Host tissue specificity of selected South African isolates of Rift Valley fever virus

by

Moabi Rachel Maluleke

Submitted in partial fulfilment of the requirements for the degree

Philosophiae Doctor

in the Faculty of Veterinary Science

University of Pretoria

Pretoria

DECLARATION

I, Moabi Rachel Maluleke, declare that the thesis, which I hereby submit for the degree, Philosophiae Doctor at the University of Pretoria, is my own work and has been submitted by me for the degree at this tertiary institution.

Signature ……. Date ……

ACKNOWLEDGEMENTS

A word of special acknowledgement and appreciation to the following people and institution for their contribution to the successful completion of this study:

- The Almighty God, CREATOR of all the opportunities for giving me the strength and wisdom I needed to make this study a success.

- Dr Ben Mans and Professor Estelle Venter, my promoters for their excellent guidance, patience and everlasting support during my studies. You were so amazing and this thesis would not have been possible without you. I thank you.

- Dr Phelix Majiwa, who conceived the project and supervised part of the work.

- Dr Antoinette van Schalkwyk, for always listening and assisting me with some techniques.

- Mr John Putterill, Dr Sonja Maree and Dr Eudri Venter for assistance with microscopy techniques.

- Agricultural Research Council – Onderstepoort Veterinary Research for allowing me to do research in the laboratories.

- Meat Industry Trust, University of Pretoria and Joy Liebenberg grant for financial assistance.

- My husband, John and daughters Dorothy, Tenyiko and Nkhensani for their moral support, encouragement, believing in me and always praying for me.

- Finally, to my family, friends and colleagues at ARC-OVR for their moral support.

SUMMARY

Host tissue specificity of selected South African isolates of Rift Valley fever virus

By

Moabi Rachel Maluleke

Promoter: Dr B.J. Mans
Agricultural Research Council
Onderstepoort Veterinary Research

Co-promoter: Prof E.H. Venter
Department of Veterinary Tropical Diseases
Faculty of Veterinary Science
University of Pretoria

College of Public Health Medical and Veterinary Sciences
James Cook University
Australia

For the degree PhD

Rift Valley fever (RVF), is a mosquito-borne viral disease affecting humans and some species of ruminants including sheep, cattle, goats, buffalos and to a lesser extent wild animals. It is a re-emerging disease responsible for major losses in livestock production, with negative impacts on livelihoods of both commercial and resource- poor farmers in sub-Saharan African and some countries in the Middle East. It remains a threat to both endemic and non-endemic countries where competent mosquito vectors exist.

The RVF virus (RVFV) causes the disease and though only a single serotype exists, differences in virulence and pathogenicity of the virus have been observed in a wide range of affected mammalian host species. This necessitates the need for a detailed genetic characterization of various isolates of the virus and whether the causal factors for host tissue tropism can be explained.

Therefore, the aims of this study were to obtain comprehensive information on the genetic composition of the RVFVs circulating in South Africa between 2008 and 2010 and to differentiate these isolates based on cell infectivity and genomic parameters.

In the first chapter the status of some published literature on the disease as well as the virus are reviewed. Viral characteristics, replication, assembly and release of the viral particle from the cell as well as virus-host receptors documented are also mentioned in this chapter.

Chapter two focused on the genetic composition of RVFVs that caused outbreaks during 2008-2010 in South Africa. Complete genome sequence analysis of isolates from different hosts and tissues collected at discrete foci of outbreaks were analysed and compared with virus sequences from earlier outbreaks in South Africa and from other countries. Phylogenetic analysis indicated that viruses that caused outbreaks during 2008-2010 were most probably reassortants, resulting from exchange of portions of the genome of different isolates, particularly of Segment M. In addition, the analysis indicated that the viruses were not introduced from outside the country but mutated in time and caused the outbreaks when the environmental conditions became favourable. Although no clear association between the virus genotype and phenotype has been established, various amino acid substitutions have been implicated for changes in the phenotype.

The third chapter describes the characterization of isolates derived from different hosts (bovine and ovine), but from the same tissue (liver). The isolates from bovine liver presented a different growth phenotype in a cell culture-based system as well as some amino acid substitutions when compared with isolates from ovine livers. Although the codon usage patterns of the six isolates were the same, they differed with those of their hosts. Further investigation of the coding regions of the genome, molecular modelling of glycoproteins and codon usage bias failed to explain the phenotypic changes.

The fourth chapter focused on an attempt to identify RVFV glycoprotein receptors using the yeast two-hybrid (Y2H) system. Baby hamster kidney cells were chosen as host cells in the laboratory because hamsters are known to be highly susceptible to RVFV. The complexity of the cDNA library constructed from BHK cells were assessed by random sequencing of 100 clones and revealed that 51 clones were genes from mRNA from the Syrian/Golden hamster using BLAST. The constructed library can also be used to study other animal pathogens

such as bluetongue virus and African horse sickness virus. The constructed bait plasmids did not show any autoactivation or toxicity in yeast, thus making them suitable to be used in the Y2H system. Twelve unique clones (4 clones using transformants of the glycoprotein Gn and 8 clones using transformants of glycoprotein Gc) were screened from the cDNA library. Identification and further characterization of the clones is necessary.

Sampling of the isolates that caused the 2008-2010 outbreaks in South Africa and full genome sequencing indicated that the isolates were genetically distinct, grouping in different clades, namely C and H. Reassortment have been identified in some of these isolates, particularly in their M segments. The majority of isolates that emerged in the outbreaks accumulated mutations over time while circulating in South Africa. The impact of these mutations on the pathogenicity of RVFV should be further investigated. Sequencing should be done on clinical samples directly to have a better idea of the phenotype and the effect of amino acid substitutions. Different phenotypes observed between cattle and sheep in tissue culture systems should be further investigated including investigation of different phenotypes *in vivo* using small experimental animals. The study has laid a foundation in understanding the pathogenicity of RVFV and necessitates the importance of understanding molecular mechanisms of the virus.

PUBLICATIONS AND CONFERENCE CONTRIBUTIONS

Publication:

Moabi R. Maluleke, Maanda Phosiwa, Antoinette van Schalkwyk, George Michuki, Baratang A. Lubisi, Phemelo S. Kegakilwe, Steve J. Kemp , Phelix A.O. Majiwa. **A comparative genome analysis of Rift Valley fever virus isolates from foci of the disease outbreak in South Africa in 2008-2010.** *Plos Negl Trop Dis*. 2019 Mar 21;13(3):e0006576

Conference contributions:

Poster presentations:

Interregional Conference on Rift Valley fever in the Middle East and Horn of Africa, 21 - 23 April 2015, Djibouti City, Djibouti
Title: Comparative genome sequence analysis of RVF virus isolates from 2008-2010 outbreaks in South Africa
M.R Maluleke, M. Phosiwa, B.A Lubisi, G. Michuki, P.S Kegakilwe, S.J Kemp and P.A.O Majiwa

11th Annual Sequencing, Finishing and Analysis in the Future (SFAF) conference, 1st - 3rd June 2016, Santa Fe, NM, USA
Title: Genome sequence of Rift Valley fever virus isolates from the 2008-2010 disease outbreaks in South Africa
M.R Maluleke, A. Lubisi, G. Michuki, M. Phosiwa, P.S Kegakilwe, Steve J. Kemp and Phelix A.O. Majiwa

University of Pretoria, Faculty of Veterinary Science, Faculty day 23th August 2018, SA
Title: Screening of host proteins that interact with Rift Valley fever virus glycoproteins using yeast two hybrid system
M.R Maluleke, E.H Venter and B. Mans

Oral presentation:
University of Pretoria, One Health Symposium, 27 November 2018, University of Pretoria, SA
Title: A comparative genome analysis of Rift Valley fever virus from foci of disease outbreak in South Africa in 2008-2010

M.R Maluleke, M. Phosiwa, B.A Lubisi, G. Michuki, P.S Kegakilwe, S.J Kemp and P.A.O Majiwa

LIST OF FIGURES

B: Transformants of pGBKT7-Gc and cDNA in a prey plasmid streaked twice on QDO/X/A plates. QDO/X/A = SD/-Ade/His/-Leu/-Trp/X-α-alpha/AbA.

LIST OF TABLES

LIST OF ABBREVIATIONS

A	Aureobasidin A
ARC-OVR	Agricultural Research Council - Onderstepoort Veterinary Research
BHK	Baby Hamster Kidney
CPE	Cytopathic effect
DDO	Double dropout media
DMEM	Dulbecco Modified Eagle media
EC	Eastern Cape
ELISA	Enzyme linked immunosorbent assay
FAO	Food and Agricultural Organization
FBS	Fetal bovine serum
FS	Free State
GA	Glutaraldehyde
GP	Gauteng Province
KZN	KwaZulu-Natal
LB	Luria broth
LP	Limpopo Province
MEGA	Molecular Evolutionary Genetics Analysis
MOI	Multiplicity of infection
MP	Mpumalanga Province
NC	Northern Cape
NGS	Next Generation Sequencing
NP/N	Nucleoprotein/Nucleocapsid
NSm	Non-structural protein of M segment
NSs	Non-structural protein of S segment
OIE	World Organisation for Animal Health
PBS	Phosphate buffered saline
PFU	Plaque forming units
Phyre2	Protein Homology/analogy Recognition Engine V 2.0
QDO	Quadruple dropout media
RPM	Ramp per minute
RVF	Rift Valley fever
RVFV	Rift Valley fever virus
SD	Minimal, synthetic defined medium for yeast

SDS PAGE	Sodium dodecyl sulphate polyacrylamide gel electrophoresis
SEM	Scanning electron microscope
SISPA	Sequence independent single primer amplification
TBST	Tris buffered saline, with Tween 20
TEM	Transmission electron microscope
tRNA	Transfer RNA
X	X-alpha galactosidase
Y2H	Yeast two-hybrid
YPDA	Yeast peptone dextrose adenine

Table of Contents

CHAPTER 1: LITERATURE REVIEW

1.1 INTRODUCTION

Rift Valley fever (RVF) is an acute mosquito-borne viral disease affecting humans and a wide diversity of animals including sheep, cattle, goats and some species of wild animals (Daubney *et al.,* 1931; Swanepoel and Coetzer, 2004; Ikegami and Makino, 2011). The disease was first identified and characterized in 1931 when it killed thousands of sheep on a farm in the Rift Valley in Kenya (Daubney *et al.,* 1931). Rift Valley fever is a notifiable disease in terms of the South African Animal Disease Act (Act 35 of 1984) (Habjan *et al.,* 2009), as well as in Europe and the United States of America (USA); it is classified as a potential biological weapon (Bouloy and Weber, 2010), a Category A Priority pathogen and a high–consequence pathogen (OIE, 2019). The increasing number of human deaths caused by RVF virus (RVFV) in eastern Africa and the ability of the RVFV to cross national and geographic borders makes this virus a high-risk pathogen of importance (Shope *et al.,* 1982; Bird *et al.,* 2008).

The occurrence of RVF epidemics is associated with heavy rainfall and flooding conditions, which provides an excellent environment for mosquito breeding (Anyamba *et al*., 2010). During these periods, *Aedes* mosquitoes multiply rapidly, transmit and amplify RVFV in animals (Linthicum *et al*., 1999). Human infection may be through mosquito bites but mostly is through direct contact with infectious aerosols. Rift Valley fever is characterised by high numbers of abortions and mortality among new-born animals. Clinical signs vary between animal species and animal age. Small ruminants (sheep and cattle) show clinical signs, whereas other animals such as dogs, adult cats and some monkeys may become viraemic without severe disease. The disease is more severe in young animals, such as lambs and calves, with mortality rates ranging from 90-100% (Swanepoel and Coetzer, 2004).

Rift Valley fever outbreaks cause large economic losses resulting from trade cessation of livestock and livestock-related products (Dautu *et al*., 2012). The disease is also of economic concern because of the cost associated with monitoring the introduction of disease in unaffected areas (Kasye *et al*., 2016). In humans, RVF outbreaks in the last few decades have worsened, affecting their social and economic impacts (Baba *et al*., 2016). For RVF survivors, neurological and visual complications are likely to be lifelong, including loss in disability-adjusted life (Baba *et al*., 2016).

Although there is no specific treatment for RVF, vaccination of livestock against RVF represents the most sustainable strategy to prevent and control its spread. Currently, there are two types of vaccines available and commonly used in endemic countries: the live attenuated vaccine, Clone 13, and a formalin-inactivated vaccine (Barnard and Botha, 1977; Alhaj, 2016). There is major improvement reported towards the novel vaccines development and the achievements have resulted in teamwork between human and veterinary research groups: a “One Health” approach to fight RVF, a major zoonotic threat (Faburay *et al*., 2017).

It is unclear why RVFV infection causes differ in different hosts and result in different outcomes. Pregnant ruminants are subjected to a high rate of abortion, while new-born animals, such as lambs, usually die (Ikegami and Makino, 2011). The susceptibility to RVFV differs between hosts and in the affected hosts certain tissues/organs are targeted. For example, in adult sheep and cattle the most affected organs are liver and spleen, while in pregnant animals the virus targets the placenta. The mechanism of interaction between RVFV and the receptor molecules on the surface of the host cells that facilitates viral attachment and entry is unknown. Therefore, this work will focus on the interaction between virus and receptors with specific attention devoted to the isolates from South Africa.

1.2 SOCIO-ECONOMIC IMPORTANCE OF RVF

Rift Valley fever has a great impact on both livestock and humans. Loss of livestock, especially young animals, is associated with huge economic loss threatening the lives of both people and animals. In many African countries (e.g. Kenya, Somalia and Tanzania) livestock is an important source of livelihood, valuable goods and services. It provides products such as milk, meat, manure, transport and wool, which lead to financial benefits (Sindato *et al*., 2011). The disease has a direct and indirect impact on both livestock-keepers and non-livestock keepers. Livestock-keepers lose their livestock through death and abortions. Loss of animals in this manner could result in production losses lasting for several years. Benefits provided by livestock, such as transport and food, are also lost during a disease outbreak. Sheep and cattle that survive abortions often suffer from infertility, which leads to a decrease in animal products (Shope *et al*., 1982). Loss of livestock, especially young animals, is a great disruption on herd dynamics that could result in production losses lasting for several years (Kasye *et al*., 2016).

Communities experience psychological stress and trauma due to the loss of family members to the disease, the possibility of contracting the disease or fear of death or losing animals (Peyre *et al*., 2015). In some communities, which depend on animals as a source of income, the presence of the disease also changes their lifestyle; i.e. meat consumption has to be reduced due to the high risk of infection and even transport becomes a challenge due to the fear of coming into contact with sick animals. This again leads to competition for alternative protein sources such as fish, chicken, pork and vegetables to replace meat (Chengula *et al*., 2013).

In some African countries, such as Tanzania where people's houses are next to animal kraals, family members might also contract the disease while taking care of their animals (Sindato *et al*., 2011), or when slaughtering sick animals (Anyangu *et al*., 2010). This will not only lead to a decrease in economic activities among these people and loss of income, but will also increase medical expenses (Anyangu *et al*., 2010).

Livestock trade drops due to animal deaths and strict export policies on animals and animal products will be impeded in countries affected by the disease. These conditions influence both internal and external markets, resulting in closure of some businesses. In countries in the Horn of Africa (Somalia, Ethiopia and Kenya), which are actively involved in livestock trading, livestock bans have a great impact, including adverse effects on public treasury, foreign exchange rates and prices of imported goods (Sindato *et al*., 2011). A demand for livestock during religious feasts such as Ramadan and Feast of Sacrifices in these countries drops during outbreaks, which also affects economic activities (Kasye *et al*., 2016).

Outbreaks also cause great financial loss due to costs associated with the control of the disease where sample collection and animal vaccination are involved. Funding is also needed for training of personnel and campaigns to raise public awareness (Narrod *et al.,* 2012).

1.3 GEOGRAPHICAL DISTRIBUTION OF RIFT VALLEY FEVER

Rift Valley fever has the capacity to cross borders and emerge in areas where it had never been reported before or re-emerge after long periods where it had once occurred. Since the time the disease was first reported in Kenya numerous outbreaks of RVF have been reported in sub-Saharan countries moving through the Rift Valley from Kenya to Tanzania, Somalia, Sudan, Zambia and Zimbabwe (Abd EI-Rahim *et al.*, 1999; Gerrard and Nichol, 2007; Chevalier *et al.,* 2010). In 1973, the disease spread through the Nile Valley to the White Nile into Sudan and in 1977, spread north of the Sahara Desert outside East Africa into Egypt

(Himeidan *et al.,* 2014). This resulted in a major epidemic with more than 200 000 clinical cases and about 600 human deaths reported (Meegan, 1979; Imam *et al.,* 1979). Epidemics are now more frequently experienced in Africa and the Middle East. The largest outbreak recorded was in sub-Saharan Africa in the Garissa District of Kenya in 1997 with human infections estimated at 27 500 (Woods *et al*., 2002).

In West Africa, Senegal and Mauritania the disease was first recorded in 1974 and 1987, respectively (Zeller *et al*., 1997). The disease spread from continental Africa to Madagascar in 1991 and was reported in Saudi Arabia and Yemen in 2000 (Ahmad, 2000; Sissoko *et al*., 2009). This was the second outbreak outside East Africa and the first time the disease was detected outside Africa (Swanepoel and Coetzer, 2004). It raised concerns that the disease might spread further into Asia and more West into Europe (Ahmed *et al.,* 2011; WHO, 2010).

In some African countries (such as Angola, Nigeria, Cameroon and Ethiopia), no RVF outbreaks have been reported, but virus isolation or serological evidence of the disease has been reported (LeBreton *et al*., 2006; Davies, 2010; Liu *et al.*, 2016). This indicates endemic circulation of the virus with mild or subclinical manifestation (Fafetine *et al*., 2013).

1.3.1 RVF outbreaks in South Africa

Records indicate that RVF outbreaks were first reported in South Africa in 1951 in three different areas: Western (North West Province), Southern (Gauteng Province) and South-Western Transvaal (Free State Province) (Gear *et al*., 1955). The outbreak started in December 1950 and continued until April 1951. At first, the disease was not known, reported as a strange and unusual disease and only recognized when people became ill soon after contact with tissues of infected sheep and cattle. This epidemic resulted in over 100 000 deaths and 500 000 abortions among sheep (Gear *et al.,* 1955).

Disease outbreaks then occurred in 1955 in the Orange Free State (Free State Province) with several farmers, farm labourers and a woman working in the kitchen getting sick after handling meat (Alexander, 1951; Gear *et al*., 1955). During this outbreak, young lambs were dying, ewes were either aborting or dying and cattle were becoming sick with a small number aborting. This outbreak was followed by several outbreaks, which occurred in successive years (1955-1956, 1956-57, 1969-1970), affecting both animals (especially sheep and cattle) and humans (Pienaar and Thompson, 2013).

The second major epidemic occurred in 1974/75 in the farming districts of the Orange Free State (Free State Province) and the Cape Province (Eastern Cape Province). This outbreak lasted for three years. Human cases were more severe, with many deaths reported during this period (McIntosh *et al*., 1980a).

In 2008, four provinces (Mpumalanga, North West, Gauteng and Limpopo) reported the disease outbreaks among cattle, goats, sheep and buffaloes (Figure 1.1 and Figure 1.2). The outbreak started close to the Kruger National Park, Mpumalanga Province in January 2008 after heavy rainfall and continued until August of the same year. The most affected animals were cattle. During this period, 18 laboratory cases of humans were reported and these were people who had close contact with infected animals. It was concluded that the disease outbreak resulted from re-emergence of the virus from reservoir hosts such as wild animals (Grobbelaar *et al*., 2011).

The 2009 outbreak in South Africa started in February and continued until May 2009 with many cases reported in KwaZulu-Natal, Eastern Cape and Mpumalanga provinces (Figure 1.1). The most affected species during this outbreak were cattle and sheep. Reports of abortion and sudden deaths, mostly in new-born and young animals, were recorded. Towards the end of that year (October to November), an outbreak was reported again, this time starting in the Northern Cape Province (in an area called Kakamas) (Figure 1.1) near the border of Namibia and continued towards the interior regions of the country (Kegakilwe, 2010; Glancey *et al*., 2015). No confirmed human cases were reported during this period. However, this second outbreak in 2009 was unusual; the outbreak did not follow any heavy rainfall (Kegakilwe, 2010). It occurred in the Northern Cape Province, next to the Gariep (Orange River) and was associated with irrigation of land (Kegakilwe, 2010).

The third major epidemic experienced in South Africa was in 2010 with 14 342 animal cases reported and 8 877 animal deaths confirmed by laboratory tests (National Institute for Communicable Diseases, 2012). The disease outbreak appeared to have started in the Free State Province in February 2010. The outbreak continued (until June) and other provinces were then also affected. High abortion rates in ewes and death of new-born lambs were recorded in the Free States and in the Northern Cape Provinces (Figure 1.1). This was the first time that RVF outbreaks were experienced during winter in South Africa (Pienaar and Thompson, 2013). The most affected animals during the outbreaks were sheep, cattle and goats and to a lesser extent buffaloes. During this period, some cases were reported in neighbouring countries; Namibia and Botswana. No outbreak was reported in KwaZulu-Natal Province in 2010 (Glancey *et al*., 2015).

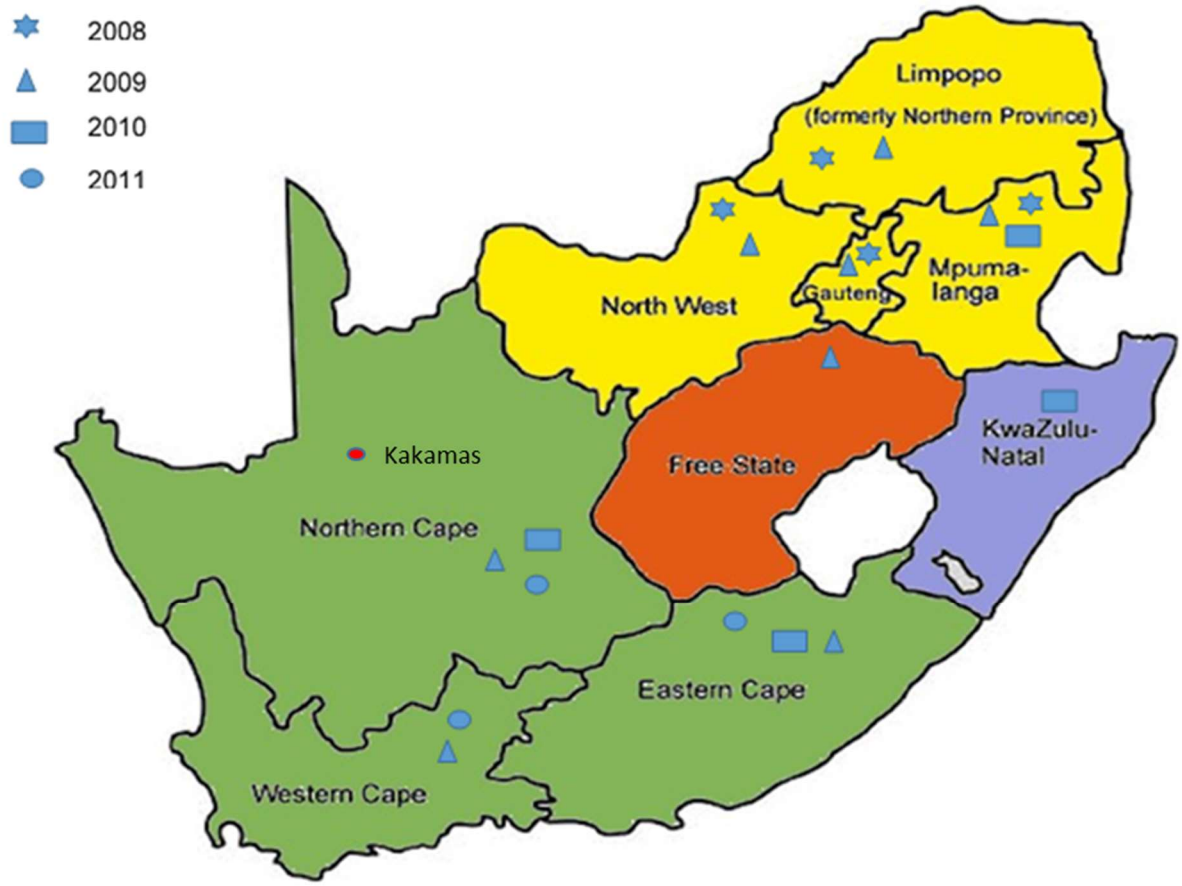

Figure 1.1: Map of South Africa showing the nine provinces. Map adapted from www.globalsecurity.org. The provinces indicated by stars experienced outbreaks in 2008; those indicated by rectangles experienced outbreaks in 2009; those indicated by triangles experienced outbreaks in 2010 and those provinces indicated by circles experienced outbreaks in 2011. The town Kakamas is indicated by a red dot.

A small outbreak of RVF was experienced in November 2010 in the Eastern Cape Province and continued to the Western and Northern Cape provinces until June 2011. Most RVF cases in animals were diagnosed at the Agricultural Research Council-Onderstepoort Veterinary Research (ARC-OVR) (Archer *et al.,* 2011). During this period, 242 laboratory-confirmed human cases with 26 deaths were reported (National Institute for Communicable Diseases, 2012) as illustrated in Figure 1.2. In addition to livestock infections, camels (*Camelus dromedaries*), waterbucks (*Kobus ellipsiprymnus*) and other wildlife species were also infected during this outbreak in South Africa (Glancey *et al*., 2015). The 2008 and 2009 outbreaks were relatively small compared to those of 2010 and 2011.

Although the disease may be inapparent in non-pregnant animals, death in adult animals such as cattle and sheep were also reported during the 2010 outbreak (Kegakilwe 2010). In most of the reported cases in South Africa, a seasonal pattern was observed from January to June and from October to June of the next year, except in the second 2009 outbreak, which did not follow the period of heavy rainfalls. Persistent heavy rainfalls result in abundant vegetation associated with appearance and survival of large numbers of mosquitoes, which serve as vectors of many diseases, including RVF. In most of the areas that were affected, susceptible hosts; i.e. sheep, cattle and goats were present, which contributed to the high number of cases reported.

Reports revealed that the circulating RVFV during 2008 and 2009 grouped within Lineage C viruses, similar to viruses that caused an outbreak in African buffaloes (*Syncerus caffer*) in the Kruger National Park in 1999 (Grobbelaar *et al*., 2011). A virus associated with Lineage H caused the outbreaks in 2010 and 2011 (Grobbelaar *et al*., 2011). During the 2010 epidemic, a virus with similar sequence identity corresponding to Lineage H was co-circulating in the neighbouring country Namibia (Monaco *et al*., 2013).

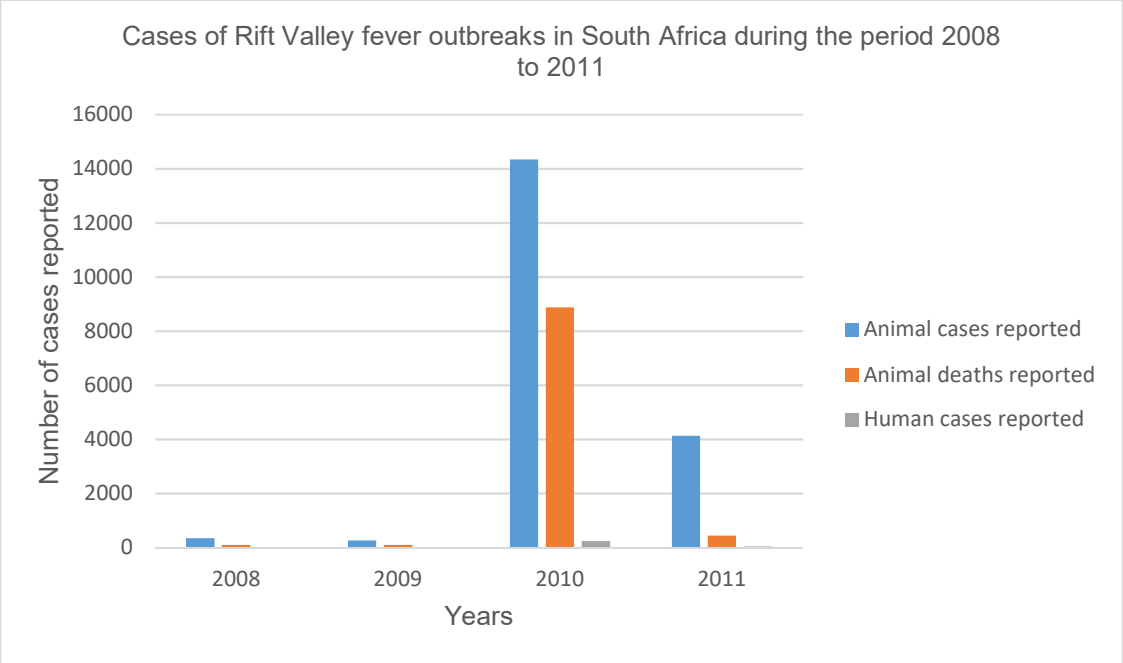

Figure 1.2: Summary of animal and human cases reported during RVF outbreaks experienced in South Africa during the period 2008 to 2011 (National Institute for Communicable Diseases, 2012; Pienaar and Thompson, 2013).

1.4 RISK FACTORS ASSOCIATED WITH THE SPREAD OF RVF

1.4.1 Water borne risk factors

Rift Valley fever occurrence typically follows periods of unusually widespread and heavy rainfall. Heavy rainfall is associated with flooding and increase in the vegetation cover that favours high vector density and vector amplification (Linthicum *et al*., 1985). During dry seasons, dambo areas (low-lying areas of soil often located near rivers) dry out and leave cracked surfaces that fill up with water during rainy seasons (Chevalier *et al*., 2011). These areas are habitats of mosquito vectors. Above normal and persistent rainfall cause the dambo areas to flood, and this increases the hatching of infected mosquito eggs that were lying dormant in the soil. These infected eggs produce new generations of infected mosquito females that transmit RVFV to nearby livestock and wildlife animals (Linthicum *et al*., 1985).

Large shallow wetlands that are created by floods are also suitable for mosquito breeding. Furthermore, the construction of dams also provides breeding sites for mosquito vectors, while the presence of susceptible breeds along the systems, serve as amplifying hosts (Jupp *et al*., 2002; Pepin *et al*., 2010).

During heavy rainfall, dams flood and increase the spread of the disease (Barnard and Botha, 1977; Gerdes, 2004), as was experienced during the construction of the Aswan dam in Egypt in 1977 (Meegan, 1979). The outbreak in Sudan originated in the White Nile State, where the Nile River (with a wide basin) floods annually during rainy seasons (Himeidan *et al.,* 2014). The second outbreak experienced in South Africa in 2009 was associated with irrigation systems along the Orange River at the border of Namibia; while the outbreaks in Madagascar in 2008-2009 were also associated with water systems used as resources for irrigation (Nicolas *et al*., 2013; Métras *et al*., 2015).

Environmental factors, such as the type of soil, is also associated with outbreaks of RVF. During heavy rainfall, clay and loam soil retain water for long periods of time, which renders this condition suitable for breeding and survival of mosquito vectors (Himeidan *et al*., 2014; Baba *et al*., 2016).

Furthermore, infected mosquito eggs can survive for several years in the soil. Once the conditions are favourable (during rainy seasons), they hatch and give rise to new generations of infected mosquitoes, which start a new outbreak (Linthicum *et al*., 1985; Chevalier *et al*., 2011).

1.4.2 The role of wildlife and subclinically infected animals, in the epidemiology of the disease

Studies have shown that many wild animals [including black rhino (*Diceros bicornis*), African buffalo, kudu (*Tragelaphus strepsiceros*), impala (*Aepyceros melampus*), African elephant (*Loxodonta*) and waterbuck] are seropositive for neutralizing antibodies specific to RVFV during inter-epidemic periods (Evans *et al*., 2008; LaBeaud *et al.,* 2011; Fafetine *et al*., 2013). This is an indication that these animals serve as RVFV reservoirs that may undergo mild or asymptomatic infections or maintain the virus at low levels (Olive *et al*., 2012). In another study, high levels of RVFV antibodies were reported in black rhinos, buffalos, impala and waterbucks from different species of wildlife collected from Kenya during the 1999-2005 inter-epidemic periods (Evans *et al.,* 2008). Circulation of RVFV among wild ruminants, especially African buffaloes and some small ruminants, may lead to dead-end infections (Olive *et al*., 2012).

1.4.3 Risk factors during outbreaks

Movement of infected animals during an outbreak is a major risk factor for translocation of RVF. Outbreaks in Saudi Arabia and Yemen in 2000 were thought to have been the result of importation of animals from the Horn of Africa, which is similar to the outbreaks in Egypt in 1977 (Gad *et al*., 1987). Importation of wild animals from infected areas can also be a possible means of introduction of the disease to an unaffected area (Olive *et al*., 2012). During an outbreak, the consumption of raw milk and meat that is not properly cooked may result in the spread of the disease to humans (Anyangu *et al.,* 2010).

Human cases reported in the first outbreaks in South Africa, were due to contact with sick animals or animal materials (Gear *et al*., 1955). This is also a major problem in some rural areas as most cattle, sheep, goats and camels stay close to their owners, and if they are infected, their owners may get infected from their saliva, nasal discharges and other materials (Seufi and Galal, 2010). Likewise, caring for animals during birth and coming into contact with the aborted animal foetus have become a major risk factor during outbreaks. Aborted animal foetuses contain high quantities of virus; thus, they need to be handled with extreme care (with personal protective equipment) to prevent the risk of infection from blood splash and aerosols, and should be destroyed by buried or burnt their carcasses (Anyangu *et al*., 2010).

1.5 CONTROL OF RIFT VALLEY FEVER

1.5.1 Vaccination of animals

Vaccination of livestock has been and continues to be the most effective method of protecting livestock against diseases. There are two types of vaccines used for the control of RVF: live attenuated and inactivated vaccines. The most commonly used live RVF vaccine; is the Smithburn. The Smithburn strain was isolated from mosquitoes in Uganda and has been used throughout Africa and the Middle East (Ikegami and Makino, 2009; Dungu *et al*., 2013). Although it provides lifelong immunity and is relatively cheap (less than 60 USD per 100ml), the Smithburn vaccine causes abortions in ewes, cattle and goats and malformations in the foetus of vaccinated and pregnant animals (Botros *et al*., 2006, Dungu *et al*., 2013). Furthermore, the Smithburn vaccine has poor antibody responses in vaccinated cattle (Barnard and Botha, 1977). Therefore, its use is not recommended in countries where RVFV has not been introduced (Ikegami and Makino, 2009). The attenuated MP-12 vaccine, obtained from a virulent Egyptian strain ZH548, did not cause abortions in ewes after 90-110 days of gestation and was reported to be non-pathogenic (Morrill *et al.,* 1987). However, more recently this vaccine was shown to cause abortions and teratogenesis (in new-born lambs) during early stages of pregnancy in ewes during animal trials in South Africa (Hunter and Bouloy, 2001). A developed recombinant candidate vaccine derived from MP-12, referred to as arMP-12ΔNSm21/384 that has shown to be safe and efficacious in sheep in Canada, has been tested in goats from Tanzania wherein it elicited neutralising antibodies (Nyundo *et al*., 2019).

A new vaccine called RVFV Clone 13 was registered in South Africa in 2008. The vaccine is based on a virus isolated from a human case of RVF in the Central African Republic, which has a large deletion (about 70%) of nucleotides in the NSs gene (Muller *et al*., 1995). Subsequently, the safety and efficacy of the vaccine was evaluated in both sheep and cattle, and neither abortion nor teratogenic effects in offspring were observed (Dungu *et al*., 2010, von Teichman *et al*., 2011). The Clone 13 vaccine was used to control the disease during the 2009 – 2010 RVF outbreaks in South Africa, Namibia, Botswana and other countries (Kortekaas *et al*., 2011).

A licenced formalin-inactivated vaccine, which is a derivative of the Smithburn vaccine, is biologically safe and poses no risk of reversion to virulence. However, it has poor immunity in cattle and requires multiple inoculations and regular boosters in order to maintain effective

immunity (Barnard and Botha, 1977; Morrill *et al*., 1991; Hunter *et al.,* 2002). This annual revaccination prevents its use in endemic areas (Alhaj, 2016).

Viral vectors such as lumpy skin disease virus, alphavirus, baculovirus and virus-like particles remain promising approaches to control RVF (Wallace *et al*., 2006; Liu *et al*., 2008; Heise *et al*., 2009). The vaccine construct, ChAdOx1 RVF, is based on a replication-deficient simian adenovirus vector (ChAdOx1) encoding the RVFV Gn and Gc glycoproteins, is still undergoing further developments in livestock trials and humans (Stedman *et al*., 2019). This candidate vaccine has shown to be safe to use in cattle, camels, pregnant sheep and goats (Warimwe *et al*., 2016; Stedman *et al*., 2019). Animal vaccination during the time of an outbreak should be done cautiously, avoiding the reuse of needles that can increase the spread of the disease (FAO, 2002).

Currently, there is no safe vaccine available for human use however, TSI-GSD 200, a formalin-inactivated vaccine derived from RVFV vaccine NDBR-103 (Randall *et al*., 1962), is a safe vaccine candidate for human use (Pittman *et al*., 1999; Faburay *et al*., 2017). The drawback of this vaccine is that it is expensive and difficult to produce. In addition, for maximum immunity, follow-up booster administrations are required (Bouloy and Flick, 2009; Ikegami and Makino, 2009). The MP-12 as a human vaccine, is still under development. Clinical trials in humans demonstrated that its use induces neutralizing antibodies with a single dose for at least several years (n=5). Although a single dose of MP-12 has proved to elicit long term immunity in humans, further assessment of its safety in healthy, immunosuppressed human individuals, pregnant women and children is still required (Ikegami, 2017).

1.5.2 Surveillance and Prevention

The occurrence of RVF is unpredictable; therefore, surveillance to monitor circulation of the virus should be encouraged even in unaffected areas. Surveillance may be done 2 to 4 times a year and any suspicious illness should be reported and investigated. In some cases, where the level of circulating virus in animals is low and cannot be detected, regular reporting of the disease (passive surveillance) is not easy. Therefore, it is advisable that surveillance is focused on vectors and serology of susceptible ruminants (Corso *et al.,* 2008). In high risk areas, laboratories are required to provide information of the disease to authorities. This type of surveillance (active) will provide an estimation of the disease frequency and will help in restraining the outbreaks of RVF by using vaccines or put other control measures in place (Lichoti *et al.,* 2014).

Public and farmer awareness/education programmes and campaigns educating people on the nature of the disease, consequences and description of benefits arising from disease prevention should be implemented. Adoption of appropriate protective measures when engaging in activities such as slaughtering and butchering should be emphasized and possible contact with mosquitoes and sick animals should be avoided. Consumption and handling of uncooked or undercooked animal products such as milk and meat should be avoided (Seufi and Galal, 2010). Clothes with long sleeves should be worn, and insect repellents be applied to prevent contracting RVF through the bite of mosquitoes (Schulz, 1951; Centres for Disease Control and Prevention, 2000).

Since mosquitoes are the most common way that RVF can spreads, eradication of their breeding sites will reduce the spread of the disease (Kasye *et al*., 2016). Since these sites are known to be on or near edges of a river, dams and other waterways, managing these sites by using insecticides will destroy mosquito eggs lying dormant, kill larvae and some adult mosquitoes (Lernout *et al*., 2013).

Movement of humans or animals can introduce the disease into areas that were previously free from the disease. Therefore, during disease outbreaks, these movements should be controlled to prevent infected animals from moving to unaffected areas (Chevalier *et al*., 2010). Outbreaks of RVF in Saudi Arabia and Egypt were caused by the importation of animals from Kenya and Sudan, respectively (Hassan *et al.,* 2011; Kamal, 2011). The recent RVF outbreak in Mayotte was the result of illegal animal movements, the presence of susceptible animals and favourable environment for mosquito vectors (WHO, 2019).

1.5.3 Diagnostic methods

Laboratory diagnosis of RVF is based on many techniques. Appropriate samples for laboratory diagnosis include liver, spleen, brain, aborted foetuses, serum or blood (OIE, 2019). The following sections discuss the various laboratory diagnostic procedures or approaches commonly used.

Virus isolation

Virus isolation can be done from specimens such as liver, spleen, kidney and blood (in heparin). Various cell cultures including African green monkey kidney [Vero, (CCL-81, ATCC)], baby hamster kidney [BHK-21 (CCL-10, ATCC)], chicken embryo reticulum [CRL, (CRL-12203, ATCC)] and AP61 mosquito cells (CVCL-2362, ATCC), are used for *in vitro* RVFV isolation (OIE, 2019). Cells infected with the virus show clear cytopathic effect (CPE) after 2-

5 days post infection. Although the method is sensitive and specific, further tests confirming the presence of the virus are required. Virus isolation also involves use of live virus, therefore requires an adequate biosafety facility.

Histopathology and immunohistochemistry

Diagnosis of RVF can be done from liver samples collected from dead animals or aborted foetus. Examination of infected liver samples using microscopy may indicate characteristic RVF liver lesions (Coetzer, 1982; Odendaal *et al*., 2019). The RVF viral antigens have aslo been identified in infected tissue samples using the antibodies against RVFV (Dodd *et al*., 2014; Wichgers Schereur *et al*., 2016).

Electron microscopy

Electron microscopy can be used to confirm and characterize the morphology of the virus. The microscopic technique is reliable and the process can take at least 24 hours upon receipt of the sample; but it is expensive and highly skilled personnel are required (Goldsmith and Miller, 2009).

Serological methods

Enzyme-linked immunosorbent assays (ELISA) and serum neutralization tests (SNT) are the most reliable and most often used serological methods to detect antibodies against RVFV in serum (Nicklasson *et al*., 1984; Zaki *et al*., 2006). The SNT is highly specific and can be applied to blood from any species. Although regarded as the gold standard and prescribed for international trade (OIE, 2019), the virus neutralization test (VNT) method is laborious, expensive and involves use of live virus requiring a biosafety facility (Pepin *et al*., 2010).

There are different types of ELISA for RVF, including indirect IgG (Paweska *et al*., 2003), Ig-sandwich and IgM capture ELISA (Paweska *et al*., 2005). The advantages of these methods are that they are rapid, specific, sensitive and inexpensive. Besides the fact that the sandwich ELISA for antigen detection (sAg-ELISA) is safe, it is suitable for use with large numbers of samples and therefore useful for surveillance and diagnosis in endemic areas (Jansen van Vuren and Paweska, 2009). Furthermore, the various approaches of ELISAs that are developed have the potential to replace traditional diagnostic methods that pose health risks (Pepin *et al.,* 2010).

Classical methods such as haemagglutination inhibition (HAI), complement fixation test, immunofluorescence (IF) and agar gel immune diffusion (AGID) have also been used (OIE, 2019). Disadvantages of these techniques include cross-reactions between RVF viruses and other phleboviruses such as sandfly fever sicilian virus (Pepin *et al.,* 2010), and pose health

threats to laboratory personnel (McIntosh *et al.*, 1980a). Furthermore, the methods are less sensitive and time-consuming (Kendall *et al*., 1999).

Molecular methods

There are two types of molecular techniques used to detect viral genomes in specimens: nucleic acid probes for hybridization and amplification methods. Hybridization processes that required labelled DNA/RNA segments serving as probes, or involving dot blot assays, are not in general use anymore (Cobo, 2012).

Highly sensitive PCR methods for detecting viral nucleic acid in tissues and blood samples have been reported. The methods include quantitative real-time PCR (RT-PCR) (Garcia *et al*., 2001; Sall *et al.,* 2002) and conventional reverse transcriptase PCR (Drosten *et al*., 2002; Bird *et al*., 2007). Another method, called reverse transcription loop-mediated isothermal amplification (RT-LAMP), has been developed and validated for RVFV RNA amplification (Peyrefitte *et al*., 2008). The latter technique is efficient, fast and inexpensive (Le Roux *et al*., 2009). A quantitative reverse transcribed PCR (qRT- PCR) is also used to detect and quantify the amount of viral RNA present in a sample (Njenga *et al*., 2009).

Sequencing provides detailed information about the origin of a pathogen. Genetic information on viruses can be obtained through nucleotide sequencing that can be done using Sanger sequencing and Next Generation Sequencing (NGS). Platforms, including NGS, 454/Roche and Illumina/Solexa, which are broadly applied to metagenomics, are still used, even though Sanger sequencing, with its low error rate, long read length and large insert size, is still considered the gold standard for sequencing (Thomas *et al*., 2012; Mokili *et al*., 2012; Smits and Osterhaus, 2013). Sequencing generates genetic data that provide insights into disease pathogenesis and therapeutic strategies (Boyd, 2013). The challenges faced with sequencing as a diagnostic tool includes expensive equipment, processing and interpretation of results by trained personnel and storage of the amount of data generated. The use of NGS technologies as a routine application requires a further decrease in costs and run times (Prachayangprecha *et al*., 2014).

A new prototype called RVF lateral flow test (LFT) or immune-chromatographic strip was developed and evaluated for rapid detection of RVF in the field at the site of a suspected outbreak (Cêtre-Sossah *et al*., 2019). It uses monoclonal antibodies against the nucleoprotein of RVFV to bind antigens captured by immobilized membrane and form a red band indicating the presence of RVFV. This RVF LFT is a promising diagnostic tool that is rapid, inexpensive and simpler to use and it provides immediate results which are visible to the naked eye (Cêtre-Sossah *et al*., 2019).

1.6 PREDICTION OF RVF DISEASE OUTBREAKS AND CLIMATE MODELS

Rift Valley fever outbreaks in East Africa have been associated with periods of heavy rainfall. Most of these outbreaks are associated with El Nino Southern Oscillation (ENSO), which warms the eastern Pacific and western Indian oceans. This causes a change in ocean temperatures, which is accompanied by changes in rainfall patterns (Anyamba *et al*., 2002).

Heavy rainfall boosts food supplies, elevates rodent populations and creates appropriate conditions for mosquito breeding and propagation, thereby fascilitating increased spread of diseases. Prediction models used to predict RVF outbreaks are based on several satellite-derived measurements (Linthicum *et al*., 1999). These include normalized difference vegetation index (NDVI), Sea Surface Temperatures (SST), Southern Oscillation Index (SOI) and rainfall (Linthicum *et al*., 1999, Anyamba *et al*., 2009, Anyamba *et al*., 2010). Through the use of Normalized Difference Vegetation Index (NDVI) measurement, the conditions suitable for the earliest stages in RVF outbreaks have been detected in East Africa (Linthicum *et al*., 1999) and this rainfall indicator was shown to correlate with RVF outbreaks in identified regions (Nderitu *et al.,* 2011). The NDVI data is available the same day and provides confirmation of predicted rainfall events with sea surface temperatures (Linthicum *et al*., 1999). The model used to predict the occurrence of RVF may be efficient in the Horn and East Africa, but needs to be adjusted for other countries such as Madagascar and Zambia. Reported cases of RVF in Madagascar in 2008 and 2009 were in areas that fall outside the endemic RVF areas predicted by the model (Anyamba *et al*., 2002; Andriamandimby *et al*., 2010). Regular and consistent heavy rainfalls lead to regular and consistent low-level activity of RVF. Because the methods are based on elevated RVF activity, in countries that receive regular and consistent rainfalls, the detection of anomalous vegetation conditions using these models may be problematic (Anyamba *et al*., 2002). Methods that use NDVI were unable to predict areas in South Africa that would be affected by RVF in 2010 and 2011. This might suggest that the difference in environmental and RVF dynamics between eastern and southern Africa also exist within South Africa (Glancey *et al*., 2015).

1.7 HOST RANGE

Although the RVFV infects many animal species including humans, it has been noted that not all animals are equally susceptible to infections. Daubney *et al.* (1931) reported that RVF is more prevalent in livestock species, such as sheep, cattle and goats, with sheep being more

susceptible than cattle or goats. This susceptibility has been seen in naturally infected sheep and proven in experimentally infected sheep (Daubney *et al.,* 1931; Easterday, 1965). Furthermore, during outbreaks of RVF in South Africa in 1951, both sheep and cattle aborted (Gear *et al*., 1955; Easterday, 1965). Again, young animals such as lambs, calves and new–born kids are most susceptible to the disease, with the mortality rate being very high (100%) in lambs as compared to calves and kids. However, calves usually die within 24 hours of infection (Gerdes, 2004).

Experimentally inoculated pigs did not show any clinical signs, but antibodies against RVFV were detected in sera of pigs, suggesting that pigs may act as reservoir hosts for RVFV (Daubney *et al.,* 1931; Easterday, 1965, Youssef, 2009). Davies and Karstad (1981) noticed that during outbreaks of the disease when sheep and cattle abort, camels also abort without showing any clinical signs. Antibodies have also been detected in camels from Kenya (Scott, 1963). Other animal species that include monkeys, domestic cats (*Felis catus*) and dogs (*Carnivora*) have demonstrated susceptibility to RVFV by subcutaneous, intraperitoneal and respiratory routes during experimental infections (Findlay, 1932; Davies *et al*., 1972). Rift Valley fever viruses have also been isolated from mosquitoes in an area where a dead buffalo and a sick buffalo calf were observed (Smithburn *et al*., 1948). However, birds, amphibians and reptiles are not susceptible to the virus (Ikegami and Makino, 2011).

The host range of RVF has also been tested by experimental inoculation of different species. Among the species inoculated gerbil (*Meriones unguiculatus*), rhesus monkeys (*Macaca mulatta*) and baboons (*Papio anubis*) have proven to be highly susceptible to RVF (Easterday, 1965; Ikegami and Makino, 2011). Hamsters are the most susceptible rodents with a mortality rate of about 100% (Easterday and Murphy, 1963). A high mortality rate among rats was also reported during the first outbreak of RVF in Kenya (Daubney and Hudson, 1933).

Rift Valley fever virus has the capacity to infect and cause severe disease in humans (Hoogstraal *et al.,* 1979; Easterday, 1965; Meegan, 1981). During the first outbreak in Kenya and in South Africa, every person engaged in herding sheep on the affected farms had been ill for some days and complained of fever and severe muscular pains (Daubney and Hudson, 1933; Gear *et al*., 1955).

1.8 CLINICAL FEATURES OF THE DISEASE

1.8.1 Animals (sheep and cattle)

Although the disease signs are non-specific, there are specific signs to look for during or after heavy prolonged rainfalls; these include sudden abortion in pregnant animals and dying of lambs and kids together with disease in humans. Clinical signs vary depending on the age and the health conditions of the animal. Sheep, cattle and goats are less susceptible than new-born lambs, calves and kids (Swanepoel and Coetzer, 2004). Lambs and kids usually develop high fevers of 40-42ºC (Easterday, 1965) and may be too weak to suckle or to stand. New-borns usually die within 36-40 hours after the onset of symptoms (Daubney *et al.,* 1931). Clinical signs in calves are the same as in lambs with occurrence of fever, weakness and bloody diarrhoea with death occuring two to three days after infection (Coetzer, 1977; Swanepoel, 1981). A small proportion of lambs and calves may develop jaundice. In pregnant animals, abortion is the first sign of the disease and this may occur at any stage of pregnancy because of infection of the foetus (Swanepoel and Coetzer, 2004). Abortion rate in sheep range between 35-40% and pregnant ewes that aborted may die because of secondary complications (Coetzer, 1977). The abortion rate seems higher compared to that in cattle (20-30%). During the South African outbreak in 1951, most sheep were found dead in the morning with no signs of illness observed the previous day (Gear *et al.,* 1955). Infected cattle may develop staring coats, refuses to eat and have a decreased in milk production (Daubney *et al.,* 1931).

The organs that show the greatest damage in infected animals such as sheep are the liver and spleen with the liver being the most damaged organ (Daubney *et al*., 1931; Coetzer 1977; Swanepoel and Coetzer, 2004). Liver lesions are the most common characteristics in affected animals and these lesions depend on animal age and susceptibility of the animal (Findlay, 1932). Lesions are more severe in young animals than in older animals. In young lambs, naturally or experimentally infected, liver lesions are constant (Easterday and Murphy, 1963). The lesions extend throughout the liver in such a way that the organ loses its shape and becomes congested (Daubney *et al*., 1931; Gear *et al*., 1955; Easterday, 1965). In severe cases, liver necrosis may affect most of the tissue. The necrotic foci start as small white spots of up to 1 mm in diameter and are distributed evenly throughout the whole organ (Daubney *et al*., 1931; Coetzer, 1982; Odendaal *et al*., 2019). The affected area may turn yellowish. In adult sheep the liver lesion is different from that of the lamb in that it has red mottled appearance and the necrotic foci are well-defined and easily recognizable (Daubney *et al.,* 1931).

1.8.2 Humans

The virus causes different disease symptoms in humans. Some people may not show any signs at first while others may have fever as the first sign. The time from infection to visible symptoms varies from 2-6 days (Ikegami and Makino, 2011). At the start of illness, affected people experience fever, physical weakness, back pain and dizziness. Patients experienced the same symptoms during the South African outbreak in 1953 (Gear *et al*., 1955). Headache, backache and muscular pains were also experienced as clinical symptoms of RVF. In some cases fatigue, loss of appetite, vomiting, neck stiffness and bodily unease accompany these symptoms. Although most infected people recover within 4 to 7 days, some patients take weeks to recover (Easterday, 1965) and a small percentage (8-10%) may develop complications including haemorrhagic fever, neurological disorder and loss of vision (Ikegami and Makino, 2011; Pepin, 2010). In less than 1% of the patients, death may occur within 3-6 days after the development of haemorrhagic fever. Although the fatality rate of the haemorrhagic fever varies between epidemics, the overall documented fatalities have been less than 1%. Mild disease in humans can be resolved spontaneously within 2 weeks with neither complications nor death (WHO, 2010).

1.9 TRANSMISSION OF THE VIRUS

Rift Valley fever virus is primarily transmitted by a broad range of mosquito species belonging to the genera *Aedes*, *Anopheles*, *Culex*, *Eretmapoites*, *Mansonia* and *Coquillettidia* with the main vectors *Aedes* (*Aedimorphus*) *vexans arabiensis* and *Culex poicilipes* (*Diptera: Culicidae*) (Smithburn *et al.,* 1948; Steyn and Schulz, 1955; Davies, 1975; McIntosh *et al*., 1980b; Logan *et al*., 1991). Sand flies (*Phlebotominae*) could also serve as vectors for RVFV (Hock *et al*., 1984; Turell and Perkins, 1990).

Infected female mosquitoes of *Aedes* species transfer the virus directly to their offspring through eggs and when eggs hatch, they produce a new generation of infected mosquitoes (Linthicum *et al*., 1985). Infected eggs can survive for long periods in dry conditions and hatch after showers. Transmission of the disease from animal to animal can occur by vertical transmission from pregnant animals to their foetus and by mechanical transmission from repeated use of contaminated needles during herd vaccination. The virus can also be spread by aerosols and enter the skin through abrasions (FAO, 2002).

Humans can become infected through the bite of infected mosquitoes. However, this happens rarely and the majority of infections are through direct contact with infected body fluids, blood, tissues or products of aborted animals and during the slaughter of infected animals (Njenga *et al.,* 2009). The virus can also infect humans by entering through wounds or broken skin (Gear *et al*., 1955) and inhalation of aerosols produced through slaughtering of infected animals (Bouloy and Flick, 2009). People at risk are farmers, shepherds, abattoir workers, veterinarians and families who shelter animals (Bouloy and Flick, 2009). Laboratory staff/technicians are at risk of infection by inhalation of aerosols from samples to be tested. During outbreaks, ingestion of raw milk and meat that has not been properly cooked also contributes to infection (Sissoko *et al.,* 2009; Anyangu *et al*., 2010).

Although no human-to-human infection has been reported, vertical transmission is possible in pregnant women (Adam and Karsany, 2008). Studies have found that pregnant women infected with RVFV were significantly associated with miscarriages (Baudin *et al.*, 2016). In another case, a pregnant woman who was ill, delivered a child that was IgM positive for RVFV. The infant developed severe haemorrhagic symptoms that led to the child's death within days of admission (Arishi *et al.*, 2006).

Rift Valley fever virus may be carried from one country to another by movement of infected hosts (domestic animals) or infected vectors (mosquitoes) resulting in the disease establishing itself in areas previously free from the virus (Chevalier *et al.,* 2010). The RVF virus can also be introduced directly to ruminants or to wild animals and persist at low levels in the environment for a very long period after the epizootic/epidemic has ended. The virus will then emerge at a later stage when conditions are favourable to cause outbreaks (Linthicum *et al.*, 1985; Fafetine *et al*., 2013).

The detection of RVF viral RNA in infected human urine and semen may reveal another mode of transmission of the disease, which is through sexual contact but this still needs to be proven (Hanecke *et al*., 2016). Insemination by bulls vaccinated with attenuated vaccines may pose danger to inseminated cows as the virus has been detected in semen three weeks after vaccination. Transmission of RVFV through semen has not been proven (Kamal, 2011).

Findings of the studies by Evans *et al*. (2007) and Lichoti *et al*. (2014) in Kenya and East Africa respectively suggested the presence of RVFV cycling during inter-epidemic periods (IEPs) involving continuous but low-level infection of livestock, wildlife and humans. The maintained virus is transmitted by mosquito vectors in ecosystems that are characterised by certain soil types vertisols, solonerts and nitisols and low annual rainfall during non-El-Nino climatic seasons (Njenga and Bett, 2019).

1.10 SURVIVAL OF RVFV

In the environment

Aedes mcintoshi infected with RVFV lay drought resistant eggs. The virus persists in these eggs for some years during dry conditions and as soon as the conditions become favourable (i.e. during heavy rainfalls), the eggs hatch and newly infected mosquitoes appear. The virus can survive in mosquito eggs laid in soil for 5-15 years (Linthicum *et al*., 1999; Baba *et al*., 2016).

In wildlife

Antibodies against RVFV have been detected in wild animals (Evans *et al*., 2008). Studies have indicated that RVFV has been circulating among apparently healthy ruminants, wildlife and humans in Mayotte for several years (Lernout *et al*., 2013). The virus has also been detected in blood of healthy and naturally infected camels in Egypt and Sudan (Imam *et al.,* 1979). Detection of RVF antibodies in areas where the disease has never been reported (Easterday, 1965) is a confirmation that the virus can circulate at a very low level without clinical signs being observed in infected animals (Lichoti *et al*., 2014; OIE, 2019). Antibodies against RVFV have been detected in buffalo sera collected during inter-epidemic periods in the Kruger National Park and Hluhluwe-iMfolozi Park providing evidence that RVFV transmission occurs in African buffaloes (Fafetine *et al*., 2013; Fagbo *et al*., 2014).

In animal products and by-products

Blood of infected animals have a high concentration of virus, but as soon as the animal is slaughtered, the virus concentration decreases (Pepin *et al*., 2010). The drop in pH (to less than 6.8) during meat processing rapidly destroys the virus (Gerdes, 2004; Ahmed *et al.,* 2011). The virus is susceptible to acidic environments but can survive for up to 3 months in dried blood (FAO, 2001). Persistence of the virus in dead animal skins, wool, bones, faeces and urine has not been demonstrated except when these products have been contaminated with blood (OIE, 2019; Pepin *et al*., 2010).

Low concentrations of virus have been detected in milk (but inactivated by pasteurization) and in body fluids of domestic animals during the epidemic in Saudi Arabia (Easterday, 1965; Al-Hazmi *et al*., 2003; Sissoko *et al*., 2009).

The virus can be destroyed by strong sunlight, lipid solvents and disinfectant solution containing sodium hypochlorite, chloroform, ether or formalin and acetic acid but can be maintained for many years when stored in temperatures below 0^{o}C (FAO, 2001).

1.11 AETIOLOGY

1.11.1 Structure of the virus

Rift Valley fever virus belongs to the order *Bunyavirales.* Viruses in this order are grouped into twelve different families: *Fimoviridae*, *Arenaviridae*, *Cruliviridae*, *Hantaviridae*, *Nairoviridae*, *Peribunyaviridae*, *Phasmaviridae*, *Phenuiviridae*, *Mypoviridae*, *Leishbuviridae*, *Wupedeviridae* and *Tospoviridae* (Abudurexiti *et al*., 2019). Several viruses of the family *Phenuiviridae*, including RVFV, comprise major pathogens producing mild to severe diseases in humans, animals and sometimes in both. The genus *Phlebovirus* consists of different species including *Rift Valley fever phlebovirus* (e.g. RVFV), *Sandfly fever Naples phlebovirus* (e.g. Toscana virus), *Punta Toro phlebovirus* (e.g. Punta Toro virus) and *Uukuniemi phlebovirus* (e.g. Uukuniemi virus) (Abudurexiti *et al.,* 2019).

Electron microscopic images of RVFV show a pleomorphic or spherical appearance, with a diameter of 80 to 120 nm (Elliot, 1990; Liu *et al*., 2008; Pepin *et al*., 2010). The viral particle is composed of a lipid bilayer and anchored glycoproteins Gn (also termed G2 and Gc (also termed G1) (Bouloy and Weber, 2010) which, when examined under the electron microscope, form spike-like projections facing outwards (Figure 1.3). The spikes are about 9 nm long and embedded in a 7 nm lipid bilayer (Freiberg *et al*., 2008). Like in many other viruses, low pH treatment changes viral surface projections from a tall (10-18 nm) to a flat (8 nm) appearance (Ellis *et al*., 1988; Överby *et al*., 2008). When RVF virions were examined by cryoelectron microscopy, the viral envelope showed 720 heterodimers of Gn (54 kDa) and Gc (56 kDa) forming 110 cylinder-shaped hexamers and 12 pentamers according to a T=12 icosahedral lattice (Freiberg *et al*., 2008).

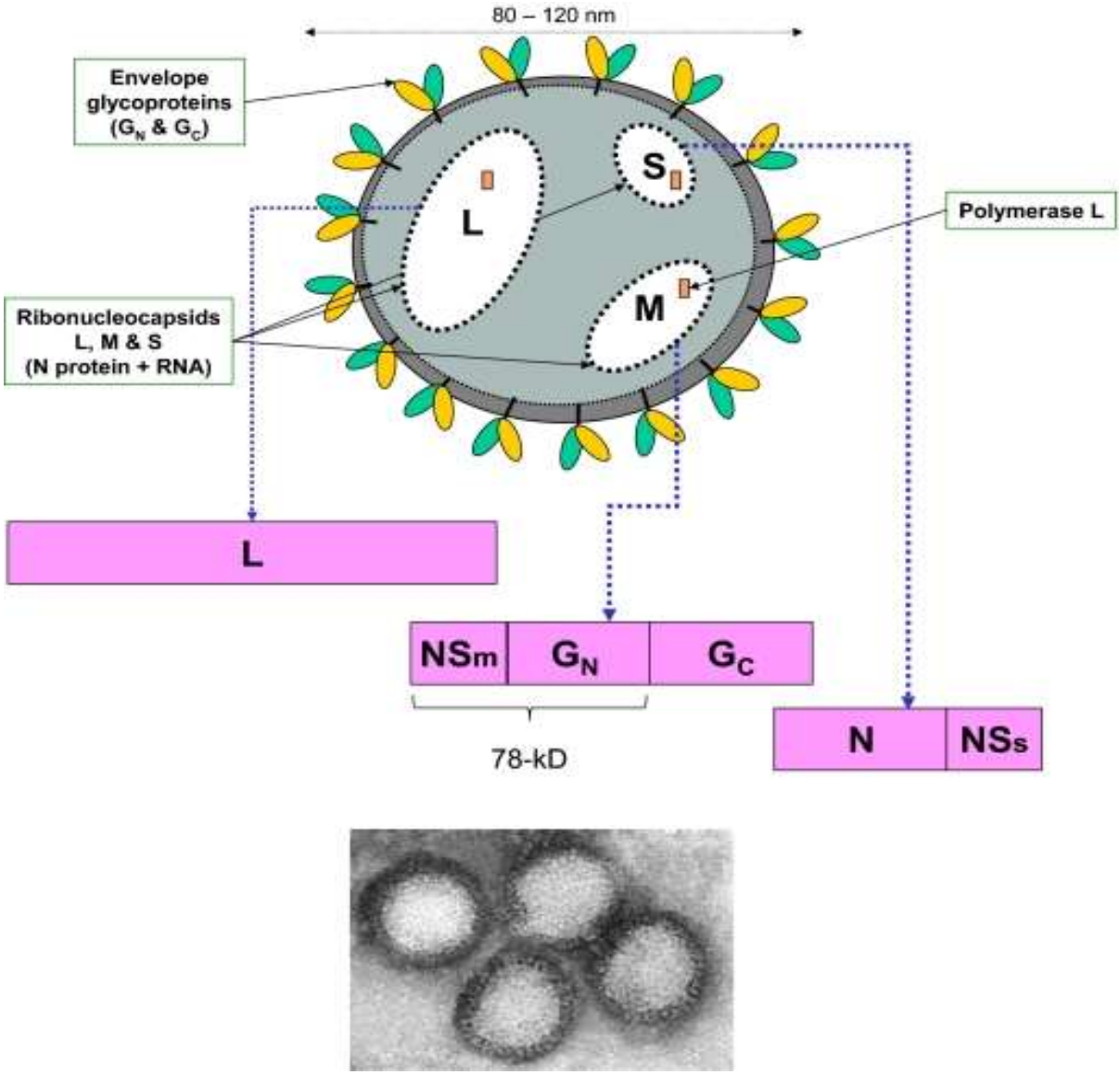

Figure 1.3: The electron microscopic photo and schematic diagram of RVFV indicating all major components of the virus (Pepin *et al*., 2010). Indicated are the L, M and S segmented genome and the genes coded for, namely, the envelope glycoproteins Gn and Gc, polymerase, non-structural protein NSm, non-structural protein NSs and the nucleocapsid (N).

Viruses of the family *Phenuiviridae* are characterised by a tri-segmented single stranded RNA genome of negative or ambisense polarity. Each segment is enclosed by a ribonucleoprotein (RNP) packaged inside the envelope (Figure 1.3). The RNP is filamentous and thought to have a panhandle structure (Ikegami, 2012). The viral RNPs serve as templates for synthesis of two types of RNA's: messenger RNA (mRNA) and complementary RNA (cRNA). The three segments are termed large (L), medium (M) and small (S). The *Bunyavirales* are the only negative-sense RNA viruses that lack a matrix underlying the envelope (Freiberg *et al*., 2008). The matrix protein links the viral envelope with the virus and may prevent assembly and

stabilization of the virus (Elliot, 1990). In Phlebovirus, the Gn cytoplasmic tail function in place of the matrix protein. It initiates the budding process and packaging of RNP into the virus particles while the viral release is facilitated by the genomic RNA and the nucleocapsid (Överby *et al*., 2008; Piper *et al*., 2011).

1.11.2 Molecular biology of the virus

Large (L) segment- polymerase protein (6.4kb)

The L segment, which is approximately 6.4 kb in length, encodes the viral RNA-dependent RNA polymerase (L-protein: 2087 amino acids) using the negative polarity. The polymerase protein synthesizes two types of RNAs: mRNA and complementary RNA (cRNA) (Muller *et al*., 1994). The cRNA is the full-length copy of the genome RNA. The protein is packaged together with the genomic RNA segments inside the viral particle and is responsible for viral transcription and replication (Liu *et al*., 2008).

Medium (M) segment – non-structural proteins and glycoproteins (3.8kb)

The M segment has an approximate length of 3.8 kb. This segment encodes five proteins: two non-structural proteins (the 78 kDa also called NSm1 and the 14 kDa named NSm2), two structural envelope glycoproteins (Gn, encoded by the amino-terminal of the protein and Gc, encoded by the carboxy-terminal sequences), and the NSm-Gn polyprotein starting from the nucleotide 135-2090 (Kakach *et al.,* 1988; Kreher *et al*., 2014). The five proteins are encoded in a single open reading frame using the negative polarity (Suzich *et al.,* 1990; Gerrard and Nichol, 2007). The entire mRNA has five-in frame (AUG) initiation codons, upstream of the Gn and the Gc sequences (Bouloy and Flick, 2009). The first AUG codon initiates the synthesis of a 78 kDa protein which is dispensable for virus replication (Won *et al*., 2006). The 78 kDa consists of pre-Gn and Gn regions. The NSm proteins are not essential for viral multiplication, packaging and assembly in cell culture, but play an accessory role in the maintenance of RVFV in nature (Gerrard *et al.,* 2007). The second AUG codon produces the NSm protein, which is probably involved in pathogenesis (Bird *et al*., 2007). It suppresses virus-induced apoptosis in the infected cell (Pepin *et al*., 2010).

Translation from the 3th and 4th codons results in a single precursor polyprotein which is co-translationally cleaved by host proteases. Cleavage occurs when the polyprotein enters the secretory system of the host cell to give rise to mature Gn and Gc glycoproteins (Collett *et al*., 1985, Gerrard and Nichol, 2007). The length of both Gn and Gc are the same in all RVFV isolates; and the N-glycosylation sites are also conserved in all the 33 isolates analysed by

Bird *et al*. (2007). The glycoproteins play an important role in penetration of the virus during infection (Whitehouse, 2004). They mediate entry of the virus through the unidentified receptor on the host cell (Pepin *et al.,* 2010) and this entry is activated by low pH predicted to employ a class II fusion mechanism (Rönkä *et al*., 1995; Garry and Garry, 2004; Filone *et al*., 2006).

Small (S) segment – nucleocapsid/nucleoprotein and non-structural protein (1.6kb)

The S segment is approximately 1.6 kb in length and encodes two proteins: the nucleocapsid protein (NP) in the genomic sense and the non-structural (NSs) protein in the anti-genomic sense (Bird *et al.,* 2007; Bouloy and Weber, 2010). NSs is a major virulence factor of RVFV. The functions of the NSs (non-structural protein encoded by the S segment) include counteracting the host cell interferon response (Bouloy *et al.,* 2001; Pepin *et al*., 2010). Non-structural proteins of the S segment form filamentous structure in the nucleus of infected cells and are highly conserved (Swanepoel and Blackburn, 1977). NSs is also not essential for virus replication hence the name accessory protein. An intergenic sequence of 82 nucleotides consisting of unique poly C or poly G tracts divides the NSs and NP (Giorgi *et al.,* 1991). The NP protein has a role in the assembly process. It encapsulates the copy RNA to form ribonucleocapsid and is required for transcription and RNA replication (Ikegami *et al*., 2007).

1.11.3 Replication of the virus

Attachment and entry

The virus uses a host receptor for attachment and entry into their hosts. Cell surface receptors provide functions essential for productive infection. They are used to activate specific signalling pathways facilitating viral entry (Grove and Marsh, 2011).

Viral glycoproteins (Gn and Gc) which are the most exposed components of the virus are responsible for virus attachment and penetration of the host cell (Överby *et al*., 2008; Lozach *et al*., 2010). Both processes (attachment and entry) happen when the viral envelope fuses with the cellular membrane to deliver the genome segments into the cytoplasm. Bunyaviruses use many receptors to target and infect many tissues of different species. A few possible receptors documented are summarized in Figure 1.4 (Spiegel *et al*., 2016). These are dendritic cells (DC) specific intercellular adhesion molecule 3-grabbing Nonitegrin (SIGN), nonmuscule myosin heavy chain 11A (NMHC-11A) and a ribonuclease kappa (RNASEK). Once the virus attaches to a receptor molecule, the virion is internalized by endocytosis. It has been suggested that after endocytosis the acidic environment of endosomal compartments activates virus fusion (Garry and Garry, 2004). Exposure of the viral particle to acidic pH

converts the viral Gc protein from metastable to a highly stable oligomer (De Boer *et al*., 2012). It has been confirmed that at alkaline pH, the Gn glycoprotein shields the hydrophobic loops of the Gc glycoprotein and rearrange at acidic pH to expose the hydrophobic loops, allowing insertion into the endosomal membrane followed by fusion (Halldorsson *et al*., 2018).

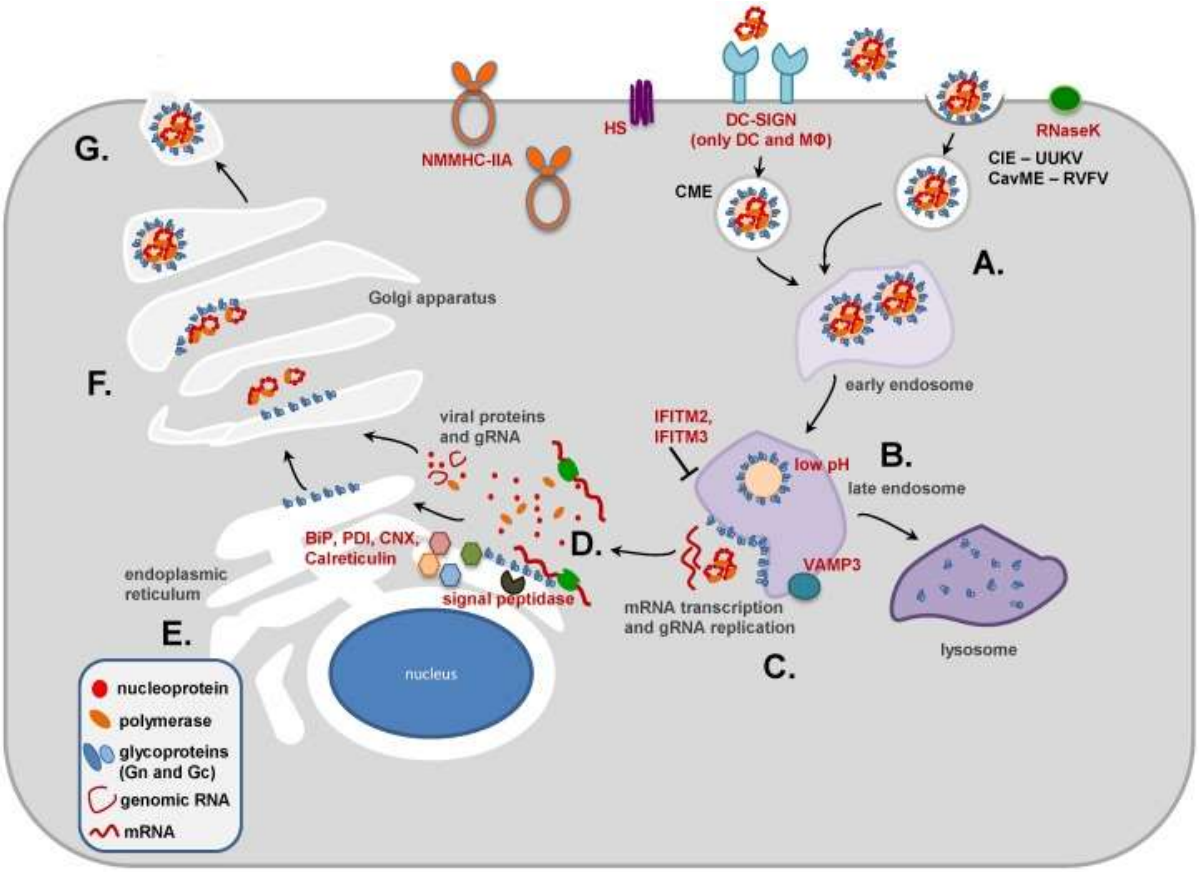

Figure 1.4: Replication cycle of phleboviruses (Spiegel *et al*., 2016). Host cell factors: DC-SIGN, HS, NMMHC-IIA responsible for attachment of phleboviruses are shown on the outside of a cell. The CavME, CIE and RNaseK are responsible for internalization of different phleboviruses. **A**: Cellular attachment, **B**: Late endosomes, **C**: Fusion of viral and endosomal membranes, **D**: Translation of glycoproteins Gn and Gc, **E**: Folding of Gn and Gc, **F**: Transportation of Gn and Gc into the Golgi Apparatus, **G**: Release of new viral particles.

Entry is predicted to employ a class II fusion mechanism (Garry and Garry, 2004). The type of proteins exhibits a parallel orientation relative to the viral membrane and a high content of ß-sheets. A trigger, which can be either low pH or receptor binding, will induce the membrane fusion proteins facilitated by marked conformational changes in glycoproteins (Spiegel *et al*., 2016; Halldorsson *et al*., 2018). The Gn and Gc proteins are localized to Golgi apparatus via co-expression, but when expressed individually the Gn is retained in the Golgi while Gc is accumulated in the endoplasmic reticulum (ER) (Gerrard and Nichol, 2007; Filone *et al*., 2006).

Experiments have shown that when glycoproteins are overexpressed using an alphavirus replicon vector, they become localised in the cell membrane where they induce cell-cell fusion (Filone *et al.,* 2006).

Heparan sulphate, a sulphated polysaccharide, which is present in mammalian cells and in the extracellular matrix (Liu and Thorp, 2002; Parish, 2006; Sarrazin *et al*., 2011), has been proven to facilitate RVF viral entry into the cell (De Boer *et al.,* 2012). Many viruses may target a sugar moiety that covers all eukaryotic cells as part of their strategy to infect cells. However, dendritic cells (DC) which are present in the dermis are among the first cells to encounter the incoming viruses (Lozach *et al*., 2010). These dermal DC express DC-specific intercellular adhesion molecule 3-grabbing Nonitegrin (DC-SIGN), a C-type lectin that captures and presents foreign antigens (Van Kooyk, 2008; Léger *et al*., 2016; Spiegel *et al*., 2016). Lozach and co-workers (2011) reported virus binding and internalization of different phleboviruses (UUKV, RVFV, Punta Toro virus and Toscana virus) using DC-SIGN-expressing cell systems and concluded that DC-SIGN is an authentic receptor required by RVFV for both attachment and endocytosis. It has been proposed that these phlebovirses use another C-type lectin DC-SIGN related protein L-SIGN, as attachment to infect cells expressing the lectin ectopically (Léger *et al*., 2016). Although the two lectins share 77% amino acid identity, they are expressed on different cell types with DC-SIGN expressed on dendritic cells, certain tissue macrophages and platelets, whereas L-SIGN is expressed on the endothelial cells of liver and lymph node sinuses (Soilleux *et al*., 2000; Phoenix *et al*., 2016; Spiegel *et al*., 2016). Another critical factor, nonmuscule myosin heavy chain 11A (NMHC-11A), has been shown to contribute to severe fever with thrombocytopenia syndrome virus (SFTSV) (another member of *Bunyavirales*) infection and the recombinant Gn is capable of binding this factor. This indicates that Gn is more likely a receptor-binding protein for SFTSV (Sun *et al*., 2014; Wu *et al*., 2017).

Not all cell lines susceptible to phlebovirus infection express the DC-SIGN, thus indicating that these cells have other receptors used for entry (Spiegel *et al*., 2016). In addition to the statement above, bunyaviruses also infect a large number of tissues that do not express the lectin (Léger *et al*., 2016).

A mechanism independent of clathrin coats called clathrin-independent endocytosis is involved in the uptake of UUKV virion, a phlebovirus related to RVFV and the process takes minutes to occur (Lozach *et al*., 2010). Research has also shown that RVFV entry depends on caveolin-1-mediated endocytosis (CavME) (Harmon *et al*., 2012) and a ribonuclease kappa (RNASEK), which is required for the initial stages of internalization of diverse pH-dependent viruses (Hackett *et al*., 2015).

Replication in the infected cell

After fusion of viral and endosomal membranes, the three segments are released into the cytoplasm. Transcription and replication occur in the cytoplasm of infected cells and follows mechanisms similar to those of viruses with negative single stranded RNA genomes (Elliot, 1990; Pepin *et al*., 2010). The ribonucleoproteins (RNPs) are templates for the synthesis of the two types of RNAs (mRNA and genomic RNA), (Gauliard *et al.*, 2006; Bouloy and Weber, 2010). The cRNA of the S segment associated with incoming virions serves as template for the synthesis of NSs mRNA and is expressed immediately after the virus has entered the cell (Schmaljohn and Hooper, 2001). During replication, nucleocapsid (N) monomers enclose the viral genome and antigenome thereby protecting the viral RNA from degradation and preventing the formation of double stranded RNA intermediate; a process that is proposed to occur in the 5' to 3' direction (Raymond *et al*., 2012; Ellenbecker *et al*., 2014). Replication process starts around 1 to 2 hours after infection and the process increases the amount of viral mRNA and proteins. Reports indicate that in other bunyaviruses, RNP assemble into virions by interacting with the cytoplasmic regions of the envelope glycoproteins at the Golgi apparatus and this process is probably also happening during RVFV replication (Rusu *et al*., 2012; Ferron *et al*., 2011). Although glycoproteins are expressed as a precursor polypeptide, this polypeptide is co-translationally cleaved prior to maturation of the glycoproteins (Wasmoen *et al*., 1988).

Assembly and release of the viral particle from the cell

The assembly process is initiated by recruitment of RdRp and encapsidated genome as a complex to the Golgi apparatus (Piper *et al*., 2011). Viral particle assembly takes place in the Golgi complex. The N protein interact with the Gn cytoplasmic tail and this interaction occurs during budding thus triggering the release of the virion (Spiegel *et al*., 2016). Mature virus particles are released to the plasma membrane where they are released through the process of exocytosis (Spiegel *et al*., 2016).

1.12 VIRUS-RECEPTOR-HOST INTERACTIONS

All viruses must enter cells to initiate their replication. Understanding how pathogens attach to host cells is of particular interest in studying infectious diseases. Pathogen proteins target different host receptors involved in molecular trafficking to the cell membrane, uptake of

nutrients and other metabolites (Hackett *et al*., 2015). Characterization of host-pathogen protein-protein interactions helps in understanding pathogen-pathogen interaction. In addition, the identification of these proteins is important to understand how pathogens evade the immune system of the host, their replication and how they persist within the organism (Huo *et al*., 2015; Nicod *et al*., 2017).

There are few methods used to study these proteins:

(a) Co-immunoprecipitation

This method uses the same technique as immunoprecipitation except that during co-immunoprecipitation an antibody against the known protein, usually called the bait is used to target that protein in the entire cell lysate. The antibody forms an immune complex with its target protein in the cell lysate and with several washes, bound proteins can be eluted and analysed using Western blot and mass spectrometry (MS). The disadvantage of this technique is that the specific immune-precipitated protein/s may be part of large complexes that will require fractionation, followed by mass spectrometry to analyse their components and to obtain antibodies of high specificity and avidity can be difficult (Xing *et al*., 2016; Avila *et al*., 2015; Miernyk and Thelen, 2008). Furthermore, the interacting proteins may be lost during stringent wash processes while non-stringent conditions might involve binding of more proteins that are not true positives (Phizicky and Fields, 1995; Klockenbusch and Kast, 2010).

(b) Pull-down assay

The approach used in this assay is the same as the one used in co-immunoprecipitation except that in the pull-down assay, a known protein fused to a tag is used to trap the interacting protein in the cell lysate. The tagged protein is captured on an immobilized affinity resin by a chemical specific for the tag. When the cell lysate containing putative prey proteins is incubated with the resin, the resin traps the bait-prey complex. After several washes to remove the unbound proteins, the complex is eluted and analysed by western blotting. The assay is useful for both confirming protein-protein interaction identified using other techniques or to identify an unknown protein interacting with the known protein (Berggard *et al*., 2007).

(c) Cross-linking

Another approach for determining protein-protein interaction is by applying a cross-linker between proteins and side chains of amino acids in a chemical reaction (Hoffman *et al*., 2015). This assay stabilises protein-protein interactions including very weak and transient interactions in the presence of cross-linkers. The cross-linker is usually a molecule with two

reactive groups on either sides separated by a spacer (Lum and Cristea, 2016). The shortest cross-linker that is used is formaldehyde with 2.3-2.7Å (Klockenbusch and Kast, 2010). Formaldehyde, a simple, inexpensive cross-linker has been widely used to freeze the native state of tissues and cells because of its high permeability towards cell membranes (Miernyk and Thelen, 2008). Cross-linked proteins can be identified by mass spectrometry, which will further reveal the peptide involved in the receptor interaction. The use of higher formaldehyde concentrations (1%) may lead to a maximum number of captured proteins (Rappsilber, 2011; Holding, 2015).

(d) Far-western blot

A molecular biological method derived from the technique of western blotting called far-western is used to detect protein-protein interaction *in vitro* (Wu *et al*., 2007). The method is specifically used to detect the interaction between protein of interest and unknown protein immobilized on a solid membrane such as nitrocellulose. In far-western blotting, cell lysate containing unknown (prey) proteins are separated on SDS PAGE, transferred to a membrane and probed with a purified labelled known (bait) protein, no antibody is used. If there is an interaction between the proteins, a protein complex will form and be detected directly (Wu *et al*., 2007). Far-western blotting involves proteins that have denatured and have been allowed to renature; allowing proteins to recover their secondary and tertiary structures (Machida and Mayer, 2009). Unlike other assays, far-western blotting detects direct binding and if binding involves a multiple protein, far-western blotting will allow the examination of interacting proteins that form complexes between them (Walsh *et al.,* 2012; Wu *et al.,* 2007). The assay can be used to either detect or confirm the interaction following pull-down or immunoprecipitation assays (Wu *et al.,* 2007).

(e) Fluorescence (Förster) Resonance Energy Transfer and Bioluminescence Resonance Energy Transfer

Interacting molecules can transfer energy between each other by non-radiative dipole-dipole interactions and if the acceptor is itself fluorescent, the process is called Fluorescence (Förster) Resonance Energy Transfer (FRET) (Corry *et al*., 2005). If the reaction is bioluminescent, it is called Bioluminescence Resonance Energy Transfer (BRET). Both FRET and BRET can detect the proximity of fluorescently labelled molecules (Xu *et al*., 1999). The techniques allow characterization of spatial organization and quantification of the interactions in living cells (Auerbach *et al*., 2003). The two techniques are related except that during FRET two fluorophores are used, one that absorbs exogenous excitation (the donor) and passes energy to the other fluorophore (the acceptor). In BRET, the donor is a luciferase and in the

presence of a substrate it generates its own luminescence emission (Sun *et al*., 2016). The disadvantage of the two techniques is that they require specialized equipment and expertise; in addition, BRET requires the use of expensive luciferase (Xie *et al*., 2011).

(f) Yeast Two-Hybrid system

Another powerful tool used, is the yeast two-hybrid (Y2H) system (Fields and Song, 1989). The Y2H system requires construction of two hybrids: a DNA binding domain fused to the protein of interest (bait) and a transcription activation domain fused to an unknown protein (prey). The two hybrids are expressed in a cell containing two or more reporter genes and if bait protein and prey protein interact, this allows association of the DNA binding and activation domains. This interaction results in expression of inducible reporter genes indicated by colour change on plates with selective media (Phizicky and Fields, 1995; Causier and Davies, 2002). The availability of bait protein clones and prey libraries can make Y2H system a relatively easy and quick method for binding proteins (Mendez-Rios and Uetz, 2010).

The Y2H system allows protein interactions to take place inside a living yeast cell. This method uses random libraries that can be made from either genomes or cDNA's to identify the unknown interacting protein. A genomic library is digested randomly, size selected, and the resulting fragments are ligated in a prey vector. A cDNA library is made through reverse transcription of mRNA collected from specific cell types or tissues (Rajapola and Uetz, 2011). Nowadays, many human and tissue specific cDNA libraries are commercially available making the system more advantageous. When compared with array screening, random libraries can find more interactions because they include fragments that may interact while full-length proteins may not (Koegl and Uetz, 2008). The method can be used to screen complex libraries for interacting prey proteins using a bait protein. The interacting prey proteins are then identified by sequencing. Because of the above advantages, Y2H was chosen as the method for identifying protein-protein interactions in this study.

1.13 JUSTIFICATION

Rift Valley fever outbreaks are usually cyclical, occurring every 5-10 years in Africa. Although only one serotype has been identified, differences in virulence and pathogenicity of the virus have been observed. Rift Valley fever infects only certain animal species (e.g. young sheep) and probably infects some animal species without the occurrence of recognizable symptoms or clinical signs (e.g. domestic pigs) (Daubney *et al*., 1931; Youssef, 2009). In an infected animal, the virus preferentially localizes to certain tissues, especially the liver, spleen and in pregnant animals, the placenta (Swanepoel, 1981). The virus causes greater levels of damage in these tissues leading to morbidity and in many instances causing death of the infected animals (Swanepoel and Coetzer, 2004).

Problem statement

Although RVFV has only one serotype, differences in virulence and pathogenicity of the virus have been observed. The casual factors of host/tissue tropism still need to be elucidated.

The overall aim of the research described herein, was to investigate potential genetic and infection characteristics, as well as receptor preferences, that may lead to understanding differences in virulence and pathogenicity between isolates. The studies utilized RVFV isolates from recent outbreaks in South Africa that were isolated from different hosts and tissues for genomic sequencing (Chapter 2). From these characterized isolates, the focus was on selected field isolates from different hosts, but from the same tissue wherein, they were compared based on growth curves, immunofluorescences and predicted protein structures. Bioinformatic analysis of protein coding genes were performed to identify possible causes of tropism (Chapter 3). The final study attempted to identify receptor molecules in BHK cells using the Y2H system to differentiate potential tropism (Chapter 4).

1.14 THE STUDY OBJECTIVE

The main objective of the study was to characterise and understand the causal factors of host tropism and its mechanism during RVFV infection.

1.14.1 Specific aims

CHAPTER 2: A comparative genome analysis of Rift Valley fever virus isolates from foci of the disease outbreaks in South Africa in 2008-2010

1. Analysis of the complete genome sequences of RVFV collected over time from animal samples at distinct foci of the outbreak, with emphasis on isolates from 2008 to 2010 outbreaks.
2. Identification of the reassortment of these isolates.
3. Determination of phylogenetic relationship of SA isolates in relation to previously published genomes.
4. Selection of isolates for further characterization.

CHAPTER 3: Differentiation of virus isolates based on cell infectivity and genomic parameters that could affect this

1. Determination of the time taken by RVFV to attach to host cells, during the cause of infection.
2. Comparison and characterization of selected isolates based on the following:
   (a) Sequence alignments (both nucleotides and amino acids)
   (b) Status of RVFV infection in BHK cells
   (c) Codon usage bias
   (d) Molecular modelling

CHAPTER 4: Identification of potential host receptors using the yeast two-hybrid system

1. Construction and evaluation of cDNA library (as prey for yeast two hybrid screening) from BHK cells
2. Construction of bait plasmids in yeast
3. Expression, autoactivation and toxicity test on baits constructed
4. Yeast two-hybrid screening using the constructed prey and baits

CHAPTER 2: A COMPARATIVE GENOME ANALYSIS OF RIFT VALLEY FEVER VIRUS ISOLATES FROM FOCI OF THE DISEASE OUTBREAKS IN SOUTH AFRICA IN 2008-2010

Data/part of this chapter has been published: *PloS Neglected Tropical Diseases* 2019 March 21;13(3):e0006576 (Maluleke *et al*., 2019)

2.1 INTRODUCTION

Rift Valley fever is a mosquito-borne viral disease, which affects humans, sheep, cattle, goats and buffaloes. The causative agent, RVFV belongs to the genus *Phlebovirus* in the family *Phenuiviridae* of the order *Bunyavirales* (Abudurexiti *et al*., 2019). The disease is characterized in livestock by an acute hepatitis, abortion storms and high mortality rates particularly in young animals. In humans, it manifests as febrile illness, resulting in retinal degeneration, severe encephalitis, haemorrhage and fatal hepatitis. Protection of animals from the disease is through vaccination. However, there is currently no approved vaccine for use in humans. The transmission of RVFV can be prevented by avoiding contact with infected tissue and animals or by eliminating the mosquito vectors (Anyangu *et al*., 2010).

The RVF virus has been isolated in Africa from more than 30 mosquito species belonging to at least six genera (*Aedes, Culex, Anopheles, Eretmapoites, Mansonia* and *Coquillettidia*). In several mosquito species isolations were performed on both the insects as well as their eggs, suggesting alternative modes of transmission (Linthicum *et al*., 1985; Turell *et al*., 1996). Eggs from floodwater mosquitoes can remain viable for many years, hatching under conducive climatic conditions associated with periods of high rainfall (Linthicum *et al*., 1985). The virus has been isolated from unfed mosquitoes reared from eggs obtained during inter-epidemic periods in Kenya (Linthicum *et al*., 1985) confirming the previous speculation by Alexander (1957) in South Africa. This contributed to the cyclic outbreaks of RVF, which is enhanced by changing climate and intensive farming systems creating conditions favorable to mosquito breeding (Anyamba *et al*., 2009).

The disease is endemic in eastern and southern Africa, although outbreaks have been reported in Egypt, Saudi Arabia, Yemen, Madagascar and Mauritania (Shoemaker *et al*., 2002; Morvan *et al*., 1992). Since no significant antigenic differences have been demonstrated among isolates from different geographic locations, only one serotype of RVFV is recognized. Despite the single serotype, differences in virulence have been observed, necessitating the

need for subsequent genetic characterization of the various isolates (Muller *et al*., 1995; Bird *et al*., 2007).

The genome of RVFV consists of three-segmented, single-stranded negative- and ambi-sense RNAs with a total size of 12 kb. The L (Large) segment encodes the RNA viral polymerase. The M (Medium) segment encodes a single precursor protein, which is cleaved to produce the envelope glycoproteins Gn and Gc; and two non-structural 78 kDa protein and NSm protein. The glycoproteins, which are located on the outer surface of the virus trigger the host humoral immune response, which produces neutralizing antibodies (Pepin *et al*., 2010).

In contrast, the ambisense S (small) segment encodes the nonstructural protein NSs in the antigenomic sense and the nucleocapsid protein N in the genomic sense (Muller *et al*., 1995; Sall *et al*., 1997; Liu *et al*., 2008; Bouloy and Weber, 2010). Due to its segmented genome, recombination through reassortment has been described as an essential contributor to RVFV evolutionary dynamics (Freire *et al*., 2015). The RVFV genome is characterized by low genetic diversity (~5%) resulting in the inability to statistically detect intragenic recombination events (Bird *et al*., 2007; Grobbelaar *et al*., 2011). Similar to other arboviruses, all the genes of RVFV are under purifying selection and evolved at distinct rates by accumulating mutations through substitutions at 1.9×10^{-4} to 2.5×10^{-4} substitutions per site per year (Freire *et al*., 2015; Bird *et al*., 2007). The previously estimated time to most recent common ancestor (TMRCA) were estimated to be approximately 124 to 133 years ago coinciding with the importation of highly susceptible European cattle and sheep breeds into Africa (Bird *et al*., 2007).

Despite the high percentage of sequence identity, partial M segment sequences of RVFV isolated over 60 years from various countries have been grouped into 15 lineages (Grobbelaar *et al*., 2011). Congruence of the phylogenetic trees constructed for the three partial genome segments indicated the presence of reassortment, with special emphasis on a 2010 isolate from a human patient in South Africa. This patient was potentially exposed to co-infection with the live animal vaccine that clustered with viruses from Lineage H. Lineage H contains mainly isolates from the 2009-2010 outbreaks in South Africa (Grobbelaar *et al*., 2011).

The first occurrence of the disease in South Africa occurred in the summer of 1950-1951 in animals and was subsequently diagnosed in humans in 1951 (Alexander, 1951; Schulz, 1951). Three major outbreaks of RVF occurred in South Africa namely in 1950-1951, 1974-1976 and recently in 2008-2011. Smaller outbreaks and individual cases of which some were not laboratory confirmed also occurred. Most of these small outbreaks occurred in the eastern part of the country (KwaZulu-Natal, Mpumalanga and Gauteng provinces) (Pienaar and Thompson, 2013). Outbreaks of RVF usually follow weather conditions, which favour an increase in mosquito populations. Such outbreaks are normally cyclical, occurring once every

30 or so years. However, this is not always the case. For example, recent outbreaks of the disease in South Africa have occurred with increasing frequency and rather unexpectedly: in 2008 (in Mpumalanga, Limpopo and Gauteng provinces), 2009 (in KwaZulu-Natal, Mpumalanga and Northern Cape provinces) and 2010 (in Eastern Cape, Northern Cape, Western Cape, North West, Free State and Mpumalanga provinces) (Figure 2.1). As of August 2010, there were 232 recorded human cases, with 26 confirmed deaths.

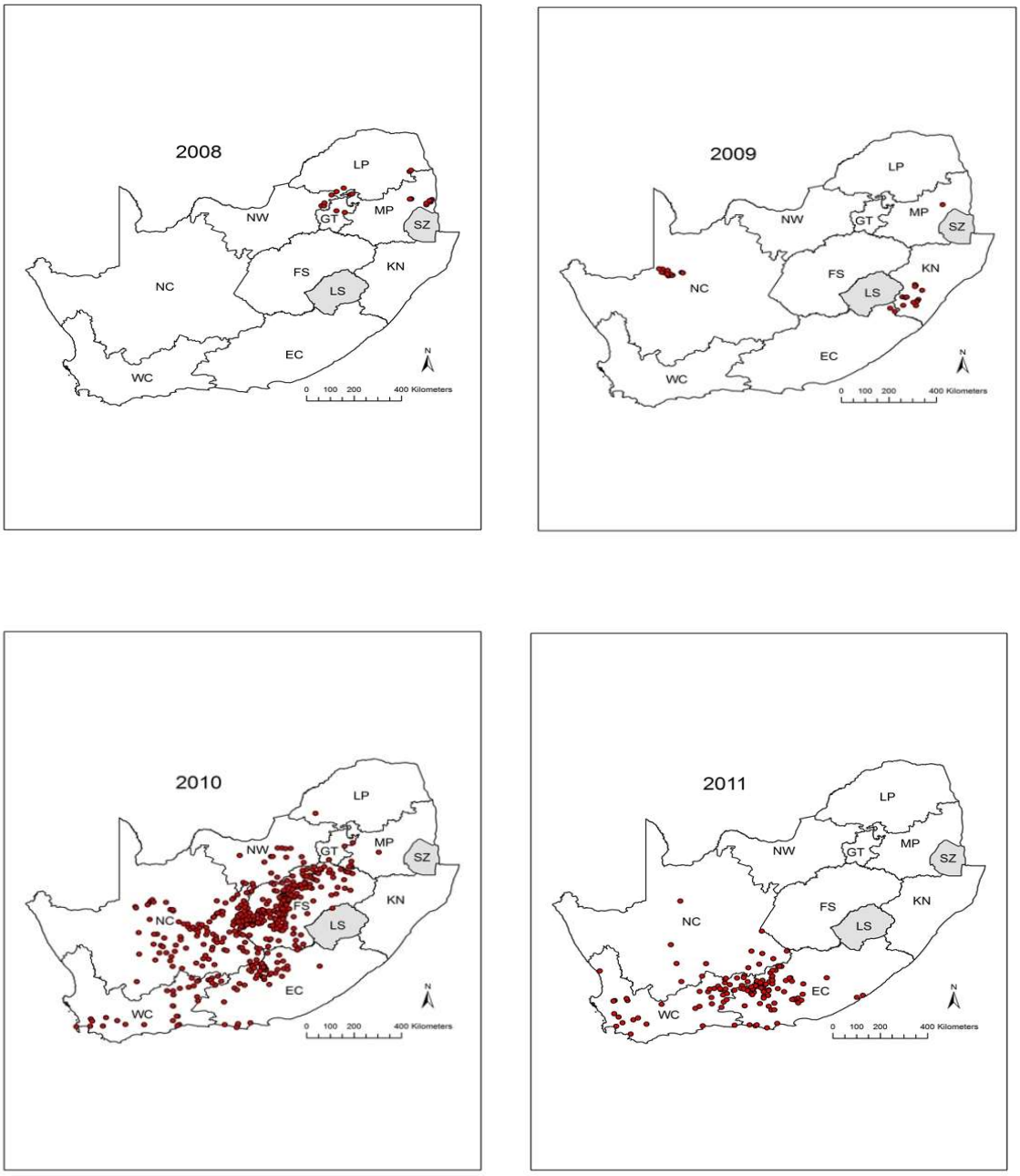

Figure 2.1: Livestock cases of Rift Valley fever in South Africa for 2008, 2009, 2010 and 2011 (Métras *et al*., 2012). Provinces are NC: Northern Cape, WC: Western Cape, EC: Eastern Cape, FS: Free State, NW: North West, KN: KwaZulu-Natal, MP: Mpumalanga, GT: Gauteng, LP: Limpopo. The light grey shaded areas are Swaziland and Lesotho (no data).

The aim of this work was to obtain comprehensive information on the genetic composition of the RVFVs circulating in South Africa. This work detailed the source of the outbreaks by comparing genomes of samples collected from these outbreaks and samples collected over

time from animals at distinct foci of outbreaks. Comparisons also included samples from earlier outbreaks in South Africa and from other countries with the aim to identify reassortment.

2.2 MATERIALS AND METHODS

2.2.1 Viruses, cells and media

All the outbreak samples used in the study were brought to the Agricultural Research Council-Onderstepoort Veterinary Research (ARC-OVR) to be tested for the presence of RVFV using PCR. The samples that tested positive for the presence of RVFV nucleic acid using real-time PCR (modified from Drosten *et al*., 2002) were confirmed by virus isolation using the method described by Digoutte *et al.* (1989). Thereafter the virus materials were propagated either in Vero or in BHK cells and stored at -80°C.

Baby hamster kidney (BHK-21) and Vero cells used throughout the study were a kind donation from Virology Division at ARC-OVR. For optimization of the growth of RVFV in the laboratory, different media; i.e. DMEM/F12, MEM and RPMI supplemented with different concentrations of fetal bovine serum (FBS) and a 1% mixture of penicillin (10 000 U/ml), streptomycin (10 000 U/ml) and amphotericin B (25 µg/ml) were used. Cells were grown at 37°C, 5% CO_2 in a humidified incubator. Confluent cells were infected with different concentrations of the M35/74 (also called the challenge strain of RVFV), an isolate of RVFV previously isolated from a liver of sheep in South Africa. Subsequently, the viruses were isolated in BHK-21 cells grown in DMEM/F12 supplemented with 5% FBS and 1% penicillin, streptomycin and amphotericin B.

2.2.2 RNA isolation and PCR

After 3 days of infection, the cells were pelleted by centrifugation at 2 500 rpm in an Eppendorf Centrifuge 5810R (Eppendorf, Germany) for 5 minutes and supernatant recovered and filtered through a 0.2 µm filter to remove all the cells and contaminants. In order to remove possible host nucleic acid contamination from the viral particles in the supernatant, the cell culture supernatant was treated with 100U DNase I and 4 µg RNase at 37°C for 2 hours. Viral RNA was then extracted using TRIZOL LS reagent (Invitrogen, USA) according to the procedure provided by the supplier. The RNA was precipitated, washed and diluted with 20 µl of RNase free water. The concentration of RNA was determined using the Nanodrop ND-1000 (Thermo Fisher Scientific).

2.2.3 cDNA synthesis and Sequence Independent Single Primer Amplification

The sequence independent single primer amplification (SISPA) method was performed according to Djikeng *et al.* (2008). A total of 170-200 ng RNA extracted as described above, was used to synthesize cDNA. Briefly, RNA was added to a mixture of 10 mM dNTP and 20 pmol/µl of the randomly-tagged primer FR26RV-N (5'-GCC GGA GCT CTG CAG ATA TCN NNN NN-3') and incubated at 65°C for 5 minutes, then placed on watery ice for another 5 minutes. A volume of 10 µl of cDNA mix (prepared using Superscript™ 111 First Strand Synthesis System for RT-PCR, Invitrogen) was added to the RNA mix prepared above. The mix was incubated at 25°C for 10 minutes followed by 50 minutes incubation at 50°C. The reaction was terminated by incubation at 85°C for 20 minutes and the unreacted RNA removed by addition of RNase H and incubation at 37°C for 20 minutes. A second strand was synthesized using Klenow exo-DNA polymerase in the presence of a random tagged and a virus specific 5' end oligo primer FR20RV (5'-GCCGGAGCTCTGCAGATATC-3'). The double stranded DNA was amplified with FR20RV primer using Accuprime Taq DNA polymerase High Fidelity (Invitrogen). The following PCR protocol was used: 94°C for 2 minutes, 35 cycles of 94°C for 30 seconds, 55°C for 30 seconds and 68°C for 1 minute with the final extension of 68°C for 10 minutes. The PCR products were analyzed on a 1% agarose gel and purified by the MinElute PCR Purification kit (Qiagen).

2.2.4 Construction of cDNA libraries

The SISPA products ranging in size from 0.2 kb to 1.5 kb were recovered from agarose gels and used in the preparation of a library for sequencing following procedures described by the manufacturer (Roche Applied Science). Sequencing was done using the Genome Sequencer 454 platform (GSFLX; 454 Life Sciences, Roche Applied Science; http://www.454.com). SISPA products from at least two random isolates were also sequenced on the Illumina platform (http://www.illumina.com).

2.2.5 Genome sequence accession numbers

The nucleotide sequences of all the segments of the RVF isolates analyzed in the current study have been deposited in GenBank with accession numbers indicated in Table 2.1.

2.2.6 Bioinformatic analyses of the sequence data

The sequence data obtained was processed and assembled into contigs using the Roche/454 Newbler software set to default values (454 Life Sciences Corporation, Software Release: 2.8 — 20120726_1306) and then further subjected to analyses using a combination of bioinformatics software. The nucleotide sequences were aligned using the Clustal W module within the Molecular Evolutionary Genetics Analysis (MEGA 6); set to optimum parameters for each sequence type (Thompson *et al*., 1994; Tamura *et al*., 2011). The best fitting nucleotide substitution model (General Time Reversible; GTR) was determined for each genome segment using MEGA 6 and this was applied to subsequent analysis. The criteria for selecting the best fitting nucleotide substitution was based on the lowest Bayesian information criterion (BIC). The sequence alignments were used in MEGA 6 to calculate the mean pairwise distances as well as to derive phylogenetic trees using Maximum likelihood under 1000 bootstrap iterations (Hall, 2013). Evidence of intragenic recombination events were analysed using different methods available from RDP3 (Heath *et al*., 2006). Rates of molecular evolution for individual genome segments were estimated using Bayesian Markov Chain Monte Carlo implemented in the BEAUTI, BEAST, Tracer and FigTree packages (Drummond *et al*., 2012). The substitution rates were estimated using both strict and relaxed uncorrelated lognormal molecular clock under the GTR model with gamma distribution (T4). The general Bayesian skyline coalescent prior was used and the MCMC allowed to run for a sufficient number of generations with sampling every 1000 states, to ensure convergence of all parameters (Drummond *et al*., 2012).

The two glycoproteins Gn starts from amino acid 154 and terminates at amino acid 691, while the Gc starts at amino acid residue 692 and ends at amino acid residue 1197. The amino acid sequences of the glycoproteins encoded by the M segment of different RVFV isolates obtained from the 2008-2010 outbreaks were compared with previously published sequences of isolates are illustrated in Table 2.2.

2.3 RESULTS

This study focused on RVF viruses isolated from diagnostic outbreak samples submitted to the ARC-OVR for testing. The identification of the isolates, hosts, tissue sources and the nearest towns where the samples were collected are outlined in Table 2.1. The year in which the samples were collected is attached to the virus identification number.

The complete genome sequences of 23 isolates were determined by using the SISPA method followed by NGS technologies. A representative profile of SISPA products (smear ranging between 200 bp and 1 500 bp) obtained from the virus isolates is indicated in Figure 2.2. The 23 isolates represent four of the 15 reported outbreaks in 2008, three of the 19 outbreaks reported in 2009 and six of the 484 outbreaks in 2010 (Table 2.1) (Pienaar and Thompson, 2013). In addition, the complete genome sequence of isolate M48/08 from Madagascar as well as historical samples M57/74, M1975Bov and M1955 isolated respectively from South African outbreaks in 1955, 1974 and 1975 were elucidated (Table 2.1). Isolates M247/09 and M260/09 were sequenced using both 454 Platform and Illumina Platform (indicated by I), in order to evaluate the efficiency of SISPA using these NGS technologies. The sequencing results indicated that either of these NGS technologies could be utilized together with SISPA to produce complete genome sequences of RVFV isolates.

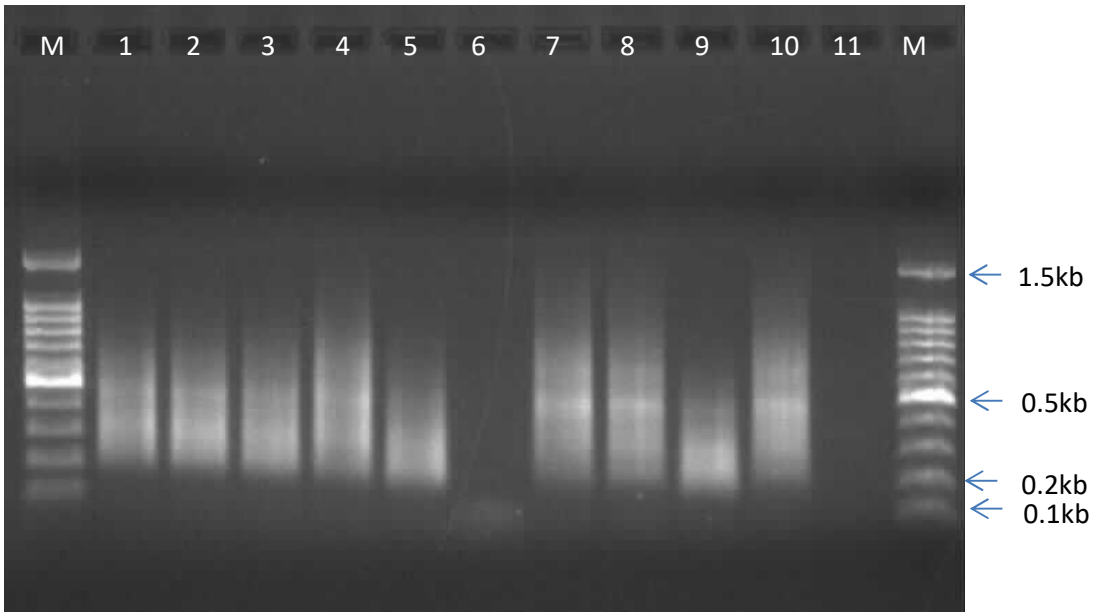

Figure 2.2: Photograph of a representative agarose gel in which SISPA products of RVFVs were resolved. Lanes contain products as follows: Lane 1: M03/10, Lane 2: M15/10, Lane 3: M06/10, Lane 4: M19/10, Lane 5: M21/10, Lane 6: M22/10, Lane 7: M23/10, Lane 8: M25/10, Lane 9: M26/10, Lane 10: M33/10, Lane 11: no DNA. Lane labeled M contain DNA size markers, with corresponding sizes of some indicated in kilobasepairs (kb).

The assembled NGS data of all the RVFV isolates generated complete sequence data for Segments S, M and L for each of the viruses and were subsequently deposited in GenBank with accession numbers indicated in Table 2.1. Alignments were generated for each of the three segments using the available sequence data from GenBank as previously indicated.

These alignments included full genome sequences from 120 – 140 isolates depending on the segment and were used to evaluate the evolutionary dynamics of each segment. Virus diversity was low for each of the segments, with percentage sequence identity differences less than 5% between isolates for Segment S and Segment L and less than 6% in Segment M.

Table 2.I. List of RVFV isolates analyzed in the study

Isolate #/year	GenBank Accession number			Host	Tissue source	Nearest town (Province)
	L segment	M segment	S segment			
M48/08	KX944866	KX944843	KX944820	Bovine	Liver	Madagascar
M47/08	KX944865	KX944842	KX944819	Bovine	Liver	Warmbad – Bela-Bela, (LP)
M39/08	KX944864	KX944841	KX944818	Buffalo calf	Whole foetus	Nelspruit – Mbombela, (MP)
M37/08	KX944863	KX944840	KX944817	Buffalo calf	Whole foetus	Hoedspruit (LP)
M85/08	KX944871	KX944848	KX944825	Bovine Calf	Carcase	Irene (GP)
M84/08	KX944870	KX944847	KX944824	Bovine	Serum	Irene (GP)
M80/08/2	KX944869	KX944846	KX944823	Bovine	Serum	Irene (GP)
M66/09	KX944868	KX944845	KX944822	bovine	liver	Modderfontein (GP)
M260/09	KX944860	KX944837	KX944814	Bovine	Foetus organ	Upington (NC)
M259/09	KX944859	KX944836	KX944812	Bovine	Serum	Upington (NC)
M247/09	KX944857	KX944834	KX944811	Ovine	Liver, lung	Upington (NC)
M127/09	KX944851	KX944828	KX944804	Bovine	Serum, fresh liver	Cascade (KZN)
M33/10	KX944862	KX944839	KX944816	Ovine	Liver	Middelburg (EC)
M29/10	KX944861	KX944838	KX944815	Bovine	Serum	Pretoria – Tshwane, (GP)
M25/10	KX944858	KX944835	KX944813	Ovine	Organs	Bultfontein (FS)
M12/10	KX944850	KX944827	KX944805	Ovine	Serum	Bultfontein (FS)
M19/10	KX944853	KX944830	KX944809	Ovine	Liver, Lung, Brain and spleen	Helderfontein (FS)
M16/10	KX944852	KX944829	KX944806	Ovine	Organs	Bultfontein (FS)
M06/10	KX944849	KX944826	KX944803	Bovine	Serum	Sterkfontein (EC)
M21/10	KX944856	KX944833	KX944810	Ovine	Liver	Bloemfontein – Mangaung, (FS)
M57/74	KX944867	KX944844	KX944821	N/A	N/A	N/A
M1975Bov	KX944855	KX944832	KX944808	Bovine	N/A	N/A
M1955	KX944854	KX944831	KX944807	N/A	N/A	N/A

N/A = Unknown

In order to determine the influence of substitution rate on biological function, the effect of differential selection pressures was estimated by calculating the rate of nonsynonymous (dN) to synonymous (dS) substitutions. All the coding regions were estimated to be under purifying selection pressure (dN/dS <1) (Table 2.2).

The estimated molecular evolutionary rates were as follows: for the L segment, 3.08 x 10^{-4} [95% highest posterior density (HPD) interval, 2.2 x 10^{-4} – 3.9 x 10^{-4}] nucleotide substitutions/site/year; for the M segment, 3.64 x 10^{-4} (95% HPD interval, 2.8 x 10^{-4} – 4.5 x 10^{-4}) nucleotide substitutions/site/year and for the S segment, 4.17 x 10^{-4} (95% HPD interval, 3.1 x 10^{-4} – 5.3 x 10^{-4}) nucleotide substitutions/site/year (Table 2.2).

Table 2.2. Bayesian coalescent estimations of RVFV isolates

Segment	TMRA (Years) [95% HPD Interval]	Substitution rate (Substitutions / site / year) [95% HPD Interval]	Mean dN/dS
Segment L	131.5 [83.3 – 140.5]	3.08 x 10^{-4} [2.2 x 10^{-4} – 3.9 x 10^{-4}]	0.045 [Log(L) = -19920.8]
Segment M	112 [86.3 -140.1]	3.64 x 10^{-4} [2.8 x 10^{-4} – 4.5 x 10^{-4}]	0.081 [Log(L) = -12337.7]
Segment S	100.9 [74.4 – 141.1]	4.17 x 10^{-4} [3.1 x 10^{-4} – 5.3 x 10^{-4}]	NS: 0.18 [Log(L) = -3206.7] NP: 0.058 [Log(L) = -2756.2]

TMRA = time to most recent common ancestor; HPD = highest posterior density; dN = nonsynonymous nucleotide substitution site; dS = synonymous nucleotide substitution site.

The phylogenetic relationships of the 23 RVFV sequences were assessed in relationship to 50 previously published sequences (Table 2.3) using maximum likelihood trees (Figures 2.3A-C).

Table 2.3. A list of previously published genome sequences of RVFV

Isolate/Name	Country of origin	Year of isolation	Segment L	Segment M	Segment S
T1: mosquito which fed on hamster infected with ZH-501	Egypt	1977	DQ375407 Egy Sha T1 77	DQ380201 Egy T1 ZH-501 77	DQ380150 Egy T1 ZH-501 77
ZH-1776	Egypt	1978	DQ375411 Egy Gha ZH-1776 78	DQ380203 Egy Gha ZH-1776 78	DQ380153 Egy Gha ZH-1776 78
ZM-657	Egypt	1978	DQ375409 Egy Sha ZM-657 78	DQ380204 Egy Sha ZM-657 78	DQ380146 Egy Sha ZM-657 78
ZS-6365	Egypt	1979	DQ375410 Egy Cha ZS-6365 79	DQ380205 Egy Gha ZS-6365 79	DQ380145 Egy Gha ZS-6365 79
ZH-548	Egypt	1977	DQ375403 Egy Sha ZH-548 77	DQ380206 Egy Sha ZH-548 77	DQ380151 Egy Sha ZH-548 77
ZC-3349	Egypt	1978	DQ375412 Egy Asy ZC-3349 78	DQ380207 Egy Asy ZC-3349 78	DQ380152 Egy Asy ZC-3349 78
763/70	Zimbabwe	1970	DQ375426 Zim Sal 763 70	DQ380188 Zim Sal 763 70	DQ380174 Zim Sal 763 70
2373/74	Zimbabwe	1974	DQ375432 Zim Sal 2373 74	DQ380194 Zim Sal 2373 74	DQ380159 Zim Sal 2373 74
2250/74	Zimbabwe	1974	DQ375413 Zim Bea 2250 74	DQ380209 Zim Bea 2250 74	DQ380143 Zim Bea 2250 74
1260/78	Zimbabwe	1978	DQ375418 Zim Sal 1260 78	DQ380214 Zim Sal 1260 78	DQ380164 Zim Sal 1260 78

1853/78	Zimbabwe	1978	DQ375424 Zim Sin 1853 78	DQ380220 Zim Sin 1853 78	DQ380168 Zim Sin 1853 78
2269/74	Zimbabwe	1974	DQ375434 Zim Sin 2269 74	DQ380222 Zim Sin 2269 74	DQ380173 Zim Sin 2269 74
MgH824	Madagascar	1979	DQ375414 Mad MgH824 79	DQ380210 Mad MgH824 79	DQ380144 Mad MgH824 79
200803166	Madagascar	1991	JF311372 Mad Ant 200803166 91	JF311381 Mad Ant 200803166 91	JF311390 Mad Ant 200803166 91
200803167	Madagascar	1991	JF311373 Mad Ant 200803167 91	JF311382 Mad Ant 200803167 91	JF311391 Mad Ant 200803167 91
200803168	Madagascar	2008	JF311374 Mad Mia 200803168 08	JF311383 Mad Mia 200803168 08	JF311392 Mad Mia 200803168 08
200803169	Madagascar	2008	JF311375 Mad Ant 200803169 08	JF311384 Mad Ant 200803169 08	JF311393 Mad Ant 200803169 08
OS-9	Mauritania	1987	DQ375397 Mau OS-9 87	DQ380183 Mau OS-9 87	DQ380179 Mau OS-9 87
OS-8	Mauritania	1987	DQ375395 Mau OS-8 87	DQ380185 Mau OS-8 87	DQ380177 Mau OS-8 87
OS-1	Mauritania	1987	DQ375398 Mau OS-1 87	DQ380186 Mau OS-1 87	DQ380180 Mau OS-1 87
Hv-B375	Central African Republic	1985	DQ375422 CAR Mba Hv-B375 85	DQ380218 CAR Aba Hv-B375 85	DQ380161 CAR Hv-B375 85
CAR-R1622	Central African Republic	1985	DQ375423 CAR Ban R1622 85	DQ380219 CAR Ban R1622 85	DQ380160 CAR R1622 85
73HB1230	Central African Republic	1973	DQ375425 CAR 73HB1230 73	DQ380221 CAR 73HB1230 73	DQ380172 CAR 73HB1230 73
Zinga	Central African Republic	1969	DQ375419 CAR Zinga 69	DQ380217 CAR Zinga 69	DQ380167 CAR Zinga 69
Kenya 56 (IB8)	Kenya	1965	DQ375427 Ken-IB8 56	DQ380190 Ken-IB8 65	DQ380176 Ken 56-IB8 65
Kenya 57 (Rintoul)	Kenya	1951	DQ375431 Ken Rintoul 57	DQ380192 Ken Rintoul-57 51	DQ380155 Ken Rintoul-57 51
Kenya 9800523	Kenya	1998	DQ375400 Ken 9800523 98	DQ380196 Ken 9800523 98	DQ380169 Ken 9800523 98
Kenya 83 (21445)	Kenya	1983	DQ375402 Ken Rui 21445 83	DQ380198 Ken Rui 21445 83	DQ380171 Ken Rui 21445 83
2007004194	Kenya	2007	EU574004 Ken Kia 2007004194 07	EU574031 Ken Kia 2007004194 07	EU574057 Ken Kia 2007004194 07
2007004193	Kenya	2007	EU574005 Ken Nai 2007004193 07	EU574032 Ken Nai 2007004193 07	EU574058 Ken Nai 2007004193 07
2007003644	Kenya	2007	EU574006 Ken Bar 2007003644 07	EU574033 Ken Bar 2007003644 07	EU574059 Ken Bar 2007003644 07
2007002060	Kenya	2007	EU574013 Ken Nai 2007002060 07	EU574039 Ken Nai 2007002060 07	EU574066 Ken Nai 2007002060 07
2007001564	Kenya	2007	EU574017 Ken Mur 2007001564 07	EU574044 Ken Mur 2007001564 07	EU574072 Ken Mur 2007001564 07
2007001292	Kenya	2007	EU574019 Ken Mer 2007001292 07	EU574046 Ken Meru 2007001292 07	EU574074 Ken Mer 2007001292 07
Saudi 2000-10911	Saudi Arabia	2000	DQ375401 SA 10911 00	DQ380197 Saudi 10911 00	DQ380170 Saudi 10911 00
SA01-1322	Saudi Arabia	2001	KX096941 SA 1322 01	KX096942 Saudi 1322 01	KX096943 Saudi 1322 01

SA-75	South Africa	1975	DQ375428 RSA 75	DQ380189 RSA 75	DQ380175 RSA 75
SA-51 (Van Wyck)	South Africa	1951	DQ375433 RSA VanWyck 51	DQ380195 RSA VanWyck 51	DQ380158 RSA VanWyck 51
M35/74	South Africa	1974	JF784386 RSA M35 74	JF784387 RSA M35 74	JF784388 RSA M35 74
Kakamas	South Africa	2009	JQ068144 RSA Kakamas 09	JQ068143 RSA Kakamas 09	JQ068142 RSA Kakamas 09
Sudan 85-2010	Sudan	2010	JQ820485 Sud Gez-85 10	JQ820488 Sud Gez-85 10	JQ820476 Sud Gez-85 10
Sudan 86-2010	Sudan	2010	JQ820484 Sud Gez 86 10	JQ820489 Sud Gez 86 10	JQ820477 Sud Gez 86 10
Sudan 2V-2007	Sudan	2007	JQ820483 Sud WNS-2V 07	JQ820490 Sud WNS 2V 07	JQ820472 Sud WNS-2V 07
Sudan 28-2010	Sudan	2010	JQ820486 Sud Gez-28 10	JQ820491 Sud Gez 28 10	JQ820474 Sud Gez 28 10
TAN/Tan-001/07	Tanzania	2007	HM586959 TAN Tan-001 07	HM586970 Tan 001 07	HM586981 Tan Tan-001 07
TAN/Dod-002/07	Tanzania	2007	HM586960 Tan Dod-002 07	HM586971 Tan 002 07	HM586982 Tan Dod-002 07
Tan 2007000323	Tanzania	2007	JF326189 Tan 2007000323 07	JF326194 Tan 2007000323 07	JF326203 Tan 2007000323 07
Entebbe	Uganda	1944	DQ375429 Uga Entebbe 44	DQ380191 Uga Entebbe 44	DQ380156 Uga Entebbe 44
Smithburn	Uganda	1944	DQ375430 Smithburn	DQ380193 Smithburn	DQ380157 Smithburn
Lunyo	Uganda	1955	KU167027 Uga Lunyo 55	KU167026 Uga Lunyo 55	EU312121 Uga Lunyo 55

Incongruence between the phylogenies generated by the individual segments was observed and subsequently the influence of recombination and reassortment were investigated (Figures 2.3A-C). Intragenic recombination events were predicted in all three segments, but with insignificant statistical support. From the 15 lineages described in Grobbelaar *et al.* (2011), 13 lineages were observed and the phylogenies of the individual three segments are illustrated in Figures 2.3A-C. All the 2008 and one 2009 isolate from South Africa and Madagascar were included as part of this study, clustered within Lineage C or Kenya-1 as previously described (Grobbelaar *et al*., 2011; Bird *et al*., 2008a). The remainder of the 2009 and 2010 isolates with the exception of isolate M259_RSA_09 clustered within Lineage H (Grobbelaar *et al*., 2011).

Sample M259_RSA_09 was isolated from a bovine serum obtained in Upington (Northern Cape Province). Both Segments L and S clustered with sample Kakamas isolated in 2009 from the town Kakamas also in the Northern Cape Province that cluster in Lineage K. In contrast, Segment M of isolate M259_RSA_09 cluster within Lineage H along with the rest of the 2009 – 2010 sequences (Figure 2.3B). Isolate M259_RSA_09 was probably a reassortment between coinfection of RVFVs belonging to Lineages H and another from Lineage K. A second sample, M1955_RSA_55, was probably also the result of reassortment with Segments L and S of this isolate which cluster with sample Van-Wyck in Lineage I isolated in South Africa in 1951 (Figures 2.3A and C). Reassortment happen like mutation. There is no likelihood factor as it can happen randomly. Segment M of M1955_RSA_55 cluster within

Lineage L along with isolates from South Africa, obtained during the 1974 and 1975 outbreaks (Figure 2.3B). Since both these reassortment events pertained to Segment M, which encode two glycoproteins (Gn and Gc), this segment was subjected to additional analysis in this study.

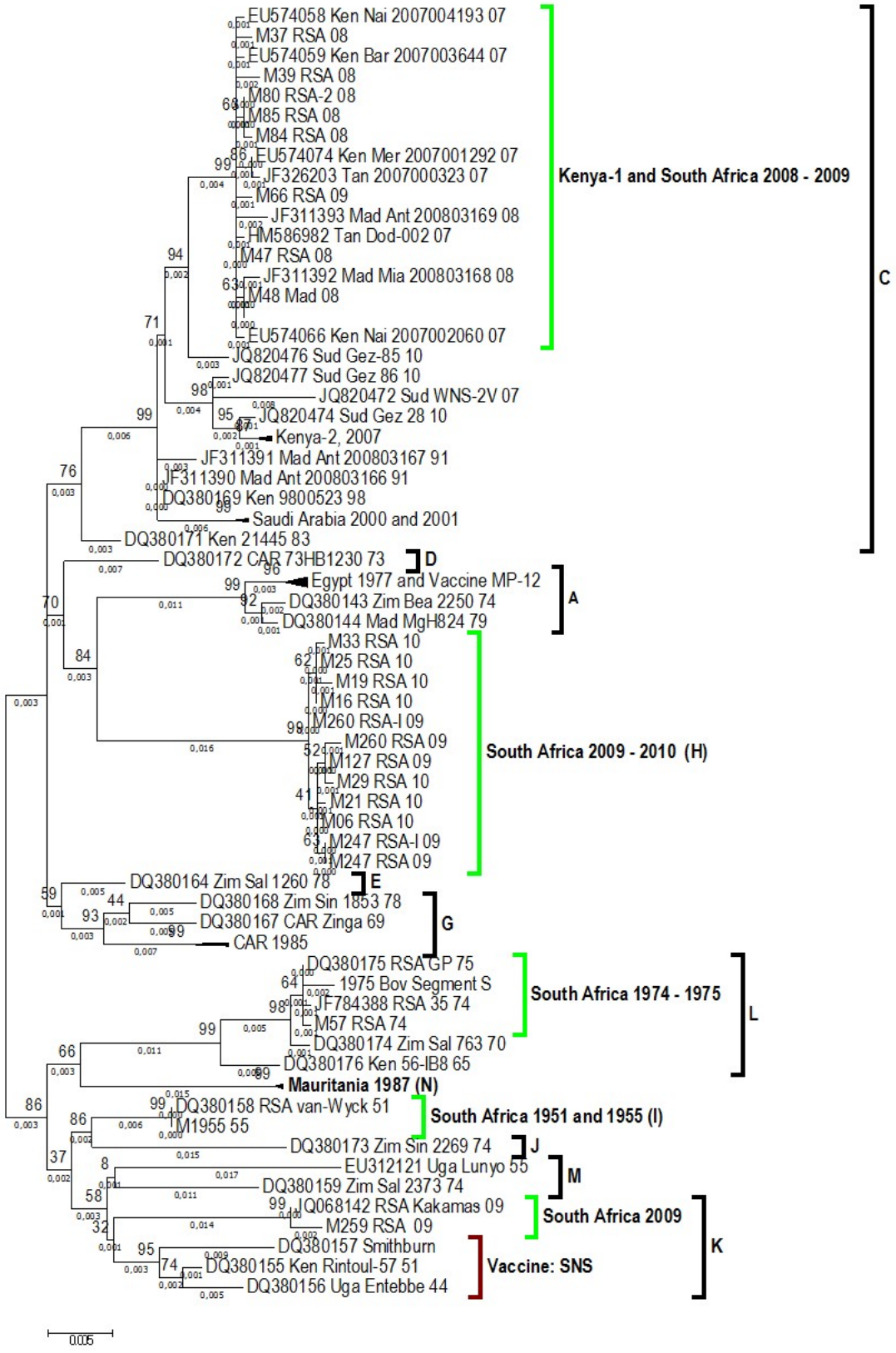

Figure 2.3A: Maximum likelihood tree of the S segment. The tree was generated using the maximum likelihood algorithm using MEGA 6. The designation of the clades follows Grobbelaar *et al*. (2011). The lineages containing RVFV isolates from South Africa are presented in green.

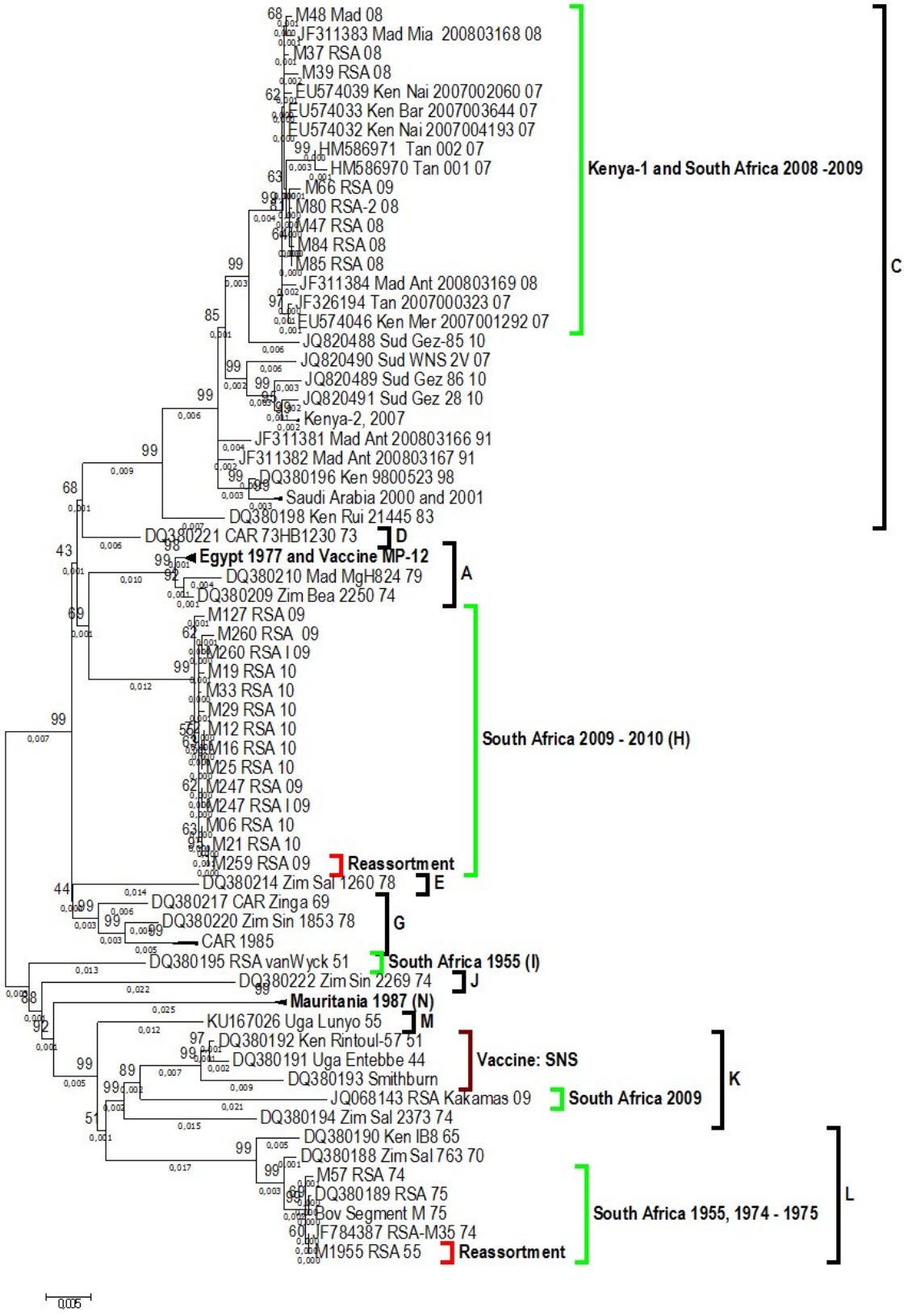

Figure 2.3B: Maximum likelihood tree of the M segment. The tree was generated using the maximum likelihood algorithm using MEGA 6. The designation of the clades follows Grobbelaar *et al*. (2011). The lineages containing RVFV isolates from South Africa are presented in green. The two specific reassortants are indicated in red.

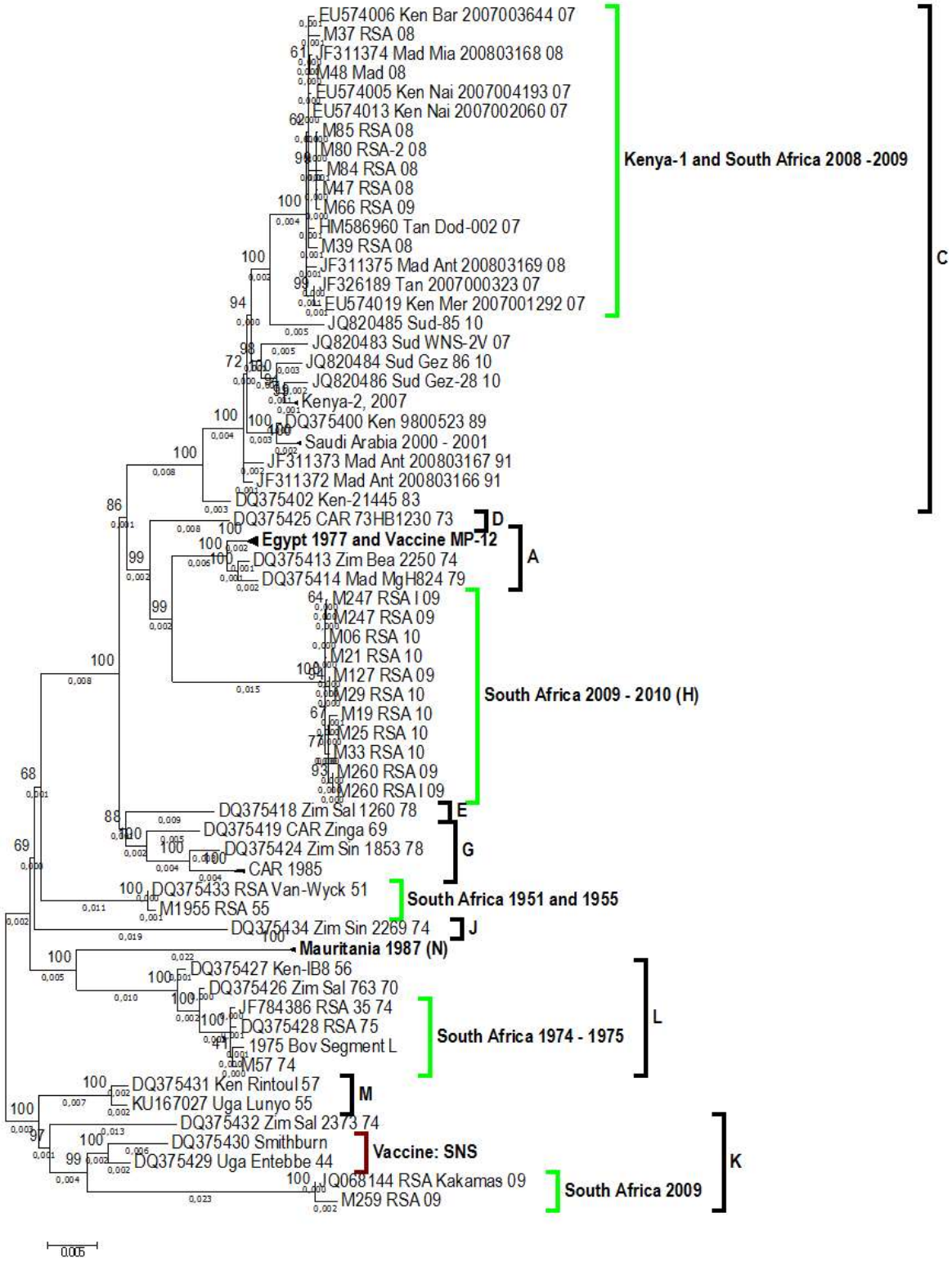

Figure 2.3C: Maximum likelihood tree of the L segment. The tree was generated using the maximum likelihood algorithm using MEGA 6. The designation of the clades follows Grobbelaar *et al*. (2011). The lineages containing RVFV isolates from South Africa are presented in green.

The predicted amino acid residues of the open reading frames of the M segment are well conserved with less than 3% sequence identity differences. Of the amino acid changes 55% are conservative changes, 9.8% will result in the loss of a charge, 17% will gain a charge (+) and 2.7% will change the charge (-).

The positions of amino acid substitution relative to the proportion of sequences with that change are indicated in Figure 2.4. Substitutions resulting in a change of charge have been indicated in Figure 2.4. The majority of the substitutions occur at the C-terminal region of the glycoprotein Gn in a low proportion of the sequences usually in only one or two, while the substitutions that are prominent in the sequence populations are conservative. The exception is a change from D (Aspartic acid) to N (Asparagine) at the amino acid position 95; this change is prominent in the 2008 – 2009 isolates clustering in Lineage C. In order to predict the impact of the amino acid changes on the antigenic properties of the virus, antigenicity predictions were performed using Welling with a window size of 11. Antigenicity plots for isolates M33_RSA_10, M37_RSA_08 and T1 ZH-501 isolated in Egypt in 1977 are presented in Figure 2.4. These isolates represent Lineage H, C and A, respectively. The major differences in antigenicity predictions between isolate ZH501-77 and the South African isolates are at positions 60 and 631 (Figure 2.4). Isolate ZH501-77 has a valine at both these positions in contrast to the isoleucine of the South African isolates.

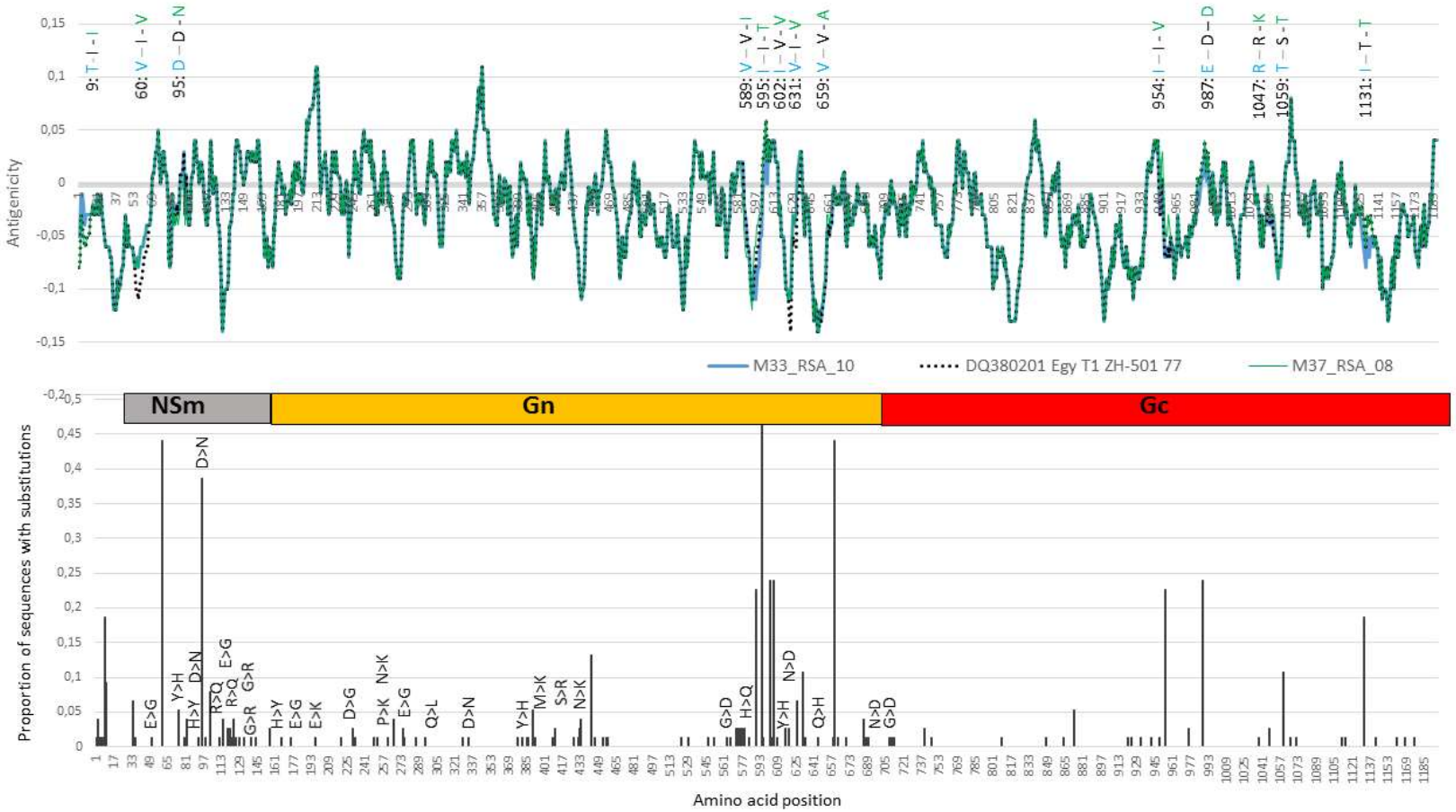

Figure 2.4: Welling antigenicity plots of Segment M for the isolates M33_RSA_10 in blue, ZH501-Egy-77 in black and M37_RSA_08 in green. Differences in amino acids between these three samples are indicated on top of the antigenicity plots with each isolate represented in its assigned colour. A graphical representation of the non-structural protein (NSm) and glycoproteins (Gn) and (Gc) regions separate the antigenicity plots from the graph depicting the proportion of substitutions per amino acid position. These proportions are representative of the 23 sequences generated during this study as well as the previously published data indicated in Table 2.3.

2.4 DISCUSSION

South Africa experienced three major outbreaks of RVF, the first in 1950-1951, the second and largest in 1974-1976 and in a period spanning 2008-2011. In this study, selected viruses from this last outbreak were sequenced and compared to sequence data obtained from GenBank.

In 2008 a total of 15 outbreaks were reported, these were all localized to a small region in Gauteng, Limpopo, North West and Mpumalanga provinces (Pienaar and Thompson, 2013). Sequence analysis of all three segments from representative isolates of the 2008 (n=7) outbreaks cluster in Lineage C among isolates from the 2007 outbreak in Kenya, known as Lineage Kenya-1 (Bird *et al*., 2007). In contrast to the localized outbreak of 2008 in Gauteng Province (Figure 2.1), 19 outbreaks were reported in 2009. One was in Mpumalanga, one in Gauteng, while the rest were either in KwaZulu-Natal and the Eastern Cape provinces or along the Orange River in the Northern Cape Province (Pienaar and Thompson, 2013). Similarly, to the isolates from 2008, the 2009 isolates (n=5) from Gauteng clustered in Lineage C within Lineage Kenya-1. This 2009 Gauteng outbreak appears to be a continuum from the 2008 RVF outbreak viruses prevalent in that region.

Isolates from outbreaks of 2009 from both the geographically distinct KwaZulu-Natal and Northern Cape provinces clustered in the same lineage, Lineage H. This includes a Segment M reassortment of sample M259_RSA_09, where both Segment L and Segment S cluster with another 2009 isolate from Kakamas in Lineage K. It is therefore possible that the majority of outbreaks occurring in 2009 in the two regions, originated from a single source.

In 2010 a total of 484 outbreaks were reported in all provinces of South Africa except KwaZulu-Natal. The initial report came from two towns, Bultfontein and Brandfort in the Free State Province and subsequently spread to the rest of the country (Pienaar and Thompson, 2013). Similar to the 2009 outbreaks from KwaZulu-Natal and the Northern Cape provinces, all the 2010 isolates (n=8) clustered in Lineage H. The eight isolates from the 2010 outbreak analyzed in this study are not statistical representatives of the 14 342 cases reported in that year; but support speculations that the 2010 outbreak was a continuum from the 2009 outbreaks in KwaZulu-Natal and Northern Cape provinces (Grobbelaar *et al*., 2011).

This study contributed full genome sequence analysis of RVFV viruses, isolate M57_RSA_74 isolated during the 1974 outbreak and isolate M1955_RSA_55 isolated from one of the 28 outbreaks during 1955 (Pienaar and Thompson, 2013). The period between 1973 and 1976

marked the largest RVF epidemic with mortality rates of 95% reported (Swanepoel and Coetzer, 2004). Outbreaks were reported in every province of South Africa and the human cases were severe with the most deaths ever reported (Pienaar and Thompson, 2013). Lineage L contains an isolate 763 from Zimbabwe isolated in 1970 and isolate IB8 from Kenya isolated in 1956 along with the 1973-1976 South African isolates (n=4). The segment M reassortment of isolate M1955_RSA_55, indicated that multiple RVFV lineages co-circulate during outbreaks and that viruses could re-emerge decades later. Evidence of reassortment within the 2006-2007 Kenya outbreaks supports the conclusion of multiple virus lineages circulating during a single outbreak (Bird *et al*., 2008a).

The evolutionary dynamics of RVFV are characterized by slow substitutions rates under strong purifying or negative selection with the major genomic diversity resulting from reassortment. Bayesian coalescent estimations of RVF viral genomes indicated that segments evolve at a mean rate between 3.9 $x10^{-4}$ and 4.17 $x10^{-4}$ substitutions per site per year regardless of the molecular model used. This is in accordance with previous Bayesian estimations (Bird *et al*., 2008a; Grobbelaar *et al*., 2011). The lack of statistical support could be due to the low genetic diversity between the sequences (Prosada *et al*., 2002). Since recombination through reassortment has been described in the segmented RVFV genome, this was further described by Grobbelaar *et al*. (2011). Similarly, the estimated TMRCA supports previous estimations of between 1880 and 1890 (Bird *et al*., 2008b; Grobbelaar *et al*., 2011). Similar evolutionary dynamics have been described in other arboviruses such as bluetongue virus and epizootic haemorrhagic disease virus due to the enforced replication of the virus in both insect vector and mammalian hosts (Wilson *et al*., 2015). The majority of reassortment events described in RVFV involves the exchange of Segment M and this was also the case for the current study (Bird *et al*., 2008a; Grobbelaar *et al*., 2011).

Although RVFV is generally known to be antigenically homogenous, various strains of the virus exhibit differences in virulence, evident upon infection of the mammalian host. A few or some of these differences may be attributable to the individual or host population; others are inherent to the virus. Differences in cytopathic effect and lethality of RVFV isolates have been observed during the experimental infection of BHK cells (Moutailler *et al*., 2011), mice (Morrill *et al*., 2010), sheep (Faburay *et al*., 2016) and cattle (Wilson *et al*., 2016).

Significant differences in mammalian pathogenesis, especially associated with the severity of the disease in humans have been observed. The latter have increased since the 1977 outbreak in Egypt to devastating effects during the 2006 - 2008 outbreaks in East Africa

(Baba *et al*., 2016). A clear association between RVFV genotype and lethal phenotype has not been established, but various amino acid substitutions have been identified to contribute to this (Bird *et al*., 2007). The most prominent substitution in the glycoproteins are I595V, R605K, I631V, V659A located in Gn and S1059T within Gc (Bird *et al*., 2007). Another variation was identified in ZH501, isolate from a human in Egypt during an outbreak in 1977, resulted in the change of amino acid from glycine to glutamic acid at position 277. The virus with the glutamic acid was shown to be more virulent in mice, compared to the one with glycine in the same position (Morrill *et al*., 2010). The majority of RVFV analysed in this study had glutamine at position 277, with the exception of the wild type isolate 763/70 from a foetus aborted during an outbreak of the disease in Zimbabwe in 1970 (Bird *et al*., 2007). This study identified additional substitutions when compared to the lethal isolate ZH501-77 from Egypt and isolates belonging to Lineage H from 2010 in South Africa. The substitutions include V602I, D987E and T1131I. A previous study indicated that virus ZH501-77, is associated with increase virulence, lethal to rats and was therefore included in this analysis as comparison between isolates from Lineage H and C (Bird *et al*., 2007). The impact of each of these substitutions on the pathogenicity of RVFV should be investigated through reverse genetics.

In order to evaluate the efficiency and reliability of the sequence data generated by different NGS platforms, two isolates (M260/09 and M247/09) were subjected to both 454 sequencing from Roche as well as Miseq technology from Illumina. The data generated by both technology platforms were comparative and produced identical sequences. The dataset analyzed in this study might however not be representative of the RVFVs circulating during the outbreak. This is due to the viruses being isolated on cell culture prior to genome determination. The dataset might have a bias towards isolates favoured by the cell culture system. A different picture of viruses and their quasispecies might emerge if the analyses included viruses sequenced directly from clinical/positive cases. This is currently unattainable within this study.

Phylogenies done for the three genome segments of RVFV indicated the presence of five lineages in South Africa as assigned by Grobbelaar *et al*. (2011). This study indicated that the viruses from 1951 and 1955 (Lineage I) persisted in the field and may have contributed to the outbreaks of 1974 and 1975 (Lineage L). The viruses analyzed from the 2008 outbreak and one 2009 isolate from Gauteng, cluster within Lineage C. The latter predominantly contains isolates from Kenya, Tanzania as well as Madagascar during their 2007-2008 outbreaks. The 2009-2010 viruses from South Africa seem to have descended from an unknown ancestor, with their closest relative been a partial sequence obtained from a virus from Namibia in 2004 (Grobbelaar *et al*., 2011). Lineage H presents a clear indication that new strains could evolve due to nucleotide substitution, albeit the slow substitution rate. It is possible that these viruses

are not introduced from elsewhere, but rather mutate in time and caused outbreaks when suitable conditions prevailed.

The most notable isolate analyzed in this study is M259_RSA_09 originating from Upington in the Northern Cape Province. The RVF outbreak in the Orange River region of the Northern Cape Province appears to have been due primarily to irrigation used in vineyards and orchards, since this is a winter-rainfall area. Similar to isolate SA184/10, isolated from a person injected with Smithburn neurotropic strain (SNS) vaccine while vaccinating sheep, M259_RSA_09 clusters with Lineage H when analyzing Segment M, but in Lineage K when segments L and S are evaluated (Grobbelaar *et al.*, 2011). Its closest association in Lineage K is the virus Kakamas, isolated in 2009 from cattle in the Northern Cape Province. Lineage K contains the sequence for Smithburn (SNS) vaccine as well as isolates Entebbe isolated in Uganda in 1844, from which the SNS vaccine was derived (Swanepoel and Coetzer, 2004). Considering that isolate SA184/10 had a direct association with the SNS vaccine, the genetic distance between M259_RSA_09 and the SNS vaccine is significant to warrant a renewed attempt to determine the sequence of the current SNS vaccine commercially available.

CHAPTER 3: COMPARISON AND CHARACTERISATION OF SELECTED SOUTH AFRICAN ISOLATES OF RIFT VALLEY FEVER VIRUS

3.1 INTRODUCTION

Rift Valley fever, an emerging zoonotic disease, associated with heavy and prolonged rainfall is endemic to African countries (Anyamba *et al*., 2009; Davies, 2010). The outbreaks are associated with high rates of abortion and high mortality in young animals. In addition to the substantial socioeconomic effects caused by the outbreaks, human health is also at risk (Archer *et al*., 2013). Since the last reported large outbreak in South Africa in 1974 and 1976, another large outbreak occurred from 2008 to 2011.

Infected mosquitoes transmit the RVF virus which is classified in the genus *Phlebovirus* (Anyamba *et al.*, 2009). The virus has a tri-segmented, negative single stranded RNA genome. Viruses with RNA genomes adapt to changing environmental conditions due to lack of proofreading activity resulting in the possibility of high mutation rates as compared to viruses with DNA genome (Elena and Sanjuán, 2005). Mutations in any of the trinucleotide can result in amino acid change that may affect the function of the protein or in a stop codon resulting in a truncated protein. Mutations can arise from substitution, insertion, deletion or frameshift.

A single amino acid residue in a protein can be encoded by more than one codon called synonymous codons (Behura and Severson, 2013). The corresponding tRNAs of these codons may differ in their relative abundance in cells and even with the speed, which they are recognized by the ribosome (Butt *et al*., 2016). During the coding of a protein, the usage of the synonymous codons is unequal and this process is called synonymous codon usage bias (SCUB) or codon usage bias (CUB) (Baker *et al*., 2015; Song *et al*., 2017; Belalov and Lukashev, 2013). The codon usage patterns vary within and among genomes (Behura and Severson, 2013).

While RVFV shows low genetic diversity (Bird *et al*., 2007; Grobbelaar *et al*., 2011), phenotypic differences between isolates has been observed including cytopathic effect, host specificity and cell culture phenotypes (Moussa *et al*., 1982; Morrill *et al*., 2010; Moutailler *et al*., 2011; Wilson *et al*., 2016). These phenotypic differences must be related to biological processes such as receptor recognition during invasion, replication and assembly of the viral capsid or final budding from infected cells. These phenotypic differences may also have a genetic origin

allowing potential discovery of the causal factors by comparative genomics. To allow for thorough analysis, a detailed knowledge of the proteins encoded by the viral genome is necessary.

The RNA polymerase encoded by the L segment is a polypeptide of 2087 amino acids and possesses three defined domains as classified by the Conserved Domain Database (Marchler- Bauer *et al*., 2015). The N-terminal domain (52-248) is an endonuclease (L-Protein N pfam15518) found in several of Bunyavirus polymerases. The endonuclease functions in mRNA transcription, by cleaving the 5' end capped host mRNA and transferring these capped oligonucleotides of 12-18 nucleotides to the mRNA, a process called cap-snatching (Reguera *et al*., 2010; Amroun *et al.,* 2017; Holm *et al*., 2018). The nuclease activity is a divalent metal ion-dependent and several residues (identified in the La Crosse orthobunyavirus) are important in the active site functioning to sequester the metal ion; notably His34, Asp52, Asp79, Asp92 and Lys108 (Reguera *et al*., 2010). These residues are also conserved in the RVFV endonuclease. This is followed by a domain of unknown function (DUF3770, pfam 12603) (249-420) that is associated with the polymerase domain (Bunya RdRp, pfam04196) from 604-1299. The polymerase RdRp domain has a right hand-like structure with finger, palm and thumb subdomains. It is responsible for both transcription and replication (Amroun *et al*., 2017). The C-terminal region from 1299-2087 has not yet been classified.

The M segment encodes the non-structural protein NSm and the envelope glycoproteins Gn and Gc. The NSm has an apoptotic function (Won *et al.,* 2007) and several potential binding partners including cleavage and polyadenylation specificity factor subunit 2 (Cpsf2), the peptidyl-prolyl cis-trans isomerase (cyclophilin) like 2 protein (Ppil2) and the synaptosome-associated protein of 25 kDa (SNAP-25) which have been identified using a yeast two-hybrid system (Engdahl *et al*., 2012). The NSm and the 78 kDa proteins are dispensable for virus maturation, replication and infection in cell culture (Won *et al*., 2006; Gerrard and Nichol, 2007). However, a virus that lacked NSm was attenuated in mice with reduced titres in murine macrophages (Kreher *et al.,* 2014). The 78 kDa protein did not have an effect on viral infection in mice but was important for propagation in mosquitoes (Kreher *et al.,* 2014). The Gn and Gc form heterodimers in the viral envelope (Huiskonen *et al*., 2009), with surface protrusions called "spikes" that are important for cell tropism and virus entry into mammalian host cells (Amroun *et al.,* 2017) (Figure 3.1A). The Gn forms a larger part of the protruding capsomer, while Gc forms the capsomer base (Rusu *et al*., 2012) (Figure 3.1B). The Gn interacts with cell surface receptors allowing viral uptake into the cell, while shielding Gc to prevent premature fusion (Halldorsson *et al*., 2016). After attachment, Gc facilitates membrane fusion and release of genomic contents from the endosomal compartments into the cytoplasm (Spiegel *et al.,* 2016). The Gn and Gc are also important for packaging of the viral genome by

interaction via the intracellular regions and directly with the ribonucleoprotein (Huiskonen *et al*., 2009). The Gn possesses a C-terminal region followed by a type 1 transmembrane region, a stem region and a head region (Wu *et al.,* 2017; Halldorsson *et al.,* 2016). The head region is composed of three domains, an N-terminal α-helical domain A, a small globular B domain and a C-terminal B-ribbon domain (Wu *et al.,* 2017; Halldorsson *et al.,* 2016). The C-terminal B-ribbon domain dimerizes with the Gc protein to form heterodimers (Halldorsson *et al*., 2016). In Gn, a single nucleotide difference that results in a substitution of E276G resulted in attenuation of a highly virulent strain to one that showed low viremia titers, did not replicate efficiently, and had low virulence (Morrill *et al.,* 2010). The Gn and Gc glycoproteins form higher order pentamers and hexamers ring-shaped assemblies (Amroun *et al*., 2017). Glutamic acid 276 is in the N-terminal domain at the top of the Gn ring with the side chain projecting towards the centre of the ring (Figure 3.1C and 3.1D). It probably interacts with the host receptor by binding to specific residues forming ionic bonds indicating the important role that receptor recognition may have on virulence, viremia and rate of replication.

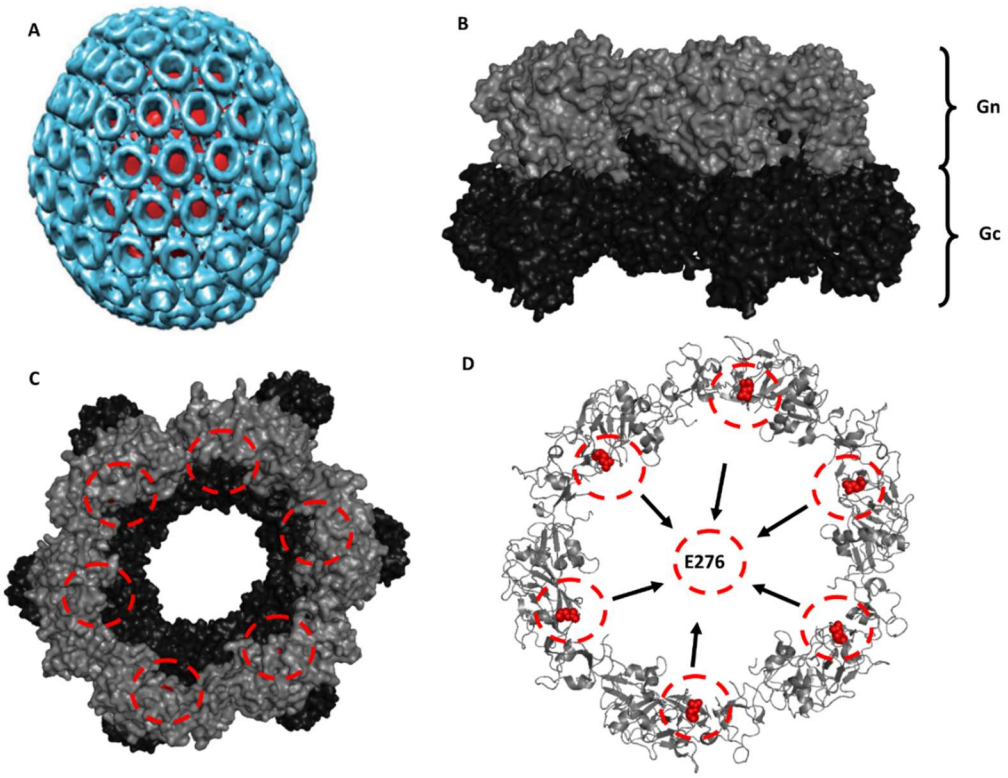

Figure 3.1: The structures of the envelope glycoproteins Gn and Gc. A) A reconstruction of RVFV at pH 7.4 (Amroun *et al.,* 2017). The blue rings represent individual capsomers formed by the 6 Gn/Gc heterodimers. B) The Gn/Gc capsomer viewed from the side. C) The Gn/Gc capsomer viewed from above. Red circles indicate the position of E276 in Gn. D) A ribbon representation of Gn in the capsomer. Indicated are E276 as a spacefilled residue.

The Gc protein is important for fusion to the endosomal membrane and release of viral content into the cytoplasm. At alkaline pH, Gn interaction with Gc shields hydrophobic loops located on Gc, which once inside the acidic endosomal compartment is exposed and inserts into the membrane (Halldorsson *et al.,* 2016). The Gc protein possesses a class II fusion protein architecture composed of three domains (Dessau and Modis, 2013). The N-terminal domain I and the C-terminal domain III forms the base of the capsomer, while the central domain II possesses the fusion loop from 818-832 residues with the important hydrophobic residues being W821, F826 and V828 as well as L779 (Dessau and Modis, 2013; Halldorsson *et al.,* 2016).

The ambisense S segment encodes the nucleocapsid protein N and the non-structural protein NSs with their open reading frames (ORF) at opposite ends. The nucleocapsid protein is responsible for formation of viral ribonucleoprotein (RNP) complexes, which is important for viral packaging, replication and transcription (Ferron *et al.,* 2011; Raymond *et al.,* 2012). The

NSs protein is a major virulence factor that hijacks the host cell and shut down defense mechanisms. It activates the cullin 1Skp1-Fbox E3 ligase complex to degrade the p62 of the transcription factor IIH complex and RNA-dependent protein kinase R proteins and facilitate ubiquitin transfer (Terasaki *et al.,* 2016). The C-terminal possesses a motif that resembles the ΩXaV motif found in nucleotide excision repair (NER) factors and transcription factors known to interact with p62 (Cyr *et al.,* 2015). It also affects cohesion and segregation of chromatin DNA and activation of the interferon-ß promoter. NSs also induces DNA damage, causes cell cycle arrest, activates p53 resulting in apoptosis (Ly and Ikegami, 2016).

The study aims to characterize and compare the six wild-type isolates of RVFV isolated from livers of bovine and ovine in South Africa from 2008 to 2010 based on their sequence alignment (both nucleotide and amino acid), cytopathic effect on mammalian cells, protein structures, and codon usage bias. The results will help in understanding the behaviour of isolates from different species. Resulting information on the codon usage bias patterns can provide significant insight on molecular evolution of genes and reveal host-pathogen coevolution and adaptation of pathogens to specific hosts (Wang *et al*., 2017; Behura and Severson, 2013; Belalov and Lukashev, 2013).

3.2 MATERIALS AND METHODS

3.2.1 Determination of viral concentration

Vero cells were seeded in 12-well plates at a density of 0.2 x 10^5 cells/well and incubated overnight at 37°C with 5% CO_2. For infection, the virus was serially diluted using 10-fold dilution in DMEM F/12 media supplemented with 2% FBS and 1% mixture of penicillin (10 000 U/ml), streptomycin (10 000 U/ml) and amphotericin B (25 µg/ml). A volume of 250 µl of each dilution was added to each well containing the Vero cell monolayer. Plates were incubated at 37°C on a rocker for 1 hour to allow virus to attach to cells. At the end of incubation, 1 ml of primary overlay [1% agarose (Merck) plus 10% DMEM F/12)] was added to each well and the plates returned to the incubator for 3 days. On the fourth day, a secondary overlay (primary overlay plus 1% neutral red) was added to the wells and plates returned to the incubator. After 24 hours, plaques were counted and viral titers were calculated. Viral titers were expressed as plaque forming units per millilitres (PFU/ml), calculated as number of plaques per well/ (dilution X inoculum).

3.2.2 Confirmation of the viral particle

Baby hamster kidney (BHK) cells infected with virus (M66/09) were harvested after 72 hours and virus was concentrated using sucrose density centrifugation. After ultra-centrifugation for 1 hour at 21 000 rpm in a Sorval Super T21 centrifuge, the viral pellet was suspended with 100 µl cold PBS and split into two tubes of equal volume. The first tube was prepared for quality purpose using transmission electron microscope (TEM). A drop of purified virus was mixed with a drop of stain in a ceramic plate well and formvar carbon coated grid floated on top of the mixture for 30 seconds. Excess fluid was blotted with paper towel. Samples were examined in a Philips CM10 (TEM) at 80 kV using negative staining with 3% phosphotungstic acid (PTA) (Sigma-Aldrich). A negative control sample containing uninfected cells was also included. The second tube was used to infect BHK cells for isolation of viral RNA to confirm the presence of viral particles. Viral RNA was isolated from the second tube using the modified method of Drosten *et al.* (2002) and RNA was then used in a reverse transcriptase PCR. The PCR primers used were RVF1-F (5' – TGT CAC ACT GCT CTC AGT GCC – 3') and RVF2-R (5' - GGA GCT TGC CTG AAT CTG TTG – 3'). The PCR conditions were as follows: 37°C for 30 minutes, 94°C for 2 minutes, followed by 35 cycles at 94°C for 30 seconds, 65°C for 30 seconds and 72°C for 30 seconds. The final extension was done at 72°C for 7 minutes.

3.2.3 Attachment of virus to host cells using electron microscopy (cell embedding)

The rate at which RVFV attaches and enters cells was investigated using TEM. The BHK cells were grown in three T75 flasks using DMEM/F12 (Gibco, Life Technology) supplemented with 5% FBS (Gibco, Life Technology) and 1% mixture of penicillin (10 000 U/ml), streptomycin (10 000 U/ml) and amphotericin B (25 µg/ml) (LONZA, BioWhitaker) as described in section 3.2.1. The cells were grown for 48 hours at 37°C, 5% CO_2 in a humidified incubator. An hour before fixation, the media was removed from the flasks. Monolayers were washed once with serum-free media and returned to the incubator. After 1 hour, media was discarded and cells were infected with the virus at a multiplicity of infection (MOI) of 0.1. After 8, 16, and 24 minute intervals, the virus suspension was removed and monolayers were washed three times with pre-warmed phosphate buffered saline solution (PBS). After the final wash, the fixation solution consisting of equal volumes of pre-warmed PBS and glutaraldehyde (GA) [2.5% GA in 0.2 M sodium cacodylate buffer pH 7.35 (Sigma-Aldrich)] was added to the infected cells and agitated gently on a rocker platform at room temperature. After 30 minutes, the solution was removed, replaced with second fixation solution (PBS and 2.5% GA) and flasks were

returned to the rocker for 90 minutes. The fixation solution was removed and replaced with 10 ml of 0.2 M Na-cacodylate buffer (pH=7.35), cells were harvested by scraping the flask with a cell scraper, transferred to a 15 ml tube and centrifuged at 1 000 rpm in an Eppendorf Centrifuge 5810R for 15 minutes. The cells were post-fixed with 1% osmium tetroxide (Sigma-Aldrich) in 100 mM phosphate buffer for 1-2 hours at 4°C. Cells were dehydrated through an ascending ethanol series: 50, 70, 90, 95 and 3 x 100% ethanol for 10 minutes each. This step was followed by resin infiltration with an intermediate transition step of 50:50, 100% ethanol: acetate or propylene oxide and a final rinse of either 100% acetone or propylene oxide. Cells were embedded into agar silicone moulds (Agar Scientific, UK) and filled with fresh resin. Moulds were placed in an oven at 60°C for 36 hours prior to sectioning with ultramicrotome to obtain thin sections (0.6 µm). The ultra-thin sections were stained with saturated uranyl acetate (Sigma-Aldrich) solution and examined using a JEOL 1400-Plus transmission electron microscope, operated at 80 kV.

3.2.4 Viral growth curves

To compare the growth rate of the isolates in cell culture, six isolates of RVFV (from South Africa) that were analysed in the previous chapter were selected (Chapter 2, Table 2.1). Isolates from the same tissue but different hosts were selected to include three from the liver of bovine and three from the liver of a sheep/ovine (Table 3.1). BHK cells grown in 12-well plates were infected with virus isolates using an MOI of 0.1. Samples were collected at time intervals (0 minutes, 30 minutes, 6 hours, 24 hours, 48 hours and 72 hours post infection). A standard plaque assay was performed on Vero cells (Section 3.2.1) to calculate viral titers. Experiments were done in duplicate.

Table 3.1. Virus isolates used in the study

Virus ID	Passage number	Year isolated	Organ	Species	Town/Province of origin
M66/09	3BHK/1Vero	2009	Liver	Bovine	Modderfontein (GP)
M127/09	1Vero/3BHK	2009	Liver	Bovine	Cascade (KZN)
M260/09	2Vero/3BHK	2009	Liver	Bovine	Upington (NC)
M21/10	4BHK	2010	Liver	Ovine	Bloemfontein (FS)
M33/10	4BHK	2010	Liver	Ovine	Middelburg (EC)
M247/09	1Vero/3BHK	2009	Liver	Ovine	Upington (NC)

(These isolates were discussed in more detail in Chapter 1)

3.2.5 Immunofluorescence assay

To visualise cells infected with RVFV isolates from the same tissue but from different species, an immunofluorescence assay was performed. BHK cells were grown in plates on coverslips until they were 70-90% confluent. Cell monolayers were infected with RVFV isolates at an MOI of 0.1. Plates were incubated at 37°C and coverslips removed from the plates at different time intervals (10 minutes, 30 minutes, 1 hour, 24 hours and 48 hours) post infection. Immediately after collection, cells were fixed with 150 µl of 3% formaldehyde for 30 minutes at room temperature. At the end of the incubation, formaldehyde was removed, followed by three washes with PBS at intervals of 5 minutes. Coverslips were dried and kept at 4°C until used. Primary antibody used was RVFV positive serum collected from sheep infected with RVFV (kind donation from Dr David Wallace, ARC-OVR). The primary antibody was diluted with 2% skim milk (in PBS), added to coverslips and incubated for 30 minutes at room temperature in the dark. This was followed by three washes with PBS and one wash with water. The secondary antibody anti-sheep IgG (whole molecule)-FITC antibody produced in rabbit was mixed with Evans Blue (1%) in a ratio 1:1. The mixture was further diluted to 1:100 with 2% milk before adding to the coverslips. Incubation with secondary conjugate was done for 30 minutes at room temperature. At the end of the incubation, coverslips were washed twice with PBS and once with water. Coverslips were air-dried and mounted upside-down (using 0.16 M sodium carbonate buffer and glycerol) on microscopic slides. Immunofluorescence confocal microscopy images were captured using Zeiss LSM 880 microscope. Coverslips with cells that were not infected with virus were included as negative controls.

3.2.6 Nucleotides and amino acid sequence alignment

The nucleotide and amino acid sequences of all the three segments of the six isolates and sequences of the segments of the strain ZH501 were aligned using CLC Genomics Workbench Version 7.5.1. The alignment parameters used were as follows: gap open cost = 10, gap extension cost = 1.0, end gap cost = as any other and the alignment mode was very accurate (slow). The nucleotide sequence accession numbers of the different samples have been discussed in the previous chapter (Section 2.3 and Table 2.1).

3.2.7 Protein structure prediction

For the protein structures, the model structures of the glycoproteins (Gn and Gc) from the M segments of the six isolates were predicted. The 3-D models of RVFV Gn and Gc were generated from their sequences by using the Protein Homology/analogy Recognition Engine V 2.0 (Phyre2) server (Kelly *et al*., 2015). Phyre2 uses the normal and intensive modes to predict the 3-D structure of a single submitted protein sequence. Phyre2 also predicts the secondary structure and convert it to a hidden Markov model (HMM). The HMM was scanned using HMM-HMM matching against pre-compiled database of HMMs of known structures. This resulted, in the alignment of query sequence and possible templates starting with the name of the top scoring model. In order to analyse the final structures, we used the PyMOL Molecular graphics system (DeLano, 2002). The PyMol server was also used to superimpose the modelled protein structures. The TOPCONS web server (http://topcons.net) was used to predict the topology of the proteins Gn and Gc and their in and out orientation relative to the membrane (Tsirigos *et al*., 2015). An additional server http://octopus.cbr.su.se was also used to predict the transmembrane in Gn and Gc proteins (Viklund and Elofsson; 2008).

3.2.8 Determination of codon usage bias

To analyse the extent of codon usage bias in RVFV Gn and Gc genes, the following codon usage parameters were investigated:

ENC: Effective number of codons. This value normally ranges from 20 (implying that only one codon is used for each kind of amino acid) to 61 (when all available codons are used equally, with no signifying bias) (Wright, 1990).

CAI: Codon Adaptation Index. This value is often used as a measure of level of gene expression. The codon usage analysis was performed using the E-CAI server available at http://genomics.urv.es/CAIcal/E-CAI (Puigbó *et al*., 2008).

RSCU: Relative synonymous codon usage. This value is the observed frequency of codon usage divided by the sum of codons per amino acid and multiplied by the actual number of codons per amino acid (Shi *et al*., 2012, Behura and Severson, 2013). To determine the influence of the host on codon usage patterns for RVFV isolates, the relative synonymous patterns of the RVFV coding sequences and those of hamsters, bovine and ovine (www.kazusa.or.jp/codon) were compared.

3.3 RESULTS

3.3.1 Selection of strains for further characterization

Six isolates were selected from those previously sequenced and described in Chapter 2. Three isolates from bovine liver (M66/09, M127/09 and M260/09) and three isolates from ovine liver (M33/10, M21/10 and M247/09) were selected. The isolate M66/09 was from Clade C, while the other isolates all clustered in Clade H (Chapter 2). The isolates used in this study are indicated with green dots in Figure 3.2. The isolates from livers were chosen because in the infected animal, the organ that is mostly affected is the liver.

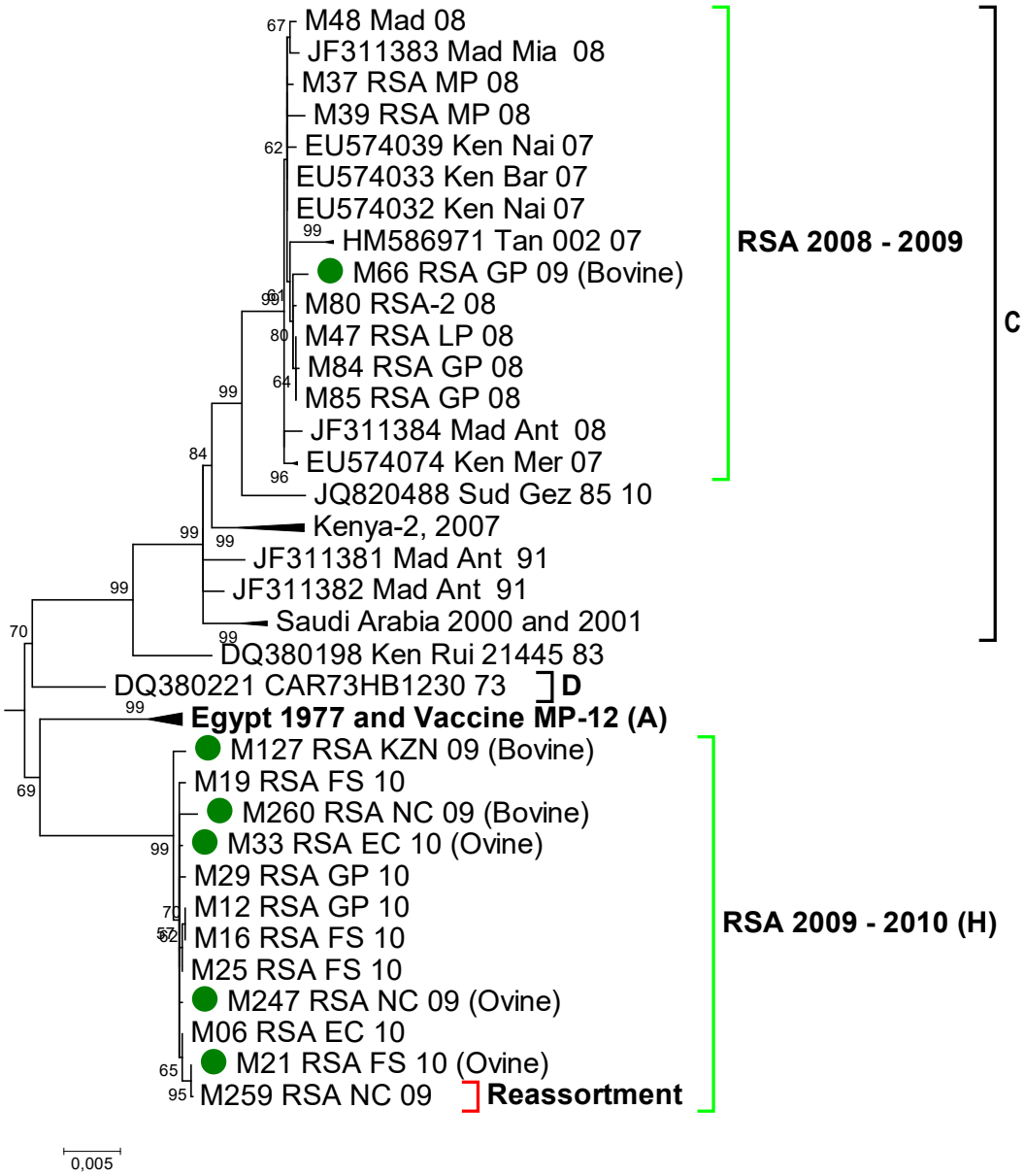

Figure 3.2: Maximum likelihood tree of the M segment (subset of Figure 2.3B). The six isolates used in this study are indicated with green circle and their origins are indicated in brackets next to their names.

3.3.2 Baby hamster kidney cells infected with RVFV

The morphological changes caused by RVFV on BHK cells are shown in Figure 3.3. The CPE in all the isolates used were 90-100% after 3 days of infection with RVFV (Figure 3.3). Results from one isolate (M66/09) are shown in Figure 3.3.

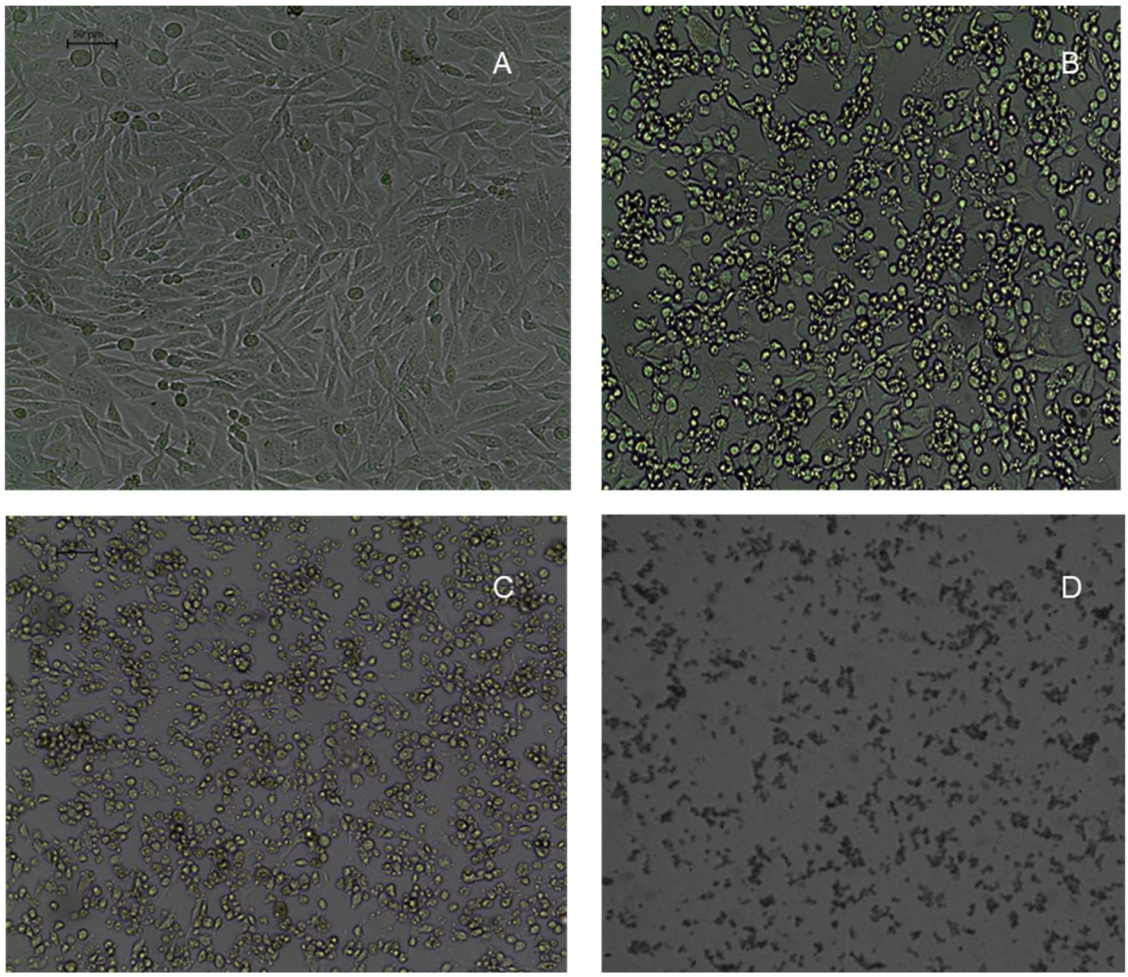

Figure 3.3: Cellular morphology of BHK cells examined using light microscopy: A: Uninfected cells. B: BHK cells 24 hours of post infection with RVFV. C: BHK cells 48 hours post infection with RVFV. D: BHK cells 72 hours of post infection with RVFV. Bar = 50µm

3.3.3 Confirmation of RVFV particle using TEM and PCR

In order to confirm the morphology of RVFV particle, TEM was used to visualize the virus in solution using isolate (M66/09). The TEM images showed different shapes of the viral particles; spherical, roughly and pleomorphic (Figure 3.4A-D). The diameter of the particles measured ranged from 70 nm to 90 nm (Figure 3.4A). No distortion or broken particles were observed. The morphology and size of viral particles observed were similar to previously reports for wild-type RVFV (Freidberg *et al*., 2008; Gerrard and Nichol, 2007; Martin *et al*., 1985).

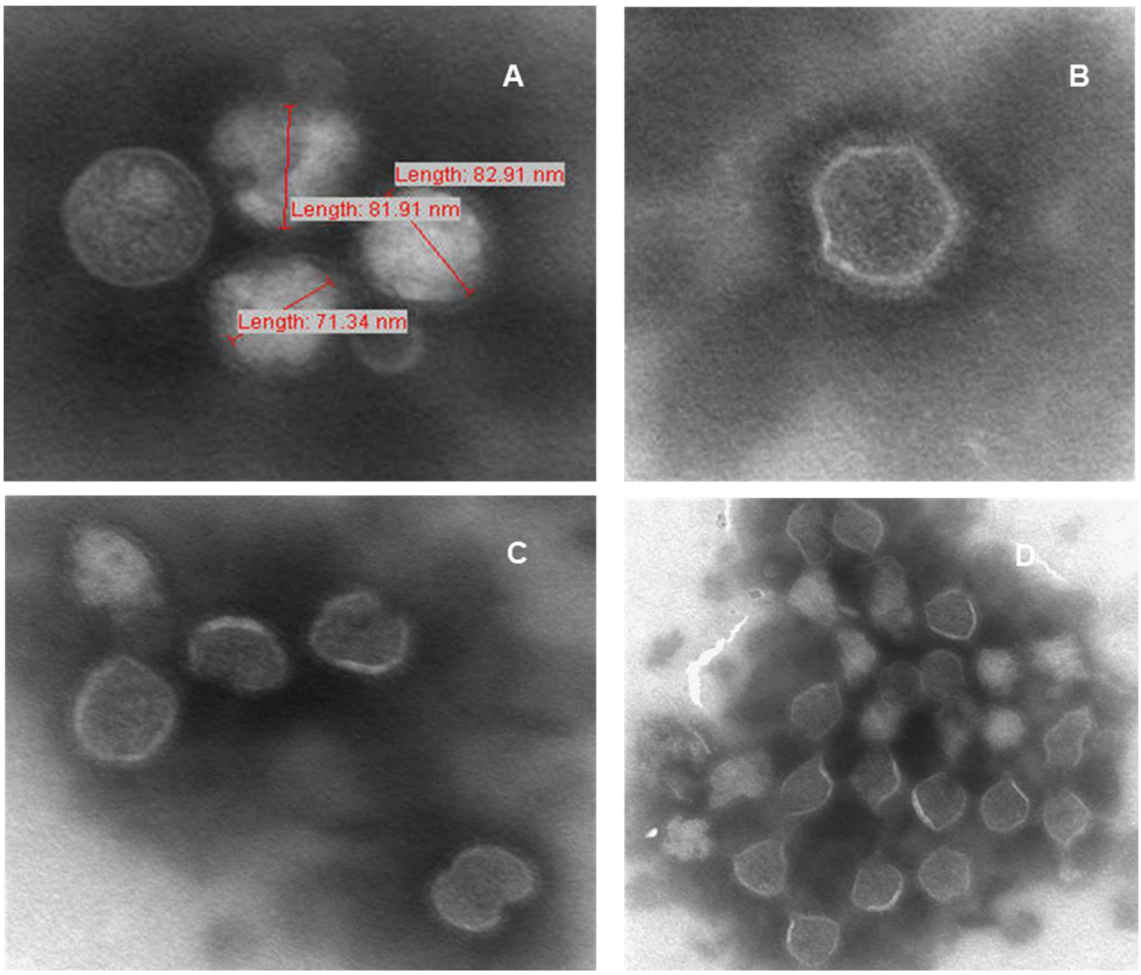

Figure 3.4: Morphology of RVFV particles revealed by negative stain transmission electron microscopy. A) Measured diameter of the viral particles ranging from 71.34 to 82.91 nm. B) The roughly spherical shape viral particle is shown. C) Pleomorphic viral particles are shown. D) Different morphologies of viral particles are shown.

PCR results confirmed that the viral particles were RVFV by amplification of a small portion of the M segment (330 bp) (data not shown).

3.3.4 Attachment of M66/09 isolate on BHK cells

The rate at which virus isolates attached to cells was determined using TEM to examine infection at specific time points (0, 8, 16 and 24). An uninfected BHK cell with nucleus is shown in Figure 3.5A. At 8 minutes post infection, the virus was already inside the cell. After 16 minutes of infection, viral particles were seen inside the cell. Longer incubation of the infected cells resulted in more viral particles infecting the cell (Figure 3.5B-D).

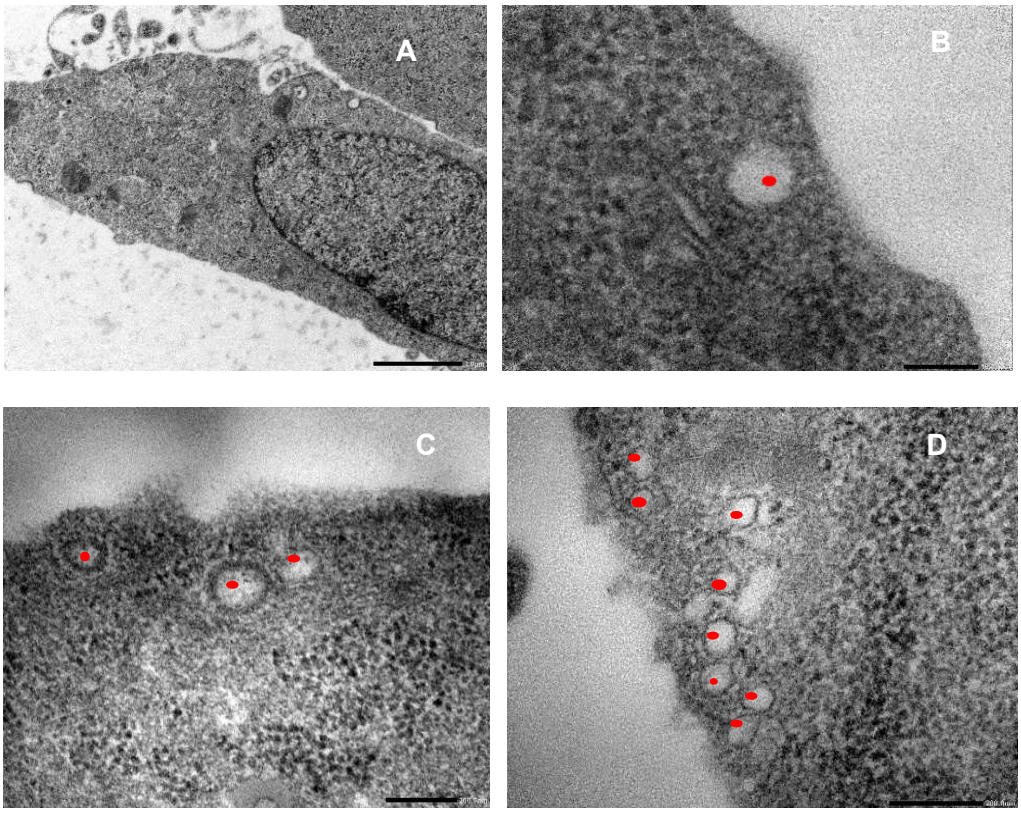

Figure 3.5: Electron micrographs showing BHK cells in the course of infection with RVFV at different time intervals (MOI of 0.1 in panels B, C and D). Electron micrograph A shows a section of an uninfected cell. Electron micrograph B shows a section of a cell infected with RVFV after 8 minutes. Electron micrograph C shows a section of a cell infected with RVFV after 16 minutes of incubation with the virus. Electron micrograph D shows a section of a cell infected with RVFV after 24 minutes of incubation with the virus. Each dot represents a viral particle. Bar in A = 1.0 µm while bars in B, C and D = 200.0nm.

3.3.5 Viral growth curves

The growth curves of RVF viruses isolated from different hosts were determined using cell culture. There were differences between the kinetic growth curves of isolates from bovine livers compared to isolates from ovine livers. Isolate M66/09 (from bovine) had the highest growth rate after 42 hours compared to the other bovine isolates followed by M127/09. The growth curve of isolate M260/09 showed some increase after 24 hours but rising slower than that of M66/09. Even after 42 hours, the growth rate increased very slow as compared to the others (Figure 3.6A). Kinetic growth curves of isolates from ovine livers are indicated in Figure 3.6B. Growth curves of the two isolates M21/10 and M247/09 seem to be rising at the same rate slower than the growth curve of isolate M33/10. At 72 hours the growth curves of the three isolates seemed to be the same. The titre of both M66/09 and M127/09 was ~10^7 PFU/ml, while those for the other isolates were less than 10^7 PFU/ml. Previous reports indicate that

10^7 PFU/ml may be considered to be normal for RVFV isolates, suggesting those isolates with lower PFU/ml may adapt more slowly to BHK cells, or may have deleterious substitutions in their genomes (Morrill *et al.,* 2010; Terasaki *et al.,* 2016).

A

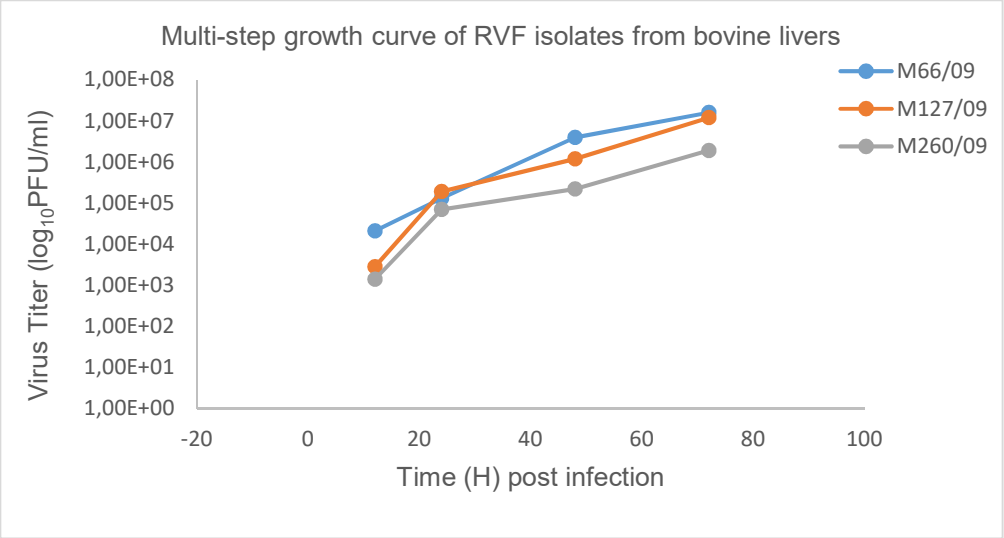

B

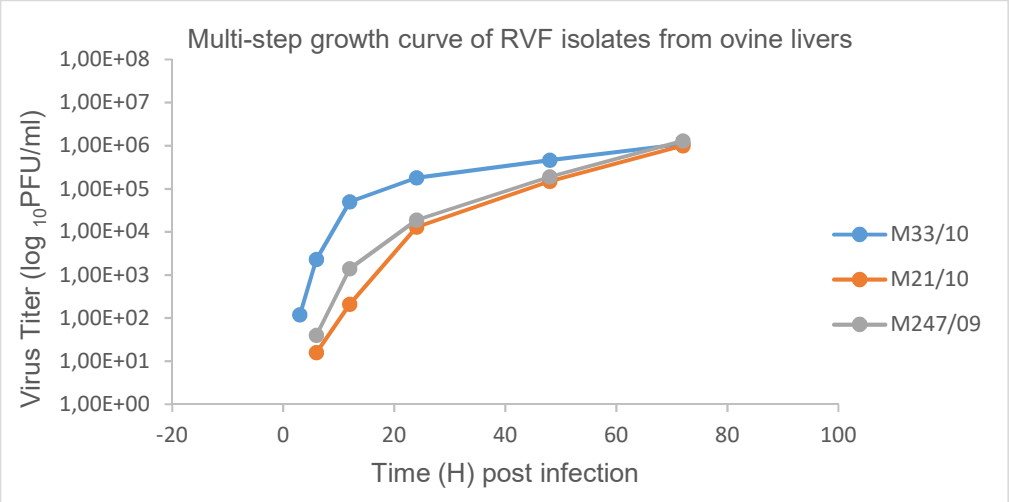

Figure 3.6: Multi-step growth curves of selected RVFV isolates. A: Growth curves of RVFV isolates from bovine livers. B: Growth curves of isolates from ovine livers. Cells were infected with RVFV isolates at MOI of 0.1 and samples collected at different time intervals. Infectious viral particles were determined using a plaque assay. Mean values are indicated by points.

3.3.6 Status of infection as visualized by immunofluorescence

The status of BHK cells infected with different isolates from different species was visualized by using an immunofluorescence assay. No fluorescence resembling any viral particle was seen in the negative control/mock-infected cells (Figure 3.7). Green fluorescence foci corresponding to viral particles were clearly visible by the confocal microscopy after 10 minutes of infection in the cells infected with some of the isolates. More viral particles were seen in cells infected with isolates M66/09, M127/09, M260/09 and M247/09. After 24 hours post infection, more viral particles were observed in cells infected with isolates M66/09, M127/09 and M260/09. At 48 hours post infection with these isolates, the majority of the cells were destroyed (Figure 3.7). An interesting point is that all these isolates were from bovine livers. Cells infected with M33/10 were also destroyed after this time, but to a lesser extent. Cells infected with the isolates M21/10, M247/09 were still visible, and their morphology still intact at 48 hours post infection. Samples collected at 72 hours post infection, did not show any cells, therefore no images are presented.

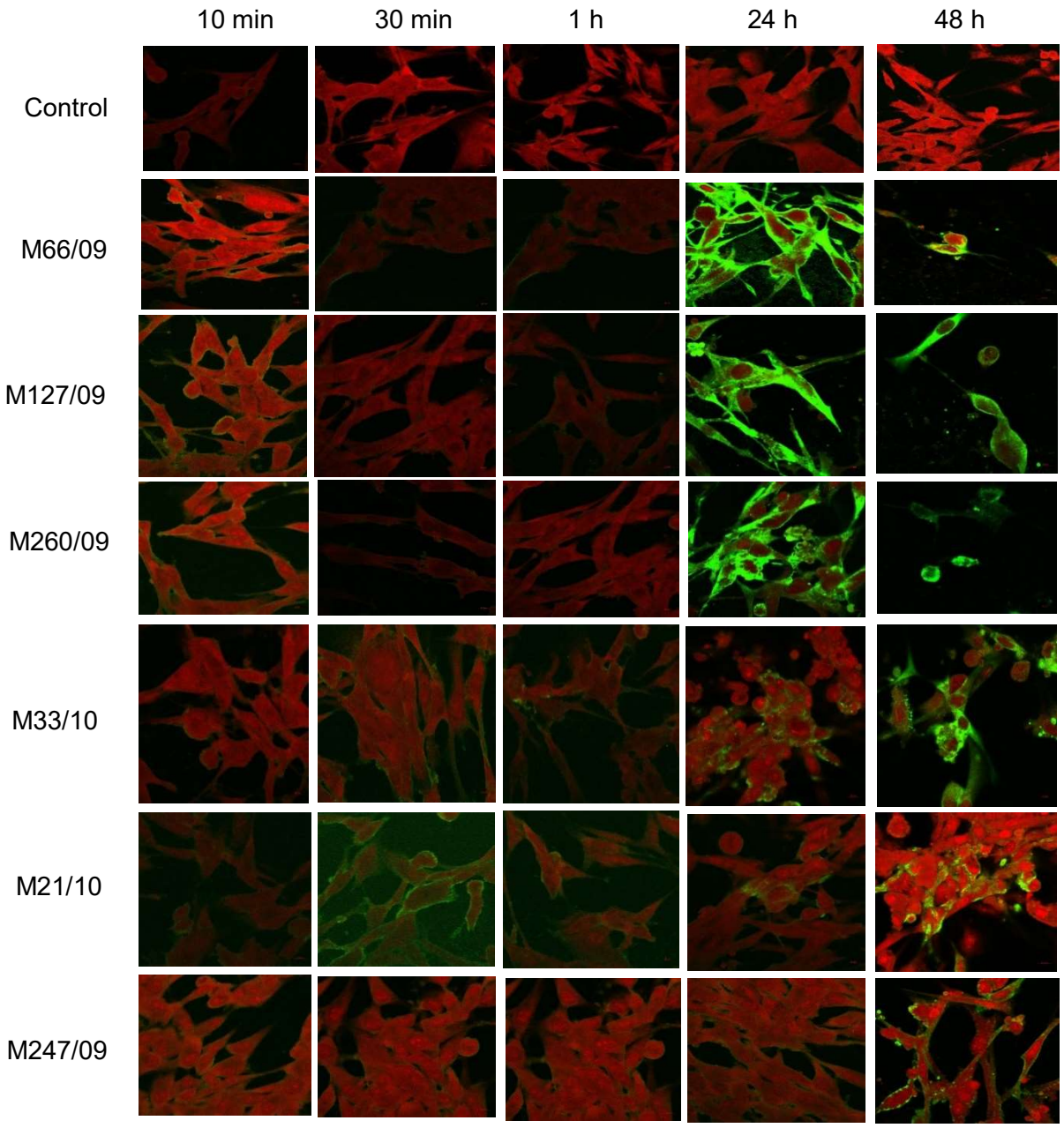

Figure 3.7: Immunofluorescence of BHK cells infected with RVFV at MOI of 0.1 and mock (uninfected cells) for the indicated time post infection. Images were taken using a Zeiss LSM 880 microscope, at a magnification of 40X.

3.3.7 Amino acid sequence alignment

The genome nucleotide and amino acid sequences of the six isolates (M66/09, M127/09, M260/09, M33/10, M21/10 and M247/09) were aligned based on their nucleotide and amino acid sequences (presented in Chapter 2). No sequence gaps in either nucleotide or amino acid sequences were identified. The Egyptian strain ZH501 was used as the reference strain

for comparing the amino acid sequences. The six isolates had many amino acid substitutions in both the L and M segments as compared to the reference strain (Table 3.2). The L segment of the six field isolates had 14 amino acid substitutions that differ from the reference strain (i.e. F23Y, V59I, M120T, E177D, S270N, N277D, N278S, D305A, V349I, A663T, G1123S, V1760I, H1852Y and R1922K). In addition to these substitutions, the M66/09 isolate had 10 unique amino acid substitutions (A288V, R249K, V302I, D435N, P440L, D446N, R947K, S1667L, R1926K and T2001A) while M260/09 and M21/10 both had one amino acid substitution (S6Q and T1683A, respectively). The M segment of the six isolates had seven amino acid substitutions that differ from ZH501 strain: one in the NSm (I9T), three in the Gn (V450I, I479V, and V507A) and three in the Gc (D297E, S369T and T441I). In addition to these substitutions, isolate M127/09 had two amino acid substitutions (I9S and Y74H), isolate M66/09 had five amino acid substitutions (D95N, D181N, V437I, I443T and I264V), isolates M21/10 and M247 both had one amino acid substitution (M114V and A280T, respectively) while isolate M260/09 had only two amino acid substitutions (C304L and V305C). Only one amino acid substitution (G159E) from the field isolates differ from that of ZH501 strain in the NP. The NSs of the field isolates had five amino acid substitutions that differ from the reference strain (F23I, A167V, V217A, I242V and E251D). In addition, the M66/09 isolate had four unique amino acid substitutions (K24R, K108R, K202R and E253G) (Table 3.2).

Table 3.2. Amino acids substitutions of field isolates as compared to those of the reference strain ZH501

Segment		Amino acid substitutions that differ from ZH501 in all of the isolates	Amino acid substitutions unique to each isolate
L		F23Y, V59I, M120T, E177D, S270N, N277D, N278S, D305A, V349I, A663T, G1123S, V1760I, H1852Y, R1922K	S6Q (M260/09), A288V (M66/09), R249K (M66/09), V302I (M66/09), D435N (M66/09), P440L (M66/09), D446N (M66/09), R947K (M66/09), S1667L (M66/09), T1683A (M21/10), R1926K (M66/09), T2001A (M66/09)
M	NSm	I9T	I9S (M127/09), Y74H (M127/09), D95N (M66/09)
	Gn	V450I, I479V, V507A	M114V (M21/10), D181N (M66/09), A280T (M247/09), C304L (M260/09), V305C (M260/09), V437I (M66/09), I443T (M66/09)
	Gc	D297E, S369T, T441I	I264V (M66/09)
S	NP	G159E	None
	NSs	F23I, A167V, V217A, I242V,E251D	K24R (M66/09), K108R (M66/09), K202R (M66/09, E253G (M66/09)

Substitutions are indicated compared to the reference strain ZH501 with the first amino acid (IUPAC) referring to the ZH501 strain, the number is the position and the second amino acid indicate the substitution in the field strain.

The L segment

Given that the L segment shows the largest number of differences between M66/09 and the other isolates, an analysis of the differences is presented below. Alignment of the endonuclease domain (residues 1-248) show that all the active site residues are conserved among all six isolates (Figure 3.8), as well as the Egyptian ZH501 isolate recently characterized (Holm *et al*., 2018). Isolate M66/09 and ZH501 share two residues that differ from those observed in the 5 isolates. Since all isolates are infective and not functional knockout strains, it is not surprising that all active site residues are conserved. However, substitutions around the active site (M120T) may lead to sterical hindrance that may impact

the rate of replication or transcription and the substitution. The E177D substitution on the other hand is located distantly from the active site residues and would be considered conserved.

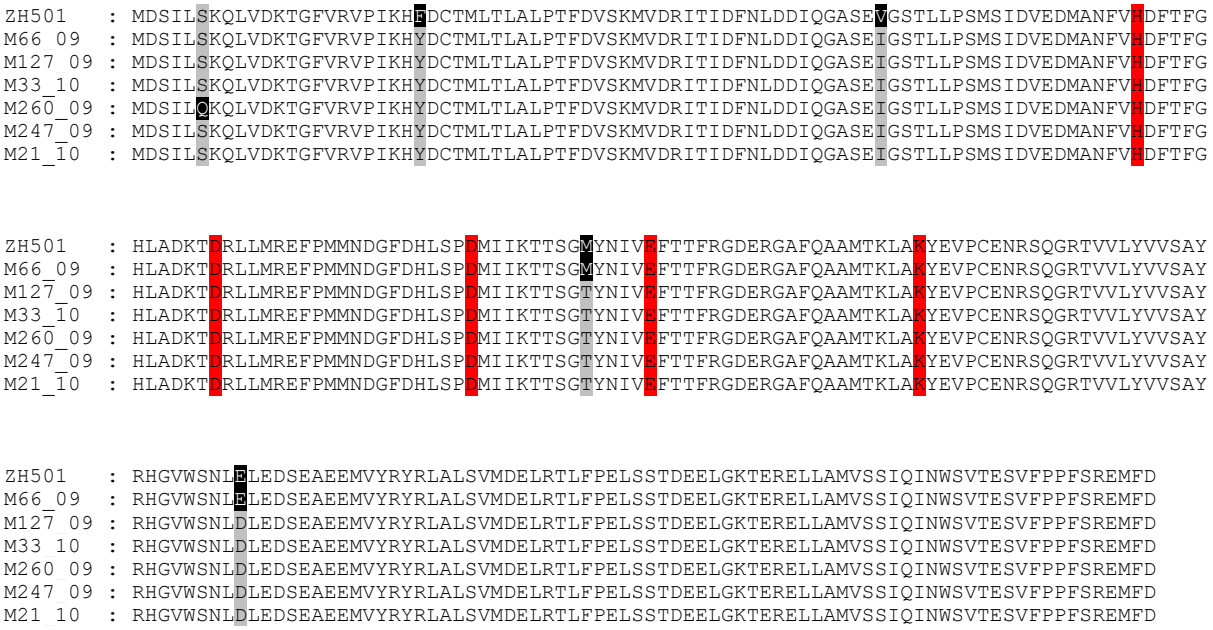

Figure 3.8: Alignment of the endonuclease domain of the polymerase encoded in the L segment (residues 1-148). Shades in red are the conserved residues involved in activity and metal ion coordination. Also shaded in black are residues conserved between isolate M66/09 and ZH501 strain that differ from the other strains (shaded in grey).

For the DUF3770 domain (residues 249-420), M66/09 showed no consistent differences beyond a S270N substitution also shared with strain ZH501 (Figure 3.9).

```
ZH501   : RFRSSPPDSEYITRIVSRCLINSQEKLINSSFFAEGNDKALRFSKNAEECSLAVERDLNQYRAEDNLRDLNDHKSTIQLPPWLS
M66_09  : KFRSSPPDSEYITRIVSRCLINSQEKLINNSFFAEGNDKVLRFSKNAEECSLAIERALNQYRAEDNLRDLNDHKSTIQLPPWLS
M127_09 : RFRSSPPDSEYITRIVSRCLISSQEKLIDNSFFAEGNDKALRFSKNAEECSLAVERALNQYRAEDNLRDLNDHKSTIQLPPWLS
M33_10  : RFRSSPPDSEYITRIVSRCLISSQEKLINNSFFAEGNDKALRFSKNAEECSLAVERALNQYRAEDNLRDLNDHKSTIQLPPWLS
M260_09 : RFRSSPPDSEYITRIVSRCLISSQEKLINNSFFAEGNDKALRFSKNAEECSLAVERALNQYRAEDNLRDLNDHKSTIQLPPWLS
M247_09 : RFRSSPPDSEYITRIVSRCLISSQEKLINNSFFAEGNDKALRFSKNAEECSLAVERALNQYRAEDNLRDLNDHKSTIQLPPWLS
M21_10  : RFRSSPPDSEYITRIVSRCLISSQEKLINNSFFAEGNDKALRFSKNAEECSLAVERALNQYRAEDNLRDLNDHKSTIQLPPWLS

ZH501   : YHDVDGKDLCPLQGLDVRGDHPMCNLWREVVTSANLEEIERMHDDAAAELEFALSGVKDRPDERNRYHRVHLNMGSDDSVYIAA
M66_09  : YHDVDGKDLCPLQGLDIRGDHPMCNLWREVVTSANLEEIERMHDDAAAELEFALSGVKDRPDERNRYHRVHLNMGSDDSVYIAA
M127_09 : YHDVDGKDLCPLQGLDVRGDHPMCNLWREVVTSANLEEIERMHDDAAAELEFALSGVKDRPDERNRYHRVHLNMGSDDSVYIAA
M33_10  : YHDVDGKDLCPLQGLDVRGDHPMCNLWREVVTSANLEEIERMHDDAAAELEFALSGVKDRPDERNRYHRVHLNMGSDDSVYIAA
M260_09 : YHDVDGKDLCPLQGLDVRGDHPMCNLWREVVTSANLEEIERMHDDAAAELEFALSGVKDRPDERNRYHRVHLNMGSDDSVYIAA
M247_09 : YHDVDGKDLCPLQGLDVRGDHPMCNLWREVVTSANLEEIERMHDDAAAELEFALSGVKDRPDERNRYHRVHLNMGSDDSVYIAA
M21_10  : YHDVDGKDLCPLQGLDVRGDHPMCNLWREVVTSANLEEIERMHDDAAAELEFALSGVKDRPDERNRYHRVHLNMGSDDSVYIAA

ZH501   : LGVNGKKHKADTLVQQMRDRSKQPFSPDHDVDHISEFLSACSSDLWATDEDLYNPLSCDKELRLAAQRIHQPSLSERGFNEIIT
M66_09  : LGVNGKKHKADTLVQQMRNRSKQLFSPDHNVDHISEFLSACSSDLWATDEDLYNPLSCDKELRLAAQRIHQPSLSEKGFNEIIT
M127_09 : LGVNGKKHKADTLVQQMRDRSKQPFSPDHDVDHISEFLSACSSDLWATDEDLYNPLSCDKELRLAAQRIHQPSLSEKGFNEIIT
M33_10  : LGVNGKKHKADTLVQQMRDRSKQPFSPDHDVDHISEFLSACSSDLWATDEDLYNPLSCDKELRLAAQRIHQPSLSEKGFNEIIT
M260_09 : LGVNGKKHKADTLVQQMRDRSKQPFSPDHDVDHISEFLSACSSDLWATDEDLYNPLSCDKELRLAAQRIHQPSLSEKGFNEIIT
M247_09 : LGVNGKKHKADTLVQQMRDRSKQPFSPDHDVDHISEFLSACSSDLWATDEDLYNPLSCDKELRLAAQRIHQPSLSEKGFNEIIT
M21_10  : LGVNGKKHKADTLVQQMRDRSKQPFSPDHDVDHISEFLSACSSDLWATDEDLYNPLSCDKELRLAAQRIHQPSLSEKGFNEIIT

ZH501   : EHYKFMGSRIGSWCQMVSLIGAELSASVKQHVKPNYFVIKRLLGSGIFLLIKPTSSKSHIFVSFAIKRSCWAFDLSTSRVFKPY
M66_09  : EHYKFMGSRIGSWCQMVSLIGAELSASVKQHVKPNYFVIKRLLGSGIFLLIKPTSSKSHIFVSFAIKRSCWAFDLSTSRVFKPY
M127_09 : EHYKFMGSRIGSWCQMVSLIGAELSASVKQHVKPNYFVIKRLLGSGIFLLIKPTSSKSHIFVSFAIKRSCWAFDLSTSRVFKPY
M33_10  : EHYKFMGSRIGSWCQMVSLIGAELSASVKQHVKPNYFVIKRLLGSGIFLLIKPTSSKSHIFVSFAIKRSCWAFDLSTSRVFKPY
M260_09 : EHYKFMGSRIGSWCQMVSLIGAELSASVKQHVKPNYFVIKRLLGSGIFLLIKPTSSKSHIFVSFAIKRSCWAFDLSTSRVFKPY
M247_09 : EHYKFMGSRIGSWCQMVSLIGAELSASVKQHVKPNYFVIKRLLGSGIFLLIKPTSSKSHIFVSFAIKRSCWAFDLSTSRVFKPY
M21_10  : EHYKFMGSRIGSWCQMVSLIGAELSASVKQHVKPNYFVIKRLLGSGIFLLIKPTSSKSHIFVSFAIKRSCWAFDLSTSRVFKPY

ZH501   : IDAGDLLVTDFVSYKLSKL
M66_09  : IDAGDLLVTDFVSYKLSKL
M127_09 : IDAGDLLVTDFVSYKLSKL
M33_10  : IDAGDLLVTDFVSYKLSKL
M260_09 : IDAGDLLVTDFVSYKLSKL
M247_09 : IDAGDLLVTDFVSYKLSKL
M21_10  : IDAGDLLVTDFVSYKLSKL
```

Figure 3.9: Alignment of the DUF3770 domain of the L segment (residues 249-420). Residues that differ from the majority consensus sequences are shaded in black, while the majority are shaded in grey.

For the RNA polymerase domain (region 604-1299) no significant differences were observed between M66/09 and the other isolates (Figure 3.10).

```
ZH501   : TNLCKCVSLMESSFSFWAEAFGIPSWNFVGDLFRSSDSAAMDASYMGKLSLLTLLEDKAATEELQTIARYIIMEGFVSPPEIPK
M66_09  : TNLCKCVSLMESSFSFWAEAFGIPSWNFVGDLFRSSDSAAMDASYMGKLSLLTLLEDKATTEELQTIARYIIMEGFVSPPEIPK
M127_09 : TNLCKCVSLMESSFSFWAEAFGIPSWNFVGDLFRSSDSAAMDASYMGKLSLLTLLEDKATTEELQTIARYIIMEGFVSPPEIPK
M33_10  : TNLCKCVSLMESSFSFWAEAFGIPSWNFVGDLFRSSDSAAMDASYMGKLSLLTLLEDKATTEELQTIARYIIMEGFVSPPEIPK
M260_09 : TNLCKCVSLMESSFSFWAEAFGIPSWNFVGDLFRSSDSAAMDASYMGKLSLLTLLEDKATTEELQTIARYIIMEGFVSPPEIPK
M247_09 : TNLCKCVSLMESSFSFWAEAFGIPSWNFVGDLFRSSDSAAMDASYMGKLSLLTLLEDKATTEELQTIARYIIMEGFVSPPEIPK
M21_10  : TNLCKCVSLMESSFSFWAEAFGIPSWNFVGDLFRSSDSAAMDASYMGKLSLLTLLEDKATTEELQTIARYIIMEGFVSPPEIPK


ZH501   : PHKMTSKFPKVLRSELQVYLLNCLCRTIQRIAGEPFILKKKDGSISWGGMFNPFSGRPLLDMQPLISCCYNGYFKNKEEETEPS
M66_09  : PHKMTSKFPKVLRSELQVYLLNCLCRTIQRIAGEPFILKKKDGSISWGGMFNPFSGRPLLDMQPLISCCYNGYFKNKEEETEPS
M127_09 : PHKMTSKFPKVLRSELQVYLLNCLCRTIQRIAGEPFILKKKDGSISWGGMFNPFSGRPLLDMQPLISCCYNGYFKNKEEETEPS
M33_10  : PHKMTSKFPKVLRSELQVYLLNCLCRTIQRIAGEPFILKKKDGSISWGGMFNPFSGRPLLDMQPLISCCYNGYFKNKEEETEPS
M260_09 : PHKMTSKFPKVLRSELQVYLLNCLCRTIQRIAGEPFILKKKDGSISWGGMFNPFSGRPLLDMQPLISCCYNGYFKNKEEETEPS
M247_09 : PHKMTSKFPKVLRSELQVYLLNCLCRTIQRIAGEPFILKKKDGSISWGGMFNPFSGRPLLDMQPLISCCYNGYFKNKEEETEPS
M21_10  : PHKMTSKFPKVLRSELQVYLLNCLCRTIQRIAGEPFILKKKDGSISWGGMFNPFSGRPLLDMQPLISCCYNGYFKNKEEETEPS


ZH501   : SLSGMYKKIIELEHLRPQSDAFLGYKDPELPRMHEFSVSYLKEACNHAKLVLRSLYGQNFMEQIDNQIIRELSGLTLERLATLK
M66_09  : SLSGMYKKIIELEHLRPQSDAFLGYKDPELPRMHEFSVSYLKEACNHAKLVLRSLYGQNFMEQIDNQIIRELSGLTLERLATLK
M127_09 : SLSGMYKKIIELEHLRPQSDAFLGYKDPELPRMHEFSVSYLKEACNHAKLVLRSLYGQNFMEQIDNQIIRELSGLTLERLATLK
M33_10  : SLSGMYKKIIELEHLRPQSDAFLGYKDPELPRMHEFSVSYLKEACNHAKLVLRSLYGQNFMEQIDNQIIRELSGLTLERLATLK
M260_09 : SLSGMYKKIIELEHLRPQSDAFLGYKDPELPRMHEFSVSYLKEACNHAKLVLRSLYGQNFMEQIDNQIIRELSGLTLERLATLK
M247_09 : SLSGMYKKIIELEHLRPQSDAFLGYKDPELPRMHEFSVSYLKEACNHAKLVLRSLYGQNFMEQIDNQIIRELSGLTLERLATLK
M21_10  : SLSGMYKKIIELEHLRPQSDAFLGYKDPELPRMHEFSVSYLKEACNHAKLVLRSLYGQNFMEQIDNQIIRELSGLTLERLATLK


ZH501   : ATSNFNENWYVYKDVADKNYTRDKLLVKMSKYASEGKSLAIQKFEDCMRQIESQGCMHICLFKKQQHGGLREIYVMGAEERIVQ
M66_09  : ATSNFNENWYVYKDVADKNYTRDKLLVKMSKYASEGKSLAIQKFEDCMRQIESQGCMHICLFKKQQHGGLREIYVMGAEERIVQ
M127_09 : ATSNFNENWYVYKDVADKNYTRDKLLVKMSKYASEGKSLAIQKFEDCMRQIESQGCMHICLFKKQQHGGLREIYVMGAEERIVQ
M33_10  : ATSNFNENWYVYKDVADKNYTRDKLLVKMSKYASEGKSLAIQKFEDCMRQIESQGCMHICLFKKQQHGGLREIYVMGAEERIVQ
M260_09 : ATSNFNENWYVYKDVADKNYTRDKLLVKMSKYASEGKSLAIQKFEDCMRQIESQGCMHICLFKKQQHGGLREIYVMGAEERIVQ
M247_09 : ATSNFNENWYVYKDVADKNYTRDKLLVKMSKYASEGKSLAIQKFEDCMRQIESQGCMHICLFKKQQHGGLREIYVMGAEERIVQ
M21_10  : ATSNFNENWYVYKDVADKNYTRDKLLVKMSKYASEGKSLAIQKFEDCMRQIESQGCMHICLFKKQQHGGLREIYVMGAEERIVQ


ZH501   : SVVETIARSIGKFFASDTLCNPPNKVKIPETHGIRARKQCKGPVWTCATSDDARKWNQGHFVTKFALMLCEFTSPKWWPLIIRG
M66_09  : SVVETIAKSIGKFFASDTLCNPPNKVKIPETHGIRARKQCKGPVWTCATSDDARKWNQGHFVTKFALMLCEFTSPKWWPLIIRG
M127_09 : SVVETIARSIGKFFASDTLCNPPNKVKIPETHGIRARKQCKGPVWTCATSDDARKWNQGHFVTKFALMLCEFTSPKWWPLIIRG
M33_10  : SVVETIARSIGKFFASDTLCNPPNKVKIPETHGIRARKQCKGPVWTCATSDDARKWNQGHFVTKFALMLCEFTSPKWWPLIIRG
M260_09 : SVVETIARSIGKFFASDTLCNPPNKVKIPETHGIRARKQCKGPVWTCATSDDARKWNQGHFVTKFALMLCEFTSPKWWPLIIRG
M247_09 : SVVETIARSIGKFFASDTLCNPPNKVKIPETHGIRARKQCKGPVWTCATSDDARKWNQGHFVTKFALMLCEFTSPKWWPLIIRG
M21_10  : SVVETIARSIGKFFASDTLCNPPNKVKIPETHGIRARKQCKGPVWTCATSDDARKWNQGHFVTKFALMLCEFTSPKWWPLIIRG


ZH501   : CSMFTRKRMMMNLNYLKILDGHRELDIRDDFVMDLFKAYHGEAEVPWAFKGKTYLETTTGMMQGILHYTSSLLHTIHQEYIRSL
M66_09  : CSMFTRKRMMMNLNYLKILDGHRELDIRDDFVMDLFKAYHGEAEVPWAFKGKTYLETTTGMMQGILHYTSSLLHTIHQEYIRSL
M127_09 : CSMFTRKRMMMNLNYLKILDGHRELDIRDDFVMDLFKAYHGEAEVPWAFKGKTYLETTTGMMQGILHYTSSLLHTIHQEYIRSL
M33_10  : CSMFTRKRMMMNLNYLKILDGHRELDIRDDFVMDLFKAYHGEAEVPWAFKGKTYLETTTGMMQGILHYTSSLLHTIHQEYIRSL
M260_09 : CSMFTRKRMMMNLNYLKILDGHRELDIRDDFVMDLFKAYHGEAEVPWAFKGKTYLETTTGMMQGILHYTSSLLHTIHQEYIRSL
M247_09 : CSMFTRKRMMMNLNYLKILDGHRELDIRDDFVMDLFKAYHGEAEVPWAFKGKTYLETTTGMMQGILHYTSSLLHTIHQEYIRSL
M21_10  : CSMFTRKRMMMNLNYLKILDGHRELDIRDDFVMDLFKAYHGEAEVPWAFKGKTYLETTTGMMQGILHYTSSLLHTIHQEYIRSL


ZH501   : SFKIFNLKVAPEMSKGLVCDMMQGSDDSSMLISFPADDEKVLTRCKVAAAICFRMKKELGVYLAIYPSEKSTANTDFVMEYNSE
M66_09  : SFKIFNLKVAPEMSKSLVCDMMQGSDDSSMLISFPADDEKVLTRCKVAAAICFRMKKELGVYLAIYPSEKSTANTDFVMEYNSE
M127_09 : SFKIFNLKVAPEMSKSLVCDMMQGSDDSSMLISFPADDEKVLTRCKVAAAICFRMKKELGVYLAIYPSEKSTANTDFVMEYNSE
M33_10  : SFKIFNLKVAPEMSKSLVCDMMQGSDDSSMLISFPADDEKVLTRCKVAAAICFRMKKELGVYLAIYPSEKSTANTDFVMEYNSE
M260_09 : SFKIFNLKVAPEMSKSLVCDMMQGSDDSSMLISFPADDEKVLTRCKVAAAICFRMKKELGVYLAIYPSEKSTANTDFVMEYNSE
M247_09 : SFKIFNLKVAPEMSKSLVCDMMQGSDDSSMLISFPADDEKVLTRCKVAAAICFRMKKELGVYLAIYPSEKSTANTDFVMEYNSE
M21_10  : SFKIFNLKVAPEMSKSLVCDMMQGSDDSSMLISFPADDEKVLTRCKVAAAICFRMKKELGVYLAIYPSEKSTANTDFVMEYNSE


ZH501   : FYFHTQHVRPTIRWIAACCSLPEVETLVARQEEASNLMTSVTEGGGSFSLAAMIQQAQCTLHYMLMGMGVSELFLEYKKAVLKW
M66_09  : FYFHTQHVRPTIRWIAACCSLPEVETLVARQEEASNLMTSVTEGGGSFSLAAMIQQAQCTLHYMLMGMGVSELFLEYKKAVLKW
M127_09 : FYFHTQHVRPTIRWIAACCSLPEVETLVARQEEASNLMTSVTEGGGSFSLAAMIQQAQCTLHYMLMGMGVSELFLEYKKAVLKW
M33_10  : FYFHTQHVRPTIRWIAACCSLPEVETLVARQEEASNLMTSVTEGGGSFSLAAMIQQAQCTLHYMLMGMGVSELFLEYKKAVLKW
M260_09 : FYFHTQHVRPTIRWIAACCSLPEVETLVARQEEASNLMTSVTEGGGSFSLAAMIQQAQCTLHYMLMGMGVSELFLEYKKAVLKW
M247_09 : FYFHTQHVRPTIRWIAACCSLPEVETLVARQEEASNLMTSVTEGGGSFSLAAMIQQAQCTLHYMLMGMGVSELFLEYKKAVLKW
M21_10  : FYFHTQHVRPTIRWIAACCSLPEVETLVARQEEASNLMTSVTEGGGSFSLAAMIQQAQCTLHYMLMGMGVSELFLEYKKAVLKW


ZH501   : NDPGLGFFLLDNPYACGLGGFRFN
M66_09  : NDPGLGFFLLDNPYACGLGGFRFN
M127_09 : NDPGLGFFLLDNPYACGLGGFRFN
M33_10  : NDPGLGFFLLDNPYACGLGGFRFN
M260_09 : NDPGLGFFLLDNPYACGLGGFRFN
M247_09 : NDPGLGFFLLDNPYACGLGGFRFN
M21_10  : NDPGLGFFLLDNPYACGLGGFRFN
```

Figure 3.10: Alignment of the RNA polymerase domain (region 604-1299). Residues that differ from the majority consensus are shaded in black, while the majority are shaded in grey.

The undefined C-terminal domain of the L-segment (region 1300-2092) shows only one potential substitution of interest namely Y1852H, in M66/09 and strain ZH501(Figure 3.11).

```
ZH501   : LFKAITRTDLQKLYAFFMKKVKGSAARDWADEDVTIPETCSVSPGGALILSSSLKWGSRKKFQKLRDRLNIPENWIELINENPE
M66_09  : LFKAITRTDLQKLYAFFMKKVKGSAARDWADEDITIPETCSVSPGGALILSSSLKWGSRKKFQKLRDRLNIPENWIELINENPE
M127_09 : LFKAITRTDLQKLYAFFMKKVKGSAARDWADEDVTIPETCSVSPGGALILSSSLKWGSRKKFQKLRDRLNIPENWIELINENPE
M33_10  : LFKAITRTDLQKLYAFFMKKVKGSAARDWADEDVTIPETCSVSPGGALILSSSLKWGSRKKFQKLRDRLNIPENWIELINENPE
M260_09 : LFKAITRTDLQKLYAFFMKKVKGSAARDWADEDVTIPETCSVSPGGALILSSSLKWGSRKKFQKLRDRLNIPENWIELINENPE
M247_09 : LFKAITRTDLQKLYAFFMKKVKGSAARDWADEDVTIPETCSVSPGGALILSSSLKWGSRKKFQKLRDRLNIPENWIELINENPE
M21_10  : LFKAITRTDLQKLYAFFMKKVKGSAARDWADEDVTIPETCSVSPGGALILSSSLKWGSRKKFQKLRDRLNIPENWIELINENPE


ZH501   : VLYRAPRTGPEILLRIAEKVHSPGVVSSLSSGNAVCKVMASAVYFLSATIFEDTGRPEFNFLEDSKYSLLQKMAAYSGFHGFND
M66_09  : VLYRAPRTGPEILLRIAEKVHSPGVVSSLSSGNAVCKVMASAVYFLSATIFEDTGRPEFNFLEDSKYSLLQKMAAYSGFHGFND
M127_09 : VLYRAPRTGPEILLRIAEKVHSPGVVSSLSSGNAVCKVMASAVYFLSATIFEDTGRPEFNFLEDSKYSLLQKMAAYSGFHGFND
M33_10  : VLYRAPRTGPEILLRIAEKVHSPGVVSSLSSGNAVCKVMASAVYFLSATIFEDTGRPEFNFLEDSKYSLLQKMAAYSGFHGFND
M260_09 : VLYRAPRTGPEILLRIAEKVHSPGVVSSLSSGNAVCKVMASAVYFLSATIFEDTGRPEFNFLEDSKYSLLQKMAAYSGFHGFND
M247_09 : VLYRAPRTGPEILLRIAEKVHSPGVVSSLSSGNAVCKVMASAVYFLSATIFEDTGRPEFNFLEDSKYSLLQKMAAYSGFHGFND
M21_10  : VLYRAPRTGPEILLRIAEKVHSPGVVSSLSSGNAVCKVMASAVYFLSATIFEDTGRPEFNFLEDSKYSLLQKMAAYSGFHGFND


ZH501   : MEPEDILFLFPNIEELESLDSIVYNKGEIDIIPRVNIRDATQTRVTIFNEQKTLRTSPEKLVSDKWFGTQKSRIGKTTFLAEWE
M66_09  : MEPEDILFLFPNIEELESLDSIVYNKGEIDIIPRVNIRDATQTRVTIFNEQKTLRTSPEKLVSDKWFGTQKSRIGKTTFLAEWE
M127_09 : MEPEDILFLFPNIEELESLDSIVYNKGEIDIIPRVNIRDATQTRVTIFNEQKTLRTSPEKLVSDKWFGTQKSRIGKTTFLAEWE
M33_10  : MEPEDILFLFPNIEELESLDSIVYNKGEIDIIPRVNIRDATQTRVTIFNEQKTLRTSPEKLVSDKWFGTQKSRIGKTTFLAEWE
M260_09 : MEPEDILFLFPNIEELESLDSIVYNKGEIDIIPRVNIRDATQTRVTIFNEQKTLRTSPEKLVSDKWFGTQKSRIGKTTFLAEWE
M247_09 : MEPEDILFLFPNIEELESLDSIVYNKGEIDIIPRVNIRDATQTRVTIFNEQKTLRTSPEKLVSDKWFGTQKSRIGKTTFLAEWE
M21_10  : MEPEDILFLFPNIEELESLDSIVYNKGEIDIIPRVNIRDATQTRVTIFNEQKTLRTSPEKLVSDKWFGTQKSRIGKTTFLAEWE


ZH501   : KLKKIVKWLEDTPEATLAHTPLNNHIQVRNFFARMESKPRTVRITGAPVKKRSGVSKIAMVIRDNFSRMGHLRGVEDLAGFTRS
M66_09  : KLKKIVKWLEDTPEATLAHTPLNNHIQVRNFFARMESKPRTVRITGAPVKKRSGVSKIAMVIRDNFSRMGHLRGVEDLAGFTRS
M127_09 : KLKKIVKWLEDTPEATLAHTPLNNHIQVRNFFARMESKPRTVRITGAPVKKRSGVSKIAMVIRDNFSRMGHLRGVEDLAGFTRS
M33_10  : KLKKIVKWLEDTPEATLAHTPLNNHIQVRNFFARMESKPRTVRITGAPVKKRSGVSKIAMVIRDNFSRMGHLRGVEDLAGFTRS
M260_09 : KLKKIVKWLEDTPEATLAHTPLNNHIQVRNFFARMESKPRTVRITGAPVKKRSGVSKIAMVIRDNFSRMGHLRGVEDLAGFTRS
M247_09 : KLKKIVKWLEDTPEATLAHTPLNNHIQVRNFFARMESKPRTVRITGAPVKKRSGVSKIAMVIRDNFSRMGHLRGVEDLAGFTRS
M21_10  : KLKKIVKWLEDTPEATLAHTPLNNHIQVRNFFARMESKPRTVRITGAPVKKRSGVSKIAMVIRDNFSRMGHLRGVEDLAGFTRS


ZH501   : VSAEILKHFLFCILQGPYSESYKLQLIYRVLSSVSNVEIKESDGKTKINLIGILQRFLDGDHVVPIIEEMGAGTVGGFIKRQQS
M66_09  : VSAEILKHFLFCILQGPYSESYKLQLIYRVLSLVSNVEIKESDGKTKINLIGILQRFLDGDHVVPIIEEMGAGTVGGFIKRQQS
M127_09 : VSAEILKHFLFCILQGPYSESYKLQLIYRVLSSVSNVEIKESDGKTKINLIGILQRFLDGDHVVPIIEEMGAGTVGGFIKRQQS
M33_10  : VSAEILKHFLFCILQGPYSESYKLQLIYRVLSSVSNVEIKESDGKTKINLIGILQRFLDGDHVVPIIEEMGAGTVGGFIKRQQS
M260_09 : VSAEILKHFLFCILQGPYSESYKLQLIYRVLSSVSNVEIKESDGKTKINLIGILQRFLDGDHVVPIIEEMGAGTVGGFIKRQQS
M247_09 : VSAEILKHFLFCILQGPYSESYKLQLIYRVLSSVSNVEIKESDGKTKINLIGILQRFLDGDHVVPIIEEMGAGTVGGFIKRQQS
M21_10  : VSAEILKHFLFCILQGPYSESYKLQLIYRVLSSVSNVEIKESDGKTKANLIGILQRFLDGDHVVPIIEEMGAGTVGGFIKRQQS


ZH501   : KVVQNKVVYYGVGIWRGFMDGYQVHLEIENDIGQPPRLRNVTTNCQSSPWDLSIPIRQWAEDMGVTNNQDYSSKSSRGARYWMH
M66_09  : KVVQNKVVYYGVGIWRGFMDGYQVHLEIENDIGQPPRLRNVTTNCQSSPWDLSIPIRQWAEDMGVTNNQDYSSKSSRGARYWMH
M127_09 : KVVQNKVVYYGVGIWRGFMDGYQVHLEIENDIGQPPRLRNITTNCQSSPWDLSIPIRQWAEDMGVTNNQDYSSKSSRGARYWMH
M33_10  : KVVQNKVVYYGVGIWRGFMDGYQVHLEIENDIGQPPRLRNITTNCQSSPWDLSIPIRQWAEDMGVTNNQDYSSKSSRGARYWMH
M260_09 : KVVQNKVVYYGVGIWRGFMDGYQVHLEIENDIGQPPRLRNITTNCQSSPWDLSIPIRQWAEDMGVTNNQDYSSKSSRGARYWMH
M247_09 : KVVQNKVVYYGVGIWRGFMDGYQVHLEIENDIGQPPRLRNITTNCQSSPWDLSIPIRQWAEDMGVTNNQDYSSKSSRGARYWMH
M21_10  : KVVQNKVVYYGVGIWRGFMDGYQVHLEIENDIGQPPRLRNITTNCQSSPWDLSIPIRQWAEDMGVTNNQDYSSKSSRGARYWMH


ZH501   : SFRMQGPSKPFGCPVYIIKGDMSDVIRLRKEEVEMKVRGSTLNLYTKHHSHQDLHILSYTASDNDLSPGIFKSISDEGVAQALQ
M66_09  : SFRMQGPSKPFGCPVYIIKGDMSDVIRLRKEEVEMKVRGSTLNLYTKHHSHQDLHILSYTASDNDLSPGIFKSISDEGVAQALQ
M127_09 : SFRMQGPSKPFGCPVYIIKGDMSDVIRLRKEEVEMKVRGSTLNLYTKHYSHQDLHILSYTASDNDLSPGIFKSISDEGVAQALQ
M33_10  : SFRMQGPSKPFGCPVYIIKGDMSDVIRLRKEEVEMKVRGSTLNLYTKHYSHQDLHILSYTASDNDLSPGIFKSISDEGVAQALQ
M260_09 : SFRMQGPSKPFGCPVYIIKGDMSDVIRLRKEEVEMKVRGSTLNLYTKHYSHQDLHILSYTASDNDLSPGIFKSISDEGVAQALQ
M247_09 : SFRMQGPSKPFGCPVYIIKGDMSDVIRLRKEEVEMKVRGSTLNLYTKHYSHQDLHILSYTASDNDLSPGIFKSISDEGVAQALQ
M21_10  : SFRMQGPSKPFGCPVYIIKGDMSDVIRLRKEEVEMKVRGSTLNLYTKHYSHQDLHILSYTASDNDLSPGIFKSISDEGVAQALQ


ZH501   : LFEREPSNCWVRCESVAPKFISAILEICEGKRQIRGINRTRLSEIVRICSESSLRSKVGSMFSFVANVEEAHDVDYDALMDLMI
M66_09  : LFEREPSNCWVRCESVAPKFISAILEICEGKRQIKGINRTRLSEIVRICSESSLRSKVGSMFSFVANVEEAHDVDYDALMDLMI
M127_09 : LFEREPSNCWVRCESVAPKFISAILEICEGKRQIKGINKTRLSEIVRICSESSLRSKVGSMFSFVANVEEAHDVDYDALMDLMI
M33_10  : LFEREPSNCWVRCESVAPKFISAILEICEGKRQIKGINKTRLSEIVRICSESSLRSKVGSMFSFVANVEEAHDVDYDALMDLMI
M260_09 : LFEREPSNCWVRCESVAPKFISAILEICEGKRQIKGINKTRLSEIVRICSESSLRSKVGSMFSFVANVEEAHDVDYDALMDLMI
M247_09 : LFEREPSNCWVRCESVAPKFISAILEICEGKRQIKGINKTRLSEIVRICSESSLRSKVGSMFSFVANVEEAHDVDYDALMDLMI
M21_10  : LFEREPSNCWVRCESVAPKFISAILEICEGKRQIKGINKTRLSEIVRICSESSLRSKVGSMFSFVANVEEAHDVDYDALMDLMI


ZH501   : EDAKNNAFSHVVDCIELDVSGPYEMESFDTSDVNLFGPAHYKDISSLSMIAHPLMDKFVDYAISKMGRASVRKVLETGRCSSKD
M66_09  : EDAKNNAFSHVVNCIELDVSGPYEMESFDASDVNLFGPAHYKDISSLSMIAHPLMDKFVDYAISKMGRASVRKVLETGRCSSKD
M127_09 : EDAKNNAFSHVVNCIELDVSGPYEMESFDTSDVNLFGPAHYKDISSLSMIAHPLMDKFVDYAISKMGRASVRKVLETGRCSSKD
M33_10  : EDAKNNAFSHVVNCIELDVSGPYEMESFDTSDVNLFGPAHYKDISSLSMIAHPLMDKFVDYAISKMGRASVRKVLETGRCSSKD
M260_09 : EDAKNNAFSHVVNCIELDVSGPYEMESFDTSDVNLFGPAHYKDISSLSMIAHPLMDKFVDYAISKMGRASVRKVLETGRCSSKD
M247_09 : EDAKNNAFSHVVNCIELDVSGPYEMESFDTSDVNLFGPAHYKDISSLSMIAHPLMDKFVDYAISKMGRASVRKVLETGRCSSKD
M21_10  : EDAKNNAFSHVVNCIELDVSGPYEMESFDTSDVNLFGPAHYKDISSLSMIAHPLMDKFVDYAISKMGRASVRKVLETGRCSSKD


ZH501   : YDLSKVLFRTLQRPEESIRIDDLELYEETDVADDMLG
M66_09  : YDLSKVLFRTLQRPEESIRIDDLELYEETDVADDMLG
M127_09 : YDLSKVLFRTLQRPEESIRIDDLELYEETDVADDMLG
M33_10  : YDLSKVLFRTLQRPEESIRIDDLELYEETDVADDMLG
M260_09 : YDLSKVLFRTLQRPEESIRIDDLELYEETDVADDMLG
M247_09 : YDLSKVLFRTLQRPEESIRIDDLELYEETDVADDMLG
M21_10  : YDLSKVLFRTLQRPEESIRIDDLELYEETDVADDMLG
```

Figure 3.11: Alignment of the undefined C-terminal domain of the L segment (residues 2300-2092). Residues that differ from the majority consensus are shaded in black, while the majority are shaded in grey.

The M segment

The M segment of RVFV encodes four proteins: i.e., NSm, 78 kDa, Gn and the Gc proteins. All the proteins of the M segment were compared. The results showed that some field isolates had unique amino acid substitutions. These substitutions were observed in different proteins of the M segment i.e. NSm, Gn and Gc (Table 3.2 and Figure 3:17). In addition, some field strains had amino acid substitutions that differed from the five field strains.

The 78kDa and the NSm gene showed only two substitutions: i.e., I9T and D95N respectively. The substitution I9T is shared between M66/09 and ZH501 (Table 3.2), and D95N where M66/09 has the unique asparagine, while ZH501, and the other six isolates have the aspartic acid substitution (Figure 3.12). Since NSm has been shown to be dispensable for virus maturation, replication and infection in cell culture, these substitutions probably do not contribute to the growth curve differences observed between the isolates and both NSm and 78 kDa proteins can be excluded from further consideration (Won *et al*., 2006; Gerrard and Nichol, 2007).

```
ZH501    : MYVLLTILISVLVCEAVIRVSLSSTREETCFGDSTNPEMIEGAWDSLREEEMPEELSCSISGIREVKTSSQELYRALKAIIAADG
M066_09 : MYVLLTILISVLVCEAVIRVSLSSTREETCFGDSTNPEMIEGAWDSLREEEMPEELSCSVSGIREVKTSSQELYRALKAIIAADG
M127_09 : MYVLLTILSSVLVCEAVIRVSLSSTREETCFGDSTNPEMIEGAWDSLREEEMPEELSCSVSGIREVKTSSQELHRALKAIIAADG
M260_09 : MYVLLTILTSVLVCEAVIRVSLSSTREETCFGDSTNPEMIEGAWDSLREEEMPEELSCSVSGIREVKTSSQELYRALKAIIAADG
M21_10   : MYVLLTILTSVLVCEAVIRVSLSSTREETCFGDSTNPEMIEGAWDSLREEEMPEELSCSVSGIREVKTSSQELYRALKAIIAADG
M247_09 : MYVLLTILTSVLVCEAVIRVSLSSTREETCFGDSTNPEMIEGAWDSLREEEMPEELSCSVSGIREVKTSSQELYRALKAIIAADG
M33_10   : MYVLLTILTSVLVCEAVIRVSLSSTREETCFGDSTNPEMIEGAWDSLREEEMPEELSCSVSGIREVKTSSQELYRALKAIIAADG

ZH501    : LNNITCHGKDPEDKISLIKGPPHKKRVGIVRCERRRDAKQIGRETMAGIAMTVLPALAVFALAPVVF
M066_09 : LNNITCHGKNPEDKISLIKGPPHKKRVGIVRCERRRDAKQIGRETMAGIAMTVLPALAVFALAPVVF
M127_09 : LNNITCHGKDPEDKISLIKGPPHKKRVGIVRCERRRDAKQIGRETMAGIAMTVLPALAVFALAPVVF
M260_09 : LNNITCHGKDPEDKISLIKGPPHKKRVGIVRCERRRDAKQIGRETMAGIAMTVLPALAVFALAPVVF
M21_10   : LNNITCHGKDPEDKISLIKGPPHKKRVGIVRCERRRDAKQIGRETMAGIAMTVLPALAVFALAPVVF
M247_09 : LNNITCHGKDPEDKISLIKGPPHKKRVGIVRCERRRDAKQIGRETMAGIAMTVLPALAVFALAPVVF
M33_10   : LNNITCHGKDPEDKISLIKGPPHKKRVGIVRCERRRDAKQIGRETMAGIAMTVLPALAVFALAPVVF
```

Figure 3.12: Alignment of the NSm. Residues that differ from the majority consensus are shaded in black, while the majority are shaded in grey.

Substitutions that occur on the Gn domain of the field isolates include V450I, I479V and V507A as compared to the reference strain (Figure 3.13). None of these occur in the region where receptor binding would occur as indicated in Figure 3.1. While these may impact growth rates if they are involved in heterodimer assembly or genome packaging, this seems unlikely.

```
ZH501   : AEDPHLRNRPGKGHNYIDGMTQEDATCKPVTYAGACSSFDVLLEKGKFPLFQSYAHHRTLLEAVHDTIIAKADPPSCDLQSAHG
M066_09 : AEDPHLRNRPGKGHNYIDGMTQEDATCKPVTYAGACSSFDVLLEKGKFPLFQSYAHHRTLLEAVHDTIIAKADPPSCDLQSAHG
M127_09 : AEDPHLRNRPGKGHNYIDGMTQEDATCKPVTYAGACSSFDVLLEKGKFPLFQSYAHHRTLLEAVHDTIIAKADPPSCDLQSAHG
M260_09 : AEDPHLRNRPGKGHNYIDGMTQEDATCKPVTYAGACSSFDVLLEKGKFPLFQSYAHHRTLLEAVHDTIIAKADPPSCDLQSAHG
M21_10  : AEDPHLRNRPGKGHNYIDGMTQEDATCKPVTYAGACSSFDVLLEKGKFPLFQSYAHHRTLLEAVHDTIIAKADPPSCDLQSAHG
M247_09 : AEDPHLRNRPGKGHNYIDGMTQEDATCKPVTYAGACSSFDVLLEKGKFPLFQSYAHHRTLLEAVHDTIIAKADPPSCDLQSAHG
M33_10  : AEDPHLRNRPGKGHNYIDGMTQEDATCKPVTYAGACSSFDVLLEKGKFPLFQSYAHHRTLLEAVHDTIIAKADPPSCDLQSAHG

ZH501   : NPCMKEKLVMKTHCPNDYQSAHYLNNDGKMASVKCPPKYELTEDCNFCRQMTGASLKKGSYPLQDLFCQSSEDDGSKLKTKMKG
M066_09 : NPCMKEKLVMKTHCPNDYQSAHYLNNDGKMASVKCPPKYELTEDCNFCRQMTGASLKKGSYPLQDLFCQSSEDDGSKLKTKMKG
M127_09 : NPCMKEKLVMKTHCPNDYQSAHYLNNDGKMASVKCPPKYELTEDCNFCRQMTGASLKKGSYPLQDLFCQSSEDDGSKLKTKMKG
M260_09 : NPCMKEKLVMKTHCPNDYQSAHYLNNDGKMASVKCPPKYELTEDCNFCRQMTGASLKKGSYPLQDLFCQSSEDDGSKLKTKMKG
M21_10  : NPCMKEKLVMKTHCPNDYQSAHYLNNDGKVASVKCPPKYELTEDCNFCRQMTGASLKKGSYPLQDLFCQSSEDDGSKLKTKMKG
M247_09 : NPCMKEKLVMKTHCPNDYQSAHYLNNDGKMASVKCPPKYELTEDCNFCRQMTGASLKKGSYPLQDLFCQSSEDDGSKLKTKMKG
M33_10  : NPCMKEKLVMKTHCPNDYQSAHYLNNDGKMASVKCPPKYELTEDCNFCRQMTGASLKKGSYPLQDLFCQSSEDDGSKLKTKMKG

ZH501   : VCEVGVQALKKCDGQLSTAHEVVPFAVFKNSKKVYLDKLDLKTEENLLPDSFVCFEHKGQYKGTMDSGQTKRELKSFDISQCPK
M066_09 : VCEVGVQALKKCNGQLSTAHEVVPFAVFKNSKKVYLDKLDLKTEENLLPDSFVCFEHKGQYKGTMDSGQTKRELKSFDISQCPK
M127_09 : VCEVGVQALKKCDGQLSTAHEVVPFAVFKNSKKVYLDKLDLKTEENLLPDSFVCFEHKGQYKGTMDSGQTKRELKSFDISQCPK
M260_09 : VCEVGVQALKKCDGQLSTAHEVVPFAVFKNSKKVYLDKLDLKTEENLLPDSFVCFEHKGQYKGTMDSGQTKRELKSFDISQCPK
M21_10  : VCEVGVQALKKCDGQLSTAHEVVPFAVFKNSKKVYLDKLDLKTEENLLPDSFVCFEHKGQYKGTMDSGQTKRELKSFDISQCPK
M247_09 : VCEVGVQALKKCDGQLSTAHEVVPFAVFKNSKKVYLDKLDLKTEENLLPDSFVCFEHKGQYKGTMDSGQTKRELKSFDISQCPK
M33_10  : VCEVGVQALKKCDGQLSTAHEVVPFAVFKNSKKVYLDKLDLKTEENLLPDSFVCFEHKGQYKGTMDSGQTKRELKSFDISQCPK

ZH501   : IGGHGSKKCTGDAAFCSAYECTAQYANAYCSHANGSGIVQIQVSGVWKKPLCVGYERVVVKRELSAKPIQRVEPCTTCITKCEP
M066_09 : IGGHGSKKCTGDAAFCSAYECTAQYANAYCSHANGSGIVQIQVSGVWKKPLCVGYERVVVKRELSAKPIQRVEPCTTCITKCEP
M127_09 : IGGHGSKKCTGDAAFCSAYECTAQYANAYCSHANGSGIVQIQVSGVWKKPLCVGYERVVVKRELSAKPIQRVEPCTTCITKCEP
M260_09 : IGGHGSKKCTGDAAFCSAYECTAQYANAYCSHANGSGIVQIQVSGVWKKPLLCGYERVVVKRELSAKPIQRVEPCTTCITKCEP
M21_10  : IGGHGSKKCTGDAAFCSAYECTAQYANAYCSHANGSGIVQIQVSGVWKKPLCVGYERVVVKRELSAKPIQRVEPCTTCITKCEP
M247_09 : IGGHGSKKCTGDAAFCSAYECTAQYANTYCSHANGSGIVQIQVSGVWKKPLCVGYERVVVKRELSAKPIQRVEPCTTCITKCEP
M33_10  : IGGHGSKKCTGDAAFCSAYECTAQYANAYCSHANGSGIVQIQVSGVWKKPLCVGYERVVVKRELSAKPIQRVEPCTTCITKCEP

ZH501   : HGLVVRSTGFKISSAVACASGVCVTGSQSPSTEITLKYPGISQSSGGDIGVHMAHDDQSVSSKIVAHCPPQDPCLVHGCIVCAH
M066_09 : HGLVVRSTGFKISSAVACASGVCVTGSQSPSTEITLKYPGISQSSGGDIGVHMAHDDQSVSSKIVAHCPPQDPCLVHGCIVCAH
M127_09 : HGLVVRSTGFKISSAVACASGVCVTGSQSPSTEITLKYPGISQSSGGDIGVHMAHDDQSVSSKIVAHCPPQDPCLVHGCIVCAH
M260_09 : HGLVVRSTGFKISSAVACASGVCVTGSQSPSTEITLKYPGISQSSGGDIGVHMAHDDQSVSSKIVAHCPPQDPCLVHGCIVCAH
M21_10  : HGLVVRSTGFKISSAVACASGVCVTGSQSPSTEITLKYPGISQSSGGDIGVHMAHDDQSVSSKIVAHCPPQDPCLVHGCIVCAH
M247_09 : HGLVVRSTGFKISSAVACASGVCVTGSQSPSTEITLKYPGISQSSGGDIGVHMAHDDQSVSSKIVAHCPPQDPCLVHGCIVCAH
M33_10  : HGLVVRSTGFKISSAVACASGVCVTGSQSPSTEITLKYPGISQSSGGDIGVHMAHDDQSVSSKIVAHCPPQDPCLVHGCIVCAH

ZH501   : GLINYQCHTALSAFVVVFVFSSIAIICLAVLYRVLKCLKIAPRKVLNPLMWITAFIRWTYKKMVARVADNINQVNREIGWMEGG
M066_09 : GLINYQCHTALSAFVVTFVFSSTAIICLAVLYRVLKCLKIAPRKVLNPLMWITAFIRWVYKKMVARVADNINQVNREIGWMEGG
M127_09 : GLINYQCHTALSAFVVVFVFSSIAIICLAILYRVLKCLKIAPRKVLNPLMWITAFIRWVYKKMVARVADNINQVNREIGWMEGG
M260_09 : GLINYQCHTALSAFVVVFVFSSIAIICLAILYRVLKCLKIAPRKVLNPLMWITAFIRWVYKKMVARVADNINQVNREIGWMEGG
M21_10  : GLINYQCHTALSAFVVVFVFSSIAIICLAILYRVLKCLKIAPRKVLNPLMWITAFIRWVYKKMVARVADNINQVNREIGWMEGG
M247_09 : GLINYQCHTALSAFVVVFVFSSIAIICLAILYRVLKCLKIAPRKVLNPLMWITAFIRWVYKKMVARVADNINQVNREIGWMEGG
M33_10  : GLINYQCHTALSAFVVVFVFSSIAIICLAILYRVLKCLKIAPRKVLNPLMWITAFIRWVYKKMVARVADNINQVNREIGWMEGG

ZH501   : QLVLGNPAPIPRHAPIPRYSTYLMLLLIVSYASA
M066_09 : QLALGNPAPIPRHAPIPRYSTYLMLLLIVSYASA
M127_09 : QLVLGNPAPIPRHAPIPRYSTYLMLLLIVSYASA
M260_09 : QLVLGNPAPIPRHAPIPRYSTYLMLLLIVSYASA
M21_10  : QLVLGNPAPIPRHAPIPRYSTYLMLLLIVSYASA
M247_09 : QLVLGNPAPIPRHAPIPRYSTYLMLLLIVSYASA
M33_10  : QLVLGNPAPIPRHAPIPRYSTYLMLLLIVSYASA
```

Figure 3.13: Alignment of the Gn protein. Residues that differ from the majority consensus are shaded in black, while the majority are shaded in grey.

Substitutions that occur on the Gc domain of the field isolates include D297E, S369T and T441I as compared to ZH501 strain (Figure 3.14). These positions do not impact fusion loop function but occur in domain III. These substitutions are not expected to play a major role in virus entry or host receptor interaction.

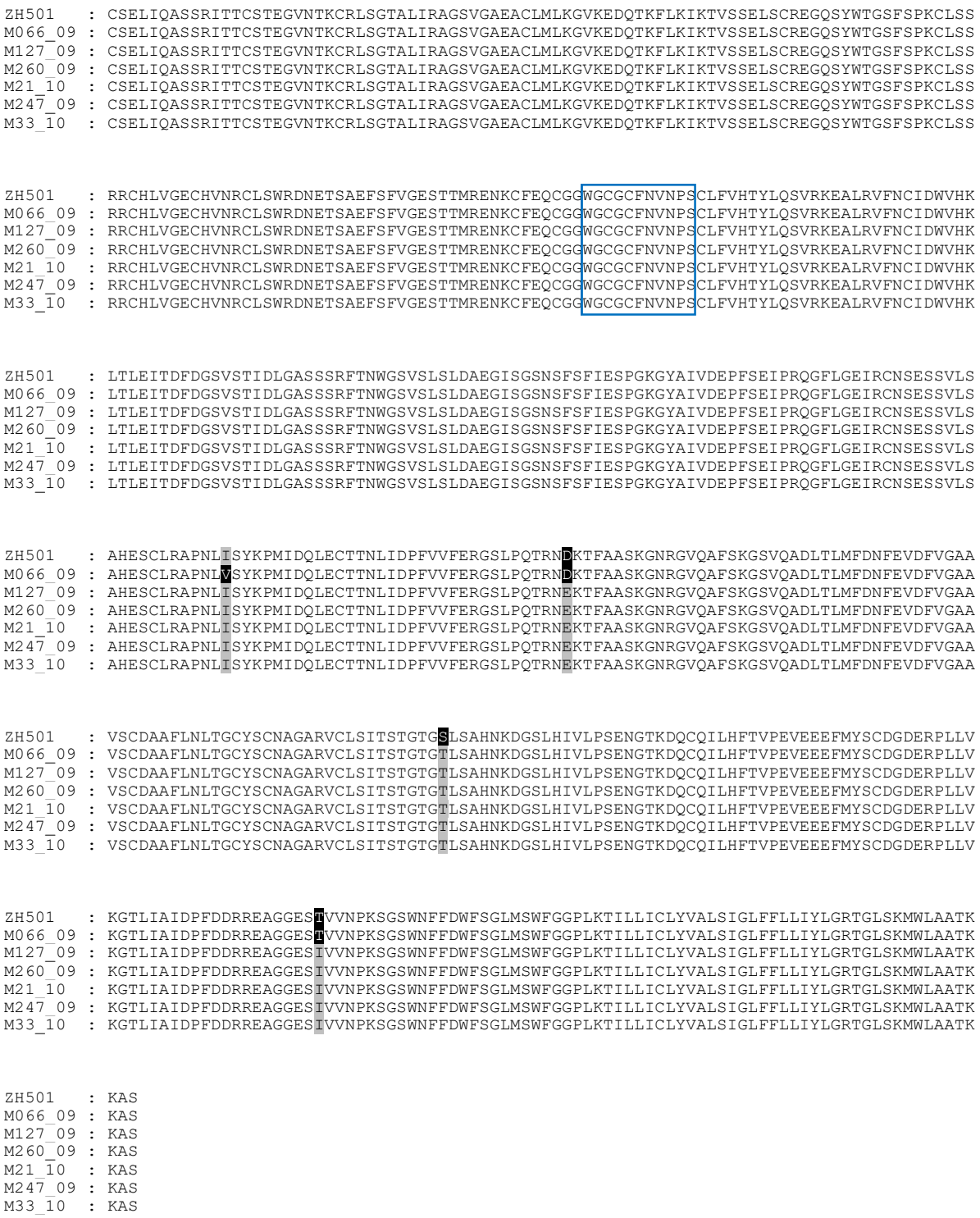

Figure 3.14: Alignment of the Gc protein. Residues that differ from the majority consensus are shaded in black, while the majority are shaded in grey. The fusion loop is indicated with a dark blue box.

The S segment

The S segment encodes two proteins in opposite directions; the nucleoprotein (NP) and the non-structural protein (NSs). Only one amino acid substitution (G159E) was found in the NP of all the six field isolates when compared to the ZH501 reference strain (Figure 3.15).

```
ZH501 : MDNYQELAIQFAAQAVDRNEIEQWVREFAYQGFDARRVIELLKQYGGADWEKDAKKMIVLALTRGNKPRRMMMKMSKEGKATVEAL
M066  : MDNYQELAIQFAAQAVDRNEIEQWVREFAYQGFDARRVIELLKQYGGADWEKDAKKMIVLALTRGNKPRRMMMKMSKEGKATVEAL
M260  : MDNYQELAIQFAAQAVDRNEIEQWVREFAYQGFDARRVIELLKQYGGADWEKDAKKMIVLALTRGNKPRRMMMKMSKEGKATVEAL
M247  : MDNYQELAIQFAAQAVDRNEIEQWVREFAYQGFDARRVIELLKQYGGADWEKDAKKMIVLALTRGNKPRRMMMKMSKEGKATVEAL
M127  : MDNYQELAIQFAAQAVDRNEIEQWVREFAYQGFDARRVIELLKQYGGADWEKDAKKMIVLALTRGNKPRRMMMKMSKEGKATVEAL
M21   : MDNYQELAIQFAAQAVDRNEIEQWVREFAYQGFDARRVIELLKQYGGADWEKDAKKMIVLALTRGNKPRRMMMKMSKEGKATVEAL
M33   : MDNYQELAIQFAAQAVDRNEIEQWVREFAYQGFDARRVIELLKQYGGADWEKDAKKMIVLALTRGNKPRRMMMKMSKEGKATVEAL


ZH501 : INKYKLKEGNPSRDELTLSRVAAALAGWTCQALVVLSEWLPVTGTTMDGLSPAYPRHMMHPSFAGMVDPSLPGDYLRAILDAHSLY
M066  : INKYKLKEGNPSRDELTLSRVAAALAGWTCQALVVLSEWLPVTGTTMDGLSPAYPRHMMHPSFAGMVDPSLPEDYLRAILDAHSLY
M260  : INKYKLKEGNPSRDELTLSRVAAALAGWTCQALVVLSEWLPVTGTTMDGLSPAYPRHMMHPSFAGMVDPSLPEDYLRAILDAHSLY
M247  : INKYKLKEGNPSRDELTLSRVAAALAGWTCQALVVLSEWLPVTGTTMDGLSPAYPRHMMHPSFAGMVDPSLPEDYLRAILDAHSLY
M127  : INKYKLKEGNPSRDELTLSRVAAALAGWTCQALVVLSEWLPVTGTTMDGLSPAYPRHMMHPSFAGMVDPSLPEDYLRAILDAHSLY
M21   : INKYKLKEGNPSRDELTLSRVAAALAGWTCQALVVLSEWLPVTGTTMDGLSPAYPRHMMHPSFAGMVDPSLPEDYLRAILDAHSLY
M33   : INKYKLKEGNPSRDELTLSRVAAALAGWTCQALVVLSEWLPVTGTTMDGLSPAYPRHMMHPSFAGMVDPSLPEDYLRAILDAHSLY


ZH501 : LLQFSRVINPNLRGRTKEEVAATFTQPMNAAVNSNFISHEKRREFLKAFGLVDSNGKPSAAVMAAAQAYKTAA
M066  : LLQFSRVINPNLRGRTKEEVAATFTQPMNAAVNSNFISHEKRREFLKAFGLVDSNGKPSAAVMAAAQAYKTAA
M260  : LLQFSRVINPNLRGRTKEEVAATFTQPMNAAVNSNFISHEKRREFLKAFGLVDSNGKPSAAVMAAAQAYKTAA
M247  : LLQFSRVINPNLRGRTKEEVAATFTQPMNAAVNSNFISHEKRREFLKAFGLVDSNGKPSAAVMAAAQAYKTAA
M127  : LLQFSRVINPNLRGRTKEEVAATFTQPMNAAVNSNFISHEKRREFLKAFGLVDSNGKPSAAVMAAAQAYKTAA
M21   : LLQFSRVINPNLRGRTKEEVAATFTQPMNAAVNSNFISHEKRREFLKAFGLVDSNGKPSAAVMAAAQAYKTAA
M33   : LLQFSRVINPNLRGRTKEEVAATFTQPMNAAVNSNFISHEKRREFLKAFGLVDSNGKPSAAVMAAAQAYKTAA
```

Figure 3.15: Alignment of the S segment nucleoprotein. Residues that differ from the majority consensus are shaded in black, while the majority are shaded in grey.

The NSs of the field isolates had five amino acid substitutions (F23I, A167V, V217A, I242V and E251D) as compared to the reference strain. In addition to these substitutions, M66/09 had four other substitutions (K24R, K108R, K202R and E253G) (Figure 3.16). All substitutions are conserved and all isolates possess the essential motifs identified for NSs functions. The substitutions in the S segment would not seem to be adequate to explain the differences observed in the growth curves. The majority of the substitutions are not linked to any active site residues. They may affect functions through steric hindrance or long-distance interactions, but no clear linkage could be found.

```
ZH501 : MDYFPVISVDLQSGRRVVSVEYFRGDGPPRIPYSMVGPCCVFLMHHRPSHEVRLRFSDFYNVGEFPYRVGLGDFASNVAPPPAKPF
M066  : MDYFPVISVDLQSGRRVVSVEYIKGDGPPRIPYSMVGPCCVFLMHHRPSHEVRLRFSDFYNVGEFPYRVGLGDFASNVAPPPAKPF
M127  : MDYFPVISVDLQSGRRVVSVEYIRGDGPPRIPYSMVGPCCVFLMHHRPSHEVRLRFSDFYNVGEFPYRVGLGDFASNVAPPPAKPF
M247  : MDYFPVISVDLQSGRRVVSVEYIRGDGPPRIPYSMVGPCCVFLMHHRPSHEVRLRFSDFYNVGEFPYRVGLGDFASNVAPPPAKPF
M260  : MDYFPVISVDLQSGRRVVSVEYIRGDGPPRIPYSMVGPCCVFLMHHRPSHEVRLRFSDFYNVGEFPYRVGLGDFASNVAPPPAKPF
M21   : MDYFPVISVDLQSGRRVVSVEYIRGDGPPRIPYSMVGPCCVFLMHHRPSHEVRLRFSDFYNVGEFPYRVGLGDFASNVAPPPAKPF
M33   : MDYFPVISVDLQSGRRVVSVEYIRGDGPPRIPYSMVGPCCVFLMHHRPSHEVRLRFSDFYNVGEFPYRVGLGDFASNVAPPPAKPF

ZH501 : QRLIDLIGHMTLSDFTRFPNLKEAISWPLGEPSLAFFDLSSTRVHRNDDIRRDQIATLAMRSCKITNDLEDSFVGLHRMIATEAIL
M066  : QRLIDLIGHMTLSDFTRFPNLREAISWPLGEPSLAFFDLSSTRVHRNDDIRRDQIATLAMRSCKITNDLEDSFVGLHRMIVTEAIL
M127  : QRLIDLIGHMTLSDFTRFPNLKEAISWPLGEPSLAFFDLSSTRVHRNDDIRRDQIATLAMRSCKITNDLEDSFVGLHRMIVTEAIL
M247  : QRLIDLIGHMTLSDFTRFPNLKEAISWPLGEPSLAFFDLSSTRVHRNDDIRRDQIATLAMRSCKITNDLEDSFVGLHRMIVTEAIL
M260  : QRLIDLIGHMTLSDFTRFPNLKEAISWPLGEPSLAFFDLSSTRVHRNDDIRRDQIATLAMRSCKITNDLEDSFVGLHRMIVTEAIL
M21   : QRLIDLIGHMTLSDFTRFPNLKEAISWPLGEPSLAFFDLSSTRVHRNDDIRRDQIATLAMRSCKITNDLEDSFVGLHRMIVTEAIL
M33   : QRLIDLIGHMTLSDFTRFPNLKEAISWPLGEPSLAFFDLSSTRVHRNDDIRRDQIATLAMRSCKITNDLEDSFVGLHRMIVTEAIL

ZH501 : RGIDLCLLPGFDLMYEVAHVQCVRLLQAAKEDISNAVVPNSALIVLMEESLMLRSSLPSMMGRNNWIPVIPPIPDVEMPSEEESDD
M066  : RGIDLCLLPGFDLMYEVAHVQCVRLLQAAREDISNAVVPNSALIALMEESLMLRSSLPSMMGRNNWIPVVPPIPDVEMPSGEESDD
M127  : RGIDLCLLPGFDLMYEVAHVQCVRLLQAAKEDISNAVVPNSALIALMEESLMLRSSLPSMMGRNNWIPVVPPIPDVEMDSEEESDD
M247  : RGIDLCLLPGFDLMYEVAHVQCVRLLQAAKEDISNAVVPNSALIALMEESLMLRSSLPSMMGRNNWIPVVPPIPDVEMDSEEESDD
M260  : RGIDLCLLPGFDLMYEVAHVQCVRLLQAAKEDISNAVVPNSALIALMEESLMLRSSLPSMMGRNNWIPVVPPIPDVEMDSEEESDD
M21   : RGIDLCLLPGFDLMYEVAHVQCVRLLQAAKEDISNAVVPNSALIALMEESLMLRSSLPSMMGRNNWIPVVPPIPDVEMDSEEESDD
M33   : RGIDLCLLPGFDLMYEVAHVQCVRLLQAAKEDISNAVVPNSALIALMEESLMLRSSLPSMMGRNNWIPVVPPIPDVEMDSEEESDD

ZH501 : DGFVEVD
M066  : DGFVEVD
M127  : DGFVEVD
M247  : DGFVEVD
M260  : DGFVEVD
M21   : DGFVEVD
M33   : DGFVEVD
```

Figure 3.16: Alignment of the S segment non-structural protein. Residues that differ from the majority consensus are shaded in black, while the majority are shaded in grey.

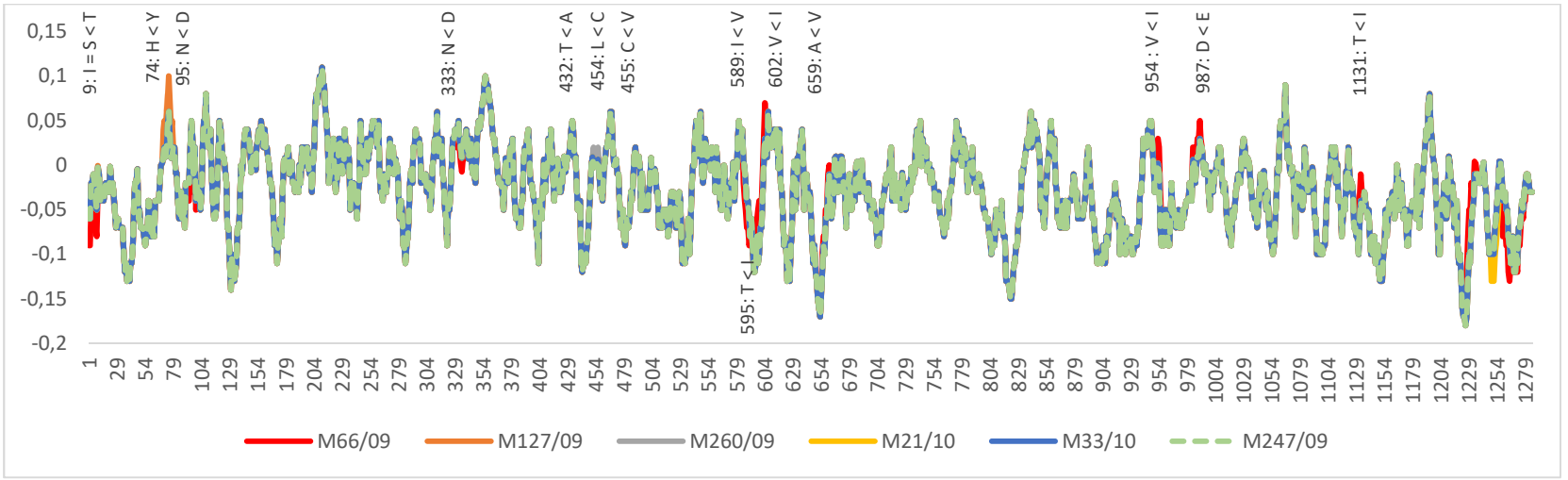

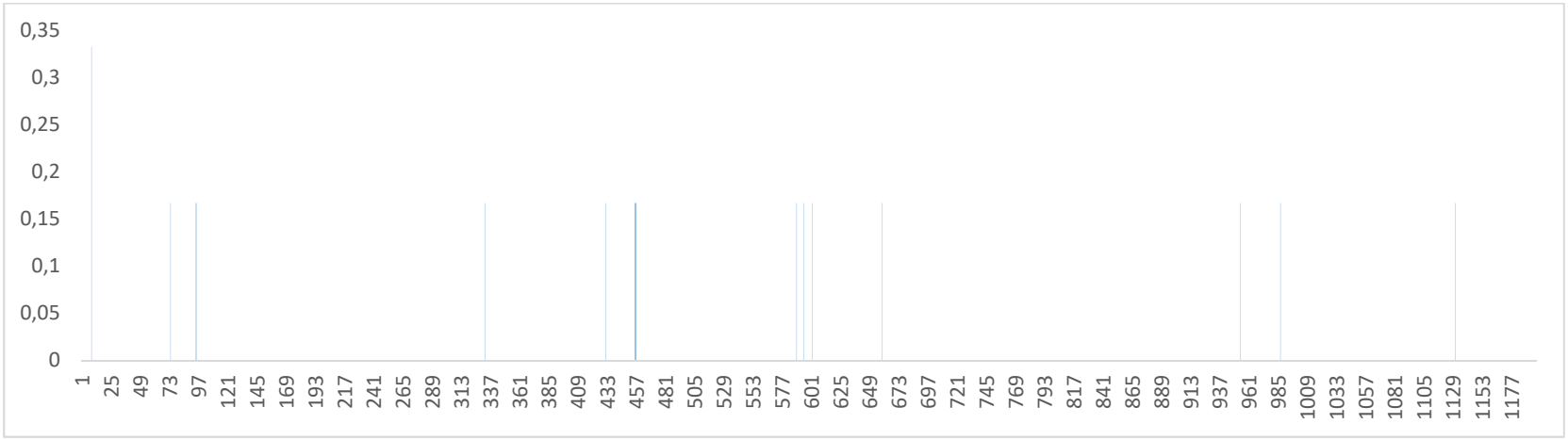

Figure 3.17: Welling antigenicity plots of the six isolates for the M segment. Differences in amino acids between these isolates are indicated on top of the plots. The lines show the positions where major amino acid changes are observed.

3.3.8 Protein structure modelling

Protein structures of Gn and Gc were predicted to determine whether gross structural changes could have occurred that would explain the phenotypic differences in the growth curves. The Phyre2 server was used in the normal mode of modelling. The models for Gn and Gc were obtained by homology modelling using the experimental structures of Gn and Gc that exist in the Protein Databank. The models agreed with alignments found using other fold recognition methods, thereby increasing our confidence in the fold predictions. The Gn models predicted in the study based on the published structure (c5y0yA) (Wu *et al*., 2017; Halldorsson *et al*., 2018) are shown in Figure 3.18A and B. Superposition of the 3-D structures predicted were the same for all the Gn structures of the different isolates (Figure 3.18A). The root mean square deviation (RSMD) value between the models was 0.002, while RMSD value of the models versus the template was 0.065 (Figure 3.18A and B; structures A and B respectively). Alignment of the template (c5y0yA) and the sequences used in the study showed that 289 amino acid residues (54% of the sequence) were modelled with 100% confidence and 99% identity. The secondary and predicted structures predicted using Phyre2, suggested the following percentages: disordered = 29%, alpha helix = 33%, beta strand = 29% and transmembrane helix = 12%. The low RMSD values for the superimposed structures suggest that Gn from all isolates would have the same overall backbone structure, with a very similar orientation of the side chain residues.

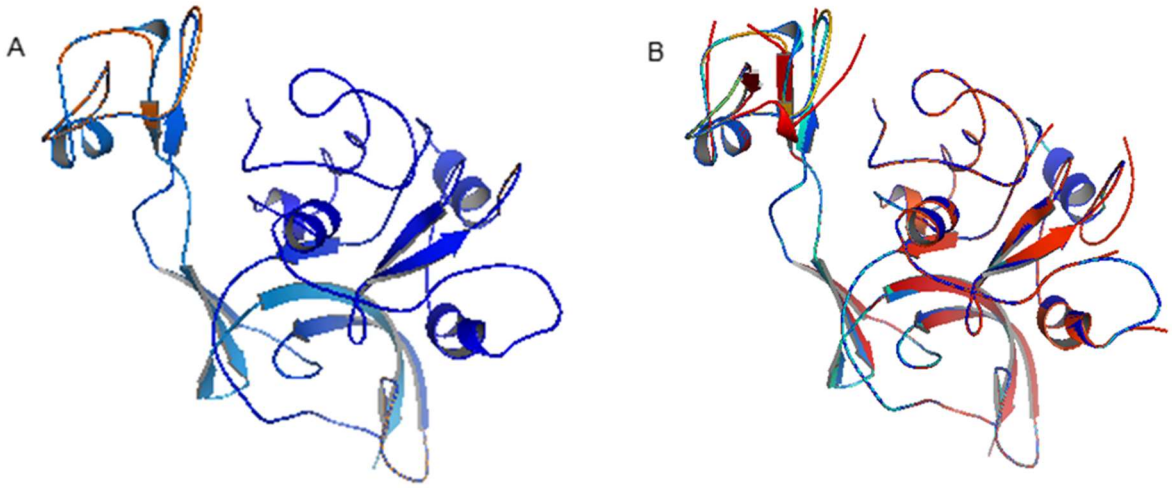

Figure 3.18A and B: The three-dimensional structure models of RVFV Gn protein. Figure A shows the modelled Gn protein structures of six isolates: M21/10, M33/10, M66/09, M127/09, M260/09 and M247/09 superimposed with a mean RMSD of 0.02. Figure B shows Gn protein structures of the six isolates superimposed with the template c5y0yA with a mean RMSD of 0.065.

Since some of the substitutions observed did not localize within known structural regions, but lie closer to the membrane regions, the predictions of membrane topology were also performed to assess whether isolates may differ in this. The TOPCONS consensus server predicted the topology of the Gn protein having three transmembrane helices at positions 430-450, 462-482 and 516-536 (data not shown). The results obtained were not considered reliable for Gn topology; therefore, an additional server; OCTOPUS (http://octopus.cbr.su.se) was used to predict the Gn topology (Viklund and Elofsson; 2008). In this server, residue preference scores derived from sequence profiles and artificial neural networks (ANNs) are combined into a final topology (Viklund and Elofsson; 2008). The OCTOPUS server predicted that the Gn protein has two transmembrane regions towards the end of the amino acid sequence (Figure 3.19). The results obtained using this server correspond with those previously published and this increased our confidence (Rusu *et al*., 2012; Halldorsson *et al*., 2018).

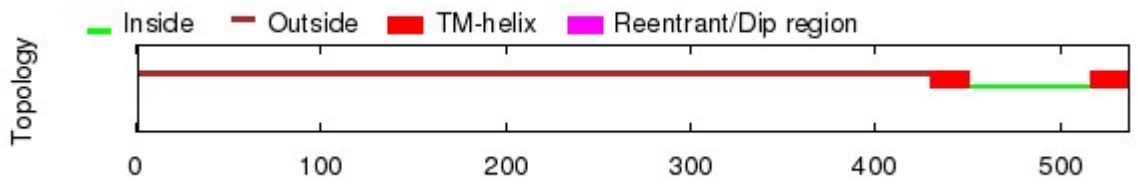

Figure 3.19: The topology prediction of Gn protein. The summary was taken from the server (http://octopus.cbr.su.se) with its explanatory colouring key at the top. Green indicates inside, brown indicates outside, red indicates the transmembrane helix, purple indicates dip region which is not present in this topology.

A number of the substitution differences observed between M66/09 and the other five isolates (V589I, I595T, I602V, and V659A) occur outside the membrane regions, presumably within the cytoplasmic tail. These may have an impact on viral assembly, especially the I595T substitution that may be considered nonconserved.

The Gc models were modelled on the existing structure of c4hj1A from the RCSB Protein Databank (Dessau and Modis, 2013). Like the Gn, the 3-D structures of Gc modelled were similar for all the isolates (Figure 3.20A and B). The RSMD value for the models was 0.000, while RMSD value of the models versus the template was 0.001 (Figure 3.20A and B; structures A and B respectively). Alignment of the top template and the protein sequences of the isolates used in the study showed that 428 amino acid residues (84% of our sequence)

were modelled with 100% confidence and 100% identity. The substitution of amino acids at positions 297 (D>E) and 369 (S>T) within the isolates sequences did not have an effect on the modelling confidence. The secondary structure and predicted structure suggested the following percentages: disordered = 33%, alpha helix = 9%, beta strand = 56% and transmembrane helix = 6%. The low RMSD values suggest that all of the isolate structures would be close to identical.

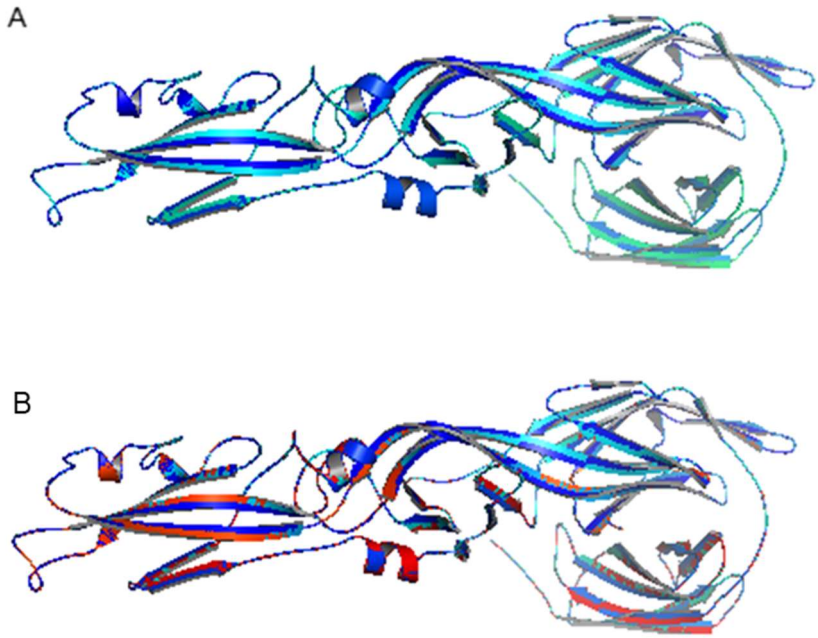

Figure 3.20A and B: The three dimensional structure models of RVFV Gc protein. Figure A shows the modelled Gc protein structures of six isolates: M21/10, M33/10, M66/09, M127/09, M260/09 and M247/09 superimposed with a mean RMSD of 0.000. Figure B shows Gc protein structures of the six isolates superimposed with the template c4hj1A with a mean RMSD of 0.001.

The predicted topology of the Gc protein using the different methods agreed with each other about the final topology results (Figure 3.21A and B). All the methods used, identified one transmembrane helix (462-492) from the membrane inside to the outside even though the identified regions differ slightly. From both topology predictions, no signal peptide region was identified using the TOPCONS consensus. Phyre2 server predicted Gc topology anchoring a signal peptide from region 1 to 25 at the N-terminal (Figure 3.21C). The transmembrane helix identified by Phyre2 is at the same region as the one identified by the method SPOCTPUS of the TOPCONS (from 463 to 493). Prediction of the Gc protein structure using the OCTOPUS server indicated that the there is only one transmembrane region on the protein structure (Figure 3.21D). The topology results obtained using different servers in this study correspond with each other and with those published (Dessau and Modis; 2013).

All substitution differences between M66/09 and the other five isolates occur on the external domain and not in the cytoplasmic tail as predicted by the topology server. Beyond the potential amino acid differences in the cytoplasmic tails, structural modelling did not suggest that the three-dimensional structures would differ significantly. Since these are static models, they may not reveal substitutions that have a destabilizing effect on the structures.

A

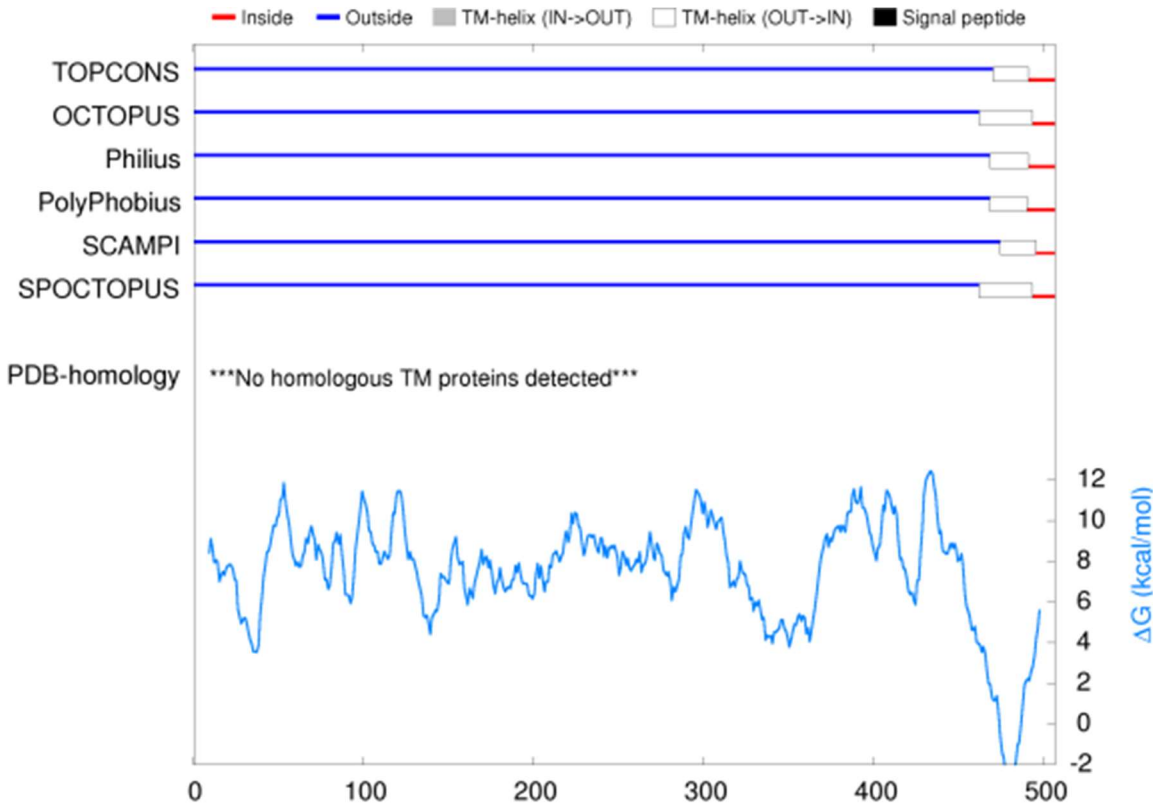

B

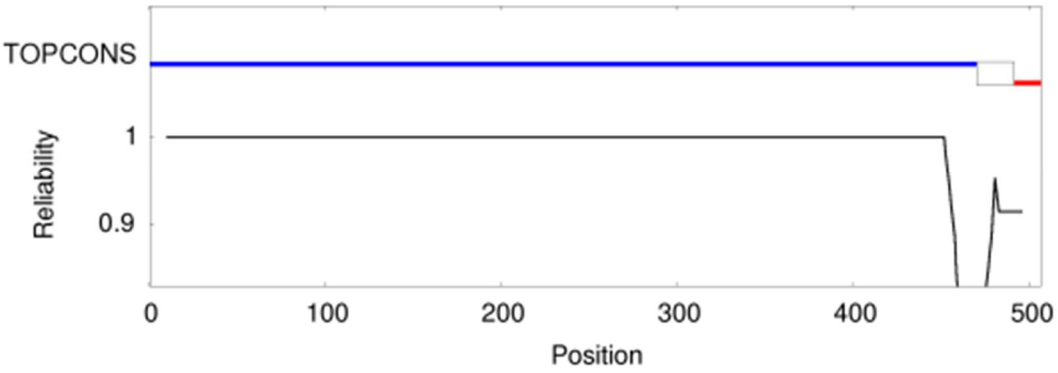

Figure 3.21A and B: The topology prediction of the Gc protein. Figure A shows the summary of the TOPCONS predictions including the individual methods (identified by the names of the methods on the left side). The summary was taken from the server with its explanatory colouring key at the top (http://topcons.net). Blue and red lines indicate outside and inside, respectively, while boxes indicate transmembrane regions. The predicted ΔG values across the sequence are on the right side. Figure B is considered the most probable reliable prediction.

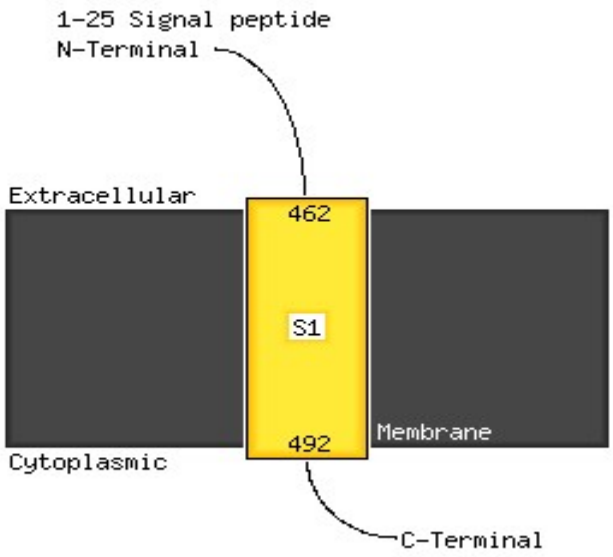

Figure 3.21C: Predicted topology of the transmembrane helix of the sequence of the Gc glycoprotein. The extracellular and cytoplasmic sides of the membrane and the beginning and end of the transmembrane helix are indicated. The numbers indicate the residue indexes.

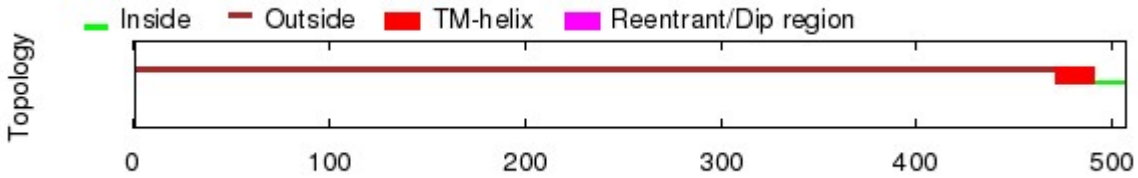

Figure 3.21 D: The topology prediction of Gc protein. The summary was taken from the server (http://octopus.cbr.su.se) with its explanatory colouring key at the top. Green indicates inside, brown indicates outside, red indicates the transmembrane helix, purple indicates dip region which is not present in this topology.

3.3.9 Relationship between codon usage patterns of RVFV and their hosts

While no significant differences could be detected at the amino acid substitution level that may explain the differences observed in the growth curves, adaptation of viruses to specific hosts may be due to codon usage bias. In order to understand the relationship of codon usage bias of virus isolates, the codon usage bias of the coding sequences of the six isolates were compared with their hosts (bovine, ovine and hamster). The results showed that the codon usage patterns of selected RVFV isolates were a mixture of correspondence and bias to their

hosts; which means that some codon usage patterns of the isolates correspond with those of the hosts (15.3%), while others were not corresponding (49%) (Table 3.3). All host codon preferences were similar between bovine, ovine and hamster, except for CAU (His) that showed a much higher prevalence in sheep. However, no difference for codon usage for this codon was observed between the isolates. The preferred codons for 9 out of the 38 were common for selected RVFV and its hosts. These included CUG (Leu), GUG (Val), AGC (Ser), ACC (Thr), CAG (Gln), AAC (Asn), UGC (Cys), CGC (Arg) and GGC (Gly). All common preferred codons between isolates and their hosts were G/C-ended (three ending with G and six ending with C). All the preferred codons were the same for all isolates. Codons that differed in usage between virus and host, included UUU (Phe) preferred by the isolates and UUC (Phe) preferred by the hosts. The same is seen for CCG (Pro) preferred by the isolates, while CCU, CCC and CCA (Pro) are preferred by the hosts. Similarly, GCG (Ala) is preferred by the isolates, while GCU and GCC (Ala) are preferred by the hosts.

Isolates also preferred UAU (Tyr), while the hosts preferred UAC (Tyr). Isolates preferred CAU (His) and AAA (Lys), while hosts preferred CAC (His) and AAG (Lys). Isolates also preferred GAU (Asp) and GAA (Glu), while hosts preferred GAC (Asp) and GAG (Glu). While no clear codon bias differences on preferences is evident between isolates and their respective hosts, it may still be possible that the subtle differences that exist between isolates could impact on translation efficiency in the host.

Table 3.3. The relative synonymous codon usage (RSCU) patterns of RVFV and its hosts.

AA	Codon	RVFV isolates						Hosts		
		RVFV (M66/09)	RVFV (M127/09)	RVFV (M260/09)	RVFV (M21/10)	RVFV (M33/10)	RVFV (M247/09)	Bovine *Bt*	Sheep *Oa*	Hamster *Ma*
Phe	UUU	**1.899***	**1.899***	**1.899***	**1.966***	**1.966***	**1.933***	0.83	0.94	0.82
	UUC	0.101	0.101	0.101	0.034	0.034	0.067	**1.15***	**1.06***	**1.18***
Leu	UUA	0.068	0.051	0.051	0.034	0.034	0.017	0.37	0.24	0.32
	UUG	0.119	0.120	0.120	0.069	0.069	0.051	0.71	0.49	0.79
	CUU	0.170	0.154	0.154	0.051	0.051	0.103	0.71	0.74	0.75
	CUC	0.119	0.137	0.137	0.051	0.051	0.086	**1.26***	**1.8***	**1.22***
	CUA	0.170	0.137	0.137	0.086	0.086	0.051	0.36	0.24	0.41
	CUG	**5.352***	**5.400***	**5.402***	**5.709***	**5.709***	**5.691***	**2.58***	**2.46***	**2.50***
Ile	AUU	**2.833***	**2.819***	**2.819***	**2.944***	**2.944***	**2.861***	0.98	0.63	1.02
	AUC	0.083	0.097	0.097	0.042	0.042	0.069	**1.57***	**1.74***	**1.57***
	AUA	0.083	0.083	0.083	0.014	0.014	0.069	0.46	0.63	0.41
Val	GUU	0.287	0.270	0.271	0.063	0.063	0.206	0.6	0.46	0.60
	GUC	0.143	0.159	0.159	0.095	0.095	0.063	**1.01***	0.91	**1.04***
	GUA	0.032	0.032	0.032	0.000	0.000	0.032	0.40	0.36	0.42
	GUG	**3.538***	**3.540***	**3.538***	**3.841***	**3.841***	**3.698***	**1.95***	**2.27***	**1.94***
Ser	UCU	0.142	0.141	0.141	0.053	0.053	0.088	**1.04***	**0.91**	**1.16***
	UCC	0.089	0.088	0.088	0.053	0.053	0.035	**1.37***	**1.27***	**1.39***
	UCA	0.160	0.158	0.159	0.035	0.035	0.124	0.79	0.52	0.80
	UCG	0.018	0.018	0.018	0.018	0.018	0.000	0.40	0.30	0.31
	AGU	0.089	0.088	0.088	0.018	0.018	0.071	0.87	**1.48***	0.70
	AGC	**5.503***	**5.507***	**5.506***	**5.824***	**5.824***	**5.682***	**1.53***	**1.58***	**1.45***
Pro	CCU	0.337	0.335	0.336	0.120	0.120	0.216	**1.08***	**1.27***	**1.19***
	CCC	0.120	0.120	0.120	0.024	0.024	0.096	**1.40***	**1.29***	**1.31***
	CCA	0.289	0.287	0.287	0.096	0.096	0.192	**1.00***	**1.03***	**1.14***
	CCG	**3.253***	**3.257***	**3.257***	**3.760***	**3.760***	**3.497***	0.53	0.42	0.37
Thr	ACU	0.178	0.178	0.177	0.110	0.110	0.066	0.89	0.78	0.95
	ACC	**3.689***	**3.689***	**3.691***	**3.779***	**3.779***	**3.912***	**1.55***	**2.05***	**1.54***
	ACA	0.089	0.089	0.088	0.066	0.066	0.022	**1.00***	0.78	**1.11***
	ACG	0.044	0.044	0.044	0.044	0.044	0.000	0.56	0.38	0.41
Ala	GCU	0.353	0.323	0.323	0.258	0.258	0.065	**1.00***	**1.19***	**1.16***
	GCC	0.145	0.177	0.177	0.113	0.113	0.065	**1.71***	**1.55***	**1.63***
	GCA	0.241	0.242	0.242	0.145	0.145	0.097	0.80	0.90	0.87

	GCG	**3.258***	**3.258***	**3.258***	**3.484***	**3.484***	**3.773***	0.48	0.37	0.35
Tyr	UAU	**1.891***	**1.909***	**1.910***	**1.964***	**1.964***	**1.946***	0.79	0.72	0.84
	UAC	0.109	0.091	0.090	0.036	0.036	0.054	**1.21***	**1.28***	**1.17***
His	CAU	**1.848***	**1.870***	**1.868***	**1.956***	**1.956***	**1.912***	0.76	**2.15***	0.80
	CAC	0.152	0.130	0.132	0.044	0.044	0.088	**1.25***	0.92	**1.20***
Gln	CAA	0.052	0.069	0.069	0.052	0.052	0.017	0.46	0.57	0.47
	CAG	**1.948***	**1.931***	**1.931***	**1.948***	**1.948***	**1.983***	**1.54***	**1.43***	**1.53***
Asn	AAU	0.138	0.144	0.143	0.071	0.071	0.071	0.81	0.49	0.82
	AAC	**1.862***	**1.856***	**1.857***	**1.929***	**1.929***	**1.929***	**1.18***	**1.51***	**1.19***
Lys	AAA	**1.870***	**1.870***	0.870	**1.887***	**1.887***	**1.983***	0.79	0.68	0.72
	AAG	0.130	0.130	0.130	0.113	0.113	0.017	**1.22***	**1.32***	**1.28***
Asp	GAU	**1.876***	**1.888***	**1.888***	**1.944***	**1.944***	**1.944***	0.84	0.66	0.82
	GAC	0.124	0.112	0.112	0.056	0.056	0.056	**1.16***	**1.34***	**1.18***
Glu	GAA	**1.839***	**1.823***	**1.823***	**1.919***	**1.919***	**1.903***	0.78	0.75	0.78
	GAG	0.161	0.177	0.177	0.081	0.081	0.097	**1.22***	**1.25***	**1.22***
Cys	UGU	0.055	0.055	0.055	0.000	0.000	0.055	0.85	0.72	0.85
	UGC	**1.945***	**1.945***	**1.942***	**2.000***	**2.000***	**1.945***	**1.15***	**1.28***	**1.15***
Arg	CGU	0.149	0.149	0.149	0.059	0.059	0.089	0.49	0.82	0.56
	CGC	**4.990***	**5.020***	**5.020***	**5.554***	**5.554***	**5.465***	**1.18***	**1.15***	**1.08***
	CGA	0.149	0.149	0.149	0.089	0.089	0.059	0.68	0.88	0.72
	CGG	0.119	0.089	0.089	0.089	0.089	0.000	**1.32***	0.87	**1.12***
	AGA	0.297	0.238	0.238	0.089	0.089	0.149	**1.13***	**1.13***	**1.26***
	AGG	0.297	0.356	0.356	0.119	0.119	0.238	**1.21***	**1.16***	**1.27***
Gly	GGU	0.086	0.069	0.069	0.034	0.034	0.034	0.63	0.92	0.71
	GGC	**3.657***	**3.672***	**3.672***	**3.862***	**3.862***	**3.810***	**1.43***	**1.33***	**1.30***
	GGA	0.086	0.086	0.086	0.000	0.000	0.086	0.95	**1.05***	**1.02***
	GGG	0.172	0.172	0.172	0.103	0.103	0.069	0.98	0.71	0.98

Abbreviations: AA – amino acid; *Bt – Bos Taurus; Oa - Ovies aries*; *Ma – Mesocricetus auratus*. The preferred codons (RSCU>1) are shown in bold and a star.

The codon adaptation index (CAI) and the estimated codon adaptation index (CAI) values of all ORFs for all segments were calculated (with the E-CAI server) using the codon usage tables for hamster, bovine and ovine and the normalised CAI values were obtained for each segment (Table 3.4). A score for each ORF was calculated using the CAI, which indicates the level of gene expression. The CAI values from 0.75 to 1.0 indicate a high gene expression whereas the CAI value less than 0.75 indicates low gene expression. The CAI values of all the ORFs of the 3 segments of the isolates ranged from 0.671 to 0.735 in relation to hamster, while in relation to bovine/ovine, the CAI value of genes of isolates from bovine were higher (ranging from 0.720 to 0.762) than those of isolates from ovine (ranging from 0.687 to 0.716). The calculated normalized CAI value of genes of isolates from bovine were close to 1 and higher than those of ovine (Table 3.4), indicating codon usage adaptation towards the host.

Table 3.4. Codon usage pattern observed for RVFV glycoproteins and its relationship to potential hosts

Isolate			Hamster (*Mesocricetus auratus*)			Bovine (*Bos taurus*)		
	Protein (ORF)	Length	CAI	eCAI	CAI/eCAI	CAI	eCAI	CAI/eCAI
M66/09	L	6276	0.733	0.762	0.962	0.757	0.760	0.996
	M	3591	0.735	0.762	**0.965**	0.762	0.760	**1.002**
	S	1530	0.687	0.762	0.902	0.721	0.760	**0.949**
M127/09	L	6276	0.733	0.762	0.962	0.757	0.760	0.996
	M	3591	0.734	0.762	0.963	0.762	0.760	**1.000**
	S	1530	0.687	0.762	0.902	0.720	0.760	0.947
M260/09	L	6276	0.733	0.762	0.962	0.757	0.760	0.997
	M	3591	0.734	0.762	0.963	0.762	0.760	**1.000**
	S	1530	0.687	0.762	0.902	0.720	0.760	0.947
			Hamster (*Mesocricetus auratus*)			Ovine (*Ovis aries*)		
M21/10	L	6276	0.731	0.762	0.959	0.703	0.745	0.943
	M	3591	0.734	0.762	0.963	0.715	0.745	0.960
	S	1530	0.671	0.762	0.881	0.688	0.745	0.923
M33/10	L	6276	0.733	0.762	0.962	0.704	0.745	0.945
	M	3591	0.734	0.762	0.963	0.715	0.745	0.961
	S	1530	0.671	0.762	0.881	0.687	0.745	0.922
M247/09	L	6276	0.733	0.762	0.962	0.704	0.745	0.945
	M	3591	0.735	0.762	**0.965**	0.716	0.745	0.961
	S	1530	0.671	0.762	0.881	0.687	0.745	0.922

Codon usage tables of hamster, bovine and ovine were used as reference set for the codon adaptation index (CAI) computation. $p < 0.05$. eCAI = expected CAI value. The eCAI values were calculated using Markov method of the E-CAI server. Normalised CAI values (defined as the quotient between the CAI and its expected value).

The ENC value and gene expression are inversely correlated with each other: lower ENC value indicates a higher codon usage and a higher gene expression (Aravind *et al*., 2014). The ENC value for all the genes of the segments was 20 implying that only one codon was used for each amino acid.

3.4 DISCUSSION

From the reported outbreaks in 2008-2010 in South Africa, a number of RVFV strains have been isolated. Chapter 1 revealed that the isolated and sequenced strains, were not introduced from outside South Africa, but mutated over time and caused outbreaks when suitable conditions prevailed. Those isolates were related to isolates from previous studies indicating an ancient origin. In this chapter, six isolates, three from bovine liver and three from ovine liver were selected. These isolates were characterised and compared based on a number of criteria.

Amino acid comparisons between the six RVFV isolates and the ZH501 strain revealed a number of substitutions in the field isolates. When the amino acid sequence of isolate M66/09 was compared to those of ZH501 strain, the two were closely related and shared some of the changes. The growth curve of this isolate differs dramatically from any of the other isolates tested or used in this study. Cells infected with isolate M66/09 showed CPE at 8 hours post infection and the virus lysed all the cells within 48 hours of infection. Previous nucleotide sequence analysis indicated that isolate M66/09 grouped in Clade C while the other isolates used in the study grouped in Clade H (Chapter 2; Maluleke *et al*., 2019). The growth curves of isolates from bovine livers reached higher levels when compared to those of isolates from ovine livers. The same pattern was observed when using the immunofluorescent localization in this study. Cells infected with isolates from bovine livers were destroyed within 48 hours of infection and after 72 hours, all cells were lysed by the virus. It is well known that sheep are generally more susceptible to infection by RVFV than cattle in outbreaks and lambs are highly susceptible while calves are moderately susceptible. The rate at which these isolates adapted to a BHK cell culture environment differs. It is possible that the isolates from bovine livers were more fit and therefor adapted very fast. On the other hand, isolates from ovine livers might have difficulties in adapting to the new environment, thereby resulting in slow growth curves.

Due to the fact that corresponding tRNA of the different codons of the same amino acid differ in abundance in the cell and in the speed by which they are recognized by the ribosomes, their usage during protein translation is unequal (Burns *et al*., 2006; Hersberg and Petrov, 2008; Behura and Severson, 2013). In the study, the codon usage patterns of the selected

RVFV isolates and their hosts were computed and compared. The preferred RSCU values for the selected isolates were greater than 1, indicating that the corresponding codons were more frequently used than expected. The nine preferred codons ended with either G or C showing strong usage bias for the identified amino acids. Therefore, assumptions were made that codons ending with G and C at the third position were preferred by RVFV. Results obtained in this study showed that the codon usage pattern of all the six isolates were similar but revealed a mixture of correspondence and bias to their hosts. The mixture might reveal the influence by selection pressures by their hosts. This might have caused the fitness of the virus to adjust among its dynamic range of hosts (Butt *et al*., 2014). Both the coincident and antagonistic codon usage between virus isolates and their hosts are important as the coincident codon usage enables the corresponding amino acids to be translated efficiently, whereas the antagonistic usage may allow viral proteins to be folded properly but may result in decreased translation efficiency (Butt *et al*., 2014). A mixed codon preference has also been detected in Chikungunya, Zika and Marburg viruses, both exploiting the same hosts and vectors (Nasrullah *et al.,* 2015; Butt *et al*., 2016). Codon usage patterns in RVFV are undergoing evolutionary processes, reflecting a dynamic process of mutation selection to adapt its codon usage to different environments and hosts (Butt *et al*., 2016).

The phenomenon in which the synonymous codons are chosen within and between the genomes is termed codon usage bias. Several factors that could influence codon usage patterns including mutation and selection pressures, natural selection, secondary protein structure, natural and translational selection were identified by this phenomenon (Song *et al*., 2017; Nasrullah *et al*., 2015; Butt *et al*., 2016; Behura and Severson, 2013; Lauring *et al*., 2012). In the study, the codon usage bias and the gene expression as indicated by ENC value among the different isolates is similar and show little bias. The low codon usage bias has also been observed among other RNA viruses (Butt *et al*., 2016). The CAI value is useful for predicting the expression level of a gene and adaptation of viral genes to their hosts. Values approaching 1 indicates a strong codon usage and a higher gene expression (Aravind *et al*., 2014). In the study, CAI values of genes encoded by L and M vary from 0.704-0.734 relative to hamster and ovine, and from 0.734-0.757 relative to hamster and bovine. These values are higher than the genes encoded by S segment, indicating that there is a good variation in codon usage pattern among the different genes of RVFV. The normalized CAI values of isolates from bovine were closer to 1. Values closer to 1 also indicate codon usage adaptation towards their hosts.

Studies have indicated that some RNA viruses accumulate significant genotypic diversity and access greater phenotypic diversity in relation to few mutational steps (Lauring *et al*., 2012). In this study, M66/09 had significant genotypic diversity as compared to other isolates.

Although M66/09 isolate grouped in a different clade (Clade C), its divergence time from the ancestor is the same (52.88 years) as the other isolates used. The growth curve pattern of isolate M66/09 gave about 10^7 pfu/ml which may be regarded as normal for RVFV growth (Morrill *et al*, 2010). All three segments of this isolate showed diversity, with the L segment having the most amino acid substitutions. The genetic diversity may have contributed to the phenotype observed in the kinetic growth curves. However, the current analysis could not definitively identify specific residues that could have impacted on the growth curve phenotype and would need more detailed and empirical analysis to confirm which residues play a role in this.

The study also aimed to confirm that the structural parameters of glycoproteins have not been affected by the substitutions observed. Molecular modelling of these protein sequences revealed that the models predicted were based on known structural templates, thus increasing the confidence in the work. For both protein models, superposition of the models indicated no deviation from the expected fold. The RMSD values between the models predicted and the template models ranged from 0.000 to 0.065. While the modelled structures show that the three-dimensional structure would be conserved, it cannot be excluded that a single point mutation cannot affect the growth curves. This has been observed for the isolate where a single substitution of E276G in the Gn resulted in attenuation of a highly virulent strain to one that showed low viraemia titers, did not replicate efficiently, and had low virulence (Morrill *et al*., 2010).

The study used the TOPCONS and the OCTOPUS web servers to predict transmembrane topology of both the Gn and Gc proteins. The TOPCONS server combines a number of topology predictions into one consensus prediction and quantifies the reliability of the predictions, based on the level of agreement between the methods, both on the protein level and the level of individual transmembrane (TM) regions (Bernsel *et al*., 2009; Tsirigos *et al*., 2015). When prediction methods are different, they may disagree with the results, resulting in uncertainty about the correct topology. Thus a combination of individual topology predictions into one consensus prediction is advantageous. In the study, the TOPCONS consensus predicted three transmembrane regions [430-450, 516-536 (2 TM helix, out in) and 462-482 (TM helix, out in)]. The results obtained for for Gn protein using TOPCONS server were considered not reliable for Gn hence an additional server OCTOPUS was used. The OCTOPUS results were more reliable and corresponded with those previously published (Rusu *et al*., 2012; Halldorsson *et al*., 2018). For the Gc protein, the results from the three servers used correspond with each other. It should be noted that this section focused on transmembrane proteins because they play major roles in cellular recognition, signal transduction and transportation of substances through membranes. These proteins are targets

for a large fraction of drugs, thus pose a great pharmaceutical interest (von Heijne, 2007; Bakheet and Doig, 2009). It also showed that a number of the substitutions for Gn occur in the cytoplasmic tail and these may influence both Gn-Gc cytoplasmic tail interactions and interaction with the ribonucleoprotein during viral assembly (Huiskonen *et al*., 2009).

In conclusion, RVFV infects its host target cell through surface contact followed by internalization in a time-dependent manner. The longer the host cell is exposed to the virus, the higher the titres of primary infection. Even though various amino acid substitutions were identified, none of them could be associated with the different growth kinetic phenotypes observed in the different strains. The structure modelling also did not identify any definitive signatures associated with Gn or Gc function. While some codon usage bias exists, this also could not be linked conclusively with the growth phenotype. All bioinformatic analyses suggest that these proteins should be functional, and that the growth phenotype may depend on a combination of multiple substitutions and subtle differences in codon bias.

CHAPTER 4: THE USE OF A YEAST TWO-HYBRID SYSTEM TO IDENTIFY THE RECEPTORS OF RVFV GLYCOPROTEINS ON HOST CELLS

4.1 INTRODUCTION

The previous chapters identified genetic diversity in various RVFV strains which could be associated with a growth phenotype where some strains grew much slower than the others in BHK cell culture. Comparative bioinformatics analysis of substitutions, structure and codon bias between the strains could not conclusively identify the molecular correlates responsible for the different growth phenotypes. As a starting point for future investigation into RVFV growth phenotypes, it was decided to investigate virus attachment and entry first and develop a system that would enable physical characterization of RVFV attachment protein biology. The yeast two-hybrid (Y2H) system was investigated as a tool to identify host glycoprotein receptors.

The network of interactions between proteins expressed in a cell can be determined using proteomics-based strategies (Causier and Davies, 2002). The formation of cellular structures and many biological processes such as signal transduction involve interaction between proteins. Protein-protein interactions contribute to many diseases and may be exploited in the development of potential therapeutic strategies. Many techniques have been developed to study protein-protein interactions from biochemical approaches including immunoprecipitation, affinity chromatography and affinity blotting to molecular genetic approaches such as the Y2H system (van Criekinge and Beyaert, 1999). The use of bacterial hosts for protein expression may result in insufficient or complete lack of proper protein folding and/or postrtranslational modification. The biochemical *in vitro* handling of these expressed protein extracts, such as during immunoprecipitation, affinity purification and blotting, can negatively affect proteins. In addition, the production and purification of antibodies required in these biochemical approaches are expensive (van Criekinge and Beyaert, 1999; Phizicky and Fields, 1995).

The Y2H system, also known as interaction trapping, enables the identification of interacting proteins in living yeast cells (Fields and Song, 1989). The technology can be used to discover novel binding proteins and to confirm an interaction between two proteins (Wong *et al*., 2017). It has been applied in many systems such as binary interaction mapping, posttranslational modifications in the *Arabidopsis* genus of plants, in host-parasite interactions, and in drug

discoveries (Pires and Boxem, 2018; Lai and Lau, 2017; Liu *et al*., 2017; Wang *et al*., 2014; *Arabidopsis* Interactome Mapping Consortium, 2011; Hamdi and Colas, 2012). The system involves two hybrid proteins, the “bait” which is usually the known protein and the “prey”, the unknown protein. The bait protein is fused to the Gal4 DNA binding domain (DBD) whereas the prey protein is fused to the Gal4 activation domain (AD). The two domains are independently non-functional as a transcription factor (Stephens and Bangting, 2000). When the two proteins are expressed in an appropriate yeast strain, they interact, and the reporter genes are activated (Figure 4.1). The activation of the reporter genes is usually identified by growth on selective growth media or colour change (Brückner *et al*., 2009; Van Criekinge and Beyaert, 1999; Causier and Davies, 2002; Koegl and Uetz, 2008).

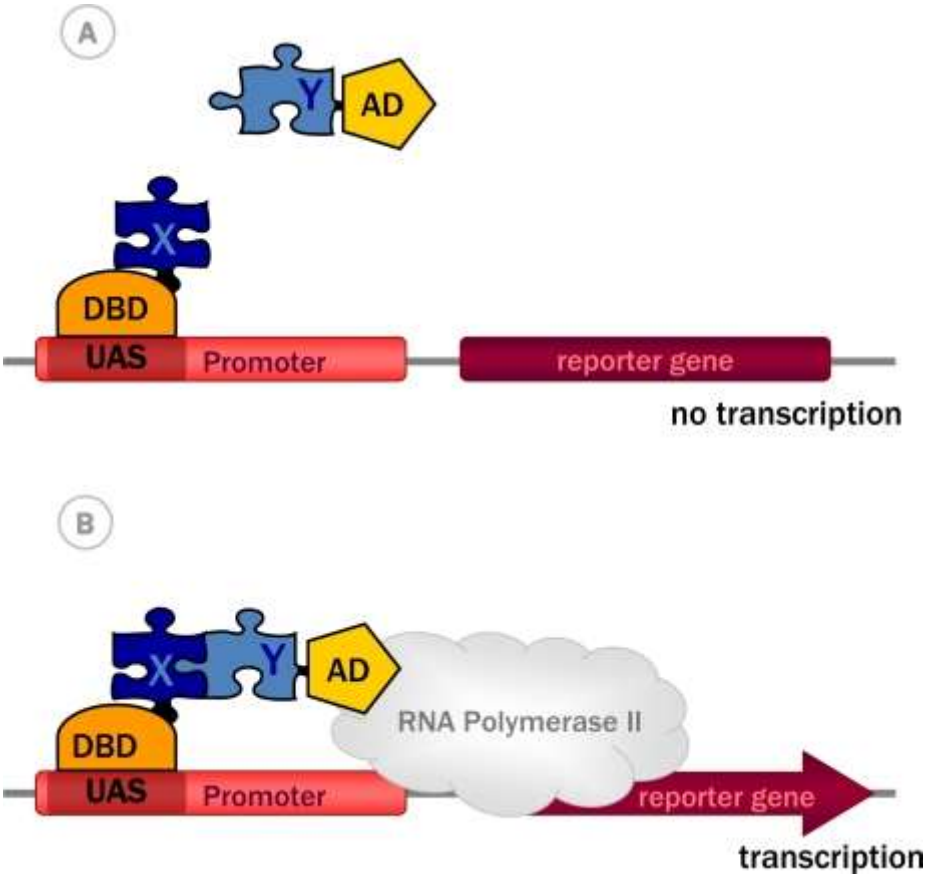

Figure 4.1: The classical yeast two-hybrid system (Brückner *et al*., 2009). A: The protein of interest known as bait (X) is fused to the DNA binding domain (DBD) to form DBD-X. The unknown protein known as prey (Y) is fused to the activation domain (AD) to form AD-Y. B: The DBD-X binds to the upstream activation sequence (UAS) of the promoter. The interaction between the two complexes recruits the AD and reconstitutes a functional transcription factor, leading to further recruitment of RNA polymerase II and subsequent transcription of a reporter gene.

Since its first report, the system has been modified in numerous ways not only for protein-protein interactions but also for DNA-protein interaction (yeast one hybrid system) and RNA-protein interaction (yeast three hybrid system) (Causier and Davies, 2002; Reece-Hoyes and Walhout, 2012; Hook *et al*., 2005).

Besides its many advantages over biochemical methods in terms of convenience and sensitivity, the Y2H system still has some drawbacks. False positives, which are often generated in two hybrid libraries, requires the use of two or more reporter genes in the assay to be eliminated, proteins that are not stably expressed or toxic when expressed in yeast cells may also prove difficult (Causier and Davies, 2002; Van Criekinge and Beyaert, 1999).

In this study the Y2H system was used to search for proteins that interact with glycoproteins of RVFV. The glycoproteins are synthesized as a precursor polyprotein that is cleaved in the endoplasmic reticulum to generate Gn and Gc (Colett *et al*., 1985; Suzich *et al*., 1990). These glycoproteins mediate the first step in virus replication, namely viral entry into the host cell by attachment and cell fusion (Överby *et al*., 2008, Spiegel *et al*., 2016). Since these proteins are mostly exposed, they are recognized by the immune system and induce the production of neutralizing antibodies, thereby playing a major protective role against the virus in the host (Pepin *et al*., 2010). Although there are many candidate receptors that might play a role in the attachment of viruses belonging to the order *Bunyavirales*, receptor molecules for RVFV has not yet been identified (Spiegel *et al*., 2016; Lozach *et al*., 2011; Lozach *et al*., 2010; Yamauchi and Helenius, 2013; Simon *et al*., 2009). It is not clear whether the Gn or Gc alone, or both simultaneously or consecutively, interact with the cell surface molecules. However, based on X-ray crystallography and reconstruction of the Gn/Gc complex it would seem as if the host receptor would interact via Gn (Halldorsson *et al*., 2018).

In this chapter, the construction and characterization of a cDNA library from BHK cells using the switching mechanism at the 5' end of the RNA transcript (SMART^{TM}) are described (Zhu *et al*., 2001). The ectodomains of Gn and Gc from wild-type RVFV isolated from samples of animals infected with RVFV were also prepared. The Y2H system was used to search for proteins which interact with ectodomains of Gn and Gc from the prepared cDNA library.

4.2 MATERIALS AND METHODS

4.2.1 Preparation of the prey (Construction of cDNA library from BHK cells)

Yeast strains and mammalian cells

The yeast strains of *S. cerevisiae*, Y2HGold and Y187 used in this study were obtained from Clontech (USA). The Y2HGold strain was used as the bait strain while Y187 strain was used as a prey strain. The Y2HGold has four reporter genes: AURI coding for inositol phosphoryl ceramide synthase enzyme, HIS3 coding for histidine, ADE2 coding for adenine and MEL1 coding for α-galactosidase and ß-galactosidase enzymes.

The BHK cells were selected for the construction of the cDNA library because this cell line has previously shown to be very susceptible to RVFV (Scharton *et al*., 2015). Cells were maintained in DMEM/F12 supplemented with 5% FBS and 1% mixture of penicillin (10 000 U/ml), streptomycin (10 000 U/ml) and amphotericin B (25 µg/ml).

RNA extraction from BHK cells

The BHK cells were grown in a T75 flask at 37°C in an atmosphere of 5% CO_2 until confluent. The cell monolayers were washed once with PBS and total RNA extracted from BHK cells using RNeasy Mini kit according to the manufacturer's protocol (Qiagen). Purification of mRNA from total RNA was carried out using GenElute mRNA Miniprep kit as per the manufacturer's protocol (SIGMA ALDRICH). The quantity and integrity of both RNA and mRNA were evaluated using a Nanodrop spectrophotometer (Thermo Fisher Scientific) and 1% denaturing formaldehyde agarose gels respectively. The absorbance ratios of the RNA at $A_{260/280}$ and $A_{260/230}$ nm were 2.0 and 1.9, respectively.

cDNA synthesis

Single stranded cDNA was synthesized using Make Your Own Mate and Plate Library System. Briefly, 2 µl (0.4 µg) of mRNA was reverse transcribed using SMART 111 (5' - AAGCAGTGGTATCAACGCAGAGTGGCCATTATGGCCGGG - 3') and CDS 111 primers (5' - ATTCTAGAGGCCGAGGCGGCCGACATG-d$(T)_{30}$VN - 3' and SMART Moloney Murine Leukemia Virus (MMLV) Reverse Transcriptase as per the manufacturer's protocol (Clontech, USA). The double stranded (ds) cDNA was amplified by long distance PCR using 2 µl of single strands cDNA product and the Advantage 2 PCR kit (Clontech, USA). The reaction parameters used were 95°C for 30 seconds, followed by 22 cycles of 95°C for 10 seconds (extension time increased by 5 seconds with each cycle), 68°C for 6 minutes and final extension at 68°C for 5 minutes. At the end of PCR, the product was analysed on 1% agarose gel to check the quality of ds cDNA. In order to remove low molecular weight cDNA and unincorporated nucleotides, the PCR products were size fractionated using CHROMA-SPIN TE 400 columns (Invitrogen). The cDNA was precipitated using sodium acetate and ethanol. The purified ds cDNA was analysed using a Nanodrop spectrophotometer and 1% agarose gels.

Construction and evaluation of the cDNA library

The purified ds cDNA (3 µg) and 3 µg of Sma1-linearized pGADT7-Rec vector were co-transformed into freshly prepared competent Y187 yeast cells using a lithium acetate method according to the protocol in Yeastmaker Yeast Transformation System 2 (Clontech, USA). Transformed yeast cells were diluted with 0.9% (w/v) NaCl solution and 100 µl of 10^{-1}, 10^{-2}, 10^{-3} and 10^{-4} were cultured on synthetically defined medium lacking leucine (SD/Leu) plates (in duplicate) and incubated at 30°C for 4 days. The purpose of diluting the yeast cells was to calculate the various parameters of the transformed library. Colonies were randomly selected to identify the size of the inserts and the recombination rate of the library. The selected colonies were subjected to PCR using the Matchmaker InsertCheck PCR Mix 2 (Clontech) and the product analysed on 1% agarose gel. Plasmid DNA were extracted from these colonies using Easy Yeast Plasmid Isolation kit (Clontech), then amplified in competent bacterial cells (DH5α) by transformation and plated on LB-ampicillin agar plates. Bacterial plasmid DNA was extracted from transformants using the QuickLyse Miniprep Kit (Qiagen, South Africa). The extracted plasmid DNA was sequenced. The remaining transformed mixture of yeast was spread on SD/Leu plates (in duplicate) and incubated at 30°C for 4 days. Transformants were then harvested, pooled in freezing media [yeast extract, peptone and dextrose medium supplemented with adenine hemisulphate (YPDA) plus 25% glycerol] and stored at -80°C in 1 ml aliquots.

4.2.2 Construction of the bait plasmids

The viral strain (M66/09) used in the study was isolated from diagnostic sample brought to ARC-OVR to be tested for the presence of RVFV. This sample tested positive using PCR and was confirmed by virus isolation as mentioned in Section 2.2.1.

Baby hamster kidney and *Escherichia coli* (DH5α) cells were obtained from the Virology and Biotechnology laboratories, ARC-OVR, respectively.

Viral RNA extraction

Baby hamster kidney cells were maintained as described in Section 3.2.1. The maintenance media was removed and replaced with 1 ml of RVFV stored in cell culture. The flask was incubated at 37°C on a rocker for 1 hour to enable attachment. At the end of incubation, the unattached virus and debris were removed and replaced with fresh DMEM/F12 supplemented with 2% FBS and 1% mixture of penicillin (10 000U/ml), streptomycin (10 000U/ml) and

amphotericin B (25 µg/ml) before a further incubation. The virus was harvested after 3 days by centrifugation at 2 500 rpm in an Eppendorf Centrifuge 5810R for 5 minutes. The supernatant was collected and the cell pellet containing cells was discarded. The supernatant was aliquoted and stored at -80°C until needed.

Viral RNA was extracted from 250 µl of a 1 ml aliquot using Trizol Reagent according to the manufacture's protocol (Invitrogen). The RNA was dissolved with 10 µl of distilled H_20. The quantity of RNA was determined using the Nanodrop spectrophotometer. A concentration of 100 ng of RNA was used to prepare cDNA using SuperScript ™ III Reverse Transcriptase according to the manufacturer's protocol (Invitrogen). The primers used are listed in Table 4.1. A simple modular architecture research tool (SMART) Genomic program was used to identify the glycoprotein transmembrane regions and the signal peptides (Letunic *et al*., 2014). PCR primers for both Gn and Gc, excluding transmembrane regions were designed (Appendix A, Figure S1). The forward primers contained restriction sites of *Eco*R1 whereas the reverse primers contained restriction sites for *Sal*1. Phusion High-Fidelity PCR Master Mix with GC Buffer (Thermo Fisher Scientific, USA) was used for amplification. For both Gn and Gc the two step PCR protocol used was the same and as follows: 98°C for 30 seconds, 35 cycles at 98°C for 10 seconds, 72°C for 45 seconds and final extension of 72°C for 10 minutes. The PCR products were analysed on a 1% agarose gel, purified using QIAquick Gel Extraction kit (Qiagen, South Africa) and digested with both *Eco*R1 and *Sal*1. After digestion, purification was done using MinElute PCR Purification kit (Qiagen, South Africa) and 100 ng of the purified products were ligated with an *EcoR1/Sal1* digested, purified yeast shuttle vector (pGBKT7) using T4 DNA ligase. The ligated mixtures were transformed in *E. coli* cells (DH5α) by heat shock method and the transformed mixture was plated on LB plates containing 50 µg/ml of kanamycin (Sambrook *et al*., 1989). Plates were incubated at 37°C overnight. A colony PCR using the insert specific primers (Table 4.1), restriction enzyme digestion analysis and DNA sequencing using pGBKT7 vector specific primers (Table 4.1) confirmed the presence of the inserts.

Table 4.1. Primer sequences used in this study

Name	Primer sequence
mGnGcF	5'-CATGGAGGCC**GAATTC**GAAGACCCCCATCTCAGAAACAGAC -3'
GnR2	5'-GACGTCGACTCAATGGTGATGGTGATGGTGCCCGGAACCACTGAGAGCAGTGTGACA-3'
mGcF	5'-CATGGAGGCC**GAATTC**TGTTCAGAACTGATTCAGGCAAGC-3'
GcR2	5'-GACGTCGACTCAATGGTGATGGTGATGGTGCCCGGAACCTTTAAGCGGCCCTCCAAA-3'
T7 Sequencing primer	5'-AATACGACTCACTATAGGG-3'
3' DNA-BD Sequencing primer	5'-TTTTCGTTTTSSSSCCTAAGAGTC-3'

Bold sequence: *Eco*R1 restriction site, underlined sequence: *Sal*1 restriction site

4.2.3 Protein analysis and bait expression in yeast cells

The recombinants pGBKT7-Gn and pGBKT7-Gc plasmids were transformed into freshly prepared yeast competent cells Y2H according to the protocol described in Yeastmaker™ Yeast Transformation System 2 user manual (Clontech). A volume of 100 µl of both a 1/10 and 1/100 dilution of the transformed mixtures were plated on medium lacking tryptophan (SD/-Trp) and incubated at 30°C for 4 days. This medium was selected because the vector pGBKT7 had a selectable *TRP1* marker. An overnight culture was prepared from colonies using 5 ml of SD/-Trp media and used to inoculate 50 ml of fresh YPDA media. The culture was incubated at 30°C with shaking at 250 rpm until an optical density reading of 0.4-0.6 at OD_{600} was reached. The culture was centrifuged at 1 000 x g in Eppendorf Centrifuge 5810R for 5 minutes at 4°C and the supernatant discarded. The pellet was dissolved in 1 ml of protein extraction buffer containing Y-Per reagent (Thermo Fisher Scientific), lysozyme (25 U/µl), benzonase (50 mg/ml) and protease inhibitor cocktail tablets (cØmplete, EDTA free) (Roche). The mixer was allowed to shake for 30 minutes at room temperature and then centrifuged for 30 minutes at 13 000 rpm (Eppendorf Centrifuge 5415). The supernatant was collected and 15 µl loaded on an SDS PAGE gel (4-12% Bis Tris plus).

Purification of proteins was done using Pierce anti-c-myc agarose according to the manufacturer's instructions (Thermo Fisher Scientific, USA). Extracted and purified proteins were loaded on 4-12% SDS PAGE gels and transferred onto PVDF membrane using the iBlot® 7-minute blotting System (Invitrogen). The membrane was blocked for 1 hour with Membrane Blocking Buffer (Invitrogen) and incubated with primary antibody (c-myc tag antibody) (diluted to 1: 1000) for 1 hour. Following three washes for 10 minutes with Tris

buffered saline (TBS) and Tween 20 (TBST), and one wash with TBS, the membrane was incubated with goat anti-mouse IgG (H+L) secondary antibody, horseradish peroxidase (HRP) conjugate for 1 hour followed by four washes with TBST. Transferred proteins were visualized using chromogenic substrate 3,3',5,5' Tetramethyl Benzidine (Thermo Fisher Scientific). Confirmation of proteins was done by probing the membrane with serum from sheep infected with RVFV (strain 35/74) (kind donation from Virology Section, ARC-OVR).

4.2.4 Autoactivation and toxicity tests of bait plasmids

The first step for Y2H screening is to confirm that the selected bait does not autonomously activate the reporter genes in the absence of a prey protein. In order to test autoactivation activity of the baits, pGBKT7-Gn, pGBKT7-Gc and empty pGBKT7 plasmids were transformed into Y2HGold competent cells. Transformants were grown on plates containing minimal yeast medium without tryptophan (SD/-Trp), or SD/-Trp supplemented with 40 µg/ml of X-α-Gal (SD/-Trp/X) or SD/-Trp supplemented with both X-α-Gal and 125 ng/ml of Aureobasidin A (SD/-Trp/X/A) and incubated for 3-5 days at 30°C. Activation of the reporter genes would be indicated by blue colonies on SD/-Trp/X/A plates, allowing expression of the reporter genes, while the absence of colonies on these plates would indicate non-autoactivation of the bait. White colonies appearing on SD/-Trp and SD/-Trp/X plates would indicate non-autoactivation of the reporter genes by the bait. For toxicity testing, the colony colour and size of Y2H transformed with bait plasmids were compared with those of Y2H cells transformed with the empty vector pGBKT7. If the bait is toxic, colonies containing bait plasmids will be smaller than those containing empty vector pGBKT7 and their colour will also differ. The bait can only be used in Y2H screening if it lacks autoactivation and does not show toxicity.

4.2.5 Yeast two-hybrid screen using co-transformation of bait and prey plasmids

The interaction between BHK cells and glycoproteins was identified using the Matchmaker Gold Yeast Two-Hybrid System according to the manufacturer's protocol (Clontech, USA). Briefly, the Y187 cells harbouring the mate and plate cDNA library cloned into pGADT7-Rec vector were co-transformed with the Y2HGold cells transformed with Gn and Gc for 24 hours at 30°C. The mated culture was spread on SD/-Leu/-Trp/X-α-Gal/AbA (DDO/X/A) plates and incubated at 30°C for 4-5 days. The presence of blue colonies on these plates will be an indication of the interaction between the bait and the prey. In order to increase the chance of

rescuing the interacting prey, the blue colonies were re-plated 2-3 times on SD/-Leu/-Trp (DDO/X), each time picking a single blue colony. The blue colonies were plated using increased stringent SD/-Ade/-His/-Leu/-Trp/X-α-alpha/AbA (QDO/X/A) plates and the plasmid DNA extracted using the Easy Yeast Plasmid Isolation kit (Clontech).

4.3 RESULTS

4.3.1 Isolation and analysis of total RNA and mRNA from BHK cells

An absorbance ratio ($A_{260}/_{280}$) of 2.0 for total RNA was obtained from BHK cells with an average concentration of 1070 ng/µl, indicating a high quality preparation. The integrity of total RNA was analysed on a 1% denaturing formaldehyde gel; the results showed two distinct 18S and 28S ribosomal bands between 1.9 kb and 4.5 kb and a faint band representing the 5S ribosomal band (Figure 4.2, Lane 1) with the ratio of the intensities of these bands being 1:2. The RNA extracted was also not degraded and therefore suitable for purifying mRNA (Figure 4.2). The concentration of mRNA was 124 ng/µl with some rRNA faintly visible (Figure 4.2, Lane 2). The RNA and mRNA showed high purity and quality for construction of cDNA library.

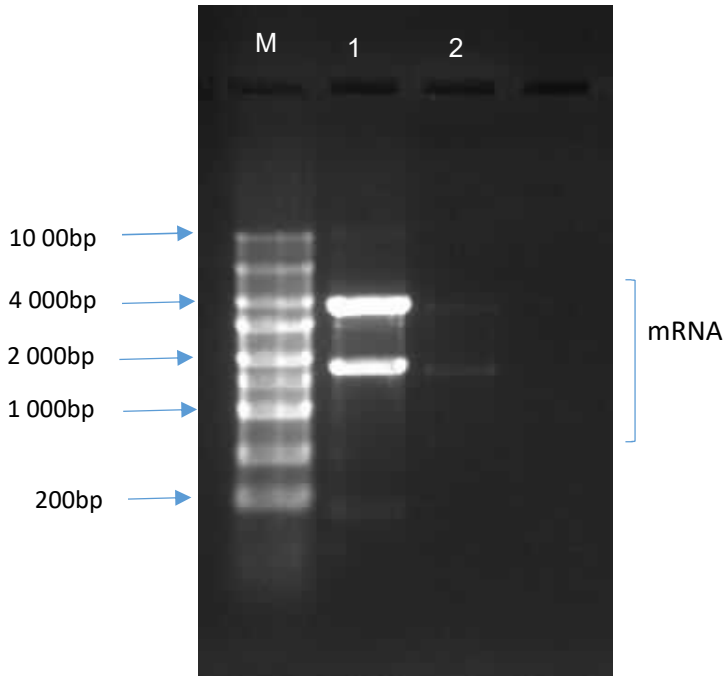

Figure 4.2: Denaturing formaldehyde gel electrophoresis of total RNA and mRNA extracted from BHK cells. Lane M: Transcript RNA Marker (SIGMA); Lane 1: Total RNA; Lane 2: mRNA.

Double stranded cDNA synthesis

A volume of 2 µl of single stranded DNA was amplified by LD-PCR and 5 µl of the product was analysed on a 1% agarose gel. The results showed a smear ranging from 100 bp to 2 500 bp in size before purification (Figure 4.3A, Lane 1). After purification using CHROMA-SPIN TE 400 columns, fragments with smaller sizes were eliminated (Figure 4.3B, Lane 1).

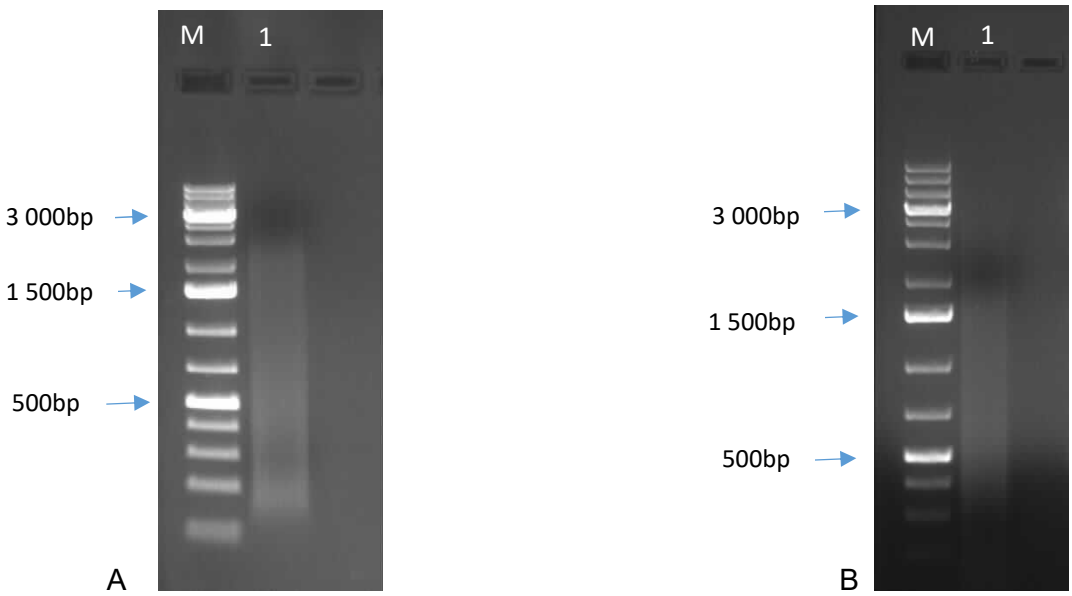

Figure 4.3: Analysis of ds cDNA from BHK cells on 1% agarose gels. (A) Unpurified ds cDNA and (B) purified ds cDNA. Lane M: O'GeneRuler 1 kb DNA ladder Plus (Thermo Fisher Scientific); Lane 1: ds cDNA.

4.3.2 Construction and evaluation of cDNA

A yeast two-hybrid cDNA library was constructed from BHK cells using the pGADT7-Rec vector in the Y187 strain. The parameters of the constructed cDNA library are described in Table 4.1. In order to identify the size of the inserts, 100 colonies were randomly picked and amplified using Matchmaker InsertCheck PCR Mix 2 and analysed on 1% agarose gels (Figure 4.4). Eighty-eight clones appeared as single bands. Six clones contained more than one band (lanes 29, 58, 63, 67, 77 and 80) indicating that a single clone possesses several plasmids, with the same origin of replication and transformed into one yeast cell. Results showed that most of the insert sizes ranged from 200-500 bp (Figure 4.5) while small fragments of cDNA of less than 200 bp were removed from the library. The following formulas were used:

Total independent clones = number of cfu/ml on SD/-Leu x resuspension volume (15 ml)

= 146 cfu/0.1 ml/0.01 x 15 ml

= 2.2 x 10^6 clones

Transformation Efficiency = cfu x suspension volume (ml) x dilution factor) / volume plated (ml) x amount of DNA (µg).

= 60 cfu x 1 000/0.1 x 6 µl of 3 µg pGADT7-Rec

= 3.0 x 10^4 µg pGADT7-Rec

Library concentration = no. of colonies / plating volume (ml) x dilution factor

= 32 cfu/0.1 x 10^3 ml

= 32 x 10^4 cells/ml

CFU = colony forming units.

Table 4.2. Parameters/measures of the quality of the cDNA library from BHK cells

Parameter	BHK cDNA library
Total independent clones	2.2 x 10^6 clones
Transformation efficiency	3.0 x 10^4 µg of GADT7-Rec
Minimum length	200 bp
Maximum length	2 500 bp
Library concentration	32 x 10^4 cells/ml

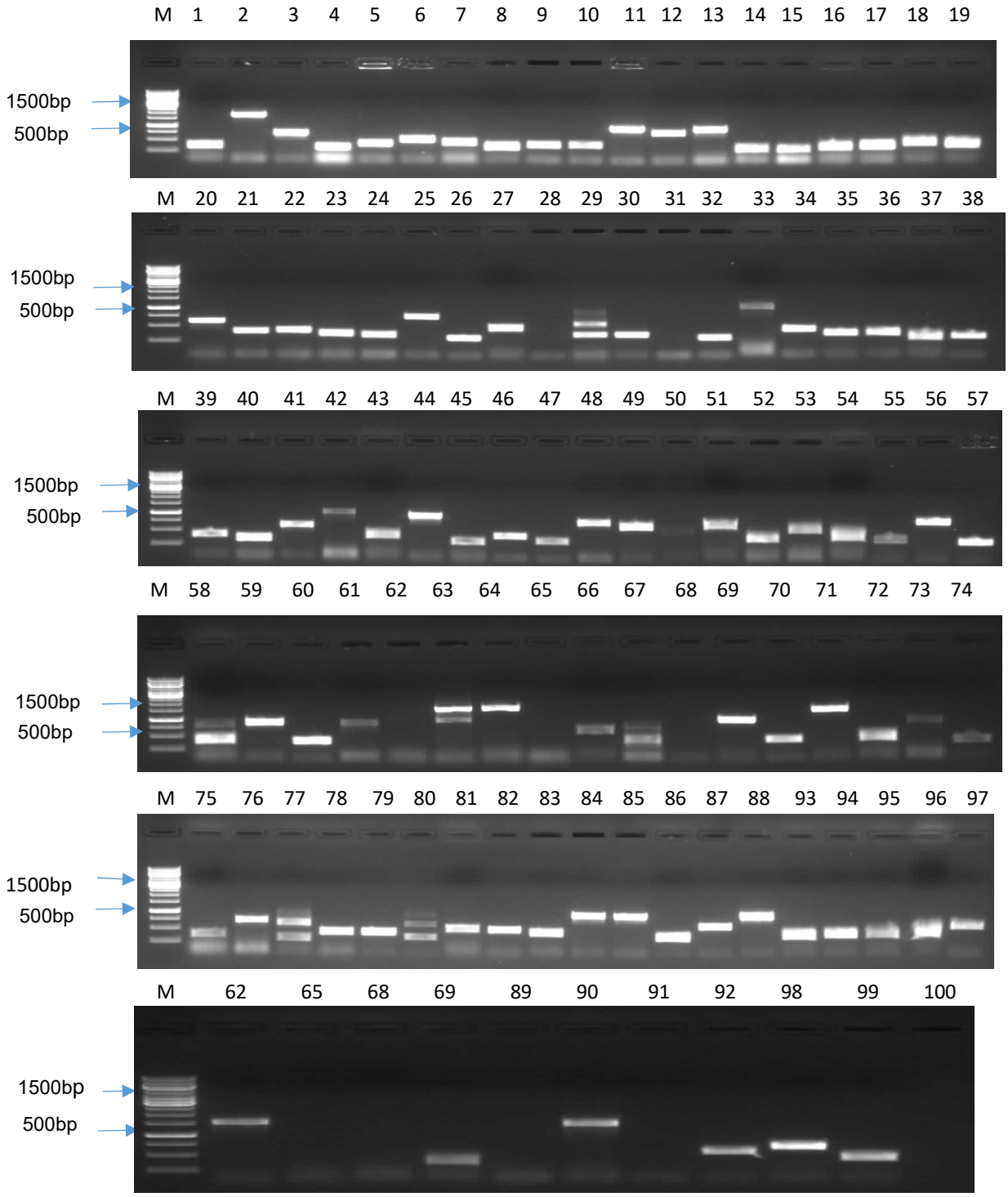

Figure 4.4: Insert check PCR of randomly selected colonies from BHK cDNA library. One hundred colonies were randomly selected from SD/-Leu plates and amplified by PCR using Matchmaker InsertCheck PCR Mix 2. The PCR products were analysed by 1% agarose gel electrophoresis to determine the size fragment. Lanes 1-100: Recombinant individual colonies; Lane M: O'GeneRuler 1 kb Plus DNA ladder (Thermo Fisher Scientific).

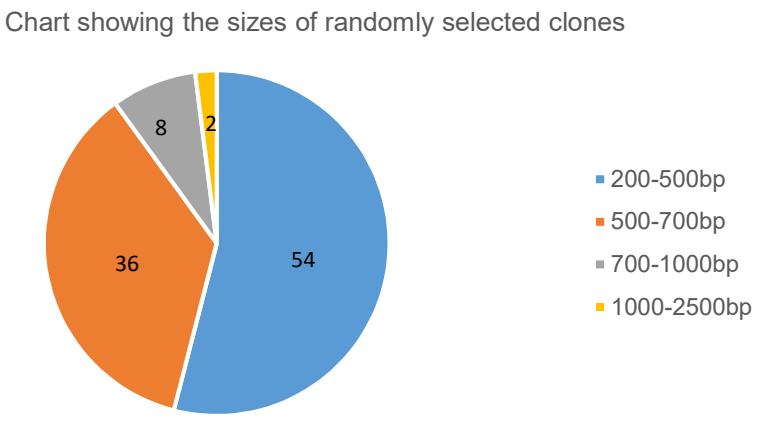

Figure 4.5: Pie chart showing sizes of the inserts. The majority of sizes were from 200-500 bp.

4.3.3 Nucleotide sequence analysis

Most of the plasmid DNA extracted from yeast colonies (from BHK cDNA library) could not be transformed in bacteria; and those that could be transformed, could not be sequenced. Therefore, sequencing was done on PCR products (n=100) of colonies using a T7 sequencing primer. The cDNA sequences were analysed using BLAST software. The genes identified from the cDNA library are outlined in Table 4.3. The five clones that contained more than one band (Figure 4.4) could not be sequenced. Thirty-seven clones contained yeast vector sequences and were not included in the analysis.

Table 4.3. Putative genes identified in cDNA clones of BHK cells

Colony number	Accession (E-value)	Organism	Lowest E-value	Description	Identity (%)
Y2	NM_001281566	*Mesocricetus auratus*	0	HtrA serine peptidase 1 (Htra1), mRNA, complete cds	99
Y3	XM_005080422	*Mesocricetus auratus*	0	Procollagen C-endopeptidase enhancer (Pcolce), mRNA	100
Y5	XM_013126271	*Mesocricetus auratus*	4.90E-31	Ribonuclease A family member 4 (Rnase4), transcript variant X2, mRNA	94
Y6	XM_021229702	*Mesocricetus auratus*	3.08E-65	Replication factor C subunit 1 (Rfc1), mRNA	100
Y7	XM_005080701	*Mesocricetus auratus*	8.84E-47	Transmembrane p24 trafficking protein 3 (Tmed3), mRNA	100
Y9	XM_005084892	*Mesocricetus auratus*	7.76E-16	Ribosomal protein L10a (Rpl10a), mRNA	100
Y10	XM_005084892	*Mesocricetus auratus*	7.76E-16	Ribosomal protein L10a (Rpl10a), mRNA	
Y11	XM_005088283	*Mesocricetus auratus*	0	L-lactate dehydrogenase A chain (LOC101835564), mRNA	100

Y12	XM_005085713	*Mesocricetus auratus*	0	TIMP metallopeptidase inhibitor 1 (Timp1), transcript variant X2, mRNA	99
Y13	XM_005067560	*Mesocricetus auratus*	0	Trafficking protein particle complex 1 (Trappc1), mRNA	99
Y18	XM_005086220	*Mesocricetus auratus*	2.89E-40	Ribosomal protein S16 (Rps16), mRNA	100
Y19	XM_005081314	*Mesocricetus auratus*	7.76E-16	NADH:ubiquinone oxidoreductase subunit A7 (Ndufa7), mRNA	100
Y20	XR_002383032	*Mesocricetus auratus*	3.09E-27	Uncharacterized LOC110341154 (LOC110341154), ncRNA	100
Y21	XM_005081664	*Mesocricetus auratus*	7.16E-24	Adenylate cyclase 9 (Adcy9), transcript variant X2, mRNA	100
Y22	XM_005066012	*Mesocricetus auratus*	8.16E-36	Triosephosphate isomerase 1 (Tpi1), mRNA	100
Y25	XM_005085725	*Mesocricetus auratus*	0	NADH:ubiquinone oxidoreductase subunit B11 (Ndufb11), mRNA	99
Y33	XM_021232574	*Mesocricetus auratus*	0	Enolase 1 (Eno1), mRNA	98
Y39	XM_005070576	*Mesocricetus auratus*	1.02E-22	Eukaryotic translation elongation factor 1 beta 2 (Eef1b2), mRNA	100
Y41	XR_002383032	*Mesocricetus auratus*	4.65E-27	Uncharacterized LOC110341154 (LOC110341154), ncRNA	100
Y42	XM_013118624	*Mesocricetus auratus*	0	Ribosomal protein L5 (Rpl5), transcript variant X2, mRNA	98
Y43	XM_005069906	*Mesocricetus auratus*	1.17E-15	Mitochondrial ribosomal protein L38 (Mrpl38), mRNA	100
Y44	XM_005087924	*Mesocricetus auratus*	0	Quinoid dihydropteridine reductase (Qdpr), mRNA	98
Y46	XM_013124303	*Mesocricetus auratus*	2.11E-31	Cyclin dependent kinase inhibitor 1A (Cdkn1a), transcript variant X2, mRNA	100
Y48	XM_005075916	*Mesocricetus auratus*	0	Ribosomal protein L23 (Rpl23), mRNA	99
Y49	XM_005088093	*Mesocricetus auratus*	8.36E-138	Ribosomal protein S11 (Rps11), mRNA	100
Y51	XM_007635938	*Cricetulus griseus*	4.06E-110	Actin gamma 1 (Actg1), transcript variant X3, mRNA	96
Y53	AH001828	*Mesocricetus auratus*	4.35E-40	Desmin gene, complete cds	100
Y56	XM_021229013	*Mesocricetus auratus*	0	Adenine phosphoribosyltransferase (Aprt), mRNA	98
Y59	XM_021235691	*Mesocricetus auratus*	1.53E-88	Serum amyloid A-3 protein-like (LOC101833293), transcript variant X1, mRNA	100
Y61	XM_005088093	*Mesocricetus auratus*	0	Ribosomal protein S11 (Rps11), mRNA	99
Y62	XM_021232924	*Mesocricetus auratus*	0	MICAL like 2 (Micall2), transcript variant X5, mRNA	98
Y64	XM_021232924	*Mesocricetus auratus*	0	MICAL like 2 (Micall2), transcript variant X5, mRNA	98
Y66	XM_005080762	*Mesocricetus auratus*	1.34E-95	Phosphoribosyl pyrophosphate amidotransferase (Ppat), mRNA	100
Y69	XM_005084365	*Mesocricetus auratus*	0	Cell division cycle associated 8 (Cdca8), mRNA	99
Y70	EU660218	*Mesocricetus auratus*	7.45E-23	Mitochondrion, complete genome	100

Y73	XM_005080434	*Mesocricetus auratus*	0	Minichromosome maintenance complex component 7 (Mcm7), mRNA	100
Y76	XM_005085713	*Mesocricetus auratus*	0	TIMP metallopeptidase inhibitor 1 (Timp1), transcript variant X2, mRNA	100
Y78	XM_005066966	*Mesocricetus auratus*	1.90E-44	Galectin 1 (Lgals1), mRNA	100
Y79	XM_005066966	*Mesocricetus auratus*	1.90E44	Galectin 1 (Lgals1), mRNA	100
Y81	XM_005084620	*Mesocricetus auratus*	1.46E-77	Reactive oxygen species modulator 1 (Romo1), mRNA	100
Y82	XM_005070347	*Mesocricetus auratus*	6.61E-82	Ribosomal protein S27a (Rps27a), mRNA	98
Y84	XM_021234483	*Mesocricetus auratus*	0	Tribbles pseudokinase 1 (Trib1), transcript variant X3, mRNA	100
Y85	XM_021234483	*Mesocricetus auratus*	0	Tribbles pseudokinase 1 (Trib1), transcript variant X3, mRNA	100
Y87	XM_005086049	*Mesocricetus auratus*	2.46E-106	TBC1 domain family member 20 (Tbc1d20), mRNA	100
Y88	XM_005079735	*Mesocricetus auratus*	0	Nascent polypeptide-associated complex subunit alpha (LOC101829818), mRNA	100
Y94	XM_005086723	*Mesocricetus auratus*	8.08E-24	Ribosomal protein S5 (Rps5), mRNA	100
Y95	XM_005086723	*Mesocricetus auratus*	8.08E-24	Ribosomal protein S5 (Rps5), mRNA	100
Y97	XM_005066966	*Mesocricetus auratus*	7.52E-132	Galectin 1 (Lgals1), mRNA	100
Y98	XM_013126271	*Mesocricetus auratus*	5.79E-108	Ribonuclease A family member 4 (Rnase4), transcript variant X2, mRNA	99
Y99	XM_021235281	*Mesocricetus auratus*	2.02E-164	Non-SMC condensin I complex subunit D2 (Ncapd2), mRNA	99
Y100	XM_007628245	*Cricetulus griseus*	3.17E-21	Acylphosphatase 2 (Acyp2), transcript variant X1, mRNA	100

4.3.4 Construction of bait plasmids (pGBKT7-Gn and pGBKT7-Gc)

PCR amplification successfully amplified fragments of Gn and Gc from wild-type RVFV isolate M66/09. The amplified sizes were approximately 1 600 bp and 1 500 bp for Gn and Gc respectively (Figure 4.6). The PCR products were digested with restriction enzymes *Eco*R1 and *Sal*1 and then cloned into the pGBKT7 vector. The successful construction of pGBKT7-Gn and pGBKT7-Gc was confirmed by colony PCR, restriction digestion and sequencing (Figure 4.7). The sequencing of products showed 100% across the entire gene length for both Gn and Gc.

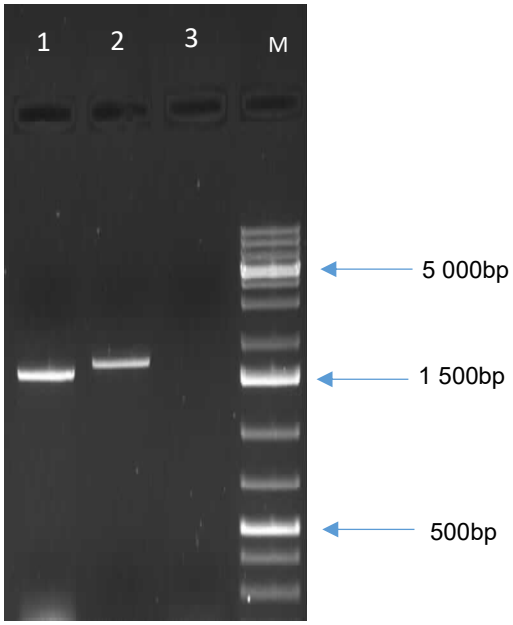

Figure 4.6: Ectodomains of genes encoding RVF viral Gc and Gn amplification. PCR-amplified portions of Segment M which encode viral glycoproteins Gc and Gn, loaded in Lane 1 and 2, respectively. Lane 3 is PCR products of a negative control. Lane M: O'GeneRuler 1 kb DNA ladder Plus (Thermo Fisher Scientific) with sizes shown in basepairs (bp).

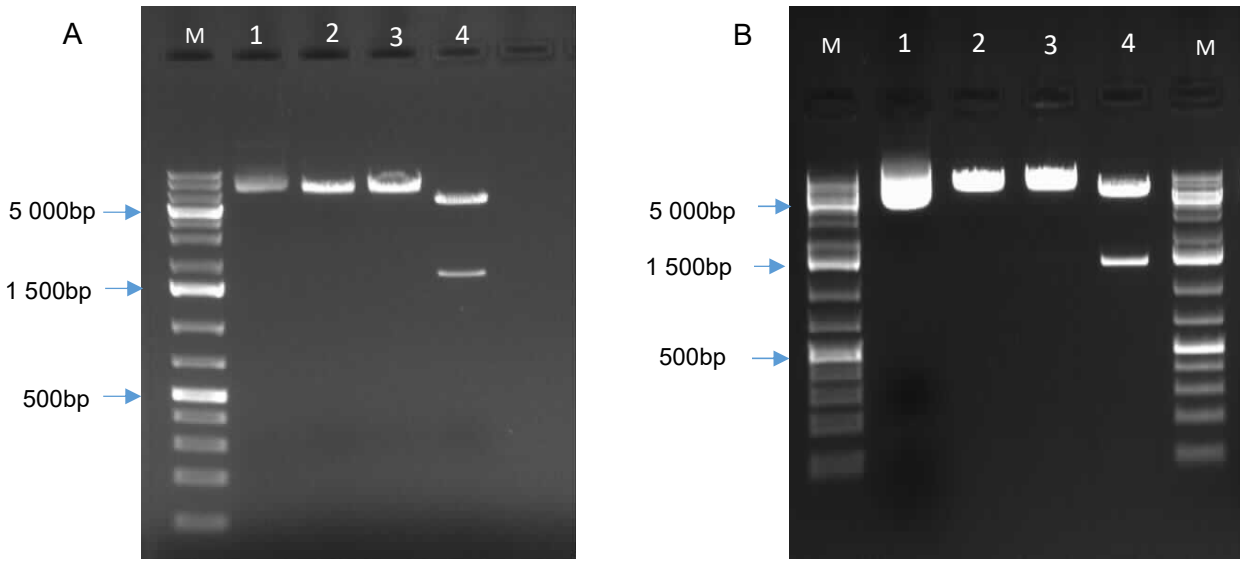

Figure 4.7: Confirmation of recombinants pGBKT7-Gn (A) and pGBKT7-Gc (B) by digestion with *Eco*R1 and *Sal*1. Lane M: Molecular marker; Lane 1: Undigested plasmid recombinants; Lane 2: plasmid recombinants digested with *Eco*R1*;* Lane 3: Plasmid recombinants digested with *Sal*1*;* Lane 4: Plasmid recombinants digested with both *Eco*R1 and *Sal*1.

4.3.5 Expression of Gn and Gc

The expression of the fusion proteins was confirmed before Y2H screening. Total proteins of baits pGBKT7-Gn and pGBKT7-Gc plasmids transformed in Y2H were extracted using Y-Per Yeast Protein Extraction Reagent (Thermo Fisher Scientific). Purification of the proteins was done using the c-myc agarose (Thermo Fisher Scientific). Proteins were detected by western blot using c-myc epitope tag antibody and goat anti-mouse IgG (H+L) secondary antibody, HRP conjugate. The molecular weight of Gn fusion protein detected was approximately 30 kDa, while that of Gc fusion detected was also approximately 30 kDa (Figures 4.8A and B, respectively). The sizes of the molecular weight detected by western blots were lower than their estimated sizes (Gn = 48.4 kDa, Gc = 52.2 kDa). Expression of Gn and Gc was proved in yeast cells. A positive control, pGBKT7-53 vector expressing a 57 kDa protein was also included and the size detected was lower than expected. A very faint band was observed around the 36 kDa region (Figure 4.8B, Lane 8 indicated by an arrow). Confirmation that these were RVFV derived proteins was confirmed using the blots with positive serum as indicated in Material and Methods (Section 4.2.3).

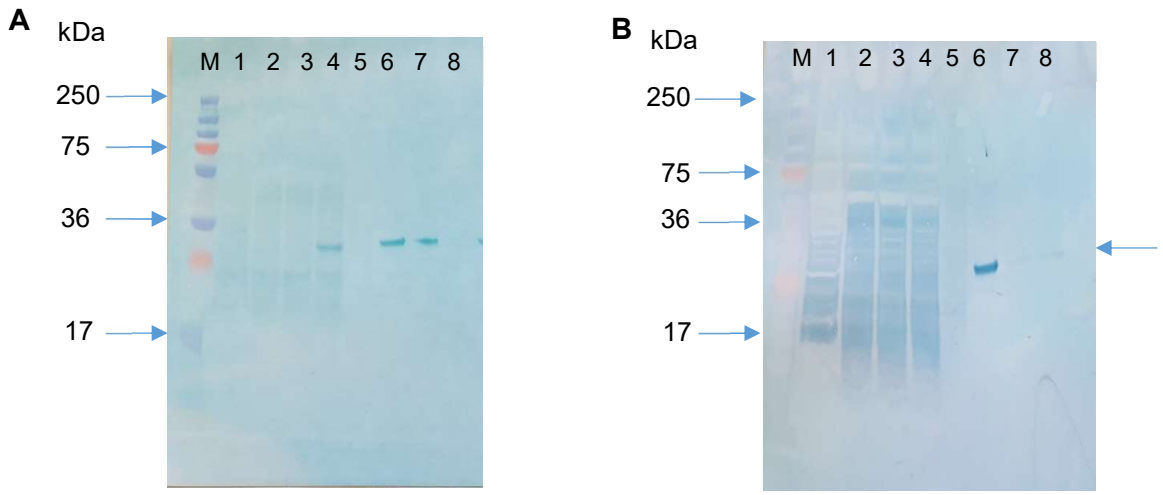

Figure 4.8: Western blotting analysis of total protein extracts of Y2HGold containing the plasmids pGBKT7-Gn (A) and pGBKT7-Gc (B). Proteins were separated on SDS PAGE (4-12%), and later probed with c-myc tag antibody. Lane M: PageRuler Plus Prestained protein Ladder (Thermo Fisher Scientific); Lane 1: Y2H yeast cells; Lane 2: Empty vector pGBKT7; Lane 3: Lysates; Lane 4: Flow-through; Lane 5: Washes; Lane 6: Eluate 1; Lane 7: Eluate 2; Lane 8: p53 (positive control indicated by an arrow).

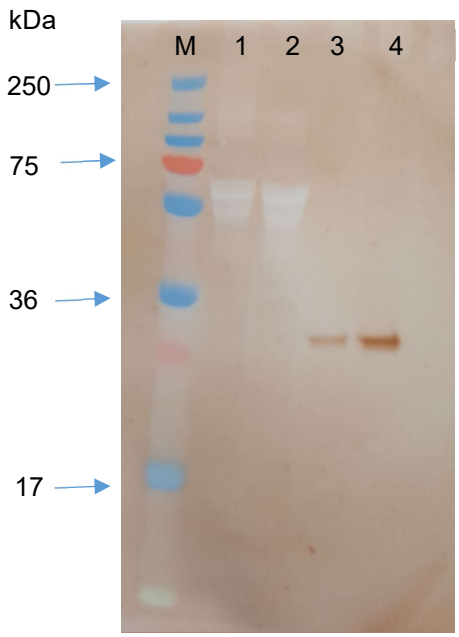

Figure 4.9: Confirmation analysis of Gn and Gc proteins of RVFV. Proteins were separated on SDS PAGE (4-12%), and later probed with positive serum from sheep infected with RVFV. Lane M: PageRuler Plus Prestained protein ladder (Thermo Fisher Scientific); Lane 1: BHK cells; Lane 2: BHK cells infected with virus; Lane 3: Gn protein; Lane 4: Gc protein.

4.3.6 Autoactivation and toxicity tests of the bait plasmids

For autoactivation activity, each bait plasmid was transformed in freshly prepared Y2H competent cells and plated on selective media (SD/-Trp, SD/-Trp/X and SD/-Trp/X/A). The presence of blue colonies on SD/-Trp/X and SD/-Trp/X/A is an indication of autoactivation that would enable expression of the reporter genes. In this experiment, the results showed that no autoactivation activity was detected from both Gn and Gc transformants (Figure 4.10). To demonstrate that baits were not toxic to yeast, both pGBKT7-Gn and pGBKT7-Gc were transformed in Y2H competent cells and plated on SD/-Trp media. An empty vector PGBKT7 was also included as a positive control. Colonies containing bait vectors and empty vectors were compared and no significant difference could be noticed (Figure 4.10). The growth rate was also compared in liquid cultures and again there was no difference. The results indicate that the baits were not toxic to yeast cells. Based on the results obtained, both pGBKT7-Gn and pGBKT7-Gc bait plasmids were used in the Y2H screening assay.

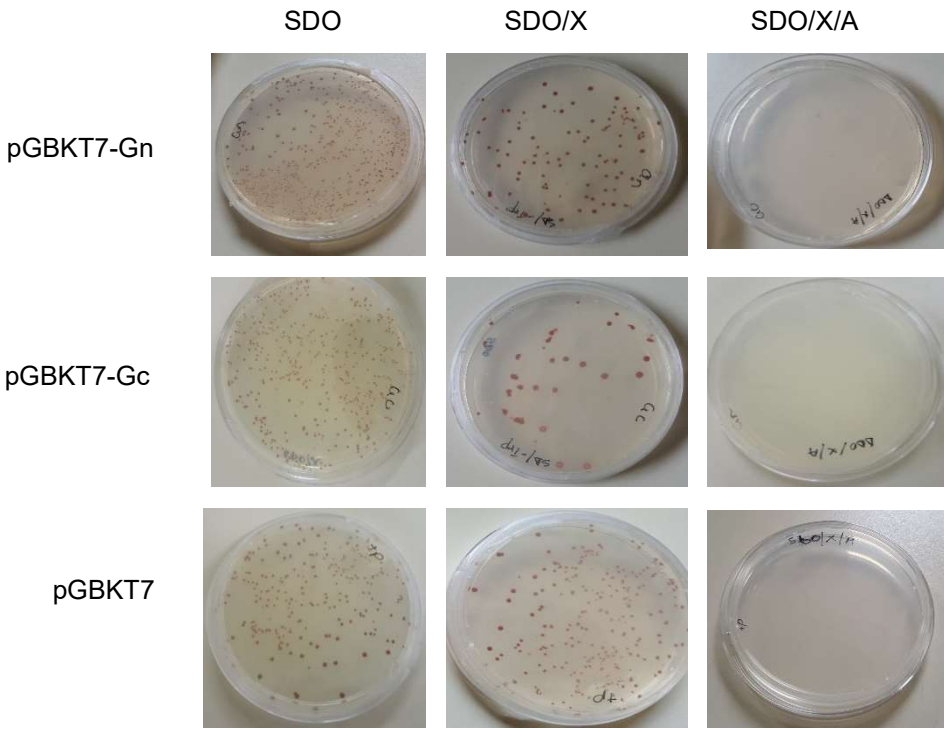

Figure 4.10: Determination of the autoactivation and toxicity activities of pGBKT7-Gn and pGBKT7-Gc bait plasmids in yeast. The bait plasmids were used to transform Y2HGold cells and grown on plates containing different media. The empty plasmid pGBKT7 was included as a control. SDO = synthetic dropout media; SDO/X = synthetic dropout media with X-alpha galactosidase; SDO/X/A = synthetic dropout media with X-alpha galactosidase and Aureobasidin A antibiotic.

4.3.7 Yeast two-hybrid screening

A total of 32 blue colonies were obtained after the co-transformation of pGBKT7-Gn and cDNA in a prey plasmid, while with the co-transformation of pGBKT7-Gc with prey plasmid 40 blue colonies were obtained. Streaking of these colonies 2 to 3 times on plates using increased stringency of SD/-Ade/His/-Leu/-Trp/X-α-alpha/AbA (QDO/X/A) reduced the number to 4 for pGBKT7-Gn and to 8 for pGBKT7-Gc (Figure 4.11). Plasmids DNA were extracted from these colonies and attempts to amplify them in bacteria failed. Sequencing of these plasmid DNA's also did not yield any results.

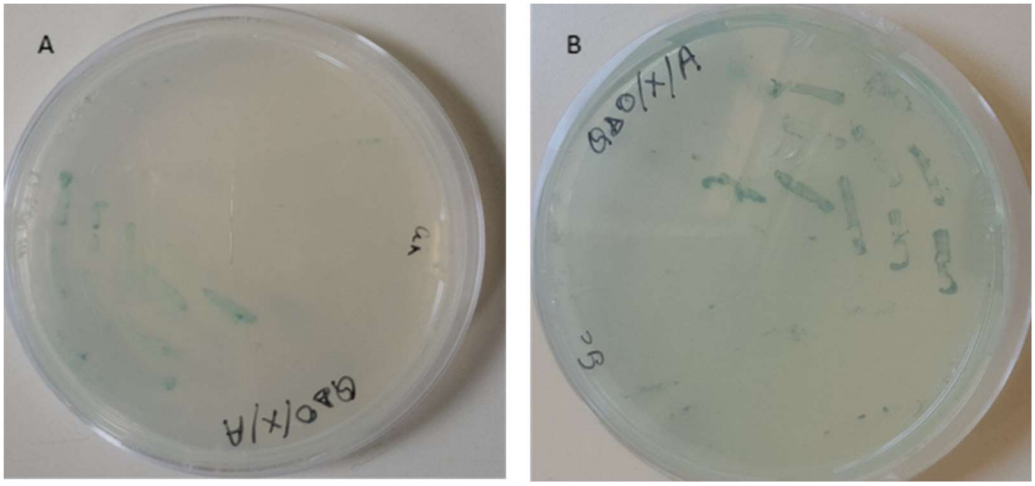

Figure 4.11: Blue colonies obtained after the co-transformation. A: Transformants of pGBKT7-Gn and cDNA in a prey plasmid streaked twice on QDO/X/A plates. B: Transformants of pGBKT7-Gc and cDNA in a prey plasmid streaked twice on QDO/X/A plates. ODO/X/A = SD/-Ade/His/-Leu/-Trp/X-α-alpha/AbA.

4.4 DISCUSSION

From previous outbreaks, it is clear that different RVFVs isolates circulate in different endemic areas and these viruses infect different host species i.e. cattle, sheep and goats. In addition, wildlife can be infected by RVFV. In an infected animal, the virus preferentially localizes to certain tissues, especially the liver, spleen and in pregnant animals, the placenta (Swanepoel, 1981). The outcome of these infections is also different in the different host species. The replication of the virus in these host species might depend on host receptor sites. It is well known that the viral glycoproteins mediate host cell attachment and are involved in viral entry into the cell (De Boer *et al*., 2012; Kakach *et al*., 1998). It possible that more than one receptor site is present in the host species. It is important to understand the interaction between the virus glycoproteins and the host cell proteins following attachment.

Characterising host pathogen protein-protein interactions help in understanding the mechanism underlying pathogen infection and broadens the understanding of molecular functions of pathogen and host proteins. Different methods have been developed and used for studying protein-protein interaction. Those methods include affinity purification, co-immunoprecipitation, pull-down assay and cross-linking assay. Some of these methods are coupled with mass spectrometry (MS) to identify the interacting partner using proteomic analysis.

The identity of specific host receptors, targeted during RVFV infection, are still not clear. In order to understand and identify the host receptors, Y2H system was used in the study to

search for BHK cell proteins that interact with viral glycoproteins Gn and Gc. For the Y2H assay, a high-quality cDNA library which expresses host proteins, is required for screening of interactions between host and virus proteins. Many cDNA libraries have been constructed from plants, animals and microorganisms and genes related to biological processes have been determined (Lee *et al*., 2012; Ma *et al*., 2011; Zhao *et al*., 2009). To date, an interaction between a mouse embryonic cDNA library and RVFV NSm protein was studied using Y2H system (Engdahl *et al*., 2012). In this study, cDNA library from BHK cell line was constructed and characterised before it could be screened for interaction with RVFV glycoproteins. A comprehensive screen for positive interactions needs a library with high complexity as possible to maximize the chances of finding relevant prey proteins (Gao *et al*., 2015). A good quality cDNA library has been identified by three aspects 1) The total independent clones/ capacity of more than 1.7 X 10^5 clones, which will ensure that the low abundance mRNAs is present in the library. 2) High transformation efficiency and 3) the average length of inserted cDNA (>1.0 kb). The average length will ensure the integrity of cDNA (Li *et al*., 2009; Al-Taweel *et al*., 2011; Liu *et al*., 2013). In this study, the total number of independent clones obtained was 2.2 X 10^6 and the transformation efficiency was 3.0 X 10^4 colonies/µg of GADT7-Rec. This means that the two aspects of the good quality library were achieved. The number of cycles used in the study was 22. It was believed that this number is small enough to minimise the chances of amplification of smaller cDNA fragments that might not have been removed during CHROMA-SPIN fractionation. In this study, the cDNA inserts ranged from 200 bp to 2 500 bp, with a large number of inserts harbouring sizes of 200-500 bp. Only 100 colonies were randomly picked up and amplified. It was possible that the number of clones amplified was too small to represent the average length of the cDNA size. Although some of the genes identified in the cDNA library were not full-length sequences, they were identified as from hamsters. The library parameters calculated indicate that the cDNA library constructed was suitable to be used as prey in Y2H system for identifying RVFV-interacting host partners.

The constructed cDNA would be a useful tool for studying RVFV host interactions. In addition, the BHK cell line is susceptible to bluetongue virus, African horse sickness virus, bovine ephemeral fever and epizootic haemorrhagic disease virus; therefore, the constructed libraries could also be useful to study host virus protein interactions for these animal pathogens (OIE, 2019; McLaughlin *et al*., 2003; Wang *et al*., 2001; Laviada *et al*., 1993).

It was postulated that the ectodomains of Gn and Gc that lack the transmembrane regions, would be the relevant baits to be used to screen the cDNA library. Because the aim of the study was to find proteins that interact with a membrane-bound protein, only the selected domains were used as baits (Kuo *et al*., 1997). Two bait plasmids pGBKT7-Gn and pGBKT7-Gc were constructed and tested for protein expression in yeast cells by western blotting.

Confirmation of the proteins was done using positive serum against RVFV and fusion constructs were confirmed to be in-frame with their fusion partners by sequencing using the T7 primer (Causier and Davies, 2002). Before the Y2H screen, plasmids were tested for autoactivation activity and toxicity. It was found that both baits did not have any autoactivation activities, were also not toxic and were suitable for use as baits for the Y2H screen.

In this study, screening of cDNA library using the ectodomains pGBKT7-Gn and pGBKT7-Gc yielded 4 blue colonies (using pGBKT7-Gn) and 8 blue colonies (using pGBKT7-Gc). Rescuing of the plasmid DNA in bacteria was unsuccessful. Neither PCR amplification of the blue colonies nor sequencing of the plasmid DNA from yeast was successful. Many factors could have contributed to the failure of rescuing the yeast DNA in bacteria. 1) Although plasmid DNA was extracted using the kit, it is possible that contaminants were not all removed and they prevented the bacteria to take up the yeast DNA. 2) The increased concentration (from 1 to 20 ng) of yeast DNA might not have been enough. 3) The size of the genes in the plasmids might be too big. 4) The open reading frame of the DNA might not had fused in frame with the GAL4 AD sequence. These factors should be looked upon in the future study.

The proteins that were fused to the DNA binding domain; pGBKT7-Gn and pGBKT7-Gc did not possess transcription activation domains that might activate the reporter genes (Causier and Davies, 2002). These proteins were tested for autoactivation and toxicity prior to testing for protein-protein interaction. There are many reasons that might have contributed to the negative results. Firstly, the proteins of RVFV are integral proteins. These types of signalling molecules including receptor tyrosine kinase, G protein-coupled receptor, membrane bound phosphatase and transporters that are hydrophobic in nature (Stephens and Banting, 2000; Iyer *et al*., 2005). This hydrophobicity property makes them difficult to be studied using the Y2H system. Truncation of the hydrophobic domains might be necessary, but this might be difficult if it involves the unknown protein. In order to solve this problem, a modified Y2H system called split ubiquitin Y2H was developed and might have been suitable for the study (Stagljar *et al*., 1998). The above system uses an ubiquitin amino acid protein that can be split into two moieties referred to as Nub1 (N-terminal fragment) and Cub (Carboxy-terminal fragment). The two fragments allow the bait to be fused to the Cub fragment, which is linked to the artificial transcription factor, while the prey is fused to the Nub fragment containing an isoleucine 13 to glycine mutation that prevents re-association of the two fragments. An interaction between the two proteins; bait and prey in a yeast host will reconstitute an active ubiquitin molecule, resulting in the proteolytic cleavage of a reporter protein from one of the ubiquitin domains (Snider and Stagljar, 2016). This will allow the transcription factor to enter the nucleus of the yeast and to activate the reporter system (Snider and Stagljar, 2016; Snider *et al*., 2010; Causier and Davies, 2002; Paumi *et al*., 2007). The use of split-ubiquitin systems in the

analysis of protein-protein interactions involving different kinds of membranes has been successful (Hooker *et al*., 2007).

Secondly, these proteins might be unstable when expressed in yeast cells and require plasmids with modified promoters to drive a low level of expression (Causier and Davies, 2002). The initial Y2H system relied on proteins that were localised to the yeast cell nucleus, but the current two hybrid vectors, encode nuclear localization signals thereby targeting non-nuclear proteins into the nucleus (Causier and Davies, 2002). Some proteins such as cyclins and homeobox gene products are toxic when expressed and targeted to the yeast nucleus. Thirdly, in the Y2H system, it is possible that both proteins, although able to interact, are never in close proximity to each other within the cell because of time/space constraints (Van Criekinge and Bayaert, 1999). The fact that Gn/Gc forms a stable capsomer complex consisting of at least six Gn/Gc units that assemble into a full virion may support the notion that single expression glycoproteins may be unstable or may assemble into capsomers that would prevent entry into the nucleus. However, none of the above problems address the fact that blue colonies were obtained.

In conclusion, a quality cDNA library was constructed and characterized from a RVFV susceptible BHK cell line. Evaluation of the library for various parameters demonstrated it to be suitable for usage as prey for studying RVFV-host protein interactions. The library constructed will lay a solid foundation for finding relevant genes that are important for viral attachment during infection and to investigate their mechanisms. Expression of the ectodomains of Gn and Gc in yeast cells was successful and the baits constructed were suitable for Y2H screening. The putative clones found in the study using Y2H screening need to be identified and characterized fully. The molecular interactions of pathogenesis related proteins involved during RVFV infection is not very clear. Identification and characterization of these proteins are of importance both in understanding the molecular mechanisms of RVFV glycoproteins and the improvement of the development of glycoprotein-targeted therapeutics against RVFV.

CHAPTER 5: GENERAL DISCUSSION AND CONCLUSION

The RVF outbreaks of 2008-2010 affected a large number of animals that included cattle and sheep. A disproportionately large number of sheep were affected during this outbreak, raising the question of whether host tropism was observed due to the difference of RVFV genotypes. Sampling of the outbreak isolates and full genome sequencing indicated that the isolates were genetically distinct, grouping in two different clades, notably Clades C and H. Isolates in Clade C were from major outbreaks in different countries including Zimbabwe (1978), Madagascar (1991), eastern Africa (1997-1998), Saudi Arabia (2000-2001), Kenya (2007) and South Africa while those in Clade H were from South Africa (2009-2010) and Namibia (2004) (Grobbelaar *et al*., 2011).

Rift Valley fever virus has a segmented genome that allows reassortment as an essential contributor to its evolutionary dynamics (Freire *et al*., 2015). In this study, two reassortants were identified. Evidence of reassortment was also seen in the viruses that caused the 2006-2007 outbreaks in Kenya where multiple virus lineages circulated during a single outbreak (Bird *et al*., 2008). The exchange of genetic material between different lineages through superinfection is possible (Bird *et al*., 2008) and this was also noticed in the current study. Reassortment can be due to transportation of one strain to a locality where another strain is circulating (Sall *et al*., 1999). Studies have shown that RVFV isolates from different geographical localities appear to have base substitutions varying from 0 to 9.6% in the M segment, indicating reassortment as a common trait in RVFV natural history (Sall *et al*., 1997).

When kinetic growth curves are produced, viruses are removed from their original environment and given a new host system. During that process, many changes involving viral entry into the host, replication in the host and shedding from the host might occur. A virus with genetic variants showing faster replication and higher viral loads is believed to produce more severe disease and a higher mortality rate (Wargo and Kurath, 2011). Growth curves in cell culture might not represent virulence in the field because the virus might have mutated to adapt to the new environment. Arbovirus populations need to adapt to the host environments and interact with the host resources including binding host proteins, folding RNA into functional secondary structures so that replication can occur efficiently (Sexton and Ebel, 2019). These processes may vary in different hosts. Alternating replication in vertebrates and arthropods imposed by arboviruses results from the presence of different evolutionary pressures, allowing the viral genomes to evolve rapidly when novel conditions arise (Ciota and Kramer, 2010; Moser *et al*., 2018; Sexton and Ebel, 2019). Future studies need to assess the virulence of the slow and fast-growing strains in animal trials to confirm association of growth phenotype and virulence.

Recombinants of RVFV can be rescued by developing efficient and reproducible reverse genetics systems. Through reverse genetic systems, manipulation of RNA molecules through its complementary DNA has been possible and this enhances the study on the biology of the virus at the phenotypic level (Kanai *et al*., 2017). Both T7 and Pol I dependent systems can be utilized for minigenome assays to characterize the viral proteins mediating transcription during RVFV infection (Bouloy and Flick, 2009). It has been shown that these systems in combination with T7 or Pol I driven expression plasmids of the corresponding *Bunyavirus* nucleoprotein N and the polymerase L enable the constitution of ribonucleoprotein templates (Bouloy and Flick, 2009; Flick and Bouloy, 2005; Flick *et al*., 2003). The latter falls outside the scope of this current study but should be an integral part of the future work.

Infectious viruses need to use host cellular components to synthesise their proteins and to replicate. Codon usage bias in the virus and in its host can affect the viral replication. Too much deviation of the viral codon usage from that of the host will inhibit or slow down the viral protein synthesis because of the inability of the corresponding tRNA. Therefore, codon usage bias of a virus and its host must coevolve for the virus to use the host machinery more efficiently and to replicate faster (Burns *et al*., 2006; Goñi *et al*., 2012). Codon usage bias did not yield a clear answer that may explain the phenotype, but codon usage bias cannot be excluded since codon usage bias at specific regions of the genome does exist even if this is not predominant. Although complete genome sequences of RVFVs are available, codon usage bias in many of these genome sequences have not been thoroughly addressed. Further studies are needed to address this in order to provide understanding of the evolution and gene expression in RVFV.

The fact that viruses have different hosts, implies that their adaptation to these hosts differ (Butt *et al*., 2016). Most viruses have high variability at nucleotide levels. For the same virus, multiple strains may exist and at each replication, new mutations are expected to appear, so that the virus can escape the host immune system and survive (Lucas *et al*., 2001).

The inability to identify any defined characteristics that could explain the phenotypic differences observed between the RVFV isolates led to the consideration that identification of host receptors, followed by subsequent characterization of receptor interaction may shed light on the role that the glycoproteins may play in the phenotype. To this end, the Y2H system was investigated as a means to identify the receptors for Gn and Gc. The Y2H system involves detection of interacting proteins in living yeast cells and this has made it a powerful novel tool used in protein-protein interactions (Brückner *et al*., 2009).

The use of yeast is advantageous since yeast is closer to higher eukaryotes than *in vitro* experiments or those systems based on bacterial hosts (Van Criekinge and Beyaert, 1999).

Although there are many Y2H-based techniques available, they all rely on a similar principle, which is the modular structure of the protein reporting the interaction (Brückner *et al*., 2009). Most of the Y2H systems require translocation of interacting proteins into the nucleus. This makes it difficult for the membrane-associated proteins, integral membrane proteins and cytosolic proteins (Sugita *et al*., 1996). Although truncated versions of these proteins are possible to use in the system, misfolding of the protein remains an obstacle. For extracellular proteins, such as receptors and ligands, which participate in a multitude of physiological processes, a system called screening for interactions between extracellular protein (SCINEX-P) was developed (Urech *et al*., 2003).

The cDNA library needed in the Y2H system is crucial. The library should be of good representation because only one out of six fused cDNAs will be in the correct frame (Van Criekinge and Beyaert, 1999). The cDNA libraries are usually generated in the activation domain plasmids and should be directionally cloned into the vector. This will ensure that one in three of the cDNAs will be in frame with the fusion partner (Causier and Davies, 2002; Gao *et al*., 2015; Mahajan *et al*., 2015). In this study, the SMART technique, a novel method for constructing cDNA libraries was used. The technique increases the lengths of cDNA clones and high-quality cDNA library by employing MMLV reverse transcriptase (Gao *et al*., 2015). The technique also adds a distinct *Sma*1 site to each end during transcription which allowed directional cloning in a *Sma*1 digested vector.

Mapping of interaction networks that occur during protein-protein networks is of crucial importance for the systems in biology. In this study, the Y2H system was chosen because it is an *in vivo* method and proteins needed posttranslational modifications to carry out their functions; so, it was believed that the proteins would be in their physiological environment and fold properly to interact. Methods that could be suitable rather than the use of Y2H include surface plasmon resonance (SPR) which is a biophysical technology involving injection of purified cellular extracts onto a sensor chip covered with immobilized binding partner that could be eluted and identified by mass spectrophotometer (Brüchner *et al*., 2009), BRET and FRET-based methods, but these techniques use expensive equipment (Xing *et al*., 2016; Rao *et al*., 2014).

The interaction between viruses and their new environments involve manipulation of resources. In a virulent relationship, many aspects of cellular metabolism and developments are changed (Agudelo-Romero *et al*., 2008). The changes that occur in the virus genome are important to adapt to the new environment. These changes might differ within isolates of the same strain and results in different growth phenotypes (Agudelo-Romero *et al*., 2008).

The current study had a number of weaknesses that should be improved in future studies. The criteria used to select the isolates for comparisons limited some possibilities. The genome sequencing and phylogenetic analysis linked with host information, allowed the selection of isolates with distinct genetic background and potential host preferences. The selection of the isolates for comparison was based on isolates obtained from liver samples and majority of the viruses were from Clade H, with one exception from Clade C. After the growth curve experiments, more members of Clade C could have been selected to test whether all members show the fast-growing phenotype. Since growth phenotypes are known phenomena in RVFV, selection of a diverse range of isolates could have helped because the primary aim was investigation of the growth phenomenon as it gives insight into the correlation of the viral cycle. This could have also helped in identifying the amino acid substitutions that are responsible for the slow growing phenotype. The study was unable to obtain sequences from the blue colonies. More time to repeat the experiment might have help to identify the problem.

While reassortment was detected in a small number of isolates, it would seem as if the majority of strains that emerged in the outbreaks accumulated over time while circulating in South Africa. Studies have described various amino acid substitutions in the glycoproteins that might contribute to the association between RVFV genotypes and lethal phenotypes (Bird *et al*., 2007). Among the variation identified is the change from glycine to glutamic acid at position 277 of the Gn gene in the strain ZH501 from a human sample during an outbreak in Egypt in 1977 (Morrill *et al*., 2010). The majority of the South African isolates analysed in the study also had glutamic acid at this position and some additional amino acid substitutions when compared to ZH501 strain. This study relates only on the impact of amino acid substitution at position 277. Further investigation on the impact of other amino acid substitutions is required to broaden the knowledge about virus pathogenicity.

The study could have been diverted resources to cell infection biology after amino acid substitution analysis because during viral attachment and entry, many of the capsid substitutions may affect the stability of the virus. Therefore, heating the virus and testing for differences in infection rate would have indicated whether the phenotype was capsid associated or not. Determination of the rate of transcription and replication using quantitative PCR and rates of translation using ELISA might have also indicated whether the L segment is responsible for the phenotype observed or not. These are additional approaches that can be considered in future studies.

Despite the weaknesses identified, the study did produce significant results. Complete genome sequences of South African isolates of RVFV that caused the disease outbreaks from 2008 to 2010 were determined. Comparison of growth rates indicates different phenotypes for

cattle- and sheep-derived strains. Comparative sequence analysis linked with functional information identified possible amino acid substitutions that may be responsible for the phenotypes, but this needs to be confirmed. In this study, the ectodomains of Gn and Gc were successfully expressed in yeast cells. The expressed proteins can be used to improve diagnostic tests for RVFV. The cDNA BHK library generated in this study will be a significant resource for animal disease research that can be used to study host-virus protein interactions for many other animal diseases such as African horse sickness, bovine ephemeral fever, epizootic haemorrhagic and bluetongue.

CHAPTER 6: REFERENCES

Abd El-Rahim IHA, El-Hakam U., Hussein M (1999) An epizootic of Rift Valley fever in Egypt in 1997. *Revue Scientifique et Technique De L'Office International Des Epizooties* 18:741-748.

Abudurexiti A, Adkins S, Alioto D, Alkhovsky SV, Avšič-Županc T, Ballinger MJ, Bente DA, Beer M, Bergeron É, Blair CD, Briese T, Buchmeier MJ, Burt FJ, Calisher CH, Cháng C, Charrel RN, Choi IR, Clegg JCS, De la Torre JC, De Lamballerie X, Dèng F, Serio FD, Digiaro M, Drebot MA, Duàn X, Ebihara H, Elbeaino T, Ergünay K, Fulhorst CF, Garrison AR, Gão GF, Gonzalez JPJ, Groschup MH,Günther S, Haenni AL, Hall RA, Hepojoki J, Hewson R, Hú Z, Hughes HR, Jonson MG, Junglen S, Klempa B, Klingström J, Kòu C, Laenen L, Lambert AJ, Langevin SA, Liu D, Lukashevick IS, Luò T, Lǚ C, Maes P, De Souza WM, Marklewitz M, Martelli GP, Matsuno K, Mielke-Ehret N, Minutolo M, Mirazimi A, Moming A, Mühlbach HP, Naidu R, Navarro B, Nunes MRT, Palacios G, Papa A, Pauvolid-Corrêa A, Paweska JT, Qiáo J, Radoshitzky SR, Resende RO, Romanowski V, Sall AA, Salvato MS, Sasaya T, Shěn S,Shi X, Shirako Y, Simmonds P, Sironi M, Song JW, Spengler JR, Stenglein MD, Sü Z, Sūn S, Táng S, Turina M, Wáng B, Wáng C, Wáng H, Wáng J, Wèi T, Whitfield AE, Zerbini FM, Zhāng J, Zhāng L, Zhāng Y, Zhang YZ, Zhāng Y, Zhou X, Zhū L, Kuhn JH (2019) Taxonomy of the order *Bunyavirales*: update 2019. *Archives of Virology* 164:1949-1965.

Adam I, Karsany MS (2008) Case report: Rift Valley fever with vertical transmission in a pregnant Sudanese woman. *Journal of Medical Virology* 80:929.

Agudelo-Romero P, Carbonell P, Perez-Amador MA, Elena SF (2008) Virus adaptation by manipulation of host's gene expression. *PLoS One* 3:e2397.

Ahmad K (2000) More details from Rift Valley fever in Saudi Arabia and Yemen. *Lancet* 356:1422.

Ahmed O, El Mamy O, Baba MO, Barry Y, Isselmou K, Dia ML, Hampate B, Diallo MY, El Kory MOB, Diop M, Lo MM, Thiongane Y, Bengoumi M, Puech L, Plee L, Claes F, de La Rocque S, Doumbia B ((2011) Unexpected Rift Valley fever outbreak, Northern Mauritania. *Emerging Infectious Diseases* www.cdc.gov/eid 17:1894-1896.

Alexander RA (1957) Discussion on both Rift Valley fever (R.V.F.) and Wesselsbron Virus Disease (W.V.D.). In Proceedings of the IVth Annual Meeting of the Inter African Advisory Committee on Epizootic Disease. *Interafrican Bureau for Epizootic Diseases* 29.

Alexander RA (1951) Rift Valley fever in the Union. *Journal of South African Veterinary Medical Association* 22:105.

Alhaj M (2016) Safety and efficacy profile of commercial veterinary vaccines against Rift Valley fever: A review study. *Journal of Immunology Research* 7346294.

Al-Hazmi M, Ayoola EA, Abdurahman M, Banzal S, Ashraf J, El-Bushra A, Hazmi A, Abdullah M, Abbo H, Elamin A, Al-Sammani EI-T, Gadour M, Menon C, Hamza M, Rahim I, Hafez M, Jambavalikar M, Arishi H, Aqeel A (2003) Epidemic Rift Valley fever in Saudi Arabia: A clinical study of severe illness in humans. *Clinical Infectious Disease* 36:245-252.

Al-Taweel K, Fernando WGD, Brûlé-Babel AL (2011) Construction and characterization of a cDNA library from wheat infected with *Fusarium graminearum* Fg 2. *International Journal of Molecular Sciences* 12:613-626.

Amroun A, Priet S, de Lamballerie X, Quérat G (2017) Bunyaviridae RdRps: structure, motifs, and RNA synthesis machinery. *Critical Reviews in Microbiology* 43:753-778.

Andriamandimby SF, Randrianarivo-Solofoniaina AE, Jeanmaire E.M, Ravololomanana L, Razafimanantsoa LT, Rakotojoelinandrasana T, Razainirina J., Hoffmann J, Ravalohery J-P, Rafisandratantsoa J-T, Rollin PE, Reynes J-MK (2010) Rift Valley fever during rainy seasons, Madagascar, 2008 and 2009. *Emerging Infectious Diseases* www.cdc.gov/eid 6:963-970.

Anyamba A, Linthicum KJ, Small J, Britch SC, Park E, de La Rocque S, Formenty[c] P, Hightower AW, Breiman RF, Chretien JP, Tucker CJ, Schnatel DC, Sang R, Haagsma K, Latham M, Lewandowski HB, Magda SO, Mohamed MA, Nguku PM, Reynes JM, Swanepoel R (2010) Prediction, assessment of the Rift Valley fever activity in east and southern Africa 2006-2008 and possible vector control strategies. *American Journal of Tropical Medicine and Hygiene* 83:43-51.

Anyamba A, Chretien JP, Small J, Tucker CJ, Formenty P, Richardson JH, Britch SC, Schnabel DC, Erickson RL, Linthicum KJ (2009) Prediction of Rift Valley fever outbreak. *Proceedings of the National Academy of Sciences of the United States of America* 106:955-959.

Anyamba A, Linthicum KJ, Mahoney R, Tucker CJ, Kelley PW (2002) Mapping potential risk of Rift Valley fever outbreaks in African Savannas using vegetation index time series data. *Photogrammetric Engineering and Remote Sensing* 68:137-145.

Anyangu AS, Gould LH, Sharif SK, Nguku PM, Omolo JO, Mutonga D, Rao CY, Lederman ER, Schnabel D, Paweska JT, Katz M, Hightower A, Njenga MK, Feikin DR, Breiman RF,

(2010) Risk factors for severe Rift Valley fever infection in Kenya. *American Journal of Tropical Medicine and Hygiene* 83:14-21.

Arabidopsis Interactome Mapping Consortium (2011) Evidence for network evolution in an Arabidopsis Interactome map. *Science* 333:601-607.

Aravind S, Kamble NM, Gaikwad SS, Khulape SA, Dey S, Dhama K, Mohan CM (2014) Bioinformatics study involving characterization of synonymous codon usage bias in the duck enteritis virus glycoprotein D (gD) gene. *Asian Journal of Animal and Veterinary Advances* 9:229-242.

Archer BN, Thomas J, Weyer J, Cengimbo A, Landoh DE, Jacobs C, Ntuli S, Modise M, Mathonsi M, Mashishi MS, Leman PA, Le roux C, Jansen van Vuren, Kemp A, Paweska JT, Blumberg L (2013) Epidemiologic investigations into outbreaks of Rift Valley fever in humans, South Africa, 2008-2011. *Emerging Infectious Diseases* 19:1918-1925.

Archer BN, Weyer J, Paweska J, Nkosi D, Leman P, Tint KS, Blumberg L (2011) Outbreak of Rift Valley fever affecting veterinarians and farmers in South Africa, 2008. *South African Medical Journal* 101:263-266.

Arishi HM, Aqeel AY, Al Hazmi MM (2006) Vertical transmission of fatal Rift Valley fever in a newborn. *Annals of Tropical Paediatrics* 26:251-253.

Auerbach D, Fetchko M, Stagljar I (2003) Proteomics approaches for generating comprehensive protein interaction maps. *Targets* 2:85-92.

Avila JR, Lee JS, Torii KU (2015) Co-Immunoprecipitation of membrane-bound receptors. *Arabidopsis Book* 13:e0180.

Baba M, Masiga DK, Sang R, Villinger J (2016) Has Rift Valley fever virus evolved with increasing in human populations in East Africa? *Emerging Microbes and Infections* 5:e58.

Baker SF, Nogales A, Martinez-Sobrido L (2015) Downregulating viral gene expression: codon usage bias manipulation for the generation of novel influenza A virus vaccines. *Future Virology* 10:715-730.

Bakheet TM, Doig AJ (2009) Properties and identification of human protein drug targets. *Bioinformatics* 25:451-457.

Barnard BJ, Botha MJ (1977) An inactivated Rift Valley fever vaccine. *Journal of South African Veterinary Association* 48:45-48.

Baudin M, Jumaa AM, Jomma HJE, Karsany MS, Bucht G, Naslund J, Ahlm C, Evander M, Mohamed N (2016) Association of Rift Valley fever virus infection with miscarriage in Sudanese women: a cross-sectional study. *Lancet Glob Health* 4:e864-e874.

Behura SK, Severson DW (2013) Codon usage bias: causative factors, quantification methods and genome-wide patterns: with emphasis on insects genomes. *Biological Reviews* 88:94-61.

Belalov IS, Lukashev AN (2013) Cause and implications of codon usage bias in RNA viruses. *PLoS One* 8:e56642.

Berggard T, Linse S, James P (2007) Methods for the detection and analysis of protein-protein interactions. *Proteomics* 7:2833-2842.

Bernsel A, Viklund H, Hennerdal A, Elofsson A (2009) TOPCONS: consensus prediction of membrane protein topology. *Nuclei Acids Research* 37:W465-W468.

Bird BH, Albarino CG, Hartman AL, Erickson BR, Ksiazek TG, Nichol ST (2008a) Rift Valley fever lacking NSs and NSm genes is highly attenuated, confers protective immunity from virulent virus challenge, and allows for differential identification of infected and vaccinated animals. *Journal of Virology* 82:2681-2691.

Bird BH, Githinji JW, Macharia JM, Kasiiti JL, Muriithi RM, Gacheru SG, Musaa JO, Towner JS, Reeder SA, Oliver JB, Stevens TL, Erickson BR, Morgan LT, Khristova ML, Hartman AL, Comer JA, Rollin PE, Ksiazek TG, Nichol ST (2008b) Multiple virus lineages sharing recent common ancestry were associated with a large Rift Valley fever outbreak among livestock in Kenya during 2006-2007. *Journal of Virology* 82:11152-11166.

Bird BH, Khristova ML, Rollin PE, Ksiazek TG, Nichol ST (2007) Complete genome analysis of 33 ecologically and biologically diverse Rift Valley fever virus strains reveals widespread virus movement and low genetic diversity due to recent common ancestry. *Journal of Virology* 81:2805-2816.

Botros B, Omar A, Elian K, Mohamed G, Soliman A, Salib A., Salman D, Saad M, Earhart K (2006) Adverse response of non-indigenous cattle of European breeds to live attenuated Smithburn Rift Valley fever vaccine. *Journal of Medical Virology* 78:787-791.

Bouloy M, Weber F (2010) Molecular Biology of Rift Valley fever virus. *The Open Virology Journal* 4:8-14.

Bouloy M, Flick R (2009) Reverse genetics technology for Rift Valley fever virus: Current and future applications for development of therapeutics and vaccines. *Antiviral Research* 84:101-118.

Bouloy M, Janzen C, Vialat P, Khun H, Pavlovic J, Huerre M, Haller O (2001) Genetic evidence for an interferon-antagonistic function of Rift Valley fever virus non-structural protein NSs. *Journal of Virology* 75:1371-1377.

Boyd S (2013) Diagnostic applications of High-Throughput DNA sequencing. *Annual Review of Pathology: Mechanisms of Disease* 8:381-410.

Brückner A, Polge c, Lentze N, Auerbach, Schlattner U (2009) Yeast two-hybrid, a powerful tool for systems biology. *International Journal of Molecular Sciences* 10:2763-2788.

Burns CC, Shaw J Campagnoli R, Jorba J, Vincent A, Quay J, Kew O (2006) Modulation of Poliovirus replicative fitness in Hela cells by deoptimization of synonymous codon usage in the capsid region. *Journal of Virology* 80:3259-3275.

Butt AM, Nasrullah I, Qamar R, Tong Y (2016) Evolution of codon usage in Zika virus genomes in host and vector specific. *Emerging Microbes and Infections* 5:e107.

Butt AM, Nasrullah I, Tong Y (2014) Genome-wide analysis of codon usage and influencing factors in Chikungunya viruses. *PLoS One* 9:e90905.

Causier B, Davies B (2002) Analysing protein-protein interactions with the yeast two-hybrid system. *Plant Molecular Biology* 50:855-870.

Centres for Disease Control and Prevention (2000) Update: Outbreak of Rift Valley fever-Saudi Arabia. August – November (2000) MMWR Morbidity and Mortality Weekly Report 49:905-908.

Cêtre-Sossah C, Pédarrieu A, Juremalm M, Jansen van Vuren, Brun A, Mamy ABO, Héraud JM, Filippone C, Ravalohery JP, Chaabihi H, Albina E, Dommergues L, Paweska J, Cardinale E (2019) Development and validation of a pen side test for Rift Valley fever. *PLoS Neglected Tropical Disease* 13:e0007700.

Chengula AA, Mdegela RH, Kasanga CJ (2013) Socio-economic impact of Rift Valley fever to pastoralists and agro pastoralists in Arusha, Manyara and Morogoro regions in Tanzania. *Springer Plus* 2:1-14.

Chevalier V, Rakotondrafara T, Jourdan M, Heraud JM, Andriamanivo HR, Durand B, Ravaomanana J Rollin PE, Rakotondravao R (2011) An unexpected recurrent transmission of Rift Valley fever virus in cattle in a temperate and mountainous area of Madagascar. *PloS Neglected Tropical Diseases* 5:e1423.

Chevalier V, Pepin M, Plee L, Lancelot R (2010) Rift Valley fever – a threat for Europe? *European Surveillance* 15:1-11.

Ciota AT, Kramer LD (2010) Insights into arbovirus evolution and adaptation from experimental studies. *Viruses* 2:2594-2617.

Cobo F (2012) Application of molecular diagnostic techniques for viral testing. *The Open Virology Journal* 6:104-114.

Codon usage database: www.kazusa.or.jp/codon.

Coetzer JAW (1982) The pathology of Rift Valley fever.11. Lesions occurring in field cases in adult cattle, calves and aborted foetuses. *Onderstepoort Journal of Veterinary Research* 49: 11-17.

Coetzer JAW (1977) The pathology of Rift Valley fever. 1. Lesions occurring in natural cases in new-born lambs. *Onderstepoort Journal of Veterinary Research* 44:205-212.

Collett MS, Purchio AF, Keegan K, Frazier S, Hays W, Anderson DK (1985) Complete nucleotide sequence of the M RNA segment of Rift Valley fever virus. *Virology* 144:228-45.

Corso B, Pinto J, Beltrán-Alcrudo D, De Simone L and Lubroth J (2008) Rift Valley fever outbreaks in Madagascar and potential risks to neighbouring countries. *FAO Empress Watch Emergency Prevention Systems* 1-5.

Corry B, Jayatilaka D, Rigby P (2005) A flexible approach to the calculation of resonance energy transfer efficiency between multiple donors and acceptors in complex geometries. *Biophysical Journal* 89:3822-3836.

Cyr N, de la Fuente C, Lecoq L, Guendel I, Chabot PR, Kehn-Hall K, Omichinski JG (2015) A ΩXaV motif in the Rift Valley fever virus NSs protein is essential for degrading p62, forming nuclear filaments and virulence. *Proceedings of the National Academy of Sciences of the United States of America* 112:6021-6026.

Daubney R, Hudson JR (1933) Rift Valley fever. *East African Medical Journal* 10:2-19.

Daubney R, Hudson JR, Garnham (1931) Enzootic hepatitis or Rift Valley fever. An undescribed virus disease of sheep, cattle and man from East Africa. *Journal of Pathology and Bacteriology* 34:545-579.

Dautu G, Sindato C, Mweene AS, Samui KL, Roy P, Noad R, Paweska JZ, Majiwa PAO, Musoke AJ (2012) Rift valley fever: Real or perceived threat for Zambia? *Onderstepoort Journal of Veterinary Research* 79:466.

Davies FG (2010) The historical and recent impact of Rift Valley fever in Africa. *American Journal of Tropical Medicine and Hygiene* 83:73-74.

Davies FG, Karstad L (1981) Experimental infection of the African buffalo with the virus of Rift Valley fever. *Tropical Animal Health and Production* 13:185-188.

Davies FG (1975) Observations on the epidemiology of Rift Valley fever in Kenya. *Journal of Hygiene* 75:219-230.

Davies FG, Clausen B, Lund LJ (1972) The pathogenicity of Rift Valley fever virus for the baboon. *Transactions of the Royal Society of Tropical Medicine and Hygiene* 66:363-365.

De Boer SM, Kortekaas J, de Haan CAM, Rottier PJM, Moormann RJM, Bosch BJ (2012) Heparin sulphate facilitates Rift Valley fever virus entry into the cell. *Journal of Virology* 86:13767-13771.

Delano WL (2002) The PyMol Molecular Graphics System. Delano Scientific, San Carlos, CA USA. http://www.pymol.org.

Dessau M, Modis Y (2013) Crystal structure of glycoprotein C from Rift Valley fever virus. *Proceedings of the National Academy of Sciences of the United States of America* 110:1696-1701.

Digoutte JP, Jouan A, Le Guenno B, Riou O, Philippe B, Meegan J, Ksiazek TG, Peters CJ (1989) Isolation of the Rift valley fever virus by inoculation into Aedes pseuscutellaris cells: comparison with other diagnostic methods. *Research in Virology* 140:31-41.

Djikeng A, Halpin R, Kuzmickas R, Depasse J, Feldblyum J, Sengamalay N, Afonso C, Zhang X, Anderson NG, Ghedin E, Spiro DJ (2008) Viral genome sequencing by random priming methods. *BioMed Central Genomics* 9:5.

Dodd KA, McElroy AK, Jones TL, Zaki SR, Nichol ST, Spiropoulou CF (2014) Rift Valley fever virus encephalitis is associated with an ineffective systematic immune response and activated T cell infiltration into the CNS in an immunocompetent mouse model. *PLos Neglected Tropical Diseases* 8:e2874.

Drosten C, Göttig S, Schilling S, Asper M, Panning M, Schmitz H, Günther S (2002) Rapid detection and quantification of RNA of Ebola and Marburg viruses, Lassa virus, Crimean-Congo hemorrhagic fever virus, Rift Valley fever virus, Dengue virus, and Yellow fever virus by real-time reverse transcription-PCR. *Journal of Clinical Microbiology* 40:2323-2330.

Drummond AJ, Suchard MA, Xie D, Rambaut A (2012) Bayesian phylogenetics with BEAUTi and the BEAST 1.7 *Molecular Biology and Evolution* 29:1969-1973.

Dungu B, Donadeu M, Bouloy M (2013) Vaccination for the control of Rift Valley fever in Enzootic and Epizootic situations. *Vaccines and Diagnostics for Transboundary Animal Diseases* 135:61-72.

Dungu B, Louw I, Lubisi A, Hunter P, von Teichman BF, Bouloy M (2010) Evaluation of the efficacy and safety of Rift Valley fever clone 13 vaccine in sheep. *Vaccine* 28:4581-4587.

Easterday BC (1965) Rift Valley fever. *Advanced Veterinary Science* 10:65-127.

Easterday BC, Murphy LC (1963) Studies on Rift Valley fever in laboratory animals. *Cornell Veterinarian* 53:423-433.

Elena S, Sanjuán R (2005) Adaptive value of high mutation tares of RNA viruses: separating causes from consequences. *Journal of Virology* 79:11555-11528.

Ellenbecker M Lanchy J-M, Lodmell S (2014) Inhibition of Rift Valley fever virus replication and perturbation of Nucleocapsid-RNA interactions by suramin. *Antimicrobial Agents and Chemotherapy* 58:7405-7415.

Elliot RM (1990) Molecular biology of Bunyaviridae. *Journal of General Virology* 71:501-522.

Ellis DS, Shirodaria PV, Fleming E, Simpson DL (1988) Morphology and development of Rift Valley fever virus in Vero cell cultures. *Journal of Medical Virology* 24:161-174.

Engdahl C, Näslund J, Lindgren L, Ahlm C, Bucht G (2012) The Rift Valley fever virus protein NSm and putative cellular protein interactions. *Virology Journal* 9:139.

Evans A, Gakuya F, Paweska JT, Rostal M, Akoolo L, Van Vuuren PJ, Manyibe T, Macharia JM, Ksiazek TG, Feikin DR, Breiman RF, Njenga MK (2008) Prevalence of antibodies against Rift Valley fever virus in Kenyan wildlife. *Epidemiology Infections* 136:1261-1269.

Faburay B, LaBeaud AD, McVey DS, Wilson WC, Richt JA (2017) Current status of Rift Valley fever vaccine development. *Vaccine* 5:1-20.

Faburay B, Gaudreault NN, Liu Q, Davis AS, Shivanna V, Sunwoo SY, Lang Y, Morozov I, Ruder M, Drolet B, Scott McVey D, Ma W, Wilson W, Richt JA (2016) Development of a sheep challenge model for Rift Valley fever. *Virology* 489:128-140.

Fafetine J, Neves L, Thompson PN, Paweska JT, Rutten PMG (2013) Serological evidence of Rift Valley fever virus circulation in sheep and goats in Zambézia, Mozambique. *PLoS Neglected Tropical Diseases* 7:e2065.

Fagbo S, Coetzer JAW, Venter EH (2014) Seroprevalence of Rift Valley fever and lumpy skin disease in African buffalo (*Syncerus caffer*) in the Kruger National Park and Hluhluwe-iMfolozi Park, South Africa. *Journal of the South African Veterinary Association* 85:1075.

FAO (2002) Preparation of Rift Valley fever contingency plans. FAO Animal Health Manual. No.15. Rome. http://www.fao.org/docrep/005/Y4140E/Y4140E00.HTM

FAO (2001) Manual of procedures for disease eradication by stamping out. FAO Animal Health Manual. No.12. Rome. http://www.fao.org/docrep/004/y0660e/Y0660E01.htm

Ferron F, Li Z, Danek EI, Luo D, Wong Y, Coutard B, Lantez V, Charrel R, Canard B, Walz T, Lescar J (2011) The hexamer structure of the Rift Valley fever virus nucleoprotein suggests a mechanism for its assembly into ribonucleoprotein complexes. *PLoS Pathogens* 7:e1002030.

Fields S, Song OK (1989) A novel genetic system to detect protein-protein interactions. *Nature* 340:245-246.

Filone CM, Heise M, Doms RW, Bertolotti-Ciarlet A (2006) Development and characterization of a Rift Valley fever virus cell-cell fusion assay using alphavirus replicon vectors. *Virology* 356:155-164.

Findlay GM (1932) Rift Valley fever or Zoonotic hepatitis. *Transactions of the Royal Society of Tropical Medicine and Hygiene* 25:229-265.

Flick R, Bouloy M (2005) Rift Valley fever virus. *Current Molecular Medicine* 5:827-834.

Flick K, Hooper JW, Schmaljohn CS, Pettersson RF, Feldmann H, Flick R (2003) Rescue of Hantaan virus minigenomes. *Virology* 306:219-224.

Freiberg AN, Sherman MB, Morais MC, Molbrook MR, Watowick SJ (2008) Three-dimensional organization of Rift valley fever virus revealed by cryoelectron tomography. *Journal of Virology* 82:10341-10348.

Freire CCM, Lamarino A, Ly Soumare PO, Faye O, Sall AA, Zanotto PMA (2015) Reassortment and distinct evolutionary dynamics of Rift Valley fever virus genomic segments. *Science Reports* 5:11353.

Gad AM, Hassan MM, el Said S, Moussa MI, Wood OL (1987) Rift Valley fever virus transmission by different Egyptian mosquito species. *Transaction of the Royal Society of Tropical Medicine and Hygiene* 81:694-698.

Gao JX, Jing J, Yu Y, Chen J (2015) Construction of a high quality yeast two-hybrid library and its application in identification of interacting proteins with Brn1 in Curvularia lunata. *The Plant Pathology Journal* 3:108-114.

Garcia S, Crance JM, Billecocq A, Peinnequin A., Jouan A, Bouloy M, Garin D (2001) Quantitative real-time PCR detection of Rift Valley fever virus and its application to evaluation of antiviral compounds. *Journal of Clinical Microbiology* 39:4456-4461.

Garry CE, Garry RF (2004) Proteomics computational analyses suggest that the carboxyl terminal glycoproteins of Bunyaviruses are class II viral fusion protein (beta-penetrenes). *Theoretical Biology and Medical Modelling* 1:10.

Gauliard N, Billecocq A, Flick R, Bouloy M (2006) Rift Valley fever virus noncoding regions of L, M and S segments regulate RNA synthesis. *Virology* 351:170-179.

Gear J, Meillon DB, Roux AFL, Kofsky R (1955) Rift Valley fever in South Africa: A study of the 1953 outbreak in the Orange Free State, with special reference to the vectors and possible reservoir hosts. *South African Medical Journal* 29:514-518.

Gerdes GH (2004) Rift Valley fever. *Revue Scientifigue et Technique De L'Office International Des Epizooties* 23:613-623.

Gerrard SR, Bird BH, Albarini CG, Nichol ST (2007) The NSm proteins of Rift Valley fever virus are responsible for maturation, replication and infection. *Virology* 359:459-465.

Gerrard SR, Nichol ST (2007) Synthesis, proteolytic processing and complex formation of N-terminally nested precursor proteins of Rift Valley fever virus glycoproteins. *Virology* 357:124-133.

Giorgi C, Accardi L, Nicoletti L, Gro MC, Takehara K, Hilditch C, Morikawa S, Bishop DH (1991) Sequences and coding strategies of the S RNAs of Toscana and Rift Valley fever viruses compared to those of Punta Toro, Sicilian Sandfly fever, and Uukuniemi viruses. *Virology* 180:738-53.

Glancey MM, Anyamba A, Linthicum KJ (2015) Epidemiologic and environmental risk factors of Rift Valley in South Africa from 2008 to 2011. *Vector-borne and Zoonotic Diseases* 15:502-511.

Goldsmith CS, Miller SE (2009) Modern uses of electron microscopy for detection of viruses. *Clinical Microbiology Reviews* 22:552-563.

Goñi N, Iriarte A, Comas V, Soñora M, Moreno P, Moratorio G, Musto H, Cristina J (2012) Pandemic influenza A virus codon usage revisited: biases, adaptation and implications for vaccine strain development. *Virology Journal* 9:263.

Grobbelaar AA, Weyer J, Leman PA, Kemp A, Paweska JT, Swanepoel R (2011) Molecular epidemiology of Rift Valley fever virus. *Emerging Infectious Diseases* 17:2270-2276.

Grove J, Marsh M (2011) The cell biology of receptor-mediated virus entry. *Journal of Cell Biology* 195:1071-1082.

Habjan M., Pichlmair A., Elliot R M, Overby AK., Glatter T, Gstaiger M, Superti-Furga G, Unger H, Weber F (2009) Ns Protein of Rift Valley fever induces the specific degradation of the double-stranded RNA-dependent protein kinase. *Journal of Virology* 83:4365-4375.

Hackett BA, Yasunaga A, Panda D, Tartell MA, Hopkins KC, Hensley SE (2015) RNASEK is required for internalization of diverse acid-dependent viruses. *Proceedings of the National Academy of Sciences of the United States of America* 112:7797-7802.

Halldorsson S, Li S, Li M, Harlos K, Bowden TA, Huiskonen JT (2018) Shielding and activation of a viral membrane fusion protein. *Nature Communications* 9:349.

Halldorsson S, Behrens AJ, Harlos K, Huiskonen JT, Elliot RM, Crispin M, Brennan B, Bowden TA (2016) Structure of phleboviral envelope glycoprotein reveals a consolidated model of membrane fusion. *Proceedings of the National Academy of Sciences of the United States of America* 113:7154-7159.

Hall BG (2013) Building phylogenetic trees from molecular data with MEGA. *Molecular Biology and Evolution* 30:1229-35.

Hamdi A, Colas P (2012) Yeast two-hybrid methods and their applications in drug discovery. *Trends in Pharmacological Sciences* 33:109-118.

Hanecke F, Leparc-Goffart I, Simon F, Hentzien M, Martinez-Pourcher V, Caumes S, Maquart M (2016) Rift Valley fever in kidney transplant recipient returning from Mali with viral RNA detected in semen up to four months from symptom onset, France, autumn 2015. *Eurosurveillance* 21:30222.

Harmon B, Schudel BR, Maar D, Kozina C, Ikegami T, Tseng C-TK, Negrete OA (2012) Rift Valley fever virus strain MP-12 enters mammalian host cells via caveola-mediated endocytosis. *Journal of Virology* 86:12954-12970.

Hassan OA, Ahlm C, Sang R, Evander M (2011) The 2007 Rift Valley fever outbreak in Sudan. *PLoS Neglected Tropical Diseases* 5:e1229.

Heath L, van der Walt E, Varsani A, Martin DP (2006) Recombination patterns in aphthoviruses mirror those found in other picornaviruses. *Journal of Virology* 80:11827-11832.

Heise MT, Whitmore A, Thompson J, Parsons M, Grobbelaar AA, Kemp A, Paweska JT, Madric K, White LJ, Swanepoel R, Burt FJ (2009) An alpha virus replicon-derived candidate vaccine against Rift Valley fever virus. *Epidemiology and Infection* 137:1309-1318.

Hershberg R, Petrov DA (2008) Selection on codon bias. *Annual Review of Genetics* 42:287-299.

Himeidan YE, Kweka EJ, Mahgoub MM, Rayah EAE, Ouma JO (2014) Recent outbreaks of Rift Valley fever in East Africa and the Middle East. *Frontiers in Public Health* 2:169.

Hoch AL, Turell MJ, Bailey CL (1984) Replication of Rift Valley fever virus in the sand fly *Lutzomyia longipalpis*. *The American Journal of Medicine and Hygiene* 33:295-299.

Hoffman EA, Frey BL, Smith LM, Auble DT (2015) Formaldehyde crosslinking: A tool for the study of chromatin complexes. *Journal of Biological Chemistry* 290:26404-26411.

Holding AN (2015) XL-MS: Protein cross-linking coupled with mass spectrometry. *Methods* 89:54-63.

Holm T, Kopicki JD, Busch C, Olschewski S, Rosenthal M, Uetrecht C, Günther S, Reindi S (2018) Biochemical and structural studies reveal differences and commonalities among cap-snatching endonucleases from segmented negative-strand RNA viruses. *Journal of Biological Chemistry* 293:19686-19698.

Hoogstral H, Meegan JM, Khalil GM, Adham FK (1979) Rift Valley fever epizootic in Egypt 1977-1978. 11. Ecological and entomological studies. *Transactions of the Royal Society of Tropical Medicine and Hygiene* 73:624-629.

Hook B, Bernstein D, Zhang B, Wickens M (2005) RNA-protein interactions in the yeast three-hybrid system: Affinity, sensitivity, and enhanced library screening. *RNA* 11:227-233.

Hooker BS, Bigelow DJ, Lin, CT (2007) Methods for mapping of interaction networks involving membrane proteins. *Biochemical and Biophysical Research Communications* 363:457-461.

https://bioinformatics.org/sms/

http://octopus.cbr.su.se

http://topcons.net

Huo T, Liu W, Guo Y, Yang C, Lin J, Rao Z (2015) Prediction of host-pathogen protein interactions between *Mycobacterium tuberculosis* and *Homo sapiens* using sequence motifs. *BioMed Central Bioinformatics* 16:100.

Huiskonen JT, Overby AK, Weber F, Grünewald K (2009) Electron cryo-microscopy and single-particle averaging of Rift Valley fever virus: evidence for GN-GC glycoprotein heterodimers. *Journal of Virology* 83:3762-3769.

Hunter P, Erasmus BJ, Vorster JH (2002) Teratogenicity of a mutagenized Rift Valley fever (MV 12) in sheep. *Onderstepoort Journal of Veterinary Research* 69:95-98.

Hunter B, Bouloy M (2001) Investigation of C13 RVF mutant as a vaccine strain. *In: Proceedings of 5th International Sheep Veterinary Congress* 21-25 Stellenbosch, South Africa.

Ikegami T (2017) Rift Valley fever vaccines: An overview of the safety and efficacy of the live–attenuated MP-12 vaccine candidate. *Expert Review of Vaccines* 16:601-611.

Ikegami T (2012) Molecular biology and genetic diversity of Rift Valley fever virus. *Antiviral Research* 95:293-310.

Ikegami T, Makino S (2011) The Pathogenesis of Rift Valley fever. *Viruses* 3:493-519.

Ikegami T, Makino S (2009) Rift Valley fever vaccines. *Vaccines* 2754:D69-D72.

Ikegami T, Won Peters CJ, Makino S (2007) Characterization of Rift Valley fever virus transcriptional terminations. *Journal of Virology* 81:8421-8438.

Imam IZE, EL-Karamany R, Darwish MA (1979) An epidemic of Rift Valley fever in Egypt 2. Isolation of the virus from animals. *Bulletin of the World Health Organization* 57:441-443.

Iyer K, Bürke L, Auerbach D, Thaminy M, Dinkel M, Engels K, Stagljar I (2005) Utilizing the split-ubiquitin membrane yeast two hybrid system to identify protein-protein interactions of integral membrane proteins. *Science's STKE: Signal Transduction Knowledge Environment* 15:13.

Jansen van Vuren P, Paweska JT (2009) Laboratory safe detection of nucleocapsid protein of Rift Valley fever virus in human and animal specimens by a sandwich ELISA. *Journal of Virological Methods* 157:15-24.

Jupp PG, Kemp A, Grobbelaar A, Leman P, Burt FJ, Alahmed AM, Al Mujalli D, Al Khamees M, Swanepoel R (2002) The 2000 epidemic of Rift Valley fever in Saudi Arabia: mosquito vector studies. *Medical and Veterinary Entomology* 16:245-252.

Kakach LT, Wasmoen TL, Collet MS (1988) Rift Valley fever virus M Segment: Use of recombinant vaccinia viruses to study *Phlebovirus* gene expression. *Journal of Virology* 62:826-833.

Kamal SA (2011) Observations on Rift Valley fever virus and vaccines in Egypt. *Virology Journal* 8:532.

Kanai Y, Komoto S, Kawagishi T, Nouda R, Nagasawa N, Onishi M, Matsuura Y, Taniguchi K, Kobayashi T (2017) Entirely plasmid-based reverse genetics system for rotaviruses. *Proceedings of the National Academy of Sciences of the United States of America* 114:2349-2354.

Kasye M, Teshome D, Abiye A, Eshetu A (2016) A review on Rift Valley fever on animal, human health and its impact on livestock marketing. *Austin Virology and Retrovirology* 3:020.

Kegakilwe PS (2010) An atypical outbreak of Rift Valley fever in the Northern Cape in October 2009. *Proceedings of the 9th Annual Congress of the Southern African Society for Veterinary Epidemiology and Preventive Medicine*. 18-20 August 2010. Farm Inn, Republic of South Africa. ISBN 978-0-620-47979-0.

Kelly LA Mezulis S, Yates CM, Wass MN, Sternberg JE (2015) The Phyre2 web portal for protein modelling, prediction and analysis. *Nature Protocols* 10:845-858.

Kendall LV, Steffen EK, Riley LK (1999) Hemagglutination inhibition (HAI) assay. *American Association for Laboratory Animal Science* 38:54.

Klockenbusch C, Kast J (2010) Optimization of formaldehyde cross-linking for protein interaction analysis of non-tagged Integrin B1. *Journal of Biomedicine and Biotechnology* 2010:927585.

Koegl M, Uetz P (2008) Improving yeast two-hybrid screening systems. *Briefings in Functional Genomics* 6:302-312.

Kortekaas J, Zingeser J, de Leeuw P, de la Rocque S, Unger H, Moorman RJM (2011) Rift Valley fever vaccine development, progress and constraints. *Emerging Infectious Diseases* 17:e1.

Kreher F, Tamietti C, Gommet C, Guillemot L, Ermonval M, Failloux A-B, Panthier J-J, Bouloy M, Flamand M (2014) The Rift Valley fever accessory proteins NSm and P78/NSm-G_N are distinct determinants of virus propagation in vertebrate and invertebrate hosts. *Emerging Microbes and Infections* 3:e71.

Kuo HJ, Maslen CL, Keene DR, Glanville RW (1997) Type VI collagen anchors endothelial basement membranes by interacting with type IV collagen. *Journal of Biological Chemistry* 272:26522-26529.

LaBeaud AD, Cross PC, Getz WM, Glinka A, King CH (2011) Rift Valley fever virus infection in African Buffalo (*Syncerus caffer*) herds in rural South Africa: Evidence of interepidemic transmission. *American Journal of Tropical Medicine and Hygiene* 84:641-646.

Lai MY, Lau YL (2017) Screening and identification of host proteins interacting with *Toxoplasma gondii* SAG2 by yeast two-hybrid assay. *Parasites and Vectors* 10:456.

Lauring AS, Acevedo A, Cooper SB, Andino R (2012) Codon usage determines the mutational robustness, evolutionary capacity, and virulence of an RNA virus. *Cell Host and Microbe* 12:623-632.

Laviada MD, Arias M, Sánchez-Vizcaino JM (1993) Characterization of African horse sickness virus serotype 4-induced polypeptides in Vero cells and their reactivity in western immunoblotting. *Journal of General Virology* 74:81-87.

LeBreton M, Umlauf S, Djoko CF, Daszak P, Burke DS, Kwenkam PY, Wolfe ND (2006) Rift Valley fever in goats, Cameroon. *Emerging Infectious Diseases* 12:702-703.

Lee LY, Wu FH, Hsu CT, Shen SC, Yeh HY, Liao D, Fang MJ, Liu NT, Yen YC Dokládal L (2012) Screening a cDNA library for protein-protein interactions directly in planta. *Plant Cell* 24:1746-1759.

Léger P, Tetard M, Youness B, Cordes N, Rouxel RN, Flamand M, Lozach PY (2016) Differential use of the C-type lectins L-SIGN and DC-SIGN for Phlebovirus endocytosis. *Traffic* 17:639-656.

Lernout T, Cardinale E, Jego M, Desprès P, Collet L, Zumbo B, Tillard E, Girard S and Filleul L (2013) Rift Valley fever in humans and animals in Mayotte, an Endemic situation? *PLoS One* 8:e74192.

Le Roux CA, Kubo T, Grobbelaar AA, Jansen van Vuren P, Weyer J, Nel LH, Swanepoel R, Morita K, Paweska JT (2009) Development and evaluation of a real-time reverse transcription-loop-mediated isothermal amplification assay for rapid detection of Rift Valley fever virus in clinical specimens. *Journal of Clinical Microbiology* 47:645-651.

Letunic I, Doerks T, Bork P (2014) SMART: recent updates, new developments and status in 2015. *Nucleic Acids Research* 43:D257-D260.

Li YP, Xia RX, Wang H, Li XS, Liu YQ, Wei ZJ, Lu C, Xiang ZH (2009) Construction of a full-length cDNA library from Chinese oak silkworm pupa and identification of a KK-42-binding protein gene in relation to pupa-diapause termination. *International Journal of Biological Sciences* 5:451-457.

Lichoti JK, Kihara A, Oriko AA, Okutoyi LA, Wauna JO, Tchouassi DP, Tigoi CC, Kemp S, Sang R Mbabu RM (2014) Detection of Rift Valley fever virus interepidemic activity in some hotspot areas of Kenya by sentinel animal surveillance, 2009-2012. *Veterinary Medicine International* 2014:379010.

Linthicum KJ, Anyamba A, Tucker CJ, Kelley PW, Myers MF, Peters J (1999) Climate and satellite indicators to forecast Rift Valley fever epidemics in Kenya. *Science* 285:397-400.

Linthicum KJ, Davies FG, Kairo A (1985) Rift Valley fever virus (family Bunyaviridae, genus *Phlebovirus*). Isolation from Diptera collected during an inter-epizootic period in Kenya. *Journal of Hygiene* 95:197-209.

Liu Q, Li FC, Elsheika HM, Sun MM, Zhu XQ (2017) Identification of host proteins interacting with *Toxoplasma gondii* GRA 15 (TgGRA 15) by yeast two-hybrid system. *Parasites and Vectors* 10:1.

Liu W, Sun FJ Tong YG, Zhang SQ, Cao WC (2016) Rift Valley fever virus imported into China from Angola. *The Lancet Infectious Disease* 16:1226.

Liu C, Liu D, Guo Y, Lu T, Li X, Zhang M, Ma J, Ma Y, Guan W (2013) Construction of a full-length enriched cDNA library and preliminary analysis of expressed sequence tags from Bengal tiger *Panthera tigris tigris*. *International Journal of Molecular Sciences* 14:11072-11083.

Liu L, Celma CCP, Roy P (2008) Rift Valley fever virus structural proteins: expression, characterization and assembly of recombinant proteins. *Virology Journal* 5:82.

Liu J, Thorp SC (2002) Cell surface heparin sulphate and its role in assisting viral infection. *Medicinal Research Revision* 22:1-25.

Logan TM, Linthicum KJ, Davies FG, Binepal YS, Roberts CR (1991) Isolation of Rift Valley fever virus from mosquitoes (Diptera: Culcidae) collected during an outbreak in domestic animals in Kenya. *Journal of Medical Entomology* 28:293-295.

Lozach PY, Kühbacher A, Meier R, Mancini R, Bitto D, Bouloy M., Helenius A (2011) DC-SIGN as a receptor for *Phleboviruses*. *Cell Host and Microbe* 10:75-88.

Lozach PY, Mancini R, Bitto D, Meier R, Oestereich L, Överby AK, Pettersson RF, Helenius, A. (2010) Entry of bunyaviruses into mammalian cells. *Cell Host and Microbe* 7:488-499.

Lucas M, Krrer U, Lucas A, Klenerman P (2001) Viral escape mechanisms – escapology taught by viruses. *International Journal of Experimental Pathology* 82:269-286.

Lum KK, Cristea IM (2016) Proteomic approaches to uncovering virus-host protein interactions during the progression of viral infection. *Expert Review of Proteomics* 13:325-340.

Ly HJ, Ikegami T (2016) Rift Valley fever virus NSs protein functions and the similarity to other bunyavirus NSs proteins. *Virology Journal* 13:118.

Ma Y, Ruan Q, Ji Y, Wang N, Li M, Qi Y, He R, Sun Z, Ren G (2011) Novel transcripts of human cytomegalovirus clinical strain found by cDNA library screening. *Genetics and Molecular Research* 10:566-575.

Machida K, Mayer BJ (2009) Detection of protein-protein interactions by far-western blotting. In protein blotting and detection. Humana Press Volume 536 pages 313-329.

Mahajan S, Sharma GK, Matura R, Subramaniam S, Mohapatra JK, Pattnaik B (2015) Construction and characterization of yeast two-hybrid cDNA library derived from LFBK cell line. *Biologicals* 43:202-208.

Maluleke MR, Phosiwa M, van Schalkwyk A, Michuki G, Lubisi BA, Kegakilwe PS, Kemp SJ, Majiwa PAO (2019) A comparative genome analysis of Rift Valley fever virus isolates from foci of the disease outbreak in South Africa in 2008-2010. *PloS Neglected Tropical Diseases* 13(3):e0006576.

Marchler-Bauer A, Derbyshire MK, Gonzales NR, Lu S, Chitsaz F, Geer LY, Geer RC, He J, Gwadz M, Hurwitz DI, Lanczycki CJ, Lu F, Marchler GH, Song JS, Thanki N, Wang Z, Yamashita RA, Zhang D, Zheng C, Bryant SH (2015) CDD: NCBI's conserved domain database. *Nucleic Acids Research* 43:D222-D226.

Martin ML, Lindsey-Regnery H, Sasso DR, McCormick JB, Palmer E (1985) Distinction between Bunyaviridae genera by surface structure and comparison with Hantaan virus using negative stain electron microscopy. *Archives of Virology* 86:17-28.

McIntosh BM, Russel D, Dos Santos I, Gear JHS (1980a) Rift Valley fever in humans in South Africa. *South African Medical Journal* 58:803-806.

McIntosh BM, Jupp PG, Dos Santos I, Barnard BJH (1980b) Vector studies on Rift Valley fever virus in South Africa. *South African Medical Journal* 58:127-132.

McLaughlin BE, DeMaula CD, Wilson WC, Boyce WM, MacLachlan NJ (2003) Replication of bluetongue virus and epizootic hemorrhagic disease virus in pulmonary artery endothelial cells obtained from cattle, sheep and deer. *American Journal of Veterinary Research* 64:860-865.

Meegan JM (1981) Rift Valley fever in Egypt: an overview of epizootics in 1977 and 1978. *Contributions to Epidemiology and Biostatistics* 3:100-113.

Meegan JM (1979) The Rift Valley fever epizootic in Egypt 1977-98. 1. Description of the epizootic and virological studies. *Transaction of the Royal Society of Tropical Medicine and Hygiene* 73:618-623.

Mendez-Rios J, Uetz P (2010) Global approaches to study protein-protein interactions among viruses and hosts*. Future Microbiology* 5:289-301.

Métras R, Jewel C, Porphyre T, Thompson PN, Pfeiffer DU, Collins LM, White RG (2015) Risk factors associated with Rift Valley fever epidemics in South Africa in 2008-11. *Scientific Reports* 5:9492.

Métras R, Porphyre T, Pfeiffer DU, Kemp A, Thompson PN, Collins LM, White RG (2012) Exploratory space-time analysis of Rift Valley fever in South Africa in 2008-2011. *PloS Neglected Tropical Diseases* 6:e1808.

Miernyk JA, Thelen JJ (2008) Biochemical approaches for discovering protein-protein interactions. *The Plant Journal* 53:597-609.

Mokili JL, Rohwer F, Dutilh BE (2012) Metagenomics and future perspectives in virus discovery. *Current Opinion in Virology* 2:63-77.

Monaco F, Pinoni C, Cosseddu, GM, Khaiseb S, Calistri P, Molini U, Bishi A, Conte A, Scacchia M, Lelli R (2013) Rift Valley fever in Namibia, 2010. *Emerging Infectious Diseases* 19:2025-2027.

Morrill JC, Ikegami T, Yoshikawa-Iwata N, Lokugamage N, Won S, Terasaki K, Zamoto-Niikura A, Peters CJ, Makino S (2010) Rapid accumulation of virulent Rift Valley fever virus in mice from an attenuated virus carrying a single nucleotide substitution in the mRNA. *PLoS One* 5:e9986.

Morrill JC, Carpenter L, Taylor D, Ramsburg HH, Quance J Peters CJ (1991) Further evaluation of a mutagen-attenuated Rift Valley fever vaccine in sheep. *Vaccine* 9:35-41.

Morrill JC, Jennings GB, Caplen H, Turell MJ, Johnson AJ, Peters CJ (1987) Pathogenicity and immunogenicity of a mutagen-attenuated Rift Valley fever virus immunogen in pregnant ewes. *American Journal of Veterinary Research* 48:1042-1047.

Morvan J, Lesbordes JL, Rollin PE, Mouden JC, Roux J (1992) First fatal human case of Rift Valley fever in Madagascar. *Transactions of the Royal Society of Tropical Medicine and Hygiene* 86:320.

Moser LA, Boylan BT, Moreira FR, Myers LJ, Svenson EL, Fedorova NB, Pickett BE, Bernard KA (2018) Growth and adaptation of Zika virus in mammalian and mosquito cells. *PloS Neglected Diseases* 12:e0006880.

Moussa MI, Wood OL, Abdel Wahab KS (1982) Reduced pathogenicity associated with a small plaque variant of the Egyptian strain of Rift Valley fever virus (ZH501). *Transactions of the Royal Society of Tropical Medicine and Hygiene* 76:482-486.

Moutailler S, Roche B, Thiberge JM, Caro V, Rougeon F, Failloux AB (2011) Host alternation is necessary to maintain the genome stability of Rift Valley fever virus. *PLoS Neglected Tropical Diseases* 5:e1156.

Muller R, Saluzzo JF, Lopez N, Dreier T, Turell M, Smith J, Bouloy M (1995) Characterization of clone 13, a naturally attenuated avirulent isolate of Rift Valley fever virus, which is altered in the small segment. *American Journal of Tropical Medicine Hygiene* 53:405-411.

Muller R, Poch O, Delarue M, Bishop DH, Bouloy M (1994) Rift Valley fever L segment: correction of the sequence and possible functional role of newly identified regions conserved in RNA-dependent polymerases. *Journal of General Virology* 75:1345-52.

Narrod C, Zinsstag J, Tiongco M, (2012) A One Health framework for estimating the economic costs of zoonotic diseases on society. *EcoHealth* 9:150-162.

National Institute for Communicable Diseases (2012) *Communicable Disease Surveillance Bulletin* 10.

Nasrullah I, Butt AM, Tahir S, Idrees M, Tong Y (2015) Genomic analysis of codon usage shows influence of mutation pressure, natural selection and host features on Marburg virus evolution. *BioMed Central Evolutionary Biology* 15:1-15.

Nderitu L, Lee JS, Omolo J, Omulo S, O'Guinn ML, Hightower A, Mosha F, Mohamed M, Munyua P, Nganga Z, Hiett K, Seal B, Feikin DR, Breiman RF, Njenga MK (2011) Sequential

Rift Valley fever outbreaks in eastern Africa caused by multiple lineages of the virus. *Journal of Infectious Disease* 203:655-665.

Nicklasson B, Peters CJ, Grandien M, Wood O (1984) Detection of human immunoglobulins G and M antibodies of Rift Valley fever virus by enzyme-linked immunosorbent assay. *Journal of Clinical Microbiology* 19:225-229.

Nicod C, Banaei-Esfahani A, Collins BC (2017) Elucidation of host-pathogen protein-protein interactions to uncover mechanisms to host cell rewiring. *Current Opinions in Microbiology* 39:7-15.

Nicolas G, Durand B, Duboz R, Rakotondravao R, Chevalier V (2013) Description and analysis of the cattle trade network in the Madagascar highlands: potential role in the diffusion of Rift Valley fever virus. *Acta Tropica* 126:19-27.

Njenga MK, Bett B (2019) Rift Valley fever virus – How and where virus is maintained during inter-epidemic periods. *Current Clinical Microbiology Reports* 6:18-24.

Njenga MK, Paweska J, Wanjala R, Rao CY, Weiner M, Omballa V, Luman ET, Mutonga D, Sharif S, Panning M, Dorsten C, Feikin DR, Breiman R (2009) Using a field quantitative real-time PCR test to rapidly identify highly viremic Rift Valley fever cases. *Journal of Clinical Microbiology* 47:1166-1171.

Nyundo S, Adamson E, Rowland J, Palermo PM, Matiko M, Bettinger GE, Wambura P, Morrill JC, Watts D (2019) Safety and immunogenicity of Rift Valley fever MP-12 and arMP-12ΔNSm21/384 vaccine candidates in goats (*Capra aegagrus hircus*) from Tanzania. *Onderstepoort Journal of Veterinary Research* 86:a1683.

Odendaal L, Clift SJ, Fosgate GT, Davis AS (2019) Lesions and cellular tropism of natural Rift Valley fever virus infection in adult sheep. *Veterinary Pathology* 56:61-77.

OIE (2019) Manual of diagnostic tests and vaccines for terrestrial animals. *World Organisation for Animal Health,* Paris.

Olive M-M, Goodman SM, Reynes J-M (2012) The role of wild mammals in the maintenance of Rift Valley fever virus. *Journal of Wildlife Diseases* 48:241-266.

Överby AK, Pettersson RF, Grunewald K, Huiskonen JT (2008) Insights into bunyavirus architecture from electron cryotomography of Uukuniemi virus. *Proceedings of the National Academy of Sciences of the United States of America* 105:2375-2379.

Parish CR (2006) The role of heparin sulphate in inflammation. *Nature Reviews Immunology* 6:633-643.

Paweska JT, Mortimer E, Leman PA, Swanepoel R (2005) An inhibition enzyme-linked immunosorbent assay for the detection of antibody to Rift Valley fever virus in humans, domestic and wild ruminants. *Journal of Virological Methods* 127:10-18.

Paweska JT, Burt FJ, Anthony F, Smith SJ, Grobbelaar AA, Croft JE, Ksiazek TG, Swanepoel R (2003) IgG-sandwich and IgM-capture enzyme-linked immunosorbent assay for the detection of antibody to Rift Valley fever virus in domestic ruminants. *Journal of Virological Methods* 113:103-112.

Paumi CM, Menndez J, Amoldo A, Engels K, Iyer KR, Thaminy S, Georgiev O, Barral Y, Michaelis S, Stagljar I (2007) Mapping protein-protein interactions for the yeast ABC transporter Ycf1p by integrated split-ubiquitin membrane yeast two-hybrid analysis. *Molecular Cell* 26:15-25.

Pepin M, Bouloy M, Bird BH, Kemp A, Paweska J (2010) Rift Valley Fever virus (*Bunyavirirdae: Phlebovirus)*: an update on pathogenesis, molecular epidemiology, vectors, diagnostics and prevention. *Veterinary Research* 41:61.

Peyre M, Chevalier V, Abdo-Salem S, Velthuis A, Antoine-Moussiaux N, Thiry E, Roger F (2015) A systematic scoping study of the socio-economic impact of Rift Valley fever: Research gaps and needs. *Zoonoses and Public Health* 62:309-325.

Peyrefitte CN, Boubis L, Coudrier D, Bouloy M, Grndadam M, Tolou HJ, Plumet S (2008) Real-time reverse-transcription loop-mediated isothermal amplification for rapid detection of Rift Valley fever virus. *Journal of Clinical Microbiology* 46:3653-3659.

Phizicky EM, Fields S (1995) Protein-protein interactions: methods for detection and analysis. *Microbiological Revision* 59:94-123.

Phoenix I, Nishiyama S, Lokugamage N, Hill TE, Huante MB, Slack OAL, Carpio VH, Freiberg AN, Ikegami T (2016) N-Glycans on the Rift Valley fever virus envelope glycoproteins Gn and Gc redundantly support viral infection via DC-SIGN. *Viruses* 8:149.

Pienaar NJ, Thompson PN (2013) Temporal and spatial history of Rift Valley fever in South Africa: 1950 to 2011. *Onderstepoort Journal of Veterinary Research* 80:a384.

Piper ME, Sorenson DR, Gerrard SR (2011) Efficient cellular release of Rift Valley fever virus requires genomic RNA. *PLoS One* 3:e18070.

Pires HR, Boxem M (2018) Mapping the polarity Interactome. *Journal of Molecular Biology* 430:3521-3544.

Pittman PR, Liu CT, CannonTL, Makuch RS, Mangaiafico JA, Gibbs PH, Peters CJ (1999) Immunogenicity of an inactivated Rift Valley fever vaccine in humans: a 12–year experiment. *Vaccine* 18:181-189.

Prachayangprecha S, Schapendonk CME, Koopmans MP, Osterhaus ADME, Schürch AC, Pas SD, van der Eijk AA, Poovorawan Y, Haagmans BL, Smits SL (2014) Exploring the potential of Next Generation Sequencing in detection of respiratory viruses. *Journal of Clinical Microbiology* 52:3722-3730.

Posada D, Crandall KA, Holmes EC (2002) Recombination in evolutionary genomics. *Annual Review of Genetics* 36:75-97.

Puigbò P, Bravo I, Garcia-Vallvé S (2008) E-CAI: a novel server to estimate an expected value of codon adaptation index (eCAI). *BioMed Central Bioinformatics* 9:65.

Rajagopala SV, Uetz P (2011) Analysis of protein-protein interactions using high-throughput yeast two-hybrid screens. In: Cagney G, Emili A. (eds) Network Biology. Methods in Molecular Biology (Methods and Protocols), Volume 781. Humana Press.

Randall R, Gibbs CJ Jr, Aulisio CG, Binn LN, Harrison VR (1962) The development of a formalin-killed Rift Valley fever virus vaccine for use in man. *Journal of Immunology* 89:660-71.

Rao VS, Srinivas K, Sujini GN, Kumar GNS (2014) Protein-protein interaction detection: Methods and analysis. *International Journal of Proteomics*: 147648.

Rappsilber J (2011) The beginning of a beautiful friendship: cross-linking/mass spectrometry and modelling of proteins and multi-protein complexes. *Journal of Structural Biology* 173: 530-540.

Raymond DD, Piper ME, Gerrard SR, Skiniotis G, Smith JL (2012) Phleboviruses encapsidate their genomes by sequestering RNA bases. *Proceedings of the National Academy of Sciences of the United States of America* 109:19208-19213.

Reece-Hoyes JS, Walhout AJ (2012) Gene-centered yeast one-hybrid assays. *Methods in Molecular Biology* 812:189-208.

Reguera J, Weber F, Cusack S (2010) *Bunyaviridae* RNA polymerases (L-protein) have an N-terminal, influenza-like endonuclease domain, essential for viral cap-dependent transcription. *PLoS Pathogens* 6:e1001101.

Rönkä H, Hildén P, Von Bonsdorff CH, Kuismanen E (1995) Homodimeric association of the spike glycoproteins G1 and G2 of Uukuniemi virus. *Virology* 211:241-250.

Rusu M, Bonneau R, Holbrook MR, Watowich SJ, Birmanns S, Wriggers W, Freiberg AN (2012) An assembly model of Rift Valley fever virus. *Frontiers in Microbiology* 3:254.

Sall AA, Macondo EA, Sene OK, Diagne M, Sylla R, Mondo M, Girault L, Marrama L, Spiegel A, Diallo M, Bouloy M, Mathiot C (2002) Use of reverse transcriptase PCR in early diagnosis of Rift Valley fever. *Clinical and Diagnostic Laboratory Immunology* 9:713-715.

Sall AA, Zanotto PM De A, Sene OK, Zeller HG, Digoutte JP, Thiongane Y, Bouloy M (1999) Genetic reassortment of Rift Valley fever virus in nature. *Journal of Virology* 73:8196-8200.

Sall AA, de Zanotto PM, Zeller HG, Digoutte JP, Thiongane Y, Bouloy M (1997) Variability of NSs protein among Rift Valley fever virus isolates. *Journal of General Virology* 78:2853-2858.

Sambrook J, Fritsch EF, Maniatis T (1989) Molecular cloning A laboratory manual 2nd Edition. 1.74-1.81, Harbor Laboratory Press, New York.

Sarrazin S, Lamanna WC, Esko JD (2011) Heparan sulfate proteoglycans. *Cold Spring Harbor Perspectives in Biology* 7:a004952.

Scharton D, Van Wettere AJ, Bailey KW, Vest Z, Westover JB, Siddharthan V, Gowen BB (2015) Rift Valley fever virus infection in Golden Syrian hamsters. *PLoS One* 10:e0116722.

Schoemaker T, Boulianne C, Vincent MJ, Pezzanite L, Al-Qahtani MM, Al-Mazrou Y, Khan AS, Rollin PE, Swanepoel R, Ksiazek TG, Nichol ST (2002) Genetic Analysis of viruses associated with emergence of Rift Valley fever in Saudi Arabia and Yemen, 2000-01. *Emerging Infectious Diseases* 8:1415-1420.

Schulz KH (1951) Rift Valley fever in South Africa. Special Report No 5/51. Union Department of Health, Plaque Research Laboratory, Johannesburg, South Africa, May 1951.

Schmaljohn C, Hooper JW (2001) *Bunyaviridae*: The viruses and their replication. In D.M Knipe, PM Howley, DE Griffin, MA Martin, RA Lamb, B Roizman, SE Straus (ed), Fields Virology, 4th edition, Lippincott, Williams and Wilkins, Philadelphia, Pennsylvania. p1581-1602.

Scott GR (1963) Pigs and Rift Valley fever. Nature 200:919-920.

Seufi AM, Galal FH (2010) Role of *Culex* and *Anopheles* mosquito species as potential vectors of Rift Valley fever virus in Sudan outbreak, 2007. *BioMed Central Infectious Diseases* 10:65.

Sexton NR, Ebel GD (2019) Effects of arbovirus multi-host life cycles on dinucleotide and codon usage patterns. *Viruses* 11:643.

Shi M, Jagger BW, Wise HM, Digard P, Holmes EC, Taubenberger JK (2012) Evolutionary conservation of the PA-X open reading frame in segment 3 of Influenza A virus. *Journal of Virology* 86:12411-12413.

Shope RE, Peters CJ, Davies FG (1982) The spread of Rift Valley fever and approaches to its control. *Bulletin of the World Health Organization* 60:299-304.

Simon M, Johansson C, Mirazimi A (2009) Crimean-Congo hemorrhagic fever virus entry and replication is clathrin-, pH- and cholesterol-dependent. *Journal of General Virology* 90:210-215.

Sindato C, Karimuribo E, Mboera LEG (2011) The epidemiology and socio-economic impact of Rift Valley fever epidemics in Tanzania: a review. *Tanzania Journal of Health Research* 13:305-318.

Sissoko D, Giry C, Gabrie P, Tarantola A, Pettinelli F, Collet L, D'Ortenzio E, Renault P, Pierre V (2009) Rift Valley fever, Mayotte, 2007-2008. *Emerging Infectious Diseases* 15:568-570.

Smithburn KC, Haddow, AJ, Gillett JD (1948) Rift Valley fever: Isolation of the virus from wild mosquitoes. *British Journal of Experimental Pathology* 30:107-121.

Smits SL, Osterhaus ADME (2013) Virus discovery: one step beyond. *Current Opinion in Virology* 3:e1-e6.

Snider J, Stagljar I (2016) Membrane yeast two-hybrid (MYTH) mapping of full-length membrane protein interactions. Article in Cold Spring Harbor Protocols Press. http://cshprotocols.cshlp.org

Snider J, Kittanakom S, Curak J, Stagljar I (2010) Split-ubiquitin based membrane yeast two-hybrid (MYTH) system: a powerful tool for identifying protein-protein interactions. *Journal of Visualized Experiments* 1:1698.

Soilleux EJ, Barten R, Trowsdale J (2000) Cutting edge: DC-SIGN; a related gene, DC-SIGNR; and CD232 form a cluster on 19p13. *Journal of Immunology* 165:2937-2942.

Song H, Liu J, Song Q, Zhang Q, Tian P, Nan Z (2017) Comprehensive analysis of codon usage bias in seven Epichloë species and their peramine-coding genes. *Frontiers in Microbiology* 8:1419.

Spiegel M, Plegge T, Pöhlmann S (2016) The role of Phlebovirus glycoproteins in viral entry, assembly and release. *Viruses* 8:202.

Stagljar I, Korostensky C, Johnsson N, Te Heesen S (1998) A genetic system based on split-ubiquitin for the analysis of interactions between membrane proteins *in vivo*. *Proceedings of the National Academy of Sciences of the United States of America* 95:5187-5192.

Stedman A, Wright D, Schreur PJW, Clark MHA, Hill AVS, Gilbert SC, Francis MJ, Van Keulen L, Kortekaas J, Charleston B, Warmwe GM (2019) Safety and efficacy of ChAdOxl RVF vaccine against Rift Valley fever in pregnant sheep and goats. *Vaccines* 44.

Stephens DJ, Banting G (2000) The use of yeast two hybrid screens in studies of protein:protein interactions involved in trafficking. *Traffic* 1:763-768.

Steyn JJ, Schulz KH (1955) *Aedes (Ochlerotatus) caballus* Theobald, the South African vector of Rift Valley fever. *South African Medical Journal* 29:1114-1120.

Sugita S, Hata Y, Sudhof TC (1996) Distinct Ca(2+)-dependent properties of the first and second C2-domains of synaptotagmin I. *The Journal of Biological Chemistry* 271:1262-1265.

Sun S, Yang X, wang Y, Shen X (2016) In vivo analysis of protein-protein interactions with Bioluminiscence resonance energy transfer (BRET): Progress and prospects. *International Journal of Molecular Sciences* 17:1704

Sun Y, Qi Y, Liu C, Gao W, Chen P, Fu L, Peng B, Wang H, Jing Z, Zhong G, Li W (2014) Nonmuscle myosin heavy chain 11A is a critical factor contributing to the efficiency of early infection of severe fever with thrombocytopenia syndrome virus. *Journal of Virology* 88:237-248.

Suzich JA, Kakach LT, Collett MS (1990) Expression strategy of a *Phlebovirus:* biogenesis of proteins from the Rift Valley fever virus M segment. *Journal of Virology* 64:1549-1555.

Swanepoel R, Coetzer JAW (2004) Rift Valley fever. In Coetzer JAW and Tustin RC (2nd editions), Infectious diseases of livestock with special reference to Southern Africa. 1037-1070. Oxford University Press, Cape Town.

Swanepoel R (1981) Observations on Rift Valley fever in Zimbabwe. *Contributions to Epidemiology and Biostatistics* 3:383-391.

Swanepoel R, Blackburn NK (1977) Demonstration of nuclear immunofluorescence in Rift Valley fever infected cells. *Journal of General Virology* 34:557-561.

Swanepoel R, Coetzer JAW (2004) Rift Valley fever. In Coetzer JAW and Tustin RC. (2nd editions), Infectious diseases of livestock with special reference to Southern Africa. 1037-1070, Oxford University Press, Cape Town.

Tamura K, Peterson D, Peterson N, Stecher G, Nei M, Kumar S (2011) MEGA5: Molecular evolutionary genetics analysis using Maximum Likelihood, Evolutionary Distance, and Maximum Parsimony methods. *Molecular Biology and Evolution* 28:2731-2739.

Terasaki K, Ramirez SI, Makino S (2016) Mechanistic insight into the host transcription inhibition function of Rift Valley fever virus NSs and its importance in virulence. *PLoS Neglected Tropical Diseases* 10:e0005047.

Thomas T, Gilbert J, Meyer F (2012) Metagenomics – a guide from sampling to data analysis. *Microbial Informatics and Experimentation* 2:3.

Thompson JD, Higgins DG, Gibson TJ (1994) CLUSTAL W: improving the sensitivity of progressive multiple sequence alignment through sequence weighting, position-specific gap penalties and weight matrix choice. *Nucleic Acids Research* 22:4673-4680.

Tsirigos KD, Peters C, Shu N, Käll L, Elofsson A (2015) The TOPCONS web server for consensus prediction of membrane protein topology and signal peptides. *Nucleic Acids Research* 43:W401-W407.

Turell MJ, Presley SM, Gad AM, Cope SE, Dohm DJ, Morrill JC, Arthur PP (1996) Vector competence of Egyptian mosquitoes for Rift Valley fever virus. *The American Journal of Tropical Medicine and Hygiene* 54:136-139.

Turell MJ, Perkins PV (1990) Transmission of Rift Valley fever virus by the sand fly, Phlebotomus duboscqi (Diptera:Psychodidae). *The American Journal of Tropical Medicine and Hygiene* 42:185-188.

Urech DM, Lichtlen P, Barberis A (2003) Cell growth selection system to detect extracellular and transmembrane protein interactions. *Biochimica et Biophysica Acta* 1622:117-127.

Van Criekinge W, Beyaert R (1999) Yeast two-hybrid: State of Art. *Biological Procedures Online* 2(1). www.biologicalprocedures.com.

Van Kooyk Y (2008) C-type lectins on dendritic cells: key modulators for the induction of immune responses. *Biochemical Society Transactions* 36:1478-1481.

Viklund H, Elofsson A (2008) OCTOPUS: Improving topology prediction by two-track ANN-based preference scores and an extended topology grammar. *Bioinformatics* 24: 1662-1668.

Von Heijne G (2007) The membrane protein universe: what's out there and why bother? *Journal of Internal Medicine* 261:543-557.

Von Teichman B, Engelbrecht A, Zulu G, Dungu B, Pardini A, Bouloy M (2011) Safety and efficacy of Rift Valley fever Smithburn and Clone 13 vaccines in calves. *Vaccine* 29:5771-5777.

Wallace DB, Ellis CE, Espach A, Smith SJ, Greyling RR, Viljoen GJ (2006) Protective immune responses induced by different recombinant vaccine regimes to Rift Valley fever. *Vaccine* 24:7181-7189.

Walsh BW, Lenhart JS, Schroeder JW, Simmons LA (2012) Far-western blotting as a rapid and efficient method for detecting interactions between DNA replication and DNA repair proteins. *Methods in Molecular Biology* 922:161-168.

Wang H, Liu S, Zhang B, Wei W (2017) Analysis of synonymous codon usage of Zika virus and its adaptation to hosts. *PLoS One* 12:e0170128.

Wang Y, Fang R, Yuan Y, Hu M, Zhou Y, Zhao J (2014) Identification of host proteins interacting with the integrin-like A domain of *Toxoplasma gondii* micronemal protein MIC2 by yeast two-hybrid screening. *Parasites and Vectors* 7:543.

Wang FI, Hsu AM, Huang KJ (2001) Bovine ephemeral fever in Taiwan. *Journal of Veterinary Diagnostic Investigation* 13:462-467.

Wargo AR, Kurath G (2011) *In vivo* fitness associated with high virulence in a vertebrate virus is a complex trait regulated by host entry, replication and shedding. *Journal of Virology* 85:3959-3967.

Warimwe GM, Gesharisha J, Carr BV, Otieno S, Otingah K, Wright D, Charleston B, Okoth E, Elena LG, Lorenzo G, Ayman EB, Alharbi NK, Al-dubaib MA, Brun A, Gilbert SC, Nene V, Hill AVS (2016) Chimpanzee adenovirus vaccine provides multispecies protection against Rift Valley fever. *Science Report* 6:20617.

Wasmoen TL, Kakach LT, Colett MS (1988) Rift Valley fever virus M segment: cellular localization of M segment-encoded proteins. *Virology* 166:275-280.

Whitehouse CA, (2004) Crimean-Congo haemorrhagic fever. *Antiviral Research* 64:145-160.

WHO, 2019 Rift Valley fever – Mayotte (France): Disease outbreak news (13 May 2019).

WHO, 2010. *Fact sheet* 207.

Wichgers Schereur, van Keulen L, Kant J, Oreshkova N, Moormann RJ, Kortekaas J (2016) Co-housing of Rift Valley fever virus infected lambs with immunocompetent or immunosuppressed lambs does not result in virus transmission. *Frontiers in Microbiology* 7:287.

Wilson WC, Davis AS, Gaudreault NN, Faburay B, Trujillo JD, Shivanna V, Sunwoo SY, Balogh A, Endalew A, Ma W, Drolet BS, Ruder MG, Morozov I, McVey DS, Richt JA (2016) Experimental infection of calves by two genetically-distinct strains of Rift Valley fever virus. *Viruses* 8:E145.

Wilson WC, Gaudreault NN, Jasperson DC, Johnson DJ, Ostlund EN, Chase CL, Ruder MG, Stallknecht DE (2015) Molecular evolution of American field strains of Bluetongue and Epizootic haemorrhagic disease viruses. *Veterinaria Italiana* 51:269-273.

Won S, Ikegami T, Peters CJ, Makino S (2007) NSm protein of Rift Valley fever virus suppresses virus-induced apoptosis. *Journal of Virology* 81:13335-13345.

Won S, Ikegami T, Peters CJ, Makino S (2006) NSm and 78-kilodalton proteins of Rift Valley fever virus are nonessential for viral replication in cell culture. *Journal of Virology* 80:8274-8278.

Wong JH, Alfatah M, Sin MF, Sim HM, Verma CS, Lane DP, Arumugam P (2017) A yeast two-hybrid system for the screening and characterization of small molecule inhibitors of protein-protein interactions identifies a novel putative Mdm2-binding site in p53. *BioMed Central Biology* 15:108.

Woods CW, Karpati AM, Grein T, McCarthy N, Gaturuku P, Muchiri E, Dunster L, Henderson A, Khan AS, Swanepoel R, Bonmarin I, Martin L, Mann P, Smoak BL, Ryan M, Ksiazek TG, Arthur RR, Ndikuyeze A, Agata NN, Peters CJ, WHO HFTF (2002) An outbreak of Rift Valley fever in Northeastern Kenya, 1997-98. *Emerging Infectious Diseases* 8:138-144.

Wright F (1990) The effective number of codons used in a gene. *Gene* 87:23-29.

Wu Y, Zhu Y, Gao F, Jiao Y, Oladejo BO, Chai Y, Bi Y, Lu S, Dong M, Zhang C, Huang G, Wong G, Li N, Zhang Y, Li Y, Feng W-h, Shi Y, Liang M, Zhang R, Qi J, Gao GF (2017) Structures of phlebovirus glycoprotein Gn and identification of a neutralizing antibody epitope. *Proceedings of the National Academy of Sciences of the United States of America* E7564-E7573.

Wu Y, Li Q, Chen XZ (2007) Detecting protein-protein interactions by far-western blotting. *Nature Protocols* 2:3278-3284.

Xie Q, Soutto M, Xu X, Zhang Y, Johnson CH (2011) Bioluminescence resonance energy transfer (BRET) imaging in plant seedling and mammalian cells. *Methods in Molecular Biology* 680:3-28.

Xing S, Wallmeroth N, Berendzen KW, Grefen C (2016) Techniques for the analysis of protein-protein interactions in vivo. *Plant Physiology* 171:727-758.

Xu Y, Piston DW, Johnson CH (1999) A bioluminescence resonance energy transfer (BRET) system: Application to interacting circadian clock proteins. *Proceedings of the National Academy of Sciences of the United States of America* 96:151-156.

Yamauchi Y, Helenius A (2013) Virus entry at a glance. *Journal of Cell Science* 126:1289-1295.

Youssef BZ (2009) The potential role of pigs in the enzootic cycle of Rift Valley fever at Alexandria Governorate, Egypt. *Journal of Egypt Public Health Association* 84:329-341.

Zaki A, Coudrier D, Yousef AI, Fakeeh M, Bouloy M, Billecocq A (2006) Production of monoclonal antibodies against Rift Valley fever virus: Application for rapid diagnosis tests (virus detection and ELISA) in human sera. *Journal of Virological Methods* 131:34-40.

Zeller HG, Fontenille D, Traore-Laminaza M, Thiongane Y, Digoutte J-P (1997) Enzootic activity of Rift Valley fever virus in Senegal. *The American Journal of Tropical Medicine and Hygiene* 56:265-272.

Zhao WJ, Zhang H, Bo X, Li Y, Fu X (2009) Generation and analysis of expressed sequence tags from cDNA library of monieza expansa. *Molecular and Biochemical Parasitology* 164:80-85.

Zhu YY, Machleder EM, Chenchik A, Li R, Siebert PD (2001) Reverse transcriptase template switching: A SMART™ approach for full-length cDNA library construction. *BioTechniques* 30:892-897.

APPENDICES

Appendix A

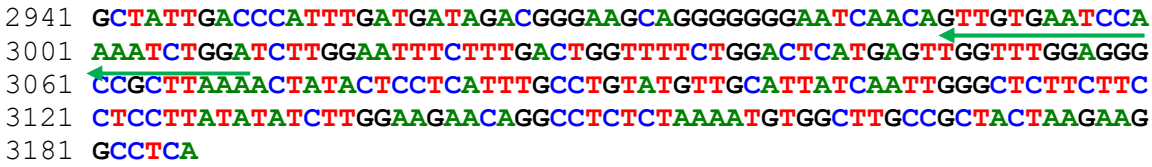

Figure S1: Sequence of the GnGc nucleotide indicating the regions amplified. Black arrows indicate the positions where the forward and the reverse primers were designed to amplify the region of the Gn. Green arrows indicate the positions where the forward and reverse primers were designed to amplify the region of the Gc.

ARC • LNR

APPROVED

Onderstepoort Veterinary Institute

AEC 18.14

Animal Ethics

Decision of the Animal Ethics Committee for the use of living vertebrates for research, diagnostic procedures and product development

APPROVAL PERIOD: 2014/ 2015

PROJECT NUMBER:	05/18/p002			
PROJECT TITLE:	Host tissue specificity of selected South African isolates of Rift Valley fever virus			
PROJECT LEADER:	Moabi Rachel Maluleke			
DIVISION:	MED			
CATEGORY:	B			
SPECIES OF ANIMAL:	Chicken			
NUMBER OF ANIMALS:	3			
NOT APPROVED:				
APPROVED:	APPROVED			

PLEASE NOTE: Should the number or species of animal(s) required, or the experimental procedure(s) change, please submit a revised animal ethics clearance form to the animal ethics committee for approval before commencing with the experiment

SIGNATURE: Dr L. Lopez
CHAIRPERSON ANIMAL ETHICS COMMITTEE

DATE: 02-12-2014

UNIVERSITEIT VAN PRETORIA
UNIVERSITY OF PRETORIA
YUNIBESITHI YA PRETORIA

Animal Ethics Committee

PROJECT TITLE	**Host tissue specificity of selected South African isolates of Rift Valley fever virus**
PROJECT NUMBER	**V050-15**
RESEARCHER/PRINCIPAL INVESTIGATOR	**MR Maluleke**

STUDENT NUMBER (where applicable)	**23282658**
DISSERTATION/THESIS SUBMITTED FOR	**PhD**

ANIMAL SPECIES	**Chickens**	
NUMBER OF ANIMALS	**4**	
Approval period to use animals for research/testing purposes		**1 July 2015 – 30 June 2016**
SUPERVISOR	**Dr.PP Majiwa**	

KINDLY NOTE:

Should there be a change in the species or number of animal/s required, or the experimental procedure/s - please submit an amendment form to the UP Animal Ethics Committee for approval before commencing with the experiment

APPROVED	Date	29 June 2015
CHAIRMAN: UP Animal Ethics Committee	Signature	

S***4285-15***

agriculture,
forestry & fisheries

Department:
Agriculture, Forestry and Fisheries
REPUBLIC OF SOUTH AFRICA

Directorate Animal Health, Department of Agriculture, Forestry and Fisheries
Private Bag X138, Pretoria 0001

Enquiries: Mr Herry Gololo • Tel: +27 12 319 7532 • Fax: +27 12 319 7470 • E-mail: HerryG@daff.gov.za
Reference: 12/11/1/1

Ms Rachel Maluleke
ARC-OVI
Onderstepoort

Dear Ms Maluleke,

RE: Dispensation on Section 20 Approval in Terms of the Animal Diseases Act, 1984 (Act No 35 of 1984) for: Host Tissue Specificity of Selected South African Isolates of Rift Valley Fever (RVF) Virus

Your application submitted 27 August 2015 refers.

A dispensation is hereby granted on point 2 of the Section 20 approval (attached):

(i) Purified antibodies may be stored at the ARC-OVI;
(ii) The stored purified antibodies may not be outsourced without prior permission from DAFF;
(iii) The use of stored purified antibodies for any further research is subject to obtaining a new Section 20 approval.

Kind regards,

DR. MPHO MAJA
DIRECTOR: ANIMAL HEALTH

Date: 2015 -10- 19

UNIVERSITEIT VAN PRETORIA
UNIVERSITY OF PRETORIA
YUNIBESITHI YA PRETORIA

FACULTY OF VETERINARY SCIENCE	
Application for approval of title of dissertation or thesis	
PLEASE NOTE: This form must be completed in **TYPING** **Please attach a summary/abstract to this form**	
Name of candidate	Moabi Rachel Maluleke
Student number	23282658
Degree	PhD
Course code	VWE901
Department	Tropical Veterinary Diseases
Name of supervisor	Dr BJ Mans
Name of co-supervisor(s)	Prof EH Venter
Protocol approved : Yes ☐ No **Date submitted/approved: 11/11/2013** **AEC approved :** Yes ☐ No **AEC Number (Certificate):** S4285-15	
Title of dissertation/thesis:	
Host tissue specificity of selected South African isolates of Rift Valley fever virus	
SIGNED BY:	
CANDIDATE	**DATE** 23/01/19
SUPERVISOR	**DATE** 23/01/2019
APPROVED BY HEAD OF DEPARTMENT	**DATE** 5/03/2019
APPROVED BY CHAIR PGC/DEPUTY DEAN	**DATE** 2019-03-20

Please submit this document to vetpg@up.ac.za or Student Administration